



Formation and reactivation of the Pyrenean-Cantabrian rift system : inheritance, segmentation and thermal evolution

Rodolphe Lescoutre

► **To cite this version:**

Rodolphe Lescoutre. Formation and reactivation of the Pyrenean-Cantabrian rift system : inheritance, segmentation and thermal evolution. Earth Sciences. Université de Strasbourg, 2019. English. NNT : 2019STRAH003 . tel-02312419

HAL Id: tel-02312419

<https://tel.archives-ouvertes.fr/tel-02312419>

Submitted on 11 Oct 2019

HAL is a multi-disciplinary open access archive for the deposit and dissemination of scientific research documents, whether they are published or not. The documents may come from teaching and research institutions in France or abroad, or from public or private research centers.

L'archive ouverte pluridisciplinaire **HAL**, est destinée au dépôt et à la diffusion de documents scientifiques de niveau recherche, publiés ou non, émanant des établissements d'enseignement et de recherche français ou étrangers, des laboratoires publics ou privés.

École Doctorale des Sciences de la Terre et de l'Environnement (ED 413)

Institut de Physique du Globe de Strasbourg (UMR 7516)

THÈSE présentée par :

Rodolphe LESCOUTRE

soutenue le : **25 avril 2019**

pour obtenir le grade de : **Docteur de l'université de Strasbourg**

Discipline/ Spécialité : Sciences de la Terre – Géologie – Tectonique

**Formation et réactivation du système de rift
pyrénéo-cantabrique:
héritage, segmentation et évolution thermique**

THÈSE dirigée par :

Pr. MANATSCHAL Gianreto

Université de Strasbourg (FR)

RAPPORTEURS :

Pr. MOUTHEREAU Frédéric

Pr. TEIXELL Antonio

Université Toulouse Paul Sabatier (FR)

Universitat Autònoma de Barcelona (ES)

EXAMINATEURS :

Pr. FERNÁNDEZ-VIEJO Gabriela

Pr. ROSENBERG Claudio

Pr. TAVANI Stefano

Universidad de Oviedo (ES)

Université Pierre et Marie Curie (FR)

Università degli Studi di Napoli Federico II (IT)



THÈSE présentée par :

Rodolphe LESCOUTRE

soutenue le : **25 avril 2019**

pour obtenir le grade de : **Docteur de l'université de Strasbourg**

Discipline/ Spécialité : Sciences de la Terre – Géologie – Tectonique

Formation and reactivation of the Pyrenean-Cantabrian rift system: inheritance, segmentation and thermal evolution

THÈSE dirigée par :

Pr. MANATSCHAL Gianreto

Université de Strasbourg (FR)

RAPPORTEURS :

Pr. MOUTHEREAU Frédéric

Pr. TEIXELL Antonio

Université Toulouse Paul Sabatier (FR)

Universitat Autònoma de Barcelona (ES)

EXAMINATEURS :

Pr. FERNÁNDEZ-VIEJO Gabriela

Pr. ROSENBERG Claudio

Pr. TAVANI Stefano

Universidad de Oviedo (ES)

Université Pierre et Marie Curie (FR)

Università degli Studi di Napoli Federico II (IT)

INVITÉS :

Pr. MUÑOZ Josep Anton

Dr. MASINI Emmanuel

Universitat de Barcelona (ES)

Total R&D - M&U sas (FR)

You see things; and you say “Why?”

But I dream things that never were; and I say “Why not?”

George Bernard Shaw (1856–1950)

Back to Methuselah, act I, *Selected Plays with Prefaces*, vol. 2, p. 7 (1949)

À mes grands-parents,

Christiane et Jean

AVANT-PROPOS

Cette thèse traite de la segmentation et de l'évolution thermique des systèmes extensifs hyper-étirés ainsi que de leur réactivation lors de l'orogénèse en choisissant la chaîne pyrénéo-cantabrique comme cas d'étude. Cette thèse, encadrée par Gianreto Manatschal, s'inscrit dans la recherche développée à Strasbourg sur l'héritage associé aux rifts hyper-étirés et leur préservation dans les chaînes de montagnes.

Ce projet a été financé par le projet Orogen, issu du partenariat associant Total, le BRGM et l'INSU sur la période 2015 à 2020.

ABSTRACT

The processes responsible for the formation of oceans and mountain chains represent a substantial part of the studies in Earth sciences. The extensional and contractional processes occurring during the Wilson cycle (Wilson, 1966) are now observed through the scope of inheritance. The latter would control the location and the mode of deformation via the reactivation of structures inherited from previous tectonic events. During rifting and prior to oceanic accretion, recent studies have revealed a strong structural and thermal asymmetry that can lead to subcontinental mantle exhumation together with a high temperature metamorphism of the sedimentary basin. The mode of deformation and the crustal architecture can significantly change along the rift axis via the occurrence of transfer zones. This 3D architecture acquired during rifting will represent the initial condition for the reactivation and the formation of the subsequent orogenic system.

The Pyrenean-Cantabrian orogenic system represents a natural laboratory to investigate these topics as it results from the inversion of segmented Mesozoic rift basins during the Late Cretaceous to Miocene Alpine orogeny. These hyperextended rift systems led to the exhumation of subcontinental mantle during mid-Cretaceous together with a High Temperature/Low Pressure metamorphic event which affected the pre- to syn-rift sedimentary sequence. Besides, the weak Alpine overprint allowed to preserve onshore the sedimentary cover as well as the basement – sediment relationship established during the rifting events. Moreover, the numerous research projects and industrial prospections provided a significant amount of data about the surface and the deep geology.

The first aim of this work is to characterise the 3D architecture of the Pyrenean-Cantabrian junction which results from the reactivation of a former segmented rift system. The second objective is to investigate how reactivation proceeds and to define the role of inheritance for the evolution of segmented domains. Finally, the third objective is to analyse the thermal evolution associated with magma-poor asymmetric rifting based on a thermo-mechanical model and on observations from the Pyrenean rift system analogue.

The first chapter investigates the present-day architecture of the Pyrenean-Cantabrian junction, in the Basque Country, where the Mauléon (Pyrenean segment) and the Basque-Cantabrian (Cantabrian segment) basins are located. It aims to provide further constrains on the existence or not of the so-called NNE-SSW Pamplona transform fault which would have decoupled the deformation between the Cantabrian and the Pyrenean segments during rifting and convergence. It also aims to provide field constrains for the kinematics of the Iberian plate

with respect to the Eurasian plate during the Mesozoic. Indeed, many geodynamic models have been proposed and remain debated due to the controversy about the origin of the magnetic anomalies. As such, N-S and E-W geological cross-sections combining field data, seismic interpretations and well information have been performed in the study area.

The results argue against the existence of a major N-S striking transform fault between rift segments. In contrast, they suggest that E-W trending mid-Cretaceous rift basins overlapped north and south of the Basque massifs, i.e. across the trace of the supposed Pamplona fault. This overlapping geometry together with the WNW-ESE striking rift structures argue for a NNE-SSW direction of extension from Aptian to Cenomanian. As such, these results provide new kinematic constraints for the displacement of the Iberian plate with respect to Eurasia at mid-Cretaceous and undermine the role of the North Pyrenean Fault for this time laps. Geological cross-sections across the Basque-Cantabrian basin also show that the mid-Cretaceous rifting event reactivated Late Jurassic to Barremian structures, highlighting the role of inheritance for the initiation of the deformation. This study raises the role of the Upper Triassic evaporites, acting as a decoupling horizon between the supra-salt sedimentary cover (thin-skinned deformation) and the crust (thick-skinned deformation) during the syn-rift and syn-orogenic evolution. In the Basque-Cantabrian basin, this decoupling horizon allowed to transport the sedimentary cover of the former exhumed mantle domain (“Nappe des Marbres”) over the Basque massifs via the reactivated Leiza fault. Finally, this study highlights the allochthony of the Basque massifs with respect to the proximal margins of the former basins that are the present-day Aquitaine and Ebro foreland basins via south-dipping and north-dipping crustal thrust faults, respectively. The Basque massifs overlain a north-dipping subducted slab composed of the former hyperextended crustal domain of the Basque-Cantabrian system. As such, despite a complex pre-orogenic framework, the final orogenic architecture of the Pyrenean-Cantabrian junction depicts a wide crustal wedge, corresponding to the Basque massifs, overlying a north-dipping slab such as described in the Pyrenean and Cantabrian ranges.

The second chapter deals with the mode of reactivation of the Cantabrian and Pyrenean rift segments and their lateral termination north and south of the Basque massifs. This study shows how inheritance and rift segmentation influence the evolution and the architecture of orogenic systems. A map of the rift domains (proximal, necking and hyperextended) have been performed across the study area together with present-day and restored N-S cross-sections, allowing to characterise newly formed and reactivated structures at both rift segments and rift segment boundaries. Moreover, the temporal and spatial evolution of rift domains and their role for the orogenic evolution have been studied in both 2D sections and 3D (map and sections). Particular attention has been paid on the mode of deformation of the rift domains with respect to

the coupling point located between the brittle hyperextended domain (coupled) and the proximal and necking domains where ductile lower crust remains (decoupled).

Results show that two different phases can be defined at rift segments during the convergence : a subduction (or underthrusting) phase from Santonian to Late Palaeocene, and a collisional phase from Eocene to Miocene. Only few evidences from the subduction phase have been recorded in the Pyrenean-Cantabrian system as this phase corresponds to the underthrusting of the hyperextended domain and to the pop-up of the sedimentary cover via the reactivation of the Upper Triassic decoupling horizon (thin-skinned deformation). The collisional phase initiates when the conjugate necking domains (landward of the coupling point) meet and corresponds to the formation of basement-involved thrust faults such as the Gavarnie and Guarga imbricate thrusts (thick-skinned deformation). The Pyrenean-Cantabrian junction shows a distinct evolution in comparison to rift segments, characterised by the formation of thick-skinned structures and the development of a proto-crustal wedge during the subduction phase. These new thrust faults, such as the north-dipping Roncesvalles fault and the south-dipping North Pyrenean Frontal Thrust, transfer the deformation at the termination of the rift segments and shortcut unstretched crustal domains. The formation of a proto-crustal wedge in the Basque massifs already during the subduction phase could be responsible for the preservation of pre-Alpine structures and the emplacement of subcontinental mantle at crustal level at the Pyrenean-Cantabrian junction. The collisional phase corresponds to the formation of an orogenic wedge composed by the Basque massifs overlying a north-dipping subducting slab corresponding to the hyperextended to proximal domains of the Ebro block. As such, the final orogenic architecture from the Central Pyrenean segment to the Cantabrian segment appears cylindrical at a first order despite the strongly segmented pre-orogenic architecture. Finally, this study shows that the subduction phase is strongly influenced by rift inheritance, whereas the collisional phase is mainly controlled by orogenic processes.

The third chapter deals with the thermal evolution of asymmetric rift systems where an upper and a lower plate develop with respect to the active detachment fault. The aim is to better characterise the role of asymmetric hyperextension on the thermal evolution and the first order thermal architecture of rift basins. As such, a thermo-mechanical model of asymmetric rifting has been performed in collaboration with Dr Sascha Brune (University of Potsdam). Top basement heat flow values have been extracted from the model at different times and different locations. Besides, the description of the Arzacq-Mauléon rift system allows to restore the basin at syn-rift stage and to define the polarity (upper-lower plate) of the system. Vitrinite reflectance data (proxy for T_{\max}) from boreholes can be replaced and permit to determine the first order thermal architecture of the basin with respect to the rift polarity.

Observations from the Arzacq-Mauléon rift system shows a strong structural asymmetry during rifting with a lower plate toward the south and an upper plate toward the north. This structural asymmetry appears to be related with a thermal asymmetry as attested by the occurrence of the highest temperatures at the transition between the upper and the lower plate. The numerical model reveals a strong asymmetry of the maximum heat flow, which is always located at the upper-lower plate transition despite rift migration. As such, the thermal asymmetry observed in the Mauléon basin can be explained by the structural asymmetry during hyperextension. Furthermore, the numerical model shows that rift migration towards the upper plate leads to the formation of extensional allochthons which migrate from the upper to the lower plate during hyperextension. As a consequence, the maximum heat flow is diachronous for each extensional allochthons, suggesting that measured peak temperatures can be diachronous within the basins and that they may have recorded a transient and punctual thermal event in relation with the upper-lower plate transition. Such a complex spatial and temporal evolution of heat flow and T_{\max} is generally not considered in thermal models of rift basins. Yet, it can potentially lead to the juxtaposition of T_{\max} that are related with different thermal events and to the determination of erroneous paleo-thermal gradients. Finally, this study shows that the β -dependent (crustal thickness) thermal model of McKenzie (1978) cannot apply to asymmetric hyperextended rift systems.

The results of this PhD thesis highlight a new approach on the processes occurring during a Wilson cycle. The syn-rift thermal evolution appears to be dependent on the mode of lithospheric deformation and might influence the style and the location of deformation during the subsequent reactivation. Moreover, the role of rift-inheritance on the reactivation is generally defined via 2D cross-sections. Yet, the variations of the 3D inherited architecture can strongly influence the reactivation pattern and eventually the local orogenic architecture. Such results should be tested in analogue orogenic systems where the architecture cannot be solely explained by orogenic processes.

RÉSUMÉ ÉTENDU

Les phénomènes responsables de la formation des océans et des chaînes de montagnes sont une part essentielle des recherches en sciences de la Terre. Les processus d'extension et de compression établis au cours du cycle de Wilson (1966) sont de plus en plus étudiés en tenant compte du concept d'héritage structural. Ce dernier contrôlerait l'emplacement et le mode de déformation au cours de ces processus par la réactivation et l'inversion des structures mises en place lors des précédents événements tectoniques. Lors du rifting et avant la mise en place d'une croûte océanique, une importante asymétrie structurale et thermique de la lithosphère a été établie par les travaux récents. Elle peut mener à l'exhumation du manteau sous-continentale associée à un métamorphisme de haute température du bassin sédimentaire sus-jacent. Le style de déformation et l'architecture crustale peuvent alors considérablement varier le long de l'axe du rift, notamment au niveau de zones de transfert. Cette architecture tridimensionnelle héritée des systèmes de rift représente l'état initial sur lequel la réactivation va s'initier lors du prochain événement tectonique.

Ainsi, trois questions se dégagent :

- *Comment l'architecture du rift contrôle l'évolution orogénique ?*
- *Comment la segmentation syn-rift influence la réactivation et l'architecture orogénique ?*
- *Quelle est l'évolution thermique dans les systèmes hyper-étirés asymétriques ?*

La cordillère pyrénéo-cantabrique représente un lieu d'étude propice pour aborder ces thématiques car elle résulte de l'inversion de bassins de rifts mésozoïques fortement segmentés lors de l'orogénèse alpine tardi-crétacée à miocène. Ces systèmes de rifts hyper-étirés ont conduit au Crétacé à l'exhumation du manteau en fond de bassin ainsi qu'à un métamorphisme de haute température/basse pression qui a affecté les séries pré- et syn-rift décollées. De plus, la faible déformation compressive alpine a permis de préserver, à terre, la couverture sédimentaire ainsi que certaines relations socle-couverture associées à l'épisode d'extension. Enfin, les nombreux projets académiques ainsi que les campagnes d'explorations pétrolières ont fourni un grand nombre de données sur la géologie de surface et profonde de cette région.

Le premier objectif de cette étude est de déterminer l'architecture 3D de la jonction pyrénéo-cantabrique qui résulte de l'inversion d'un système de rift segmenté. Le deuxième objectif est d'étudier sa réactivation afin de déterminer le rôle de l'héritage associé à l'épisode d'extension et l'évolution structurale associés à ces systèmes segmentés. Enfin, le troisième objectif est d'analyser l'évolution thermique associée aux rifts asymétriques pauvres en magma à l'aide d'un modèle numérique thermomécanique et des données sur l'analogie nord pyrénéen.

Le premier chapitre concerne l'architecture actuelle de la chaîne dans le Pays Basque où se situe la jonction entre le bassin de Mauléon (segment pyrénéen) et le bassin Basque-Cantabre (segment cantabrique). Il s'agit notamment de vérifier l'existence ou non de la faille transformante de Pampelune qui découplerait à l'échelle lithosphérique la déformation entre les deux segments le long d'un axe NNE-SSO. En effet, bien que généralement mentionnée dans la littérature par le biais d'observations indirectes, aucune étude n'a permis d'identifier cette structure ou de définir son rôle pour l'évolution du système pyrénéo-cantabrique. L'objectif est également d'apporter des contraintes de terrain à la cinématique entre la plaque Ibérique et la plaque Eurasienne au Mésozoïque et pour laquelle plusieurs modèles s'affrontent et restent largement débattus puisqu'ils sont principalement définis à partir d'anomalies magnétiques en mer à l'origine controversée. Pour cela, des coupes géologiques N-S et E-O ont été effectuées dans la zone d'étude en couplant les données de terrain, l'interprétation de lignes sismiques et les données de puits. Elles permettent de caractériser et de réinterpréter l'architecture 3D de ce domaine en y intégrant les concepts récemment développés dans les Pyrénées. Cette première étude a été réalisée en collaboration avec Josep Anton Muñoz (Universitat de Barcelona) concernant notamment l'interprétation de quelques lignes sismiques ainsi que deux jours de campagne de terrain.

Les résultats montrent que le bassin de Mauléon se propage vers l'ouest dans le bassin de St-Jean-de-Luz, au-delà de la faille supposée de Pampelune, tandis que le bassin Basque-Cantabre se propage vers l'est, au sud du massif des Aldudes. Ainsi, cette architecture infirme l'existence d'une faille majeure N-S, dite de Pampelune, à la limite entre les deux systèmes de rifts. Au contraire, elle suggère qu'au Crétacé moyen les bassins E-O se propagent et se superposent au nord et au sud des massifs basques. Cette géométrie des bassins de rift ainsi que les orientations des structures extensives syn-rift ONO-ESE vont dans le sens d'une direction d'extension NNE-SSO de l'Aptien au Cénomani. Ainsi, ces résultats imposent de nouvelles contraintes cinématiques pour le mouvement de la plaque Ibérique (ou le bloc de l'Èbre) vis-à-vis de la plaque Eurasienne au Crétacé moyen et minimisent le rôle décrochant de la Faille Nord Pyrénéenne. Les coupes à travers le bassin Basque-Cantabre montrent également que le rift crétacé moyen a réactivé des structures d'âge tardi-jurassique à crétacé inférieur, mettant en évidence le rôle de l'héritage pour l'initiation de la déformation. Cette étude souligne le rôle du sel triasique pour l'évolution syn-rift et orogénique, agissant comme une surface de découplage majeure entre la couverture sédimentaire (« thin-skinned ») et la déformation crustale (« thick-skinned ») (Fig. Résumé-1). En effet, les résultats montrent que la couverture sédimentaire du bassin Basque-Cantabre, détachée sur le sel triasique, est fortement allochtone (>20km de déplacement le long de la faille de Leiza) et recouvre vers le nord et le sud les massifs

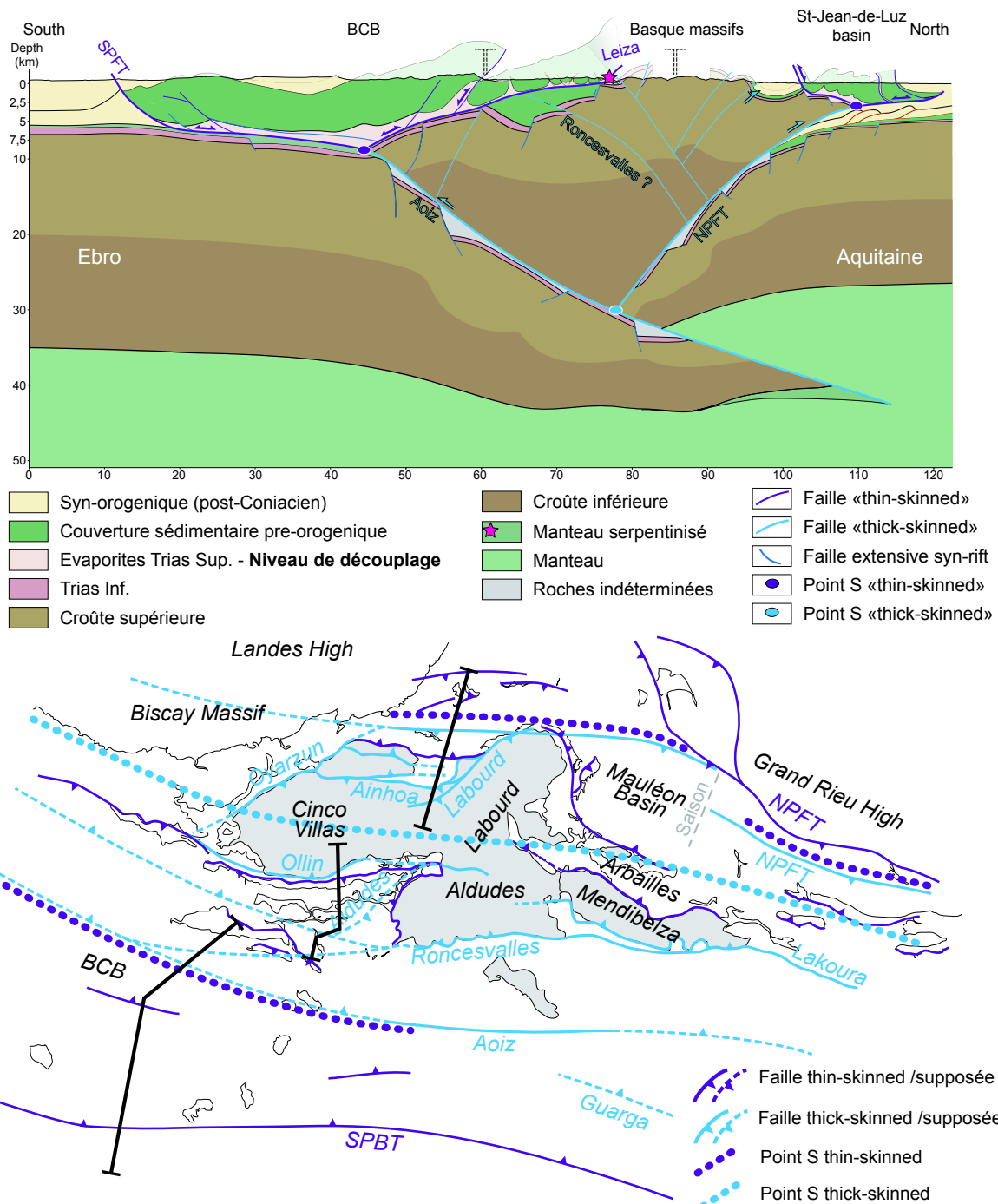


Fig. Résumé-1: Coupe nord-sud équilibrée et carte structurale simplifiée de la jonction entre le segment pyrénéen et le segment cantabrique (Pays Basque). Les deux bassins de rift (Basque-Cantabre et Mauléon/St-Jean-de-Luz) se superposent au nord et au sud des massifs basques (en gris). Ces derniers forment un prisme orogénique au-dessus de la croûte d'affinité ibérique sous-charriée vers le nord. L'architecture actuelle résulte du découplage entre la déformation « thin-skinned » (violet) affectant la couverture sédimentaire, et la déformation « thick-skinned » (bleu) affectant la croûte. Ainsi, les bassins de rift crétaqués détachés sur le sel triasique sont fortement allochtones sur les bassins d'avant-pays de l'Èbre et d'Aquitaine, ainsi que sur les massifs basques.

basques et le bassin d'avant-pays de l'Èbre, respectivement. De façon similaire, la couverture sédimentaire décollée du bassin de St-Jean-de-Luz est transportée sur le bassin d'avant-pays aquitain. D'un point de vue crustal, la partie sud des massifs basques présente majoritairement des chevauchements à vergence sud tandis que la partie nord montre des structures à vergence nord, le long desquels un fort taux de raccourcissement est déduit à partir des coupes géologiques. Ceci met en évidence l'allochtonie des massifs basques sur les domaines proximaux des marges d'Aquitaine et de l'Èbre par des structures crustales à pendage nord et sud, respectivement, au-dessus d'un sous-charriage à vergence nord correspondant aux domaines crustaux hyper-étirés. L'architecture orogénique de la jonction pyrénéo-cantabrique correspond donc à un prisme crustal associé à une subduction à pendage nord (Fig. Résumé-1) tel que décrit au centre de la chaîne, et ce malgré une architecture pré-orogénique complexe.

Le deuxième chapitre concerne l'étude du mode de réactivation des segments de rift pyrénéen et cantabrique en les comparant à leur terminaison où il se superposent de part et d'autre des massifs basques. Cette étude tente de répondre à la question du rôle de l'héritage associée à l'épisode de rifting sur l'évolution orogénique, et plus spécifiquement à l'influence de la segmentation sur la réactivation, la formation et la propagation latérale des structures lors de l'inversion. Cette partie illustre ainsi le rôle de l'héritage associé à la segmentation et aux domaines de rifts sur l'évolution et l'architecture d'un prisme orogénique. L'établissement d'une carte des domaines de rifts (proximal, necking/étranglement et hyper-étiré) à partir des résultats du premier chapitre, ainsi que de coupes N-S actuelles et restaurées à travers la zone, permettent de caractériser les structures néoformées ou réactivées à l'intérieur des segments et à la limite entre les segments de rifts. L'évolution temporelle et spatiale des domaines de rift et leur rôle lors de la convergence a été établie en représentation 2D (coupes) ainsi qu'en 3D. Une attention particulière est portée sur le mode de déformation des domaines de rifts en fonction de leur position par rapport au point de couplage situé entre le domaine cassant hyper-étiré (couplé) et le domaine de necking où la croûte inférieure est ductile (découplé).

Les résultats montrent que deux phases distinctes peuvent être observées dans les segments de rift (c.à.d. à distance des zones segmentées) lors de la convergence : une phase de sous-charriage (ou subduction) du Santonien à la fin du Paléocène, et une phase de collision de l'Éocène au Miocène. Peu d'évidences de la phase de sous-charriage sont enregistrées dans le système pyrénéo-cantabrique puisque cette phase correspond à la subduction du domaine hyper-étiré et la remontée de la couverture sédimentaire par la réactivation de la surface de décollement triasique (« thin-skinned »). La phase de collision s'installe lorsque les domaines de necking se rencontrent et forment les premiers chevauchements impliquant la croûte (« thick-skinned ») représentés par les nappes imbriquées de Gavarnie et Guarga. La terminaison des

segments de rift (c.à.d. où les segments de rift se superposent) montre une évolution distincte marquée par la formation de failles chevauchantes crustales et la formation d'un proto-prisme orogénique dès la phase de sous-charriage (Crétacé Supérieur à Paléocène). Ces failles, dont l'orientation varie de ONO-ESE à E-O autour des massifs basques (Fig. Résumé-2), relaient la déformation associée à la fermeture des bassins en recoupant les domaines non étirés, formant ainsi de nouvelles structures chevauchantes à pendage sud (Front de Chevauchement Nord Pyrénéen) à la terminaison du segment pyrénéen et à pendage nord (faille de Roncesvalles) à la terminaison du segment cantabrique. La formation du prisme cristallin dès l'initiation de la réactivation serait responsable de la préservation des structures pré-alpines à l'ouest de la faille de transfert du Saison, tels que les détachements Sud et Nord Mauléon et le bassin permien de Bidarray, ainsi que de la mise en place dans la croûte du manteau sous-continentale tel qu'observé en tomographie sismique. La phase de collision s'exprime par la formation d'un

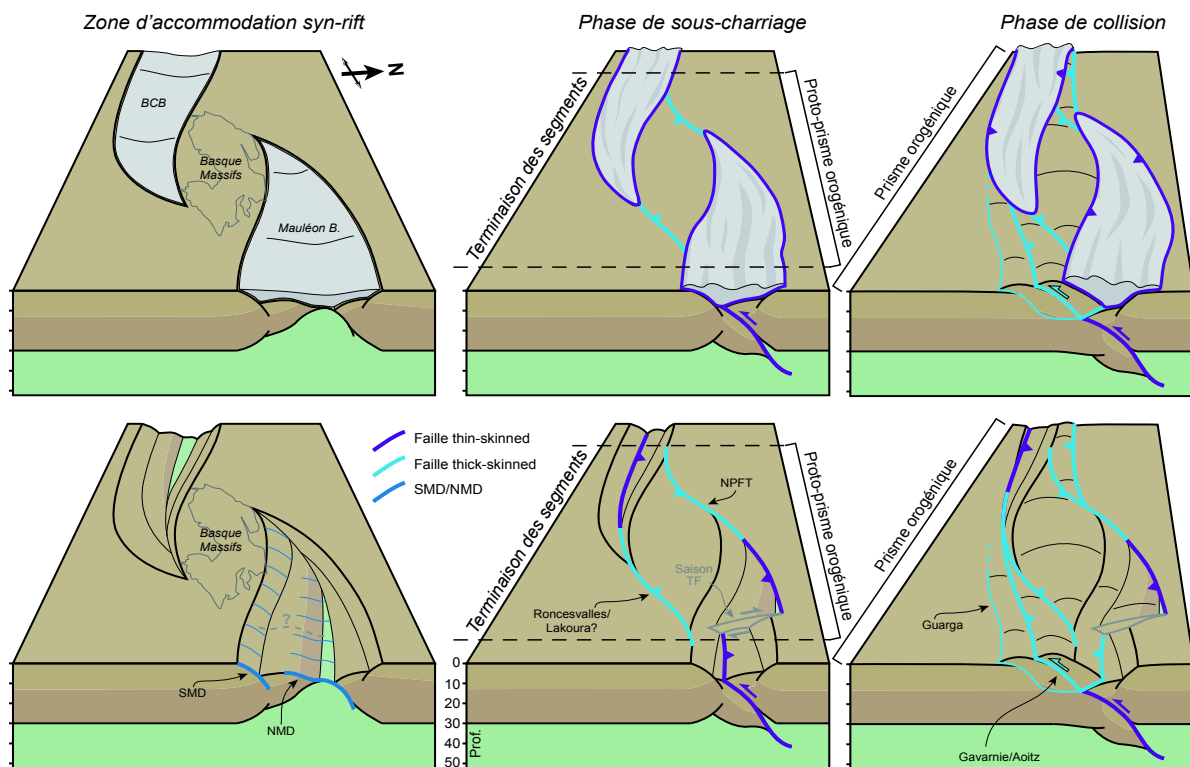


Fig. Résumé-2: Blocs 3D représentant l'évolution des segments de rift pyrénéen et cantabre lors de la convergence. L'évolution avec (haut) et sans (bas) la couverture sédimentaire supra-salifère est représentée. Deux évolutions distinctes ont été reconnues lors de la phase de sous-charriage entre les segments de rift et leur terminaison (massifs basques). Les domaines hyper-étirés sont sous-charriés vers le nord dans les segments de rift où la déformation « thin-skinned » domine, tandis qu'un proto-prisme orogénique se forme à la terminaison des segments, associé à la formation des structures « thick-skinned » néoformées de Roncesvalles et du NPFT. Ce proto-prisme orogénique est responsable de la mise en place du corps mantellique à un niveau crustal sous le bassin ouest-Mauléon ainsi que de la préservation des structures syn-rifts dans les massifs basques (SMD, NMD). La phase de collision se distingue par la formation d'un prisme orogénique et d'un sous-charriage à vergence nord de façon cylindrique à travers le système pyrénéo-cantabrique.

prisme orogénique composé des massifs Basques au-dessus d'un sous-charriage à vergence nord formé par les domaines hyper-étirés à proximaux du bloc de l'Èbre. L'architecture finale, du segment central Pyrénéen au segment Cantabrique, apparaît alors comme cylindrique au premier ordre, et cela malgré l'héritage très segmenté du système de rift. Enfin, cette étude montre que la phase de sous-charriage est fortement guidée par l'héritage de rift, tandis que la phase de collision est principalement contrôlée par les structures orogéniques néoformées.

Le troisième chapitre porte sur l'étude de l'évolution thermique associée à un système de rift asymétrique où se développent une plaque supérieure et une plaque inférieure vis-à-vis de la faille de détachement active. La migration de la déformation dite « en-séquence » va entraîner le développement d'un rift structuralement asymétrique, et est responsable de la formation d'allochtones extensifs qui vont migrer de la plaque supérieure à la plaque inférieure pendant l'hyper-étirement. Cette partie tente de répondre à la question de l'influence de l'asymétrie lithosphérique pour l'évolution thermique d'un système de rift hyper-étiré. L'objectif est de mieux caractériser le rôle de la déformation sur l'évolution et l'architecture thermique de premier ordre des systèmes hyper-étirés en utilisant un modèle numérique de rift asymétrique ainsi que l'analogie du bassin de Mauléon (Pyrénées occidentales). Ainsi, le modèle numérique thermomécanique de rift asymétrique a été élaboré en collaboration avec Dr Sascha Brune (Université de Potsdam). De ce modèle, les valeurs de flux de chaleur dans le toit du socle ont été extraites à différents endroits et à différents stades (Fig. Résumé-3). En parallèle, la description de l'évolution structurale et sédimentaire associée à l'ouverture du bassin de Mauléon permet d'identifier la polarité du système, auquel sont apposées les données de pouvoir réflecteur de la vitrinite (indicateur du pic de température) mesurées dans quatre puits du bassin. Ces données permettent de déterminer l'architecture thermique de premier ordre du bassin de Mauléon et de la comparer à la polarité du système.

Dans le système fossile ouest pyrénéen, les résultats indiquent une forte asymétrie structurale syn-rift avec une plaque inférieure au sud et une plaque supérieure au nord. Cette asymétrie structurale est combinée à une asymétrie thermique. En effet, l'analyse de la distribution des valeurs de vitrinite montre une augmentation générale de la température pour les mêmes unités sédimentaires du sud (puit d'Ainhice) vers le nord (puit Les Cassières 2) du bassin puis une forte diminution des valeurs au nord, sur l'unité du Grand Rieu. Les plus hautes températures ont été atteintes à la transition entre les plaques inférieure et supérieure (Les Cassières 2). Le modèle numérique met en évidence une forte asymétrie du flux de chaleur maximum qui se localise tout au long de l'évolution du modèle à la transition entre les plaques supérieure et inférieure malgré la migration de la déformation. L'asymétrie thermique observée dans le bassin de Mauléon peut alors s'expliquer par l'asymétrie du système lors de l'hyper-

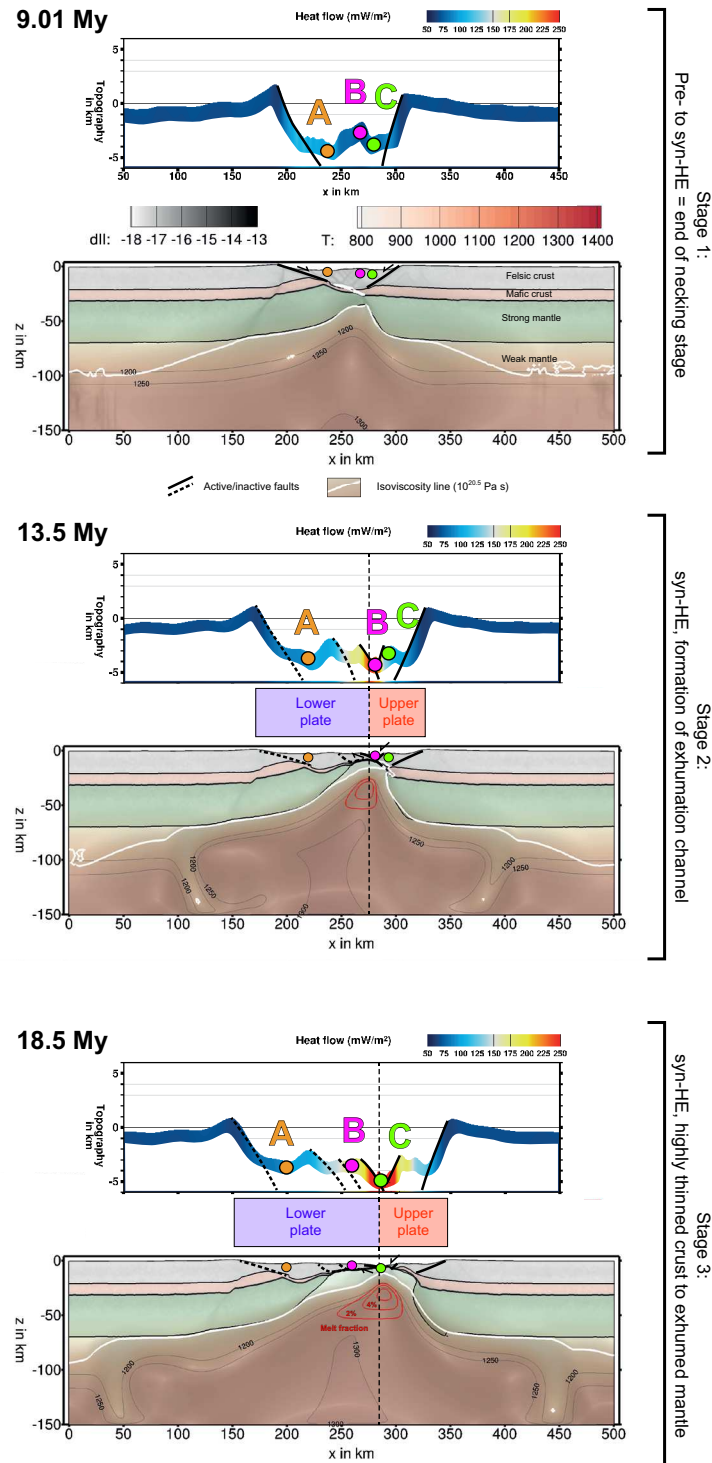


Fig. Résumé-3: Captures à différents stades (9,01 My ; 13,5 My ; 18,5 My) du modèle numérique représentant l'évolution d'un rift hyper-étiré asymétrique. La partie basse du modèle montre les différentes lithologies de la croûte et du manteau ainsi que le taux de déformation instantané en grisé tandis que la partie haute représente la topographie (attention à la différence d'échelle) et l'intensité du flux de chaleur dans le toit du socle. La ligne pointillée verticale délimite la plaque supérieure de la plaque inférieure. Les points A, B et C, correspondant à la position d'allochtones extensifs, permettent de suivre leur évolution dans le temps et dans l'espace. On remarque que chaque point va successivement migrer de la plaque supérieure à la plaque inférieure au cours du temps, et donc traverser la limite plaque inférieure-supérieure où les valeurs maximum de flux de chaleur restent localisées. Ceci montre l'asymétrie thermique ainsi que le diachronisme thermique pour chaque allochtone.

étirement. De plus, le modèle numérique montre que la migration de la déformation vers la plaque supérieure au cours de l'hyper-étirement entraîne la migration successive de blocs allochtones de la plaque supérieure vers la plaque inférieure, et l'évolution du flux de chaleur se révèle alors diachrone pour chaque bloc allochtone (Fig. Résumé-3). Ces résultats suggèrent que les pics de températures mesurés dans les bassins peuvent être diachrones et qu'ils peuvent avoir enregistré un événement thermique ponctuel associé au passage des roches dans la zone de transition entre les plaques supérieure et inférieure (Fig. Résumé-4). Sur la plaque inférieure, où l'intensité du flux de chaleur est plus faible, des sédiments peuvent se déposer au-dessus de ces allochtones et vont enregistrer des T_{max} qui seront principalement contrôlés par l'enfouissement (« burial ») et donc le taux de sédimentation. Une telle complexité spatiale et temporelle des flux de chaleur et des pics de températures n'est généralement pas prise en compte dans les

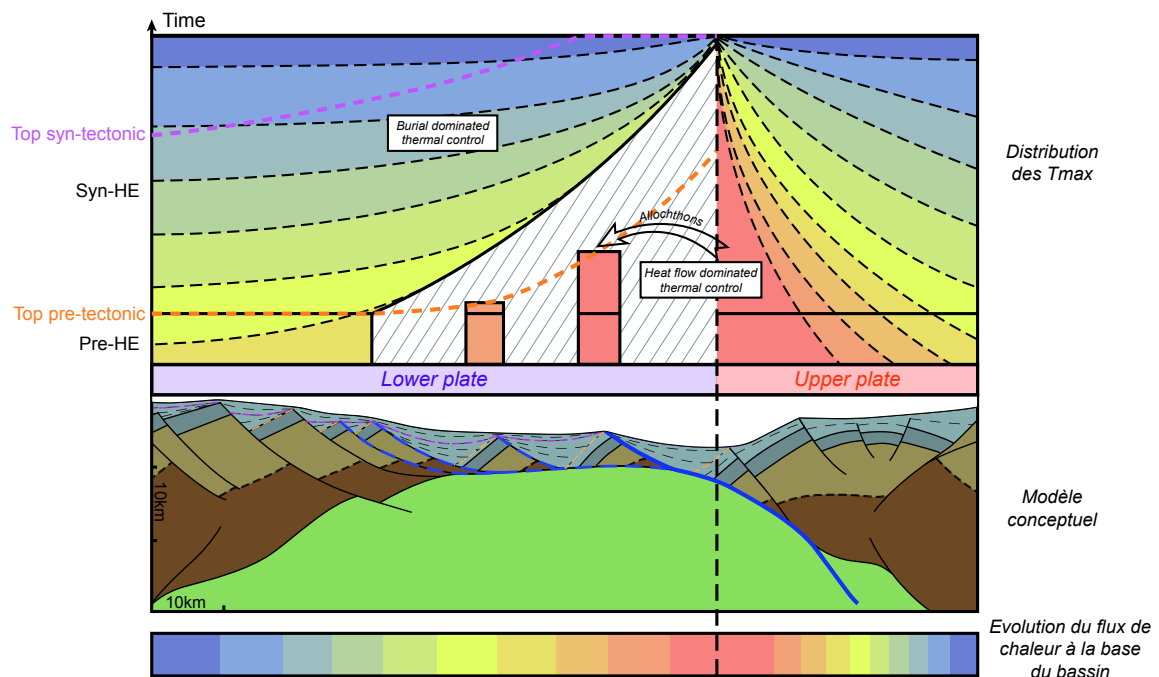


Fig. Résumé-4: Évolution thermique premier-ordre d'un système de rift hyper-étiré asymétrique. Au centre : modèle conceptuel de l'architecture des domaines distaux d'un rift asymétrique lors de l'hyper-étirement. En bas : distribution relative de l'intensité du flux de chaleur lors de l'hyper-étirement tel qu'extrait du modèle numérique. En haut : distribution supposée des T_{max} dans le bassin. Les résultats du modèle numérique montrent que les valeurs maximum de flux de chaleur dans le toit du socle restent localisées à la transition entre la plaque inférieure et supérieure pendant l'hyper-étirement. Ceci suggère, dans un modèle de bassin simplifié, que les valeurs maximum de T_{max} dans la pile sédimentaire pendant l'hyper-étirement sont également enregistrées à la transition entre la plaque supérieure et inférieure. La migration d'allochtones extensifs de la plaque supérieure à inférieure telle qu'observée dans le modèle numérique suggère que les valeurs de T_{max} sur la plaque inférieure peuvent être diachrones et allochtones. Ainsi, deux histoires thermiques pourraient être enregistrées dans ce type de bassin : un événement associé au flux de chaleur très élevé et localisé à la transition plaque supérieure-inférieure, éventuellement diachrone et allochtone ; et un événement thermique, synchrone et autochtone, distribué à l'échelle du bassin correspondant à l'enfouissement (« burial ») et donc principalement contrôlé par le taux de sédimentation.

modèles thermiques de bassins, or elle peut mener à la juxtaposition de T_{max} associés à différents évènements thermiques et à la détermination de gradients thermiques erronés. Enfin, cette étude montre que le modèle d'évolution thermique dépendant de l'épaisseur crustale proposé par McKenzie (1978) ne s'applique pas dans ces systèmes asymétriques.

En conclusion, les résultats de ces travaux de doctorat proposent une nouvelle approche des processus opérant au cours d'un cycle de Wilson. L'évolution thermique pendant le rifting est dépendante du mode de déformation et peut fortement influencer l'architecture thermique des bassins sédimentaires, notamment en juxtaposant des événements thermiques diachrones et allochtones. De plus, elle pourrait influencer le mode et la localisation de la déformation lors de la réactivation. Le rôle de l'héritage associé à l'épisode de rifting sur l'architecture orogénique est bien souvent considéré par l'analyse de coupes 2D. Cette étude montre que la segmentation syn-rift peut influencer la réactivation, notamment par le biais de structures néoformées qui vont accommoder le transfert de la déformation et contrôler localement l'évolution orogénique. Cette évolution latérale de la déformation induite par l'héritage pourrait expliquer certaines anomalies lithologique ou structurales observées dans les orogènes. De tels résultats doivent évidemment être testés sur différents analogues structuraux où l'architecture orogénique peut difficilement être expliquée par les processus orogéniques seuls.

Le **chapitre I** introduit et résume les principaux travaux scientifiques traitant de l'héritage, la réactivation, la segmentation des rifts et l'évolution thermique lors de l'extension lithosphérique. Dans un second temps, les résultats majeurs ainsi que les questions concernant l'évolution du système pyrénéo-cantabrique sont présentées, suivies des principales questions développées dans ce manuscrit. Les **chapitres II, III et IV** correspondent aux publications scientifiques associées à ces questions.

Le **chapitre II** étudie l'architecture de la jonction entre les segments Pyrénées et Cantabre et présente une nouvelle interprétation structurale et cinématique de l'ouverture des bassins de rift au Crétacé moyen. Ce travail, intitulé « *Nature, origin and evolution of the Pyrenean-Cantabrian junction* », va être soumis au journal *International Journal of Earth Sciences*.

Le **chapitre III** explore le rôle de l'héritage et de la segmentation associés à l'épisode de rifting pour l'évolution orogénique du système pyrénéo-cantabrique. De plus, il étudie le rôle des domaines de rift sur le style de déformation lors de la réactivation et l'influence de la segmentation sur l'architecture orogénique finale. Il fera l'objet d'une publication pour *Tectonics* avec pour titre « *Role of rift-inheritance and segmentation for orogenic architecture : example from the Pyrenean-Cantabrian system* ».

Le **chapitre IV** traite de l'évolution thermique des systèmes de rift hyper-étirés. Cette

étude combine les résultats d'un modèle numérique et des données du bassin de rift inversé de Mauléon afin de déterminer l'influence de l'asymétrie sur l'évolution thermique syn-rift. Ce travail a été soumis au journal *Geochemistry, Geophysics, Geosystems* sous le titre « *Thermal evolution of asymmetric hyperextended magma-poor rift systems : results from numerical modelling and Pyrenean field observations* ».

Le **chapitre V** résume les principaux résultats de ce travail de thèse et discute leurs implications pour l'évolution du système pyrénéo-cantabrique et pour les systèmes géologiques en général.

Un chapitre final recense les principales conclusions puis différentes perspectives émanantes de cette thèse sont énumérées. Enfin, les annexes se composent du matériel supplémentaire des chapitres II et IV, de différentes observations et coupes géologiques issues du travail de terrain, d'interprétations sismiques à travers le bassins Basque-Cantabre, de nouvelles descriptions et interprétations de la carotte d'Ainhice (bassin de Mauléon), ainsi que des résultats préliminaires de la campagne de cartographie magnétique par drone dans le massif du Labourd.

ACKNOWLEDGEMENTS

3 ans ! Le temps nécessaire pour comprendre le fonctionnement de la recherche, mais aussi pour faire des rencontres professionnelles ou amicales dans ce petit monde du caillou. J'avais hâte d'écrire cette partie du manuscrit mais je me rends maintenant compte de la difficulté. D'abord parce que je veux remercier avec le plus de sincérité possible toutes les personnes qui ont contribué à cette réussite, et puis parce que ça signifie que toutes les choses inhérentes à la thèse prennent fin : l'insouciance, les discussions, les voyages, ainsi que la chance de pouvoir se tromper... (Welcome to the real world!).

Je tiens tout d'abord à remercier les membres du jury, les rapporteurs **Frédéric Mouthereau** et **Antonio Teixell**, ainsi que les examinateurs **Gabriela Fernández-Viejo**, **Claudio Rosenberg** (président du jury) et **Stefano Tavani** pour avoir accepté de relire mon manuscrit de thèse et pour la discussion lors de la soutenance. J'ai sincèrement apprécié la pertinence de vos questions et de vos remarques, mais aussi d'avoir reconnu positivement la méthodologie et le travail effectués pendant cette thèse. J'aurais aimé avoir plus régulièrement ce niveau de discussion au cours de ces 3 années, puisque la science n'a de sens et d'intérêt que si elle est débattue et partagée.

Je souhaite ensuite remercier mon directeur de thèse, **Gianreto Manatschal**, pour m'avoir donné l'opportunité de faire cette thèse et pour m'avoir encouragé à chaque étape. Malgré les difficultés de la thèse, je peux dire que j'ai fait « le sujet de mes rêves », de la façon dont je voulais le faire, et tout ça c'est grâce à toi. Je pense que mon côté « têtu » n'était pas toujours là où tu l'attendais, mais ça aura été pour toi l'opportunité d'étudier un nouveau caractère, et peut-être de rajouter un critère sur la psychologie de tes doctorants !

Ces remerciements s'adressent également à **Emmanuel Masini**, qui aura été à la fois le chef du projet OROGEN, mon responsable de Master 2, le principal soutien pour l'attribution de ma thèse et le précurseur de la plupart des idées et concepts développés pendant ces 3 années. Tu m'avais impressionné pendant mon stage de Master à Total par la quantité d'idées que tu pouvais sortir à la minute (il faut dire que tu peux dire beaucoup de choses en une minute), et je dois admettre que je suis toujours autant fasciné par ton instinct géologique ! J'espère que l'avenir nous donnera l'opportunité de retravailler ensemble. Plus personnellement, je n'oublierai pas ce que tu as fait pour moi lors de mon difficile passage à Pau au début de l'année 2017...

Plus généralement, je remercie les financeurs du projet OROGEN (Total, CNRS et BRGM) ainsi que les personnes en charge de cette nébuleuse : **Sylvain Calassou**, **Manu** (again), **Isabelle Thinon** et **Olivier Vidal**.

Parce que faire une thèse c'est aussi savoir s'entourer des meilleurs, je remercie **Julie Tugend** et **Benoît Petri** qui auront été des co-encadrants indispensables à différents moments de cette épopée. Julie, tu auras essuyé les plâtres pour la rédaction du premier article « low-angle fruit pas si low-angle » et tu auras été une oreille attentive à mes déboires de jeune chercheur. Benoît, parce que ta rigueur, tes conseils, tes corrections du manuscrit et ton soutien moral auront été de précieux alliés en cette fin de thèse (et même tes graffitis bien sentis) ! On en aura fait du chemin depuis cette excursion dans les Alpes il y a 7 ans, alors que j'étais étudiant en L3 et toi tout jeune doctorant, où tu m'avais (pas si) gentiment signifié que je devais arrêter de taper comme un débile sur un gros caillou. Depuis, j'ai appris à reconnaître des grenats...

Merci **Josep Anton Muñoz** pour avoir passé du temps avec moi sur le terrain ainsi qu'à Barcelone à discuter et réfléchir sur la fameuse faille de Pampelune. Cette rencontre a très probablement sauvé ma thèse. Je suis sincèrement honoré d'avoir bénéficié de ton expérience et de tes conseils, et j'ai conscience que je fais des envieux !

Merci également à **Sascha Brune** pour la collaboration sur le papier « thermicité », ainsi que pour ton optimisme sans faille (il paraît qu'un papier est plus cité lors de la 2^{ème} soumission. Et pour la 3^{ème} ?).

Les géologues pyrénéens peuvent être (parfois) difficiles à approcher... Heureusement, quelques rencontres m'ont permis de découvrir l'envers de cette façade, et pour ça je tiens à remercier **Eneko Iriarte**, **Arantxa Bodego**, **Mikel Lopez-Horgue** et **Michel de Saint Blanquat** qui ont accepté de partager leurs connaissances au détour de différents camps de terrain.

Que seraient l'université et la recherche sans les « personnes de l'ombre » qui œuvrent à leur bon développement, donc merci à **Betty**, **Didier**, **Dilek**, **Ghenima** et **Joëlle**.

Merci également aux permanents de l'IPGS-GéOLS pour leur accueil et leur sympathie : **Mathieu**, **Julia**, **Jeff**, **Dan**, **Anne-Marie**, **Philippe**, **Karel**, **Hubert**, **Marc** et **Marc**.

Au tour des amis, d'ici ou d'ailleurs, rencontrés au détour d'un caillou puis entretenus au côté d'une bière.

Merci aux KIU, compatriotes de Licence et de Master, et particulièrement à **Val**, **Davidou** (Bella), **M-E** (tu y seras 2 fois du coup), **Patoche**, **Joseph**, **Marc**, **Jerem'** (chouquette), **Jeremie**, **Alex** (Alvaro beer™), **Vincent** le normand, **Éléonore** (il manque pas quelqu'un ?), **Dan**, **Malwina** et **Liliane** pour votre accueil à mon arrivée en terre sainte alsacienne et pour ces belles années !

Une pensée pour les camarades géologues européens (*in varietate concordia*) rencontrés à Oslo pendant mon année de M1 Erasmus : **Lars**, **Thomas**, **Simone**, **Mari** et **Daniel**.

Ces 3 années dans le bureau 111 n'auraient pas eu la même saveur sans les compatriotes de labo, thésards et postdocs ainsi que leurs +1 respectifs, qui sont peu à peu devenus des amis. **Benoît**, qui aura été un compagnon infailible de déménagement (un petit canap' ?) et de terrain, même quand les voitures basques n'en font qu'à leur tête, et **Auréli**e, qui doit quelques fois désespérer quand le trio est réuni. **Michael**, et son beau sac Dora, avec qui on aura partagé le bureau (et souvent bien plus...). **Pauline**, parce que Pamplouse c'est la loose même en mag', et qu'on est quand même dans les petits papiers des renseignements généraux (je leur ai balancé mon numéro de sécu ?). Merci également à **Francis**, **Delphine** et **Kallio** pour ces bons moments et toutes les petites attentions lors de vos retours de vacances. La seule et unique dream-team Orogen composée de **Jordi** (my Catalan boy) et **Patricia**. Les italiens **Nicolo** (grandpa) et **Gianluca** (bello), **Marie-Eva** qui cherche encore ses dents, **Morgane** qui élève son cheval en Franche-Comté, **Médéric** qui fabrique des savons décroissant en préparant la révolution anarchiste dans le Doubs avec Méluche (j'ai tout mélangé ?), **Alexis** et **Pierre**, qui ont une conception bien à eux du foot, **Simon** (qu'il est beaaauuu), **Sonia**, on aura vécu cette fin de thèse sur les rotules ensemble ! **Bruno**, qui deviendra un jour secrétaire des finances de l'UMP (Union des Méthodes Potentielles), **Shahin**, **Pauline C**, qui aura assisté à la destruction de mon coccyx et de mes lunettes le long de la faille de Leiza, **Chao** (our king), **Roza**n, **Coralie**, à qui j'aurais squatté le bureau et le PC dans les derniers jours de rédaction, **Charlotte**, qui a rapporté un peu du sud dans le Grand Est, **Paul** (sud), qui a lui ramené le Béarn et les caisses de vins, **Jeannette**, qui ne m'a pas laissé mourir de faim un soir de décembre, et **Fred**, compagnon ch'ti et fidèle acolyte de Ste-Marie-aux-Mines. Il y a aussi les nouveaux prétendants au titre de docteur à qui je souhaite bon courage : **Pierre-Olivier**, qui écoute toujours un film, **Paul** (nord) l'incollable en blind test métal, **Flora** et **Antoine**. En dehors du labo, une pensée pour **Júlia** et **Oriol** pour ces bons moments à Pontresina !

Et puis il y a les amis alsaciens, étrangers aux cailloux mais soutiens indéfectibles quand même, qui ont assisté à la lente dégradation de mon état jusqu'au jour de soutenance ! Merci **Marie**, **Léa**, **Laurent**, **Guillaume** et **Géo**. Même loin de l'Alsace mais toujours présente dans l'esprit, une pensée pour la bande de l'internat : **Regou**, **Pierro**, **Cedou**, **Nico** et **Simoon** qui sont probablement étonnés de voir mon parcours depuis le lycée !

Je tiens à remercier sincèrement la famille de Pauline, ses parents **Claudine** et **Michel**, qui m'auront hébergé durant les premières semaines de ma thèse, ainsi que **Marie-Louise**, **Jean-Paul**, **Victorien**, **Jean-Michel** et **Pierre-Louis**, pour leur immense sympathie et leur aide durant toutes ces années.

Merci vielmol !

C'est également l'occasion de dire merci à ceux qui me soutiennent depuis mes premiers jours et à qui je dois tant, **ma mère, Paul, ma sœur, mes grands-parents, Darwin, Gaspar, Cannelle** (3 d'entre eux sont des chats mais je ne dis pas lesquels) et mes amis d'enfance qui sont devenus des frères par la force des choses, **Cyril et Loïc**.

Enfin, ces derniers mots vont à celle qui m'a supporté et encouragé pendant un certain nombre d'années, et particulièrement ces derniers mois. Merci **Pauline** pour tout.

TABLE OF CONTENTS

TABLE OF CONTENTS

| | |
|---|-----|
| AVANT-PROPOS | 7 |
| ABSTRACT | 9 |
| RÉSUMÉ ÉTENDU | 13 |
| ACKNOWLEDGEMENTS | 25 |
| TABLE OF CONTENTS | 31 |
| CHAPTER I: INTRODUCTION | 35 |
| 1. General introduction | 36 |
| 2. Concepts, processes and models | 38 |
| 3. The laboratory: the Pyrenean-Cantabrian mountain ranges | 46 |
| 4. Scientific questions | 66 |
| 5. Structure of the manuscript | 67 |
| CHAPTER II: NATURE, ORIGIN AND EVOLUTION OF THE PYRENEAN-CANTABRIAN JUNCTION | 71 |
| Abstract | 73 |
| 1. Introduction | 74 |
| 2. Geological setting | 76 |
| 3. Map description of the Cantabrian-Pyrenean junction | 84 |
| 4. Cross-sections and seismic interpretations | 86 |
| 5. Discussion | 100 |
| 6. Conclusion | 109 |
| CHAPTER III: ROLE OF RIFT-INHERITANCE AND SEGMENTATION FOR OROGENIC ARCHITECTURE | 111 |
| Abstract | 113 |
| 1. Introduction | 114 |
| 2. Generalities about the Pyrenees | 115 |
| 3. The Pyrenean-Cantabrian study case | 120 |
| 4. Discussion | 129 |
| 5. Conclusion | 136 |
| CHAPTER IV: THERMAL EVOLUTION OF ASYMMETRIC HYPEREXTENDED RIFT SYSTEMS | 139 |
| Key points | 141 |
| Abstract | 141 |
| 1. Introduction | 142 |
| 2. Asymmetric rifted margins: observations and concepts | 144 |
| 3. Numerical model of asymmetric rifting | 147 |
| 4. Fossil example of asymmetric rift: observations from the Arzacq-Mauléon basin | 152 |
| 5. Discussion | 160 |
| 6. Conclusions | 164 |
| Acknowledgments | 165 |

| | |
|---|-----|
| CHAPTER V: GENERAL DISCUSSION | 167 |
| 1. What is the present-day architecture of the Pyrenean-Cantabrian junction? | 170 |
| 2. What was the pre-convergence architecture of the Pyrenean-Cantabrian junction? | 170 |
| 3. How did reactivation proceed in the segmented Pyrenean-Cantabrian system? | 172 |
| 4. What is the thermal evolution during hyperextension? | 174 |
| 5. Kinematic implication for the Iberia-Eurasia plate boundary | 176 |
| 6. General implications | 177 |
| CONCLUSION | 181 |
| 1. Architecture of the Pyrenean-Cantabrian junction | 183 |
| 2. Reactivation of the Pyrenean and Cantabrian rift segment boundaries | 183 |
| 3. Thermal evolution of asymmetric hyperextended rift systems | 184 |
| OUTLOOKS | 187 |
| 1. Cantabrian-Pyrenean rift junction from seismic tomography | 189 |
| 2. Reactivation of overlapping rift systems from numerical modelling? | 189 |
| 3. Role of rift polarity on the Pyrenean orogenic architecture | 190 |
| 4. Geodynamic evolution of Iberia, Ebro and Eurasia during the Mesozoic | 190 |
| 5. Thermal state of rift systems prior to reactivation | 190 |
| 6. Crustal thinning during mid-Cretaceous rifting: What controlling factor? | 191 |
| REFERENCES | 193 |
| ANNEXES | 221 |
| 1. Matériel supplémentaire chapitre II | 223 |
| 2. Matériel supplémentaire chapitre IV | 224 |
| 3. Interprétations sismiques dans le bassin Basque-Cantabre | 240 |
| 4. Observations et coupes de terrain | 252 |
| 5. Rapport d'observation des carottes et cuttings du puit d'Ainhice | 256 |
| 6. Caractérisation structurale et pétrologique par la méthode magnétique | 258 |

CHAPTER I:
INTRODUCTION

1. GENERAL INTRODUCTION

The theory of plate tectonics was first suggested by Wegener in 1912 based mainly on geographical and paleontological observations. However, it required almost half a century to be accepted by the scientific community after scientific breakthroughs in geophysics that led to the identification of the oceanic magnetic anomalies and the understanding of seafloor spreading. Meanwhile, based on the recognition of marine paleo-faunas in mountain chains on both sides of the Atlantic ocean, Wilson (1966) proposed that oceans and orogens formed at the same location over repeated episodes. This gave birth to the so called “Wilson cycle”, which describes the tectonic evolution taking place during repeated cycles of divergence and convergence of tectonic plates. Later, Dewey & Bird (1970) recognised that orogenic systems result from the closure of oceanic domains and that parts of the latter can be preserved within mountain belts in ophiolites. The role of inheritance was already recognized by Suess et al. (1900) but the reactivation of rift basins was described much later (e.g. Ziegler, 1978). The application of these concepts to plate boundaries as well as the reactivation of rifted margins at the initiation of orogenic formation

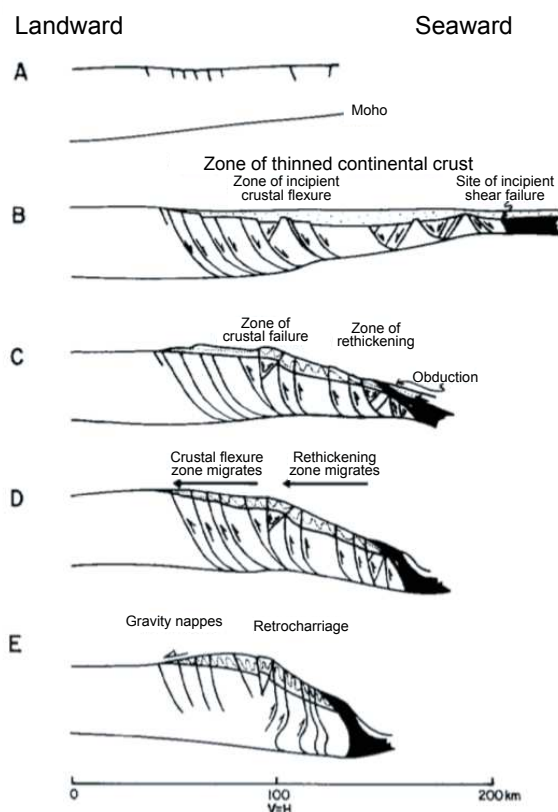


Figure I-1: Conceptual view of the formation and reactivation of a passive margin in the 80's (Cohen, 1982). Deformation during rifting was assumed to be solely controlled by high-angle listric normal faults cross-cutting the entire crust and leading to a sharp continent-ocean boundary. Tectonic inversion was governed by thick-skin tectonics via the reactivation of former normal faults.

emerged in the 80's from Cohen (1982) (Fig. I-1) and Jackson (1980). The last decades saw the development of analogue and numerical modelling that provided constraints on the physical parameters, geometry and kinematics occurring during extension or convergence (e.g. McClay, 1990). In these models, inheritance is often simplified to changes in the lithology/rheology of the layer-cake lithosphere or by adding a structural heterogeneity in the models (Fig. I-2; e.g. Bassi, 1991; Bassi et al., 1993; Corti et al., 2007; Mattioni et al., 2006; Pascal et al., 2002). However, observations from natural examples show that the processes/models presently developed cannot account for the along and across strike variability of final rift and orogenic architectures. As such, the initial condition prior to inversion might represent a substantial factor influencing the

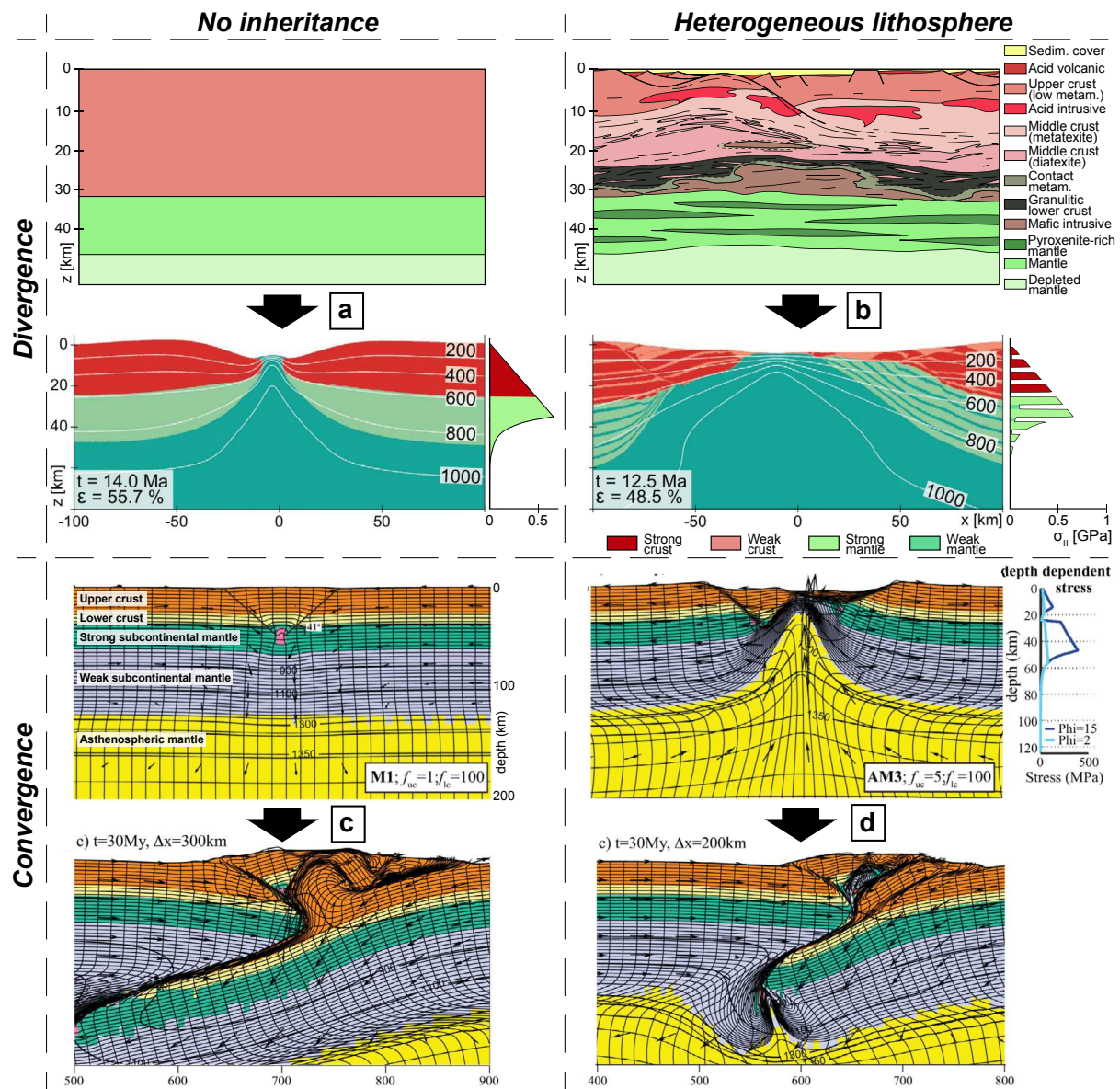


Figure I-2: Role of lithospheric inheritance for the architecture of rifted margins and collisional orogens based on numerical modelling experiments. Extensional models after Duretz et al. (2016) and contractional models after Jammes & Huisman (2012). Extensional models show the importance of pre-rift compositional architecture for rift evolution. In the scenario with an idealized brittle crust and upper mantle, the rift is abrupt and symmetrical (a), whereas for the heterogeneous lithosphere composed of ductile and brittle rheology, rift is wider and asymmetric (b). Contractional models highlight the influence of pre-convergence architecture for the orogenic evolution. In model (c) the collision initiates without inheritance (“contractional” model M3 with strong upper crust). The orogenic wedge is composed of crustal material. In model (d) the former rift system represents the pre-convergence initial condition (“accordion” model AM3 with strong upper crust). The orogenic wedge is composed of crustal and mantle rocks and involves nappe stacking in the pro-wedge. These models show that inheritance strongly affects the lithospheric evolution and the final architecture and as a consequence, it cannot be ignored in the study of natural examples.

Wilson cycle and more precisely the evolution between different tectonic phases.

In many aspects, the Pyrenean mountains represent a good natural laboratory to study processes active during a Wilson cycle as they preserve an entire cycle encompassing the Variscan orogeny, the Mesozoic rifting and the Pyrenean convergence. Yet, they also show the limitations of this theory, as the rifting did not form upon the Variscan suture, which is commonly assumed to be the weakest structure left behind from an orogen (e.g. Busch et al., 1997). Moreover, the structural and thermal evolution recorded in the Cantabrian-Pyrenean system depicts a 3D architecture that cannot be predicted from 2D models developed so far. The aim of this study is to use the Pyrenean and Cantabrian ranges as a natural laboratory to investigate the role of rift inheritance during compressional reactivation. More precisely, this study will investigate the thermal evolution associated with asymmetric rifting and the role of rift segmentation during inversion.

2. CONCEPTS, PROCESSES AND MODELS

2.1 Role of inheritance within the Wilson cycle: from historical concepts and physical models to observations

The concepts of the Wilson cycle and inheritance have been described in a few examples worldwide. Inheritance was first described by Suess et al. (1900) based on the similar direction of the post- and syn-Palaeozoic folds in the Paris basin. The modern vision in which reactivation nucleates on inherited structures of pre-structured domains was developed in the 80's based on the assumption that they correspond to weaknesses that are easier to reactivate than pristine domains. For example, reactivation of normal faults has been described in natural examples (e.g. Cohen, 1982; Gillcrist et al., 1987; Lowell, 1995) and in analogue models (Koopman et al., 1987), whilst at larger scale, Jackson (1980) proposed that most of the shortening prior to the formation of a mountain belt is accommodated by the reactivation of rift structures. Lindholm (1978) showed that compressional structures are preferentially inverted during rift initiation, especially if the structures strike perpendicular to the direction of extension (Doré et al., 1997; Ring, 1994).

However, the simple Wilson cycle template has been challenged by Krabbendam & Barr (2000), who demonstrated that about half of the Gondwana rifted margins localised parallel to former orogenic belts, whilst the other half developed obliquely to former orogenic domains.

These authors argued that orogenic systems do not necessarily correspond to the weakest domains. Indeed, orogenic belts might not be reactivated if they underwent magma-rich post-orogenic collapse, which leads to a strong mafic lower crust and a depleted subcontinental mantle (Chenin, 2016). Moreover, recent studies revealed further complexities to the concept of inheritance and showed that not only structures but every rheological variation may play a role during reactivation. This can include rock fabrics (Jammes & Lavier, 2019; Şengör, 2016; Şengör et al., 2018), inherited and not equilibrated temperature gradients or the composition of the lithosphere (Manatschal et al., 2015; Mouthereau et al., 2013; Petri et al., 2019). It shows that the initial conditions are fundamental in controlling the early stages of formation and evolution of subsequent tectonic episodes.

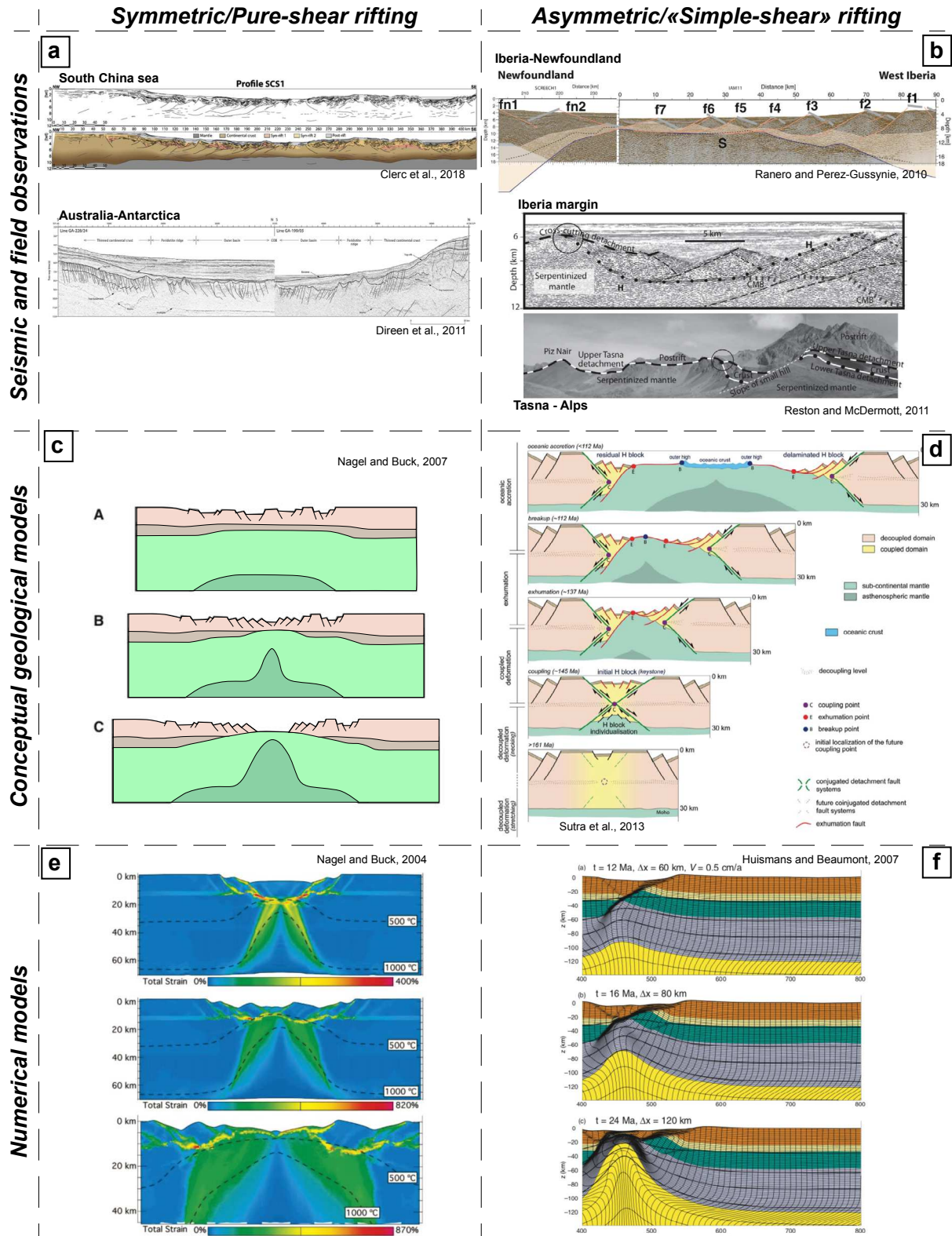
In extensional systems, former models of rifted margins depicted an abrupt continent-ocean boundary contrasting with recent models that involve a wide continent-ocean transition. This is particularly true for hyperextended, magma-poor margins which are characterised by exhumed subcontinental mantle and sparse magmatic intrusions (Boillot et al., 1987; Whitmarsh et al., 2001). Such contrasting models represent very different initial structural, thermal and compositional architectures that can influence the location and processes of reactivation during early convergence. In this manuscript, I will focus on how hyperextended rift systems develop (thermally and structurally), and how they might influence the formation and architecture of the subsequent collisional orogen. In light of the recent high quality seismic images (Ranero & Pérez-Gussinyé, 2010; Reston & McDermott, 2011), deep sea drilling campaigns (e.g. DSDP, ODP, IODP), numerical modelling (Huisman & Beaumont, 2014; Lavier & Manatschal, 2006) and observation of field analogues (Froitzheim & Eberli, 1990; Manatschal, 2004), the understanding of hyperextended rift systems significantly improved (Fig. I-3). Based on morpho-structural criteria, Sutra et al. (2013) defined rift domains. Tugend et al. (2014) showed that the limits of these rift domains are often the locus of reactivation during tectonic inversion. In particular, the exhumed serpentinitized mantle (Boillot et al., 1987) has been shown to represent a weak surface along which reactivation may initiate (Erdős et al., 2014; Lundin & Doré, 2011; Péron-Pinvidic et al., 2008; Reston & Manatschal, 2011), while the transition from the thin (<10km) to thick (>10km) crust (necking domain) has been proposed to act as a buttress where continental collision initiates (Mohn et al., 2014; Tugend et al., 2014).

In the Pyrenean-Cantabrian laboratory, a prominent mid-Cretaceous rift system has been shown to reach hyperextension and exhumation of subcontinental mantle coeval to HT/LP metamorphism (Clerc et al., 2015; Lagabrielle et al., 2010). This system never reached oceanic accretion, as it was reactivated shortly after the end of rifting. Therefore, it represents an ideal laboratory to investigate some of the processes controlling the Wilson cycle and the role of rift

domains and their boundaries during subsequent reactivation.

In this manuscript, I will address the following questions:

- Do rift domains influence the mode of deformation during reactivation?
- May the importance of rift inheritance vary during an orogenic cycle?



2.2 Segmentation: from a 2D towards a 3D vision of tectonic systems

Most of the tectonic concepts describing compression or extension have been developed in 2D systems (x-z cross-section plus time) whereas the 3D architecture (x-y-z plus time) of these systems remains ill-constrained. Segmentation is observed in orthogonal (extension/compression) and in oblique (transtension/transpression) settings (Sanderson & Marchini, 1984; Withjack & Jamison, 1986). In the latter, the direction of extension/convergence is oblique to the rift/orogen axis and favour along-strike transfer of deformation (e.g. McClay & White, 1995) via transfer zones, accommodation zones, or transform faults. Transfer zones were first described in compressional systems related to *en-échelon* faulting (Dahlstrom, 1969) or via lateral ramps. Transfer faults in extensional systems were defined in the 80's as “complex rotational, synthetic dip and strike-slip components allowing the extension to transfer style and activity along the graben” (Gibbs, 1984), and sometimes associated with a change of the dip of the faults (e.g. Lister et al., 1986). In extensional systems, transfer zones often refer to orthogonal or oblique extension accommodated by a set of relay ramps or transfer faults (Gawthorpe & Hurst, 1993), the latter striking parallel or oblique to the direction of extension and allowing to transfer strain across and between faults (Fossen, 2016). Transform faults were mainly described in oceanic domains to delimit segments at the spreading ridge (Wilson, 1965), even though they were generally extended to intra-continental strike-slip faults (Chorowicz, 1989). Accommodation zones (Fig. I-4; Chorowicz, 1989; Faulds & Varga, 1998; Reynolds & Rosendahl, 1984) were described as domains of overlapping faults or rift segment terminations linked by relay ramps (Childs et al., 1995; Morley et al., 1990; Peacock & Sanderson, 1991). In all these cases, the control of earlier structural anisotropy or suture zones (inheritance) on the initiation and geometry of these structures was suggested.

Since then, major outcomes emerged from analogue sandbox models (e.g. Acocella et al., 2005; Allken et al., 2012, 2013; Le Calvez & Vendeville, 2002) and more recently from numerical models (e.g. Le Pourhiet et al., 2017; Zwaan et al., 2016). In compressional systems, transfer zones have been shown to form in relation with variation of boundary

Figure I-3: Comparison of symmetric and asymmetric rifting. (a) Seismic interpretations in the western South China Sea (Clerc et al., 2018) and between the Australia - Antarctica conjugate margins (Direen et al., 2011) depict wide margins and a ductile lower crust. (b) Seismic interpretations from the western Iberia margin (Ranero & Pérez-Gussinyé, 2010; Reston & McDermott, 2011) showing coupled crust-mantle deformation and asymmetric architecture. Analogue observation of mantle exhumation in the Alps (Tasna). (c) Conceptual model of symmetric rifting with mainly high-angle normal faults affecting the upper crust (modified after Nagel & Buck, 2007). (d) Conceptual model of asymmetric rifting with progressive crust-mantle coupling and formation of an upper and lower plate with respect to the main active detachment fault (Sutra et al., 2013). (e) Numerical model of symmetric pure-shear rifting with decoupled upper and lower crust (Nagel & Buck, 2004). (f) Numerical model of asymmetric simple-shear rifting involved by crust-mantle coupling (Huisman & Beaumont, 2007).

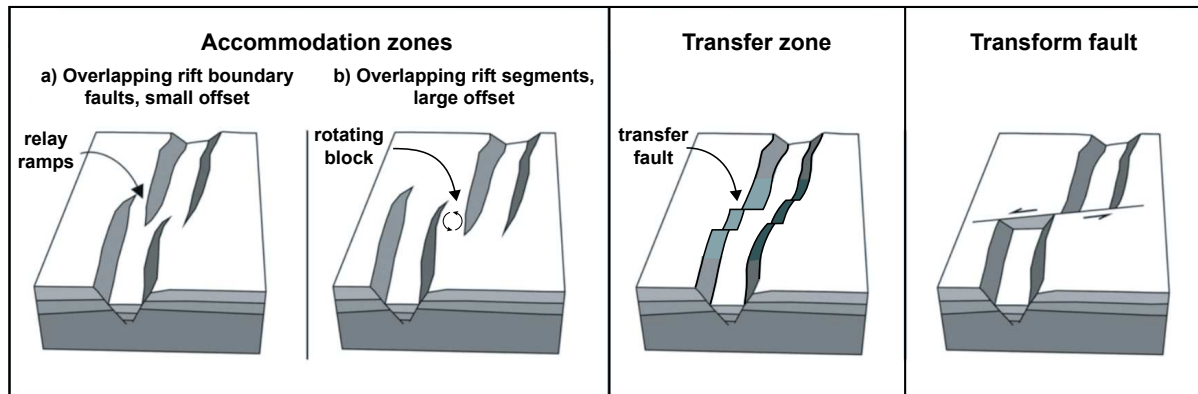


Figure I-4: Schematic 3D representation of accommodation zones, transfer zone and transform fault in an extensional setting (modified after Zwaan et al., 2016). Accommodation zones are characterized by non-connected overlapping faults associated with relay ramps in case of small offset (a) or non-connected overlapping rift segments in case of large offset (b). Transfer zones are characterised by low offset rift boundary faults via oblique to perpendicular transfer faults (c). A transform fault corresponds to a major strike-slip fault in between rift systems.

conditions (basal friction, sedimentary thickness, backstop geometry or steepness) between two adjacent segments (Calassou et al., 1993). The deformation is accommodated by imbrication of oblique thrust ramps in the transfer zone. During extension, the architecture of transfer or accommodation zones is mostly dependent on the lower crustal rheology, the offset distance between rift segments and on the direction of extension with respect to the orientation of the rift axis (i.e. oblique extension) (Le Pourhiet et al., 2017; Zwaan et al., 2016). In case of large offset between faults or rift segments, rift structures might not link at all and remain parallel to each other. Rift segments can rotate in their termination and be responsible for the formation of a rotated block between overlapping segments (Bubeck et al., 2017; Tapponnier et al., 1990) as observed at Oceanic Spreading Centre (Acocella, 2008; Tentler, 2007; Tentler & Acocella, 2010). With shorter offset, the link between rift segments and the formation of relay ramps and transfer faults will be favoured in transtensional settings (Zwaan et al., 2016). Importantly, transtensional displacement between tectonic plates has been shown to represent the dominant mode of deformation for passive margins worldwide (Brune et al., 2018), representing the most efficient way to reach continental breakup (Brune et al., 2012).

The formation and reactivation of rifted margins have been widely studied in 2D cross-sections and have been characterized in both numerical/sandbox modelling and field analogues. Besides, rift segment boundaries during extension have been explored but they often appear as inconspicuous features (Fig. I-5; e.g. Bellahsen et al., 2013; Chorowicz, 1989; Corti, 2012; Péron-Pinvidic et al., 2017). Moreover, their reactivation is restricted to very few models (Konstantinovskaya et al., 2007) or concern single structures in field examples (e.g. Benmakhoulouf et al., 2012; Quintana et al., 2006). As such, the 3D evolution of inverted rift

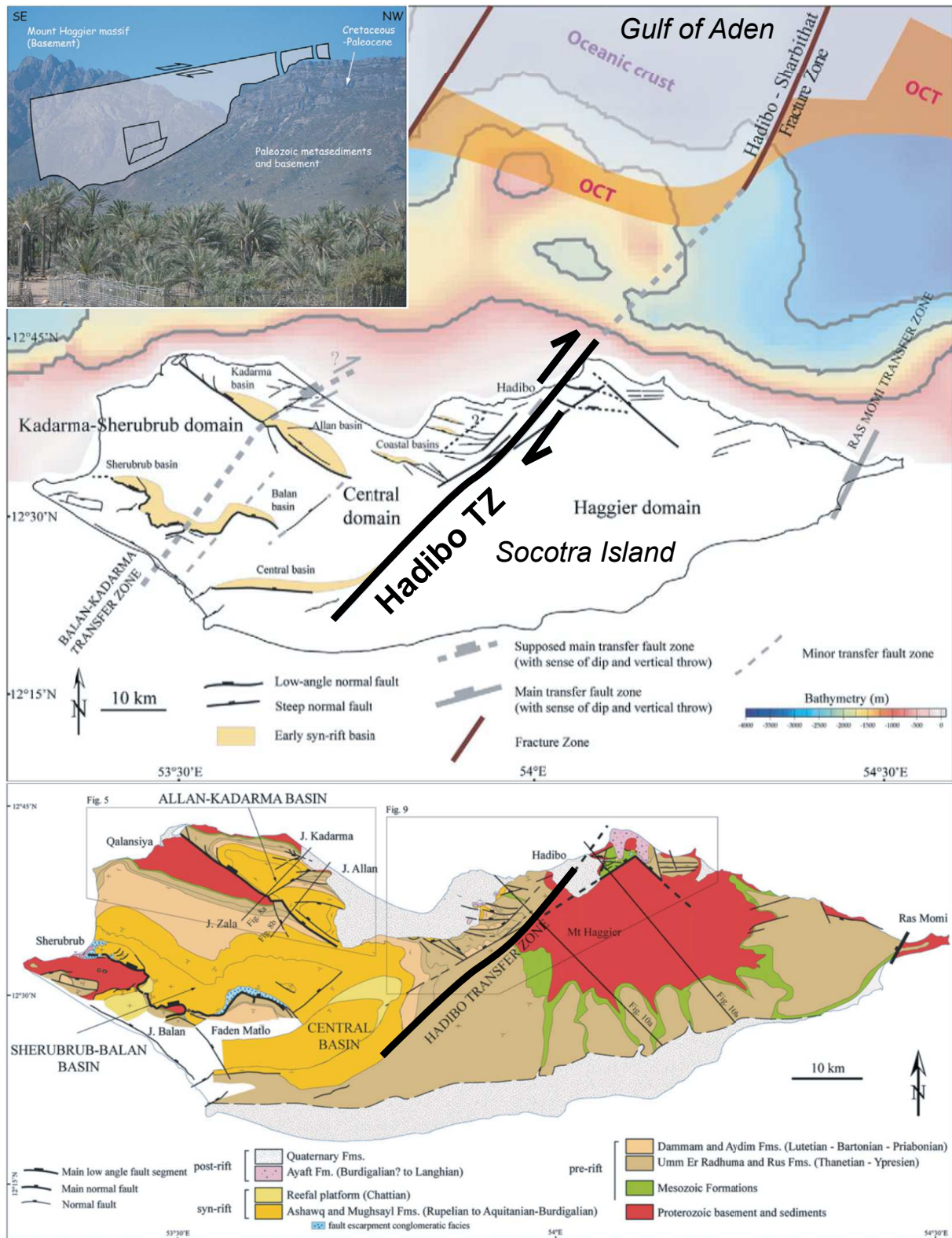


Figure I-5: Geological and structural maps of the Socotra Island and photograph of the Hadibo rift transfer zone located on the southern margin of the Gulf of Aden (modified after Bellahsen et al., 2013). The right-lateral Hadibo transfer zone delimits an uplifted eastern domain (footwall) composed of unstretched basement, from a subsided western domain (hangingwall) with syn-rift normal faults and where pre- to syn-rift sediments are cropping out. Note the difficulties to recognize and characterize a transfer zone, even on this well-defined field example.

segment boundaries is poorly known, and criteria for field recognition in orogenic systems are lacking. Therefore, key questions are:

- *How can rift segment boundary be recognized and described in the field?*
- *How are accommodation/transfer zones reactivated?*
- *Is rift segmentation responsible for the non-cylindricity of orogenic systems?*

2.3 Thermal evolution of rift systems: from the McKenzie model to new thermo-mechanical models

Heat arises from different sources and is transferred in various ways in geological systems. At the lithospheric scale, the most dominant heat sources correspond to the deep mantle (Earth interior) and to the radiogenic heat generated by the radioactive decay of isotopes in the crust and the mantle, whilst heat from shear heating or exothermic reactions represent sources being potentially more relevant at a local scale. Heat transfer occurs by conduction and convection, the latter concerning asthenospheric mantle, hydrothermal fluids or magmatic advection. All these parameters may variably evolve during the Wilson cycle, for example in relation with the depth of the base of the lithosphere (e.g. 1300°C isotherm) or with the age and thickness of continental crust.

In plate divergent settings, the most popular model to assess the thermal evolution has been proposed by McKenzie (1978), involving instantaneous rifting that thins the lithosphere under pure-shear depth-uniform extension. It is based on the assumption that passive upwelling of the asthenosphere and conduction are the main parameters controlling heat flow, which can be defined from the amount of stretching estimated from the crustal thickness (β factor). Alternatively, Wernicke (1985) proposed a model of simple shear lithospheric extension that results in a strongly asymmetric rift evolution. In this model, Buck et al. (1988) and Issler et al. (1989) showed that the highest top basement heat flow values are located in the hangingwall of the detachment fault, i.e. in the distal upper plate, raising implications for the distribution of magma (e.g. Lister et al., 1986), for the subsidence history and therefore also for the sedimentary evolution. The thermal architecture of all these models can be variably affected by the amount of magma (magma-rich vs. magma-poor), the shear heating in relation with extensional detachments (e.g. Souche et al., 2013), the circulation of hydrothermal fluids (e.g. Sclater et al., 1980; Sleep & Wolery, 1978; Smith & Chapman, 1983) or the thermal blanketing effect due to the low thermal conductivity of the sediments infilling the basin (Hutchison, 1985; Lucazeau & Le Douaran, 1985).

In convergent plate settings, the heat released during collision has been shown to be mostly provided by shear and viscous heating related to internal deformation and crustal thickening, together with the radiogenic heat involved by the continental crust (Barr & Dahlen, 1989; Burg & Gerya, 2005; England & Thompson, 1984). During subduction, the formation of a back-arc system leads to convection in the supra-slab asthenospheric corner and to significant increase of the heat flow that may also control the thermal budget of the subsequent collisional orogen (Hyndman et al., 2005). In these systems, thermal energy is transported both by magma advection and by conduction (Burg & Gerya, 2005).

More recently, new numerical models describing lithospheric extension, and inspired by field observations, have emerged and have the potential to test, predict and/or calibrate thermal systems (Fig. I-6). A model of depth-dependent extension has been proposed by Huismans & Beaumont (2011) in which the amount of mantle lithosphere thinning differs from the upper and/or lower crustal thinning (Davis & Kuszniir, 2004), eventually leading to the exhumation of lower crustal and/or mantle rocks. In these models, the crustal radiogenic heat budget may vary across the system. An alternative model involving asymmetric rift migration has been described in both conceptual (Nirrengarten et al., 2016; Ranero & Pérez-Gussinyé, 2010) and numerical models (Brune et al., 2014). Brune et al. (2014) showed, using a numerical model, that the initial thermal structure and syn-rift thermal weakening partially control the asymmetric evolution of such systems. However, the thermal evolution associated with these models, where basement rock composition evolve during rifting and the base of the lithosphere advects and migrates through time, has been only rarely tested in basin modelling (Callies et al., 2018; Hart et al., 2017).

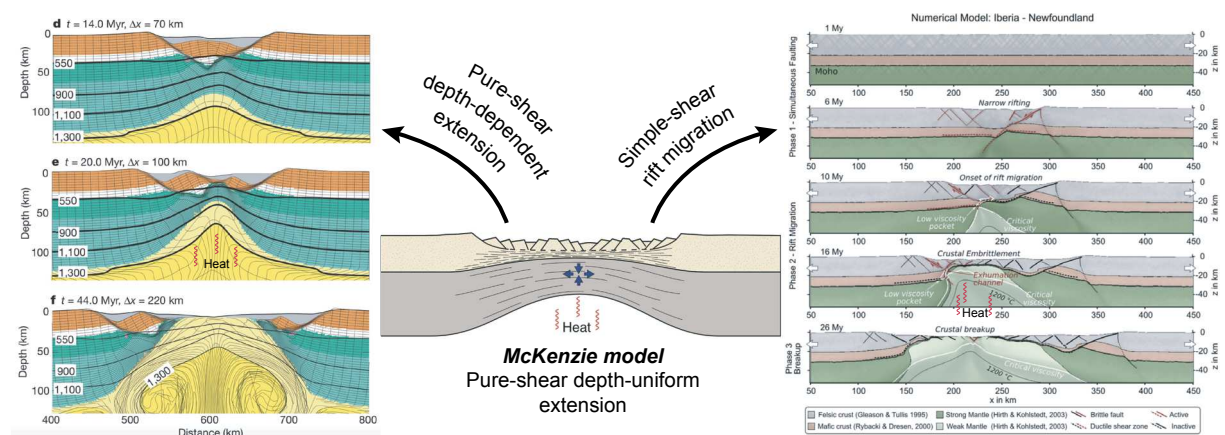


Figure I-6: New models of lithospheric extension in comparison to the typical McKenzie (1978) model (from Fossen, 2016). Huismans & Beaumont (2011) model corresponds to a permanent depth-dependent pure-shear extension with a felsic lower crust. The model shows a rather symmetrical evolution. The Brune et al. (2017) model corresponds to a simple-shear extension with a strong mafic lower crust, leading to an asymmetric structural evolution and rift migration due to asymmetric lower crustal weakening. Note the evolution of the asthenosphere-lithosphere boundary in both models.

The Pyrenean-Cantabrian system represents a rare example in which the orogenic episode did not overprint the pre-orogenic thermal imprint, allowing to study the thermal evolution associated with the mid-Cretaceous hyperextension. Studies showed that an episode of High Temperature/Low Pressure (HT/LP) metamorphism occurred coevally to mantle exhumation (Clerc et al., 2015; Lagabrielle et al., 2010). In these inverted basins, an apparent thermal asymmetry (Dauteuil & Ricou, 1989; Hart et al., 2017) and along-strike segmentation (“hot” and “cold” margins in Clerc et al., 2015) have been described from the present-day distribution of metamorphic rocks (Fig. I-7). Moreover, strong variations in the T_{max} values (maximum temperature reached by a sample rock) can be observed on sediments associated with exhumed mantle rocks (e.g. Mauléon basin, Corre, 2017; Aulus basin, Clerc et al., 2015). These observations suggest that the widely used McKenzie model for continental stretching can be merely applied in this system and that the mode of lithospheric extension may influence the thermal architecture of rift basins. This alternative thermal and structural architecture prior to reactivation may in turn influence the orogenic evolution, in particular for immature systems where the lithosphere may have not yet been thermally equilibrated. Therefore, I will attempt to answer the following questions in the third chapter of this manuscript:

- *Can an asymmetric model of lithospheric extension explain the thermal evolution of the Mauléon basin during hyperextension?*
- *What is the influence of asymmetric rifting on the thermal evolution of hyperextended domains?*
- *What do T_{max} values tell us about the thermal state of rift systems?*

3. THE LABORATORY: THE PYRENEAN-CANTABRIAN MOUNTAIN RANGES

3.1 Choice of the study area

The Pyrenean and Cantabrian mountain ranges represent an E-W striking orogenic belt across northern Spain. The Pyrenees bound the 430km long border between Spain and France, while the Cantabrian chain extends over 480km and roughly delimits the offshore Bay of Biscay from the Central Meseta. The Basque Country is at the limit between the Cantabrian and the Pyrenean mountains (Fig. I-8). I will use this geographic terminology to define the Cantabrian segment to the west and the Pyrenean segment to the east throughout the manuscript. However, note that different terminologies or geographic units have been defined in the literature (see Barnolas & Pujalte, 2004).

1 : Oligocene and post-Oligocene ; 2 : Mesozoic and Eocene ; 3 : Paleozoic basement ; 4 : area of HT-LP Pyrenean metamorphism ; 5 : Iherzolite bodies ; 6 : outcrops of granulitic basement rocks ; 7 : main external thrusts ; 8 : North Pyrenean Fault

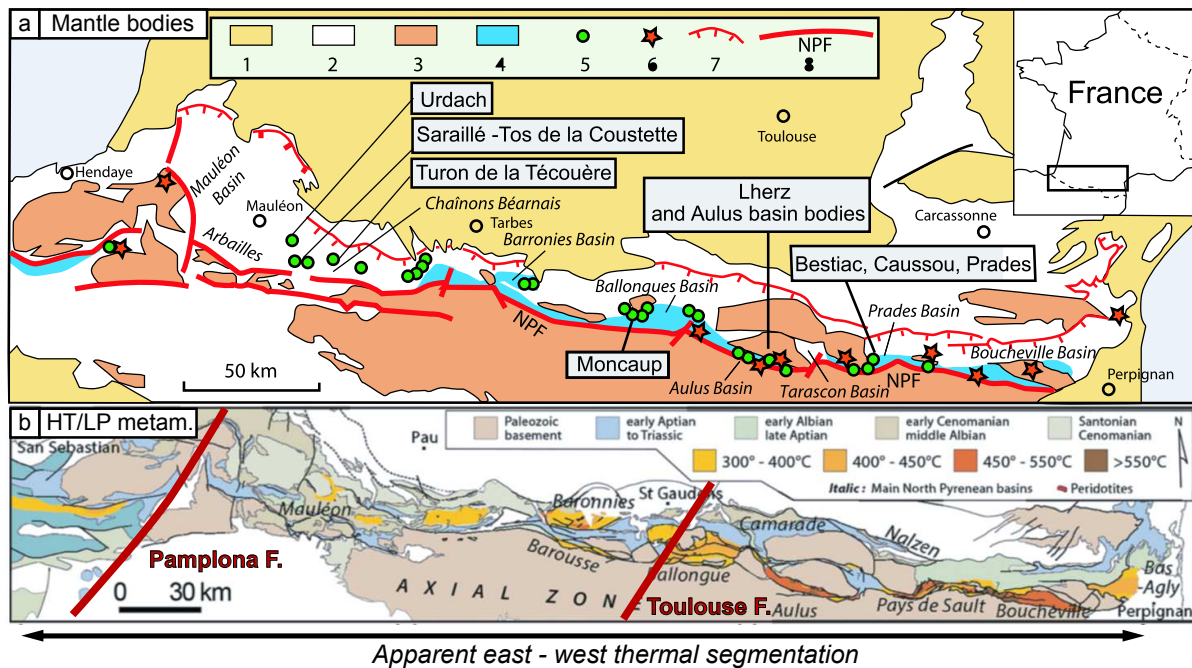


Figure I-7: Geological maps of the Pyrenees showing the distribution of (a) mantle bodies (modified after Lagabrielle et al., 2010) and (b) HT/LP metamorphic rocks (modified after Clerc et al., 2015). Note the apparent along-strike variation of the HT/LP metamorphism.

The tectonic evolution of the Pyrenean and Cantabrian segments has been widely studied since the 20th century. Several phases of divergence and convergence have been recognized starting with the Variscan orogeny subsequently affected by the Alpine cycle, which initiated with the Permo-Triassic to mid-Cretaceous rifting episode and was followed by the Late Cretaceous to Cenozoic orogenic episode (Ducasse et al., 1986b). All these episodes have been remarkably well recorded and preserved in the present-day mountain chain. However, many questions remain about the evolution from one episode to the other such as the crustal architecture and evolution during the Late Variscan period (e.g. Cochelin, 2016), the kinematics of Iberia and the implications for the Pyrenean-Cantabrian basins during the Mesozoic (e.g. Barnett-Moore et al., 2016a; Canérot, 2016, 2017), or the formation of the Alpine orogenic belt throughout the system (e.g. Teixell et al., 2018).

The main reason to study this system is that it represents a well accessible, natural laboratory that enables to investigate the role of inheritance and the processes that take place during a Wilson cycle. The area only suffered of a minor Alpine compressional imprint (thermal and structural) and allows therefore to study the syn-rift architecture and related thermal evolution. It has also been shown to represent a highly segmented rift system during the Cretaceous (Tugend et al., 2015). Moreover, it benefits from a large geological and geophysical

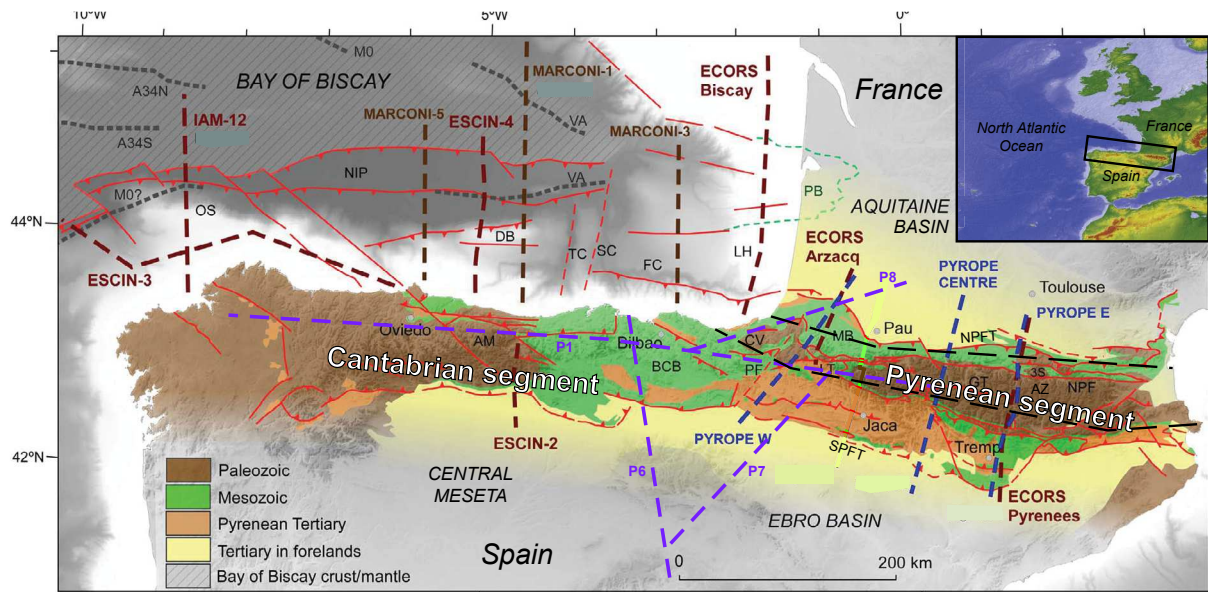


Figure I-8: Geological map of the Pyrenean and Cantabrian segments (modified from Teixell et al., 2018). Brown lines: reflection profiles; black: reflection profiles from Daignieres et al. (1982) and Gallart et al. (1981); blue: receiver function profiles; purple: refraction/wide-angle profiles from Pedreira et al. (2003); M0, A34N, A34S: oceanic magnetic anomalies; VA: V-shaped magnetic anomaly (after Sibuet et al., 2004); NIP: North Iberian thrust prism; OS: Ortelgal spur; DB: Le Danois Bank; TC, SC: Torrelavega and Santander canyons (Santander transfer zone); FC: Cap Ferret canyon; PB: Parentis basin; LH: Landes High; AM: Asturian massif; BCB: Basque-Cantabrian basin; CV: Cinco Villas massif; PF: Pamplona transfer fault; NPFT: North Pyrenean Frontal Thrust; SPFT: South Pyrenean Frontal Thrust; MB: Mauléon basin; LT: Lakora thrust; GT: Gavarnie thrust; AZ: Axial Zone; NPF: North Pyrenean fault; 3S: Trois-Seigneurs massif.

dataset acquired during the last decades. In the framework of the OROGEN project, I had access to the seismic and borehole data in France provided by Total and acquired by the SNEA (Société Nationale Elf Aquitaine), SNPA (Société Nationale des Pétroles d'Aquitaine) or Esso. Seismic and borehole data in Spain are available online or under request to the IGME service (SIGEOF). Moreover, published seismic profiles (Fig. I-8) as well as gravity and magnetic anomaly maps have been acquired from onshore and offshore campaigns, giving access to a wide and dense grid of geophysical data. Finally, it benefits from the observations and results of recent scientific projects conducted in the Pyrenees such as Pyrope, Pyramide and RGF Pyrénées.

3.2 The Wilson cycle in the Pyrenean-Cantabrian system

The aim of this section is not to summarize all the previous work done in the Pyrenean-Cantabrian system, but to provide the main information necessary to understand the questions addressed in this manuscript. Note that a more detailed geological description of the study

area can be retrieved in the geological settings of chapters II to IV. As such, this section will describe the general evolution of the system starting with the Variscan orogeny, followed by the Late Triassic to mid-Cretaceous polyphased rifting and the Late Cretaceous to Miocene Alpine orogeny. This evolution can be observed through the Wilson cycle framework among which the main episodes that occurred in the Pyrenees are summarized in the figure I-9.

3.2.1 Variscan to Late Variscan orogeny (Carboniferous to Early Permian)

3.2.1.1 Geodynamic context

The Variscan orogeny (480 to 290Ma) results from the subduction and accretion of terranes such as Avalonia and Armorica from the N-Gondwana margin against the Laurussia plate, followed by the collision of the Laurussia and Gondwana plates (Matte, 2001). The collision was associated with a HT metamorphism and melting of the lower and middle orogenic crust, which led to the emplacement of granitic plutons in the hinterland (e.g. Ballèvre et al., 2014; Martínez Catalán et al., 1997). This HT metamorphic and magmatic phase was

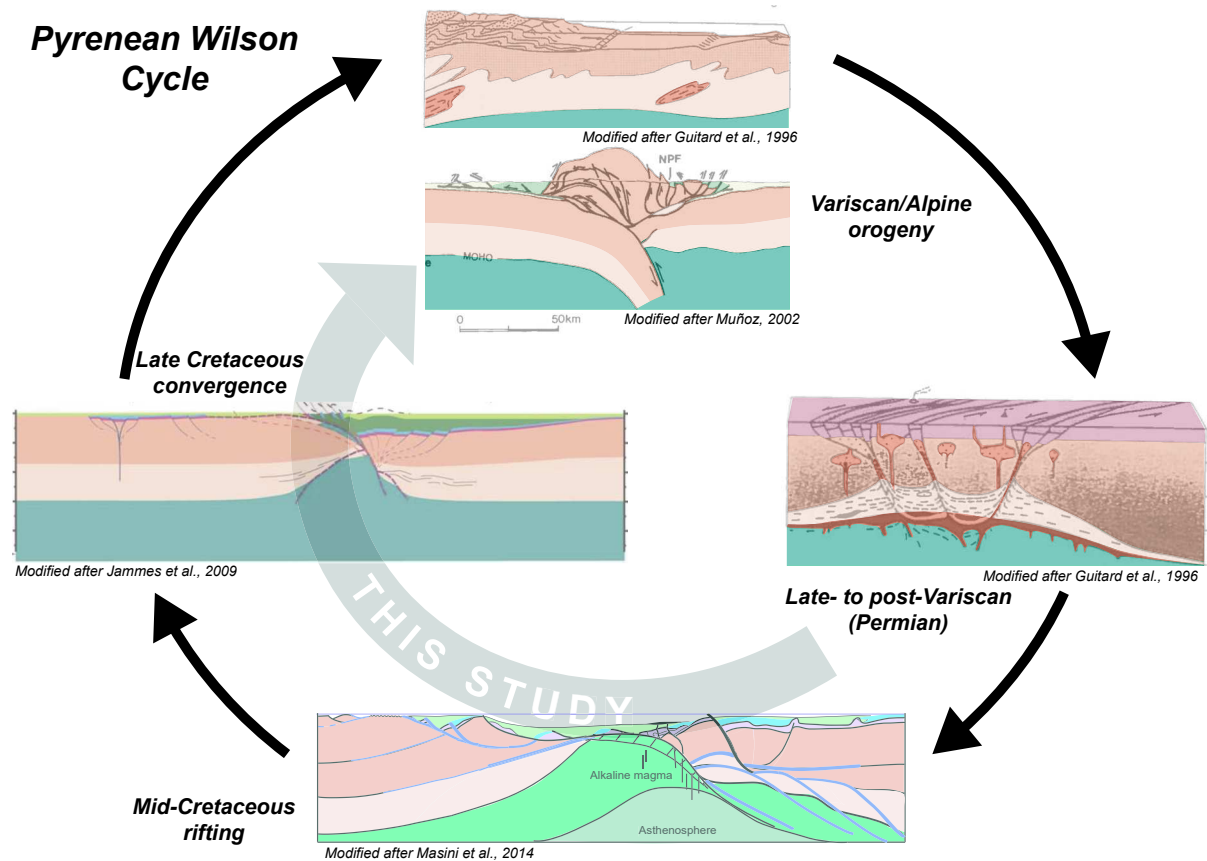


Figure I-9: Main stages in the evolution of the Pyrenean Wilson cycle.

contemporaneous with the bending of the orogen from 310 Ma onward and results in an orocline concave towards the east from the present-day NW Iberian massifs to the Armorican massifs (Fig. I-10; e.g. Ballèvre et al., 2014; Martínez Catalán et al., 2007; Martínez-García, 2013; Weil et al., 2000; Weil, 2006). This bending was also accompanied by mantle and crustal partial melting (e.g. Aguilar et al., 2014) forming extensional migmatitic domes (e.g. Denèle et al., 2009, 2014). The Pyrenees and the Cantabrian ranges represent the inner core of the oroclinal, i.e. the former southern foreland basin of the orogen and its adjacent Gondwana-derived terrane (Fig. I-10).

3.2.1.2 Evolution of the Pyrenean-Cantabrian system

The orogenic episode was characterised in the Pyrenees by the formation of a fold and thrust belt in relation with a south to south-west direction of shortening (Autran et al., 1996;

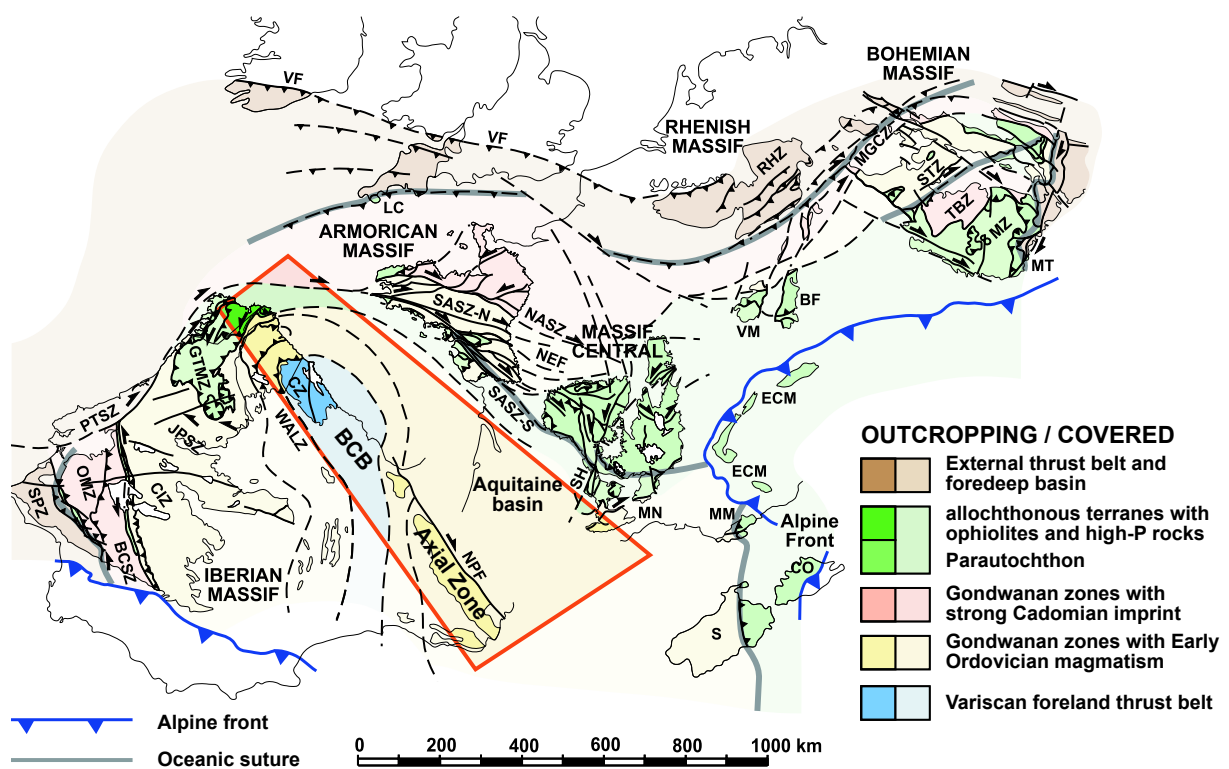


Figure I-10: Major structures and orogenic domains of the Variscan belt. Location of the future Pyrenean and Cantabrian system is indicated. Modified after Martínez Catalán et al. (2007) and Ballèvre et al. (2014). BCB: Basque-Cantabrian basin; BCSZ: Badajoz-Córdoba shear zone; BF: Black Forest; CIZ: Central Iberian zone; CO: Corsica; CZ: Cantabrian zone; ECM: External crystalline massifs of the Alps; GTMZ: Galicia-Trás-os-Montes zone; JPSZ: Juzbado-Penalva shear zone; LC: Lizard Complex; MGCCZ: Mid-German crystalline zone; MM: Maures Massif; MN: Montagne Noire; MT: Moldanubian thrust; MZ: Moldanubian zone; NASZ: North Armorican shear zone; NEF: Nort-sur-Erdre fault; NPF: North Pyrenean fault; OMZ: Ossa-Morena zone; PTSZ: Porto-Tomar shear zone; RHZ: Rhenian-Hercynian zone; S: Sardinia; SASZ: South Armorican shear zone (N and S: northern and southern branches); SH: Sillon Houillier; SPZ: South Portuguese zone; STZ: Saxo-Thuringian zone; TBZ: Teplá-Barrandian zone; VF: Variscan front; VM: Vosges Massif; WALZ: West Asturian-Leonese zone.

Delvolvé et al., 1998; García-Sansegundo et al., 2011; Gleizes et al., 1997; Mattauer et al., 1967; Pérez-Estaún et al., 1988).

The Late Variscan episode is ill-constrained in the Pyrenean and Cantabrian systems and has been attributed either to a phase of transtensional deformation in relation with the post-orogenic collapse of the hinterland or to a phase of transpression in relation with the formation of the orocline (e.g. Arthaud & Matte, 1975; Burg et al., 1994; Cochelin et al., 2017; Denèle et al., 2014; López-Gómez et al., 2019; Martínez-García, 2013). During Late Carboniferous to Early Permian, the crustal rocks suffered an episode of HT/LP metamorphism of upper-amphibolite to granulite facies in the middle and lower crust, respectively (Aguilar et al., 2014; Guitard et al., 1996; Puelles et al., 2014; Vielzeuf, 1984), while the upper crustal syn- to pre-orogenic Precambrian to Lower Carboniferous sediments suffered only low-grade metamorphism (e.g. Guitard et al., 1996). Coevally, flysch sediments of the “Culm” facies were deposited at the front of the nappes and were affected by very low-grade metamorphism (Julivert, 1971; Pérez-Estaún et al., 1988). A first episode of magmatism was responsible for the emplacement of calc-alkaline and peraluminous plutons, a magmatism that was progressively replaced by alkaline magmatism and volcanism during the Permian (e.g. Aguilar et al., 2014; Bixel, 1984; Denèle et al., 2011, 2014; Gallastegui et al., 1990; Gleizes et al., 1997; Innocent et al., 1994; Lago et al., 2004).

The transtensional/transpressional event has been proposed to be accommodated by transcurrent faults (Fig. I-11) such as the WNW-ESE North Pyrenean Fault (NPF), the NNE-SSW Pamplona or Toulouse fault or the NW-SE Ventaniella fault (e.g. Arthaud & Matte, 1975, 1977; Burg et al., 1994; Gretter et al., 2015; Laumonier, 2008; Martínez-García, 2013; Rat, 1988). This episode of crustal dislocation led to the formation of half-graben basins filled with continental deposits and controlled by NNE-SSW and ESE-WNW faults in the Western Pyrenees and NW-SE to E-W structures in the Eastern Pyrenees (Bixel & Lucas, 1983, 1987; Laumonier et al., 2014; Saura & Teixell, 2006; Soula et al., 1979). In the Cantabrian segment, Permian basins were assumed to reactivate Variscan and Late Variscan structures, the former giving rise to NE-SW to E-W trending basins and the latter leading to NW-SE striking basins (López-Gómez et al., 2019) filled with continental deposits (Virgili et al., 1976).

3.2.1.3. Key features: crustal architecture and inheritance

The Variscan to Late Variscan episode is often mentioned as a major tectonic event that deeply modified the architecture of the lithosphere and controlled the tectonic evolution of the subsequent Alpine cycle (e.g. Arthaud & Matte, 1975). However, questions remain about the thickness of the Late Variscan crust (e.g. Lemirre et al., 2016) and the metamorphic gap

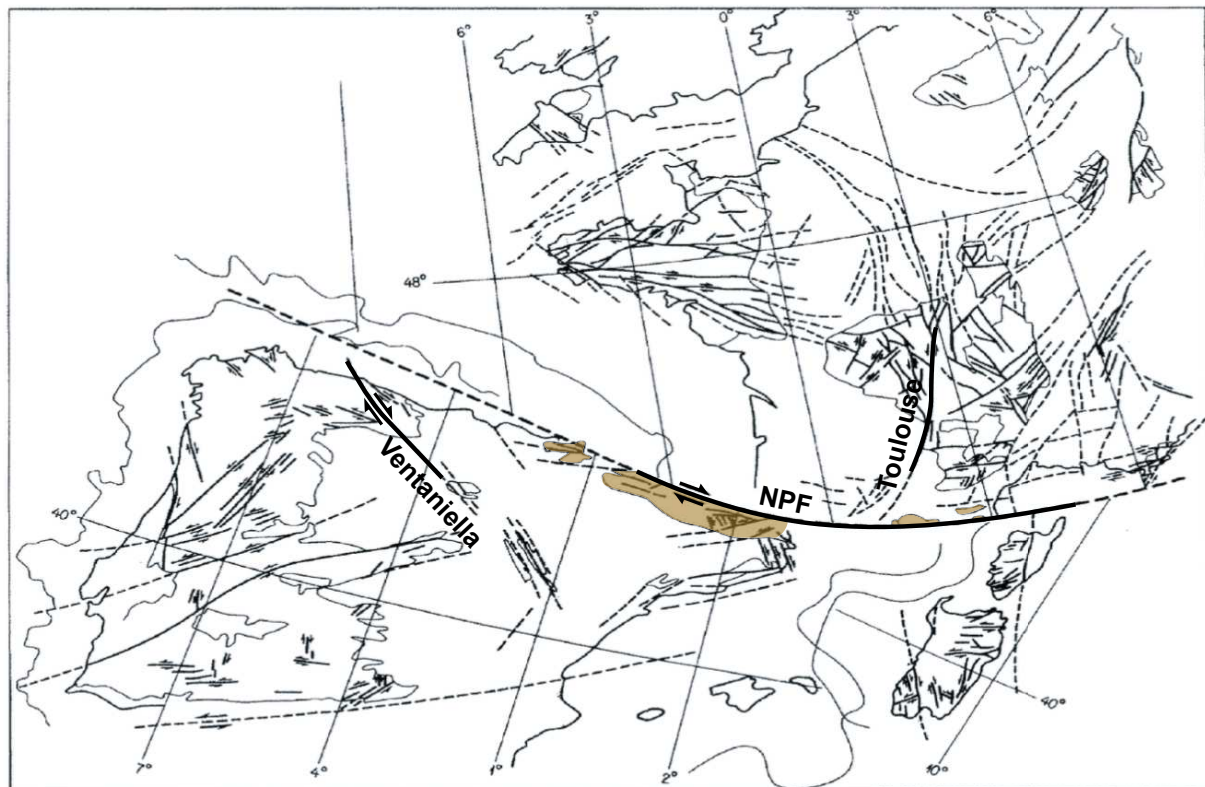


Figure I-11: Map of the Late Variscan transcurrent faults in Western Europe according to Arthaud & Matte (1975). Note the complex structural pattern and the right-lateral NPF and Ventaniella fault. Pyrenean massifs are represented in brown with the Axial Zone and the North Pyrenean massifs, shifted by the right-lateral NPF.

between the supra-structure and the infra-structure (Carreras & Capella, 1994). Moreover, the age of formation and the timing of exhumation of the granulites are still poorly constrained (e.g. Clerc & Lagabrielle, 2014; Cochelin, 2016; Jammes et al., 2009; Olivier, 2015; Petri et al., 2018; Vielzeuf, 1984).

3.2.2 Permo-Triassic: end of the Variscan and onset of the Alpine cycle

3.2.2.1 Geodynamic context

The Late Permian – Early Triassic corresponds to a transitional phase between the Variscan and the Alpine cycle. During this phase, erosion and peneplanation of the Variscan reliefs occurred throughout western Europe (Fig. I-12; Arthaud & Matte, 1977; Doré et al., 1999). This period of continental sedimentation took place in a regional transtensional regime, characterized by the formation of half-graben basins (Bixel & Lucas, 1987). It also marks the final assemblage of the Pangea supercontinent.

3.2.2.2 Evolution of the Pyrenean-Cantabrian system

In the Pyrenean-Cantabrian system, the Lower Triassic is very often composed of reddish continental sandstones, conglomerates or siltstones belonging to the Germanic Buntsandstein Formation (Stevaux & Winnock, 1974). It unconformably seals the Permian basins and plutons as well as the Palaeozoic basement in most of the study area (e.g. Genna, 2007; Virgili et al., 1976). Note that, in the Asturian massif, the Lower Triassic is lacking and the Middle Triassic sandstones represent the first sediments deposited above Palaeozoic or Permian rocks (López-Gómez et al., 2019).

Lower Triassic sediments have been deposited in NNE-SSW to E-W oriented depocenters in the Western Pyrenees and in the Aquitaine basin (Bixel & Lucas, 1987; Curnelle, 1983; Soula et al., 1979), while WNW-ESE striking boundary faults have been shown to control their deposition in the Cantabrian range (Barnolas & Pujalte, 2004; García-Mondéjar et al., 1986). These structures might potentially reflect precursor tectonic activity in relation with the Late Triassic rifting event.

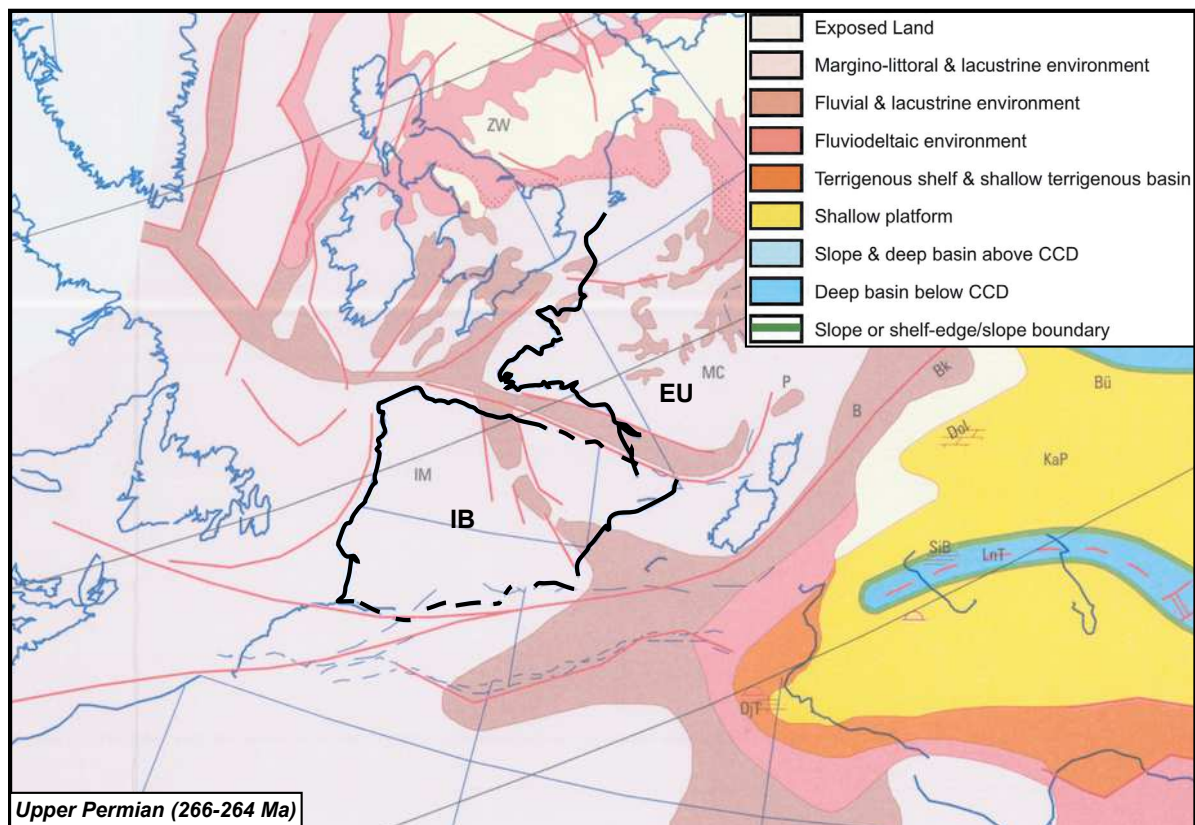


Figure I-12: Paleogeographic map of Western Europe at Late Permian (266-264 Ma) (Modified after Dercourt et al., 2000).

3.2.2.3 Key features: the Lower Triassic marker horizon

The broadly represented and characteristic Lower Triassic stratigraphic horizon represents a reasonably good marker to discriminate between deformation belonging either to the Variscan or to the Alpine cycles as well as to define the crustal position of geological units prior to the Mesozoic rifting episodes. As such, the occurrence of post-Triassic sediments directly on top of the granulites and the absence of Lower Triassic sediments suggest that the granulites were exhumed to the seafloor or below the sedimentary cover during the subsequent tectonic episodes.

3.2.3 Triassic rifting

3.2.3.1 Geodynamic context

The Late Triassic has been suggested to represent a period of crustal fragmentation in relation with the breakup of the Pangea supercontinent and the onset of rifting and oceanic spreading in the Tethys and/or Central Atlantic and/or northern North Atlantic (Fig. I-13; e.g. Doré et al., 1999; Scotese & Schettino, 2017; Stampfli & Borel, 2002). This episode shows the occurrence of marine incursion onto the former Permo-Triassic continental basins whilst the upper Late Triassic sees the development of a broad thermal and magmatic event in relation with the opening of the Central Atlantic and formation of the Central Atlantic Magmatic Province at 200Ma (CAMP; Rossi et al., 2003).

3.2.3.2 Evolution of the Pyrenean-Cantabrian system

At the scale of the Pyrenean-Cantabrian systems, the Late Triassic corresponds to a period of ill-constrained rifting that occurs along the future Iberian and Eurasian plate boundary (Boess & Hoppe, 1986; Doré et al., 1999; Montadert et al., 1974; Rat, 1988; Scotese & Schettino, 2017). A transgressive event led to the formation of shallow marine carbonate and dolomite platforms of the Muschelkalk Formation over the Lower Triassic continental deposits. It is followed by the formation and deposition of the Upper Triassic evaporites corresponding to the Keuper Formation (Fréchengues, 1993; Stevaux & Winnock, 1974), composed of variegated gypserous siltstones associated with dolomites, anhydrite and halite (Brinkmann & Logters, 1968). They are overlain by a second carbonate platform formed during the Rhaetian. The Upper Triassic evaporites are very often associated with tholeiitic dolerites (the so-called “ophites”; Walgenwitz, 1976), which were emplaced coevally with the thermo-magmatic CAMP event of the Central Atlantic. In the Asturian massif, onset of Triassic rifting occurred during the Ladinian (Middle Triassic) with the deposition of fluviatile sediments, contrasting with the

typical evaporitic facies deposited elsewhere in the Pyrenees and BCB (López-Gómez et al., 2019).

In the Pyrenean system, despite no clear basin orientation has been retrieved, authors proposed that the Upper Triassic evaporites were deposited in small troughs, potentially reactivating Late Variscan to Permo-Triassic structures, corresponding to N50-60, N80 and N110 to N140 striking normal faults (Curnelle, 1983; Muller & Roger, 1977; Peybernès & Souquet, 1984; Puigdefàbregas & Souquet, 1986; Rat, 1988; Soula et al., 1979). These faults have been suggested to form a pathway for the ascent of the Triassic ophiolites. In the Asturian massif, Middle to Late Triassic rifting has been proposed to take place in half-graben basins mainly controlled by NW-SE structures (e.g. Ventaniella fault) (García-Mondéjar et al., 1986).

3.2.3.3 Key features: the Upper Triassic evaporites

The implication of the Late Triassic rifting event for the kinematics and position of Iberia with respect to Eurasia remains debated. This is particularly important because it conditions the amount of lateral motion of the Iberian plate relative to Eurasia during Jurassic to Cretaceous

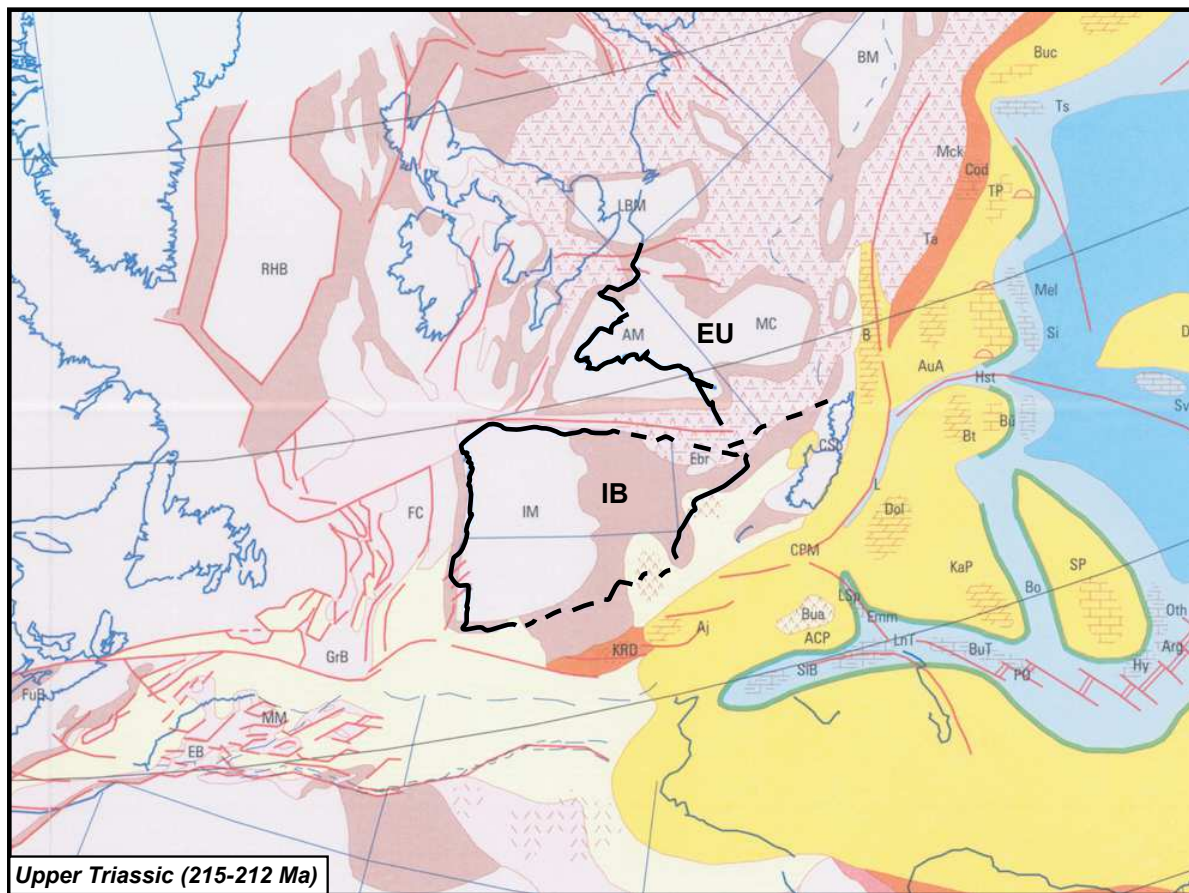


Figure I-13: Paleogeographic map of Western Europe at Late Triassic (215-212 Ma) (Modified after Dercourt et al., 2000). See caption of Fig. I-12 for details.

times. Structures associated with this event are difficult to recognize due to subsequent tectonic episodes and because of the highly mobile evaporites. The latter will strongly influence the following tectonic episodes, acting as a decoupling level between the Palaeozoic basement and the overlying sedimentary cover (e.g. Jammes et al., 2010c).

3.2.4 Late Jurassic to Cretaceous rifting

3.2.4.1 Geodynamic context

The Late Jurassic to Santonian corresponds to the opening and oceanic spreading of the southern North Atlantic and Bay of Biscay following breakup of Pangea (e.g. García-Mondejar, 1989; Le Pichon & Sibuet, 1971; Olivet, 1996; Sibuet et al., 2004; Thinon et al., 2003; Verhoef & Srivastava, 1989). However, the geodynamic evolution of the Iberian plate with respect to Eurasia during this period remains ill-constrained (see Barnett-Moore et al., 2016a and Nirrengarten et al., 2018 for a review). Indeed, none of the models proposed so far can satisfy the geophysical data (restoration of the magnetic anomalies and rotation from paleomagnetic data) and the geological observations at the same time.

As such, three main scenarios can be proposed (Fig. I-14; e.g. Tavani et al., 2018), all involving various amounts of rotation and lateral displacement or including different partitioning of the deformation through time. The three scenarios are:

- The scissor-type scenario (e.g. Sibuet et al., 2004; Vissers et al., 2016): it involves the presence of a 250km wide oceanic domain between Iberia and Eurasia before Aptian (M0), followed at mid-Cretaceous time by the closure of this oceanic domain and the opening of a back-arc basin in the present-day North Pyrenean basins. The latter would be subsequently inverted from Late Santonian onward. This model derives from the identification of the M series magnetic anomalies in the southern North Atlantic and Bay of Biscay as well as the paleomagnetic data. However, paleomagnetic data on the Iberian plate are litigious from 213 to 68 Ma (Barnett-Moore et al., 2016b; Neres et al., 2012, 2013) and the oceanic magnetic anomalies of the M-series have been shown to be ill-defined and as a consequence hardly usable for plate reconstructions (Bronner et al., 2011; Nirrengarten et al., 2017). Moreover, this reconstruction involves a large subduction and collision in the Iberian range at mid-Cretaceous time that have not been identified so far (e.g. Barnett-Moore et al., 2016a; Rat et al., 2019).
- The strike-slip scenario (e.g. Olivet, 1996; Stampfli & Borel, 2002): it involves more than 400km of left-lateral strike-slip movement along the NPF from Aptian (M0) to Santonian time resulting in the formation of pull-apart basins in the Pyrenean-Cantabrian system (e.g. Choukroune & Mattauer, 1978; Debros, 1987). This scenario corresponds to the amount

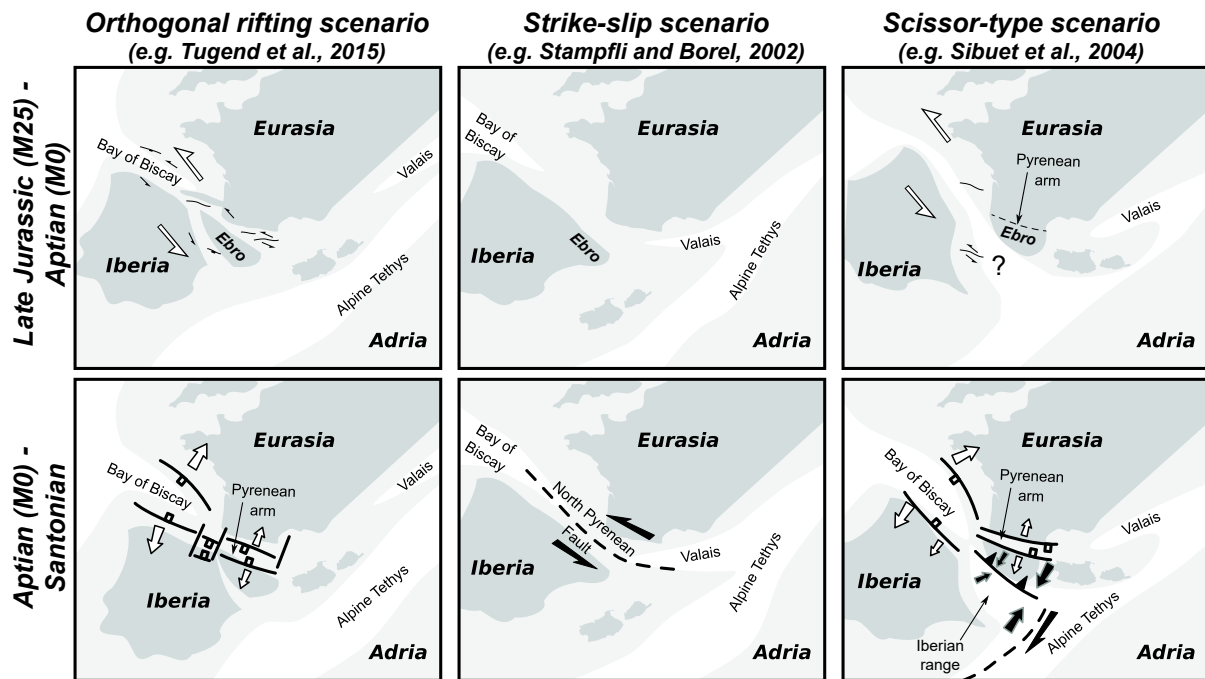


Figure I-14: Geodynamic evolution of the Iberia-Eurasia plate boundary at Late Jurassic-Aptian and at Aptian-Santonian times (modified after Tavani et al., 2018). Orthogonal rifting model after Tugend et al. (2015); Strike-slip model after Stampfli & Borel (2002); Scissor-type model after Sibuet et al. (2004). Note the variation in the mode of deformation for each model through time and space.

of vertical axis rotation defined by Van der Voo (1969) with vintage paleomagnetic data but no evidence for such an amount of strike-slip deformation can be found from field observations. Moreover, it suggests that no deformation occurred at the Iberia-Eurasia plate boundary from Late Jurassic to Aptian, contrasting with geological observations (e.g. Tavani et al., 2018).

- The orthogonal rifting scenario (e.g. Jammes et al., 2009; Tugend et al., 2015): it involves a first phase of transtensional deformation from Late Jurassic to Aptian followed by an orthogonal N-S direction of extension from Aptian to Cenomanian. Note that Tavani et al. (2018) proposed that orthogonal extension occurred from Late Jurassic to Upper Cretaceous, implying limited lateral displacement between Iberia and Eurasia from Jurassic to Late Cretaceous. This rift-perpendicular scenario mostly fits with geological field observations. However, it is hardly conciliated with an unique Iberian plate and a continuous E-W oriented seafloor spreading in the southern North Atlantic (Barnett-Moore et al., 2016b; Nirrengarten et al., 2018).

3.2.4.2 Evolution of the Pyrenean-Cantabrian system

After the Early to Middle Jurassic period, which was characterised by the formation of marine carbonate platforms and the deposition of marls in relation with a general transgression (e.g. Aurell et al., 2003), the Late Jurassic (Kimmeridgian-Tithonian) represents a new tectonic episode in the Pyrenean-Cantabrian system.

This episode, referred to as the “problemas postkimmericos” by Soler (1971), corresponds in the Cantabrian segment to the end of marine sedimentation and the formation of the continental “Purbeck-Weald complex” or “Wealden grabens” (del Pozo, 1969; Rat, 1988; Salomon et al., 1982). The Purbeck-Weald basins correspond mainly to detritic sedimentation in lacustrine to fluvial environments with very sporadic shallow marine, evaporitic or lagoonal incursions (Ábalos et al., 2008; Instituto Geológico y Minero de España (IGME), 1990; Pujalte, 1977; Rat, 1959; Salomon et al., 1982) and can reach up to 7000m in thickness (Cadenas & Fernández-Viejo, 2017).

In the Pyrenean segment, this Late Jurassic to Early Cretaceous episode is ill-defined. It shows the development of shallow water carbonates and marls but depicts stratigraphic variation from the east to the west of the Pyrenees (Fig. I-15; Barnolas & Pujalte, 2004; Puigdefàbregas & Souquet, 1986). Indeed, the Lower Cretaceous corresponds in the Eastern Pyrenees to the deposition of polymictic carbonate breccia formed from the destabilisation of the Jurassic platform, whereas detritic sandstones similar to the Cantabrian Weald facies were deposited in the Western Pyrenees (Delfaud, 1970; Rat, 1988). This distinction led Souquet et al. (1977) to propose the existence of an inherited WSW-ESE striking “faille de Bigorre” located east of the Basque massifs and bounding a domain of Atlantic affinity toward the west from a domain of Tethys affinity toward the east. Note that Neocomian bauxites have been identified in the Western Pyrenees, attesting for local aerial exposure of the basin (Canerot et al., 1978; Combes et al., 1998).

Les zones isopiques du Néocomien (Berriasien, Valanginien, Hauterivien)

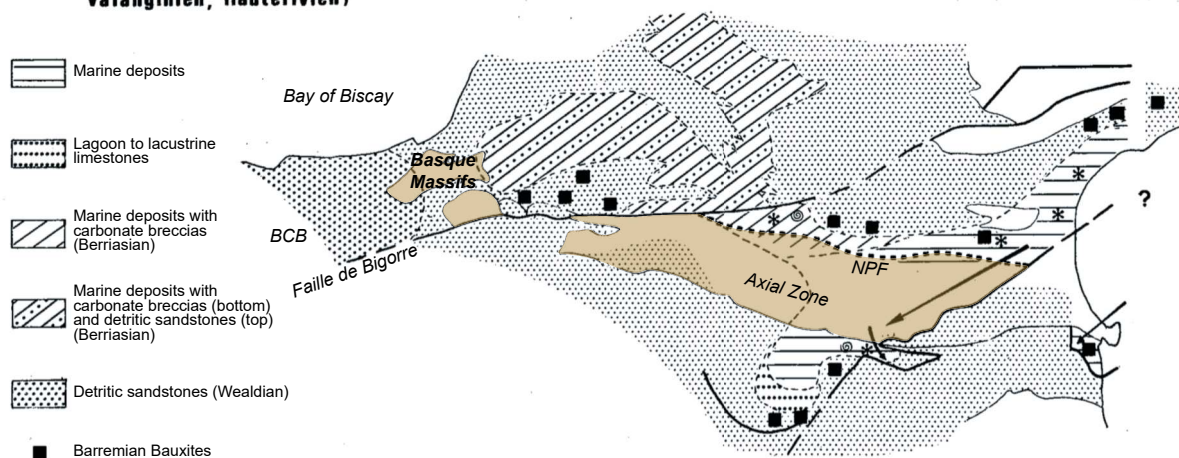


Figure I-15: Distribution of Neocomian (Berriasian to Barremian) facies in the present-day Pyrenean and Eastern Cantabrian segments (modified after Souquet et al., 1977). Pyrenean massifs are represented in brown. Note the transition from marine to continental facies from east to west.

The Aptian to Early Albian (Urgonian) corresponds to a general sea level rise that led to the formation of transgressive carbonate platforms on basin margins and deposition of marls (e.g. “marnes de Ste Suzanne”) in the deepest parts (Bouroullec et al., 1979; García-Mondéjar, 1979; Pascal, 1985; Peybernès, 1979; Puigdefàbregas & Souquet, 1986; Rat, 1959) throughout the entire Cantabrian and Pyrenean domains, suggesting a connection between the Atlantic and Tethys oceans at that time.

The Upper Albian to Cenomanian (supra-Urgonian) corresponds to the uniformization and the deepening of the depositional environment along the E-W Pyrenean-Cantabrian axis. The troughs are characterised by the deposition of deep water turbidites (the so-called “Flysch Noir” of Souquet et al., 1985) while the through margin sedimentation corresponds to deltaic or alluvial (Utrillas Fm) facies sediments overlain by Upper Cenomanian carbonate platforms (e.g. Boirie & Souquet, 1982; Camara, 1997; Debroas, 1978, 1990; Feuillée, 1971; Meschede, 1987). The Albo-Cenomanian extensional event is responsible for extreme crustal thinning and exhumation of granulite and mantle rocks (Fig. I-16; Debroas et al., 2010; Jammes et al., 2009; Lagabrielle et al., 2010; Mendia & Ibarra, 1991; Roca et al., 2011; Vielzeuf & Kornprobst, 1984). Depending on the authors and the location in the system, the exhumation of deep crustal and mantle rocks have been proposed to occur either at the seafloor or underneath the Jurassic to Lower Aptian sedimentary cover which was detached in the Upper Triassic decoupling horizon (evaporites) (Clerc et al., 2012; Corre et al., 2016; DeFelipe et al., 2017; Jammes et al., 2010c; Lagabrielle et al., 2010; Lagabrielle & Bodinier, 2008; Masini et al., 2014). The mantle rocks are generally represented by heterogeneously serpentized lherzolite bodies embedded within the Albo-Cenomanian turbidites or the Upper Triassic evaporites (Clerc et al., 2012; DeFelipe et al., 2017; Lagabrielle & Bodinier, 2008; de Saint Blanquat et al., 2016; Walgenwitz, 1976) and are crosscut by ophicalcite veins (Clerc & Lagabrielle, 2014; DeFelipe et al., 2017). The exhumation of mantle rocks occurred coevally with alkaline magmatism (Azambre & Monchoux, 1998; Azambre & Rossy, 1976; Castañares et al., 2001; Castañares & Robles, 2004; Golberg et al., 1986; Montigny et al., 1986; Rossy, 1988) and an episode of HT/LP metamorphism (< 600°C and < 4 kbar) (Albarède & Michard-Vitrac, 1978; Choukroune, 1972; Clerc et al., 2015; Golberg & Leyreloup, 1990; Golberg & Maluski, 1988; Martínez-Torres, 1992; Montigny et al., 1986; Ravier, 1959; Robert, 1971). The metamorphism (110Ma to 85Ma) together with hydrothermalism (Bernus Maury, 1984; Boulvais, 2016; Corre et al., 2018; Cuevas & Tubía, 1999; Dauteuil & Ricou, 1989; Golberg & Leyreloup, 1990; Iriarte, 2004; Poujol et al., 2010; Scharer et al., 1999) affected the Upper Triassic to Cenomanian sediments but yet remains elusive in the basement rocks (see publication of Clerc & Lagabrielle, 2014 and comments of Olivier, 2015). The Jurassic to Lower Aptian marls and carbonates display syn-metamorphic

ductile deformation in the eastern BCB and in the Central and Eastern Pyrenees (e.g. Clerc et al., 2016; Ducoux, 2017; Vauchez et al., 2013).

The structural evolution associated with this polyphase rifting remains debated (e.g. Canérot, 2017; Clerc et al., 2012; Tugend et al., 2014) in particular because the kinematics associated with the Iberia-Eurasia plate boundary is yet ill-constrained (see 3.2.4.1). In the Pyrenean domain, the Late Jurassic to Lower Cretaceous depocenters appear to be controlled by NE-SW structures (e.g. Biteau et al., 2006; Delfaud, 1970; James et al., 1996; Jammes et al., 2009; Muller & Roger, 1977; Puigdefàbregas & Souquet, 1986), while in the Cantabrian segment, sedimentation took place in NW-SE and E-W oriented basins controlled by WNW-ESE to NW-SE and NE-SW structures, potentially reactivating Late Variscan faults (Feuillée & Rat, 1971; Lepvrier & Martínez-García, 1990; del Pozo, 1969; Pujalte, 1981; Salomon et al., 1982). The Albo-Cenomanian turbidites have been proposed to be deposited either in lozenged-shaped basins (Debroas, 1990; Souquet et al., 1985) or in E-W trending basins bounded by WNW-ESE (e.g. NPF, Bilbao fault), NW-SE, and NE-SW structures (García-Mondéjar et al., 1996; Pascal, 1985; Salomon et al., 1982), and controlled by major NNE-SSW transverse structures such as the Toulouse, Pamplona, Hendaya and Santander transfer faults (Fig. I-16; Boillot, 1984; Roca et al., 2011; Tugend et al., 2015).

Kinematic indicators from field observations argue for NNE-SSW direction of extension (Granado et al., 2018; Jammes et al., 2009; Masini et al., 2014; Tavani et al., 2018; Tugend et al., 2014; Vauchez et al., 2013) whereas the sedimentary record has been proposed to better fit with NW-SE extension (Canérot, 2017). Besides, the study of the anisotropy of magnetic susceptibility (AMS) in the Cantabrian segment (and Cameros basin) argue for NNE-SSW extension from Late Jurassic to Albian except at Aptian time where E-W extension is suggested (Soto et al., 2008). In contrast, an AMS study in the Mauléon basin (Pyrenean segment) argues for NW-SE directed extension (Oliva-Urcia et al., 2010).

3.2.4.3 Key features and remaining questions

The polyphase Mesozoic rifting episode strongly modified the crustal architecture along the Iberia-Eurasia plate boundary. However, although the rift basins have been well preserved in the present-day orogenic domain, questions remain about their kinematics and their structural evolution throughout the Mesozoic. As such, this study will attempt to divide the rifting episode in different phases based on the stratigraphic evolution described above. Among these extensional events, the Aptian to Cenomanian rifting event is largely represented in the Pyrenees. However, the mode of crustal deformation that led to the formation of the basins remains debated. Whereas some authors (Clerc et al., 2016; Clerc & Lagabrielle, 2014;

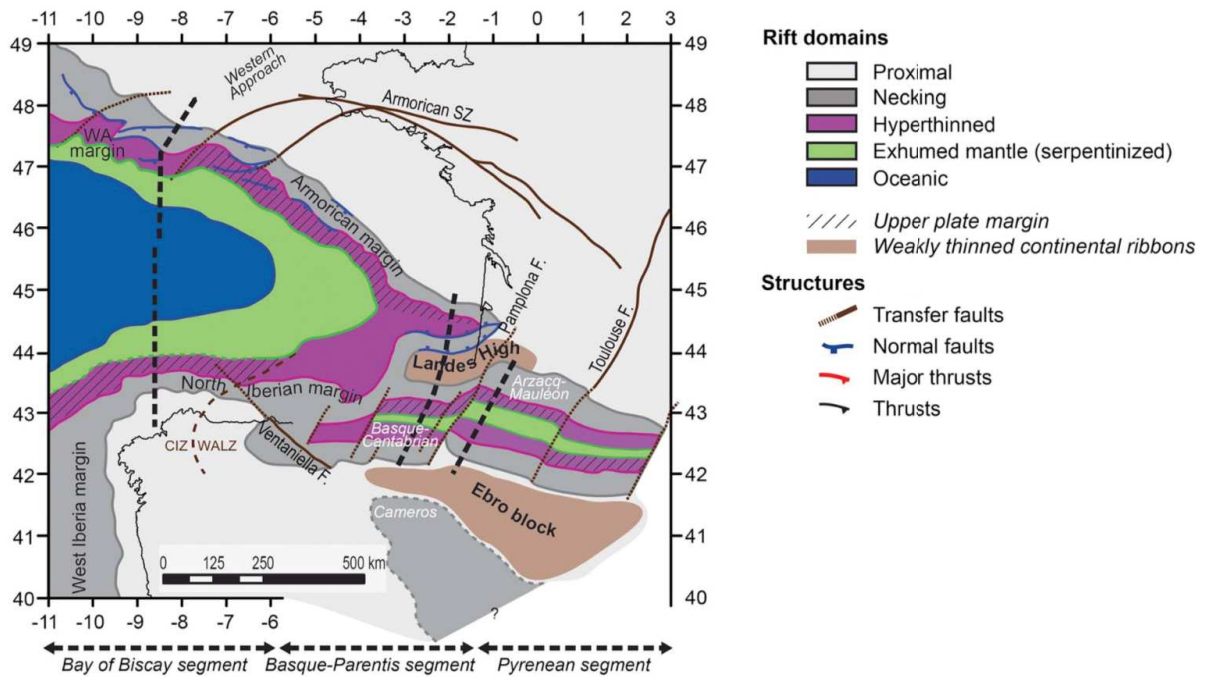


Figure I-16: Map of rift domains prior to the onset of compression (before Santonian) in the Pyrenean-Cantabrian and Bay of Biscay extensional systems (modified after Tugend et al., 2014). Note the aligned E-W striking rift systems leading to mantle exhumation and bounded by major NNE-SSW transfer/transform faults.

Corre et al., 2016; Teixell et al., 2016) propose symmetric, ductile-governed crustal extension, others suggest an asymmetric, frictional-dominated mode of deformation (Cochelin et al., 2018; Jammes et al., 2009; Masini et al., 2014; Tugend et al., 2014; Vacherat et al., 2016). Furthermore, questions remain about the existence and the role of the strike-slip NPF in the Western Pyrenees and in the Cantabrian segment (e.g. Floquet et al., 1988; Hall & Johnson, 1986; Mathey et al., 1999; Peybernes, 1978).

3.2.5 Late Cretaceous to Miocene convergence

3.2.5.1 Geodynamic context

In contrast to the Jurassic to Cenomanian geodynamic evolution, the Santonian to Miocene evolution of Iberia is well constrained by oceanic magnetic anomalies A34 and younger (e.g. Macchiavelli et al., 2017). As such, the northward migration of the African plate and the onset of N-S convergence in Western Europe is generally supposed to initiate at 83.5 Ma (e.g. Capote et al., 2002; Macchiavelli et al., 2017; Roest & Srivastava, 1991; Rosenbaum et al., 2002). During convergence, Macchiavelli et al. (2017) described a first phase of NE-SW oriented shortening at the Iberia-Eurasia plate boundary followed at the Paleocene-Eocene boundary by NW-SE convergence until Early Miocene.

3.2.5.2 Evolution of the Pyrenean-Cantabrian system

The onset of shortening in the Pyrenean-Cantabrian system is best recorded in the Eastern and Central Pyrenees. There, authors recognized shortening at Santonian-Campanian with the cessation of turbidites associated with basin inversion in the North Pyrenean Zone (Boillot & Capdevila, 1977; Grool et al., 2018) while first syn-orogenic flysch were deposited in the Southern Pyrenean Zone (Boillot & Capdevila, 1977; Garrido-Megias & Rios-Aragues, 1972) together with the reactivation of pre-Santonian extensional faults detached in the Triassic evaporites (McClay et al., 2004). The main orogenic phase lasted from Eocene to Miocene (Fig. I-17), as attested by crustal thickening and by the exhumation of the basement recorded by thermochronological data (e.g. Bosch et al., 2016; DeFelipe, 2017; Fillon et al., 2013, 2016; Fitzgerald et al., 1999; Jolivet et al., 2007; Mouthereau et al., 2014; Vacherat et al., 2016; Whitchurch et al., 2011), by subsidence analysis (Gómez et al., 2002; Grool et al., 2018) and by the deposition of flysch throughout the South Pyrenean Zone (Burbank et al., 1992; Labaume et al., 1985). Based on thermochronological data analysis, Whitchurch et al. (2011) proposed that the eastern part of the Pyrenees was exhumed before the western part, suggesting a diachronous closure of the Pyrenean basins.

At shallow level, contractional deformation was accommodated by the inversion of former rift basins (e.g. Lagabrielle & Bodinier, 2008; Roca et al., 2011; Seguret & Daignières, 1985, 1986; Tugend et al., 2014) and by the formation of north-dipping and south-dipping E-W striking thrust faults (e.g. Ábalos, 2016; Choukroune et al., 1973), locally reactivating Hercynian or Permian structures (e.g. Cochelin, 2016; Soula et al., 1986). In the Pyrenees, south-vergent nappe stacking (Central Eastern Pyrenees, Muñoz, 1992) or nappe imbricates (Western Pyrenees, Teixell, 1998) led to the formation of the Axial Zone (Mattauer & Henry, 1974) and to the formation of an asymmetric double wedge architecture (Choukroune, 1989; Muñoz, 1992; Roure et al., 1989). At depth, part of the shortening was suggested to be accommodated by the northward subduction of the Iberian plate underneath the Eurasian plate in the Pyrenean-Cantabrian system (e.g. Choukroune, 1989; Muñoz, 1992; Pulgar et al., 1996). Recent seismic imaging confirmed the existence of a subducted slab in the Pyrenean-Cantabrian system (e.g. Chevrot et al., 2014; Díaz et al., 2012; Pedreira et al., 2007; Wang et al., 2016), excepted east of the Toulouse fault, where the slab has not been recognized (Chevrot et al., 2018). Tugend et al. (2014) suggested that the slab was composed of the hyperextended domain of the former rift systems, in contrast to Teixell et al. (2018) who involve mainly the lower crust as subducting material (Fig. I-18). Note that, west of the Santander transfer zone, the north-dipping slab has been proposed to face the south-dipping oceanic crust of the inverted Bay of Biscay (e.g. Pedreira et al., 2015).

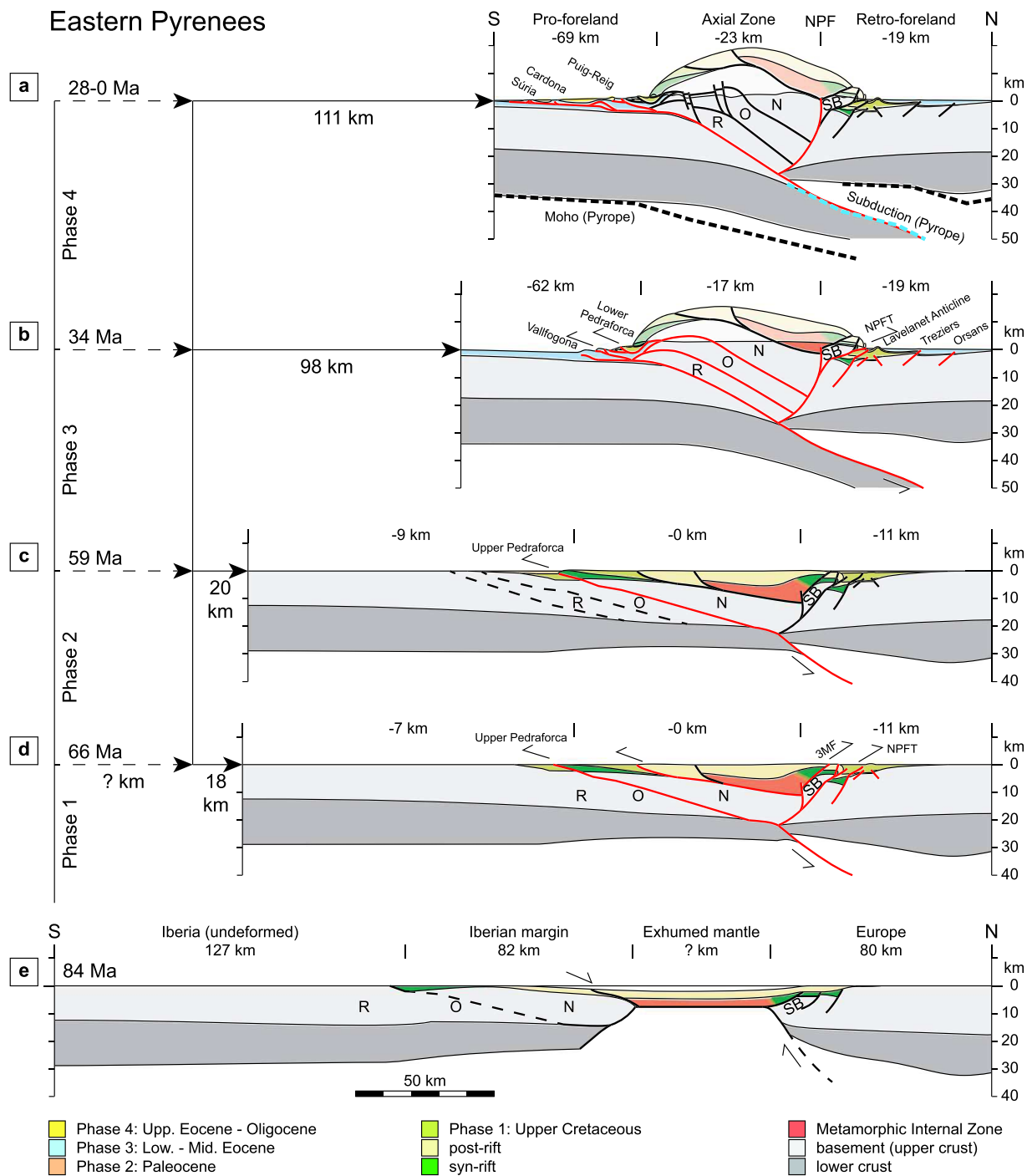


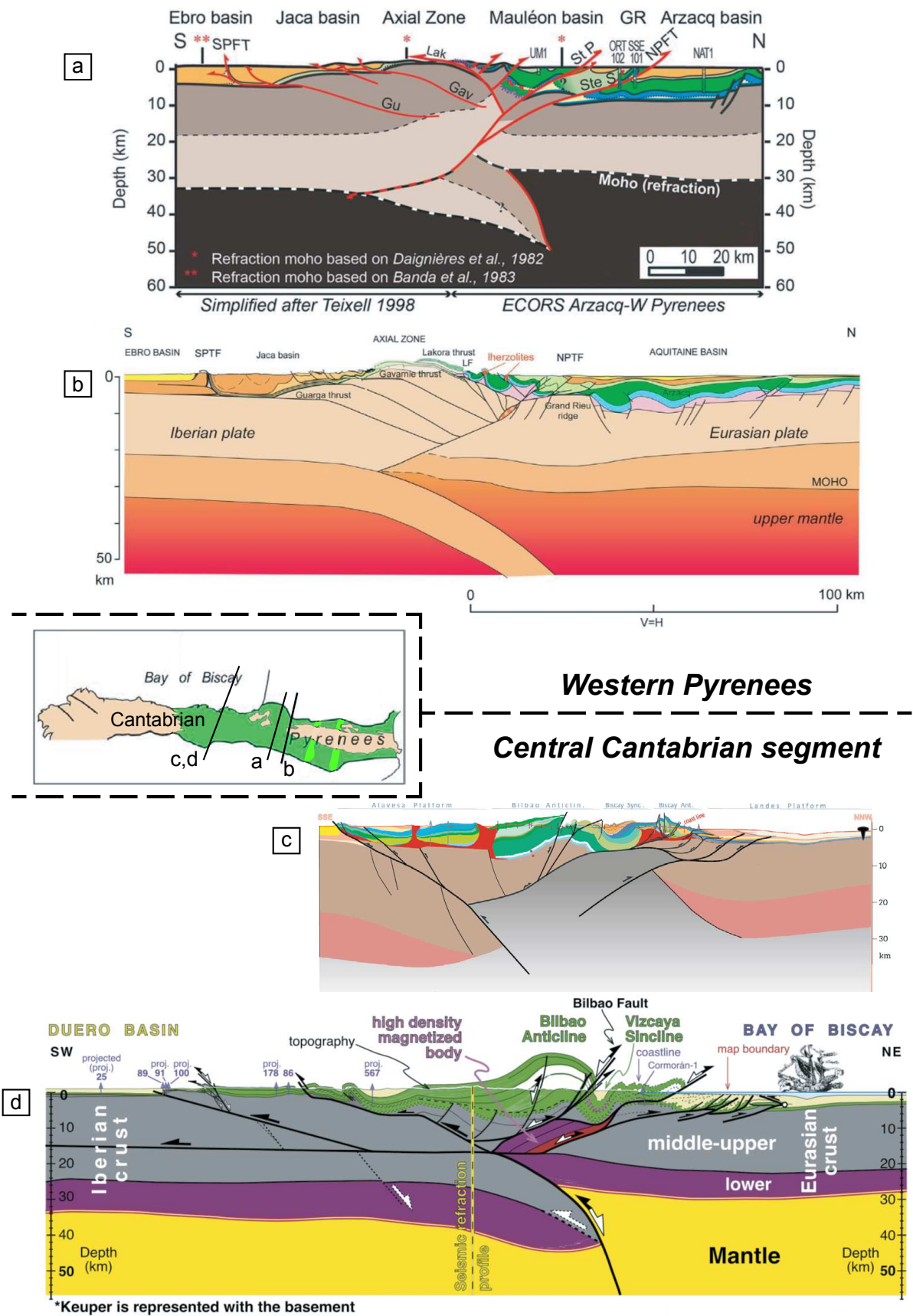
Figure I-17: Evolution of the Eastern Pyrenees from Santonian to present-day according to Grool *et al.* (2018). R: Rialp; O: Orri; N: Nogueres; SB: St Barthélémy Massif; 3MF: 3M Fault; NPFT: North Pyrenean Frontal Thrust. Note the first phases of inversion leading to the closure of the exhumed mantle domain followed from Paleocene to Eocene by the formation of south-vergent nappe stacking in the future Axial Zone. The Metamorphic Internal Zone (HT/LP metamorphic rocks) was supposedly flooring the exhumed mantle domain.

The amount and timing of shortening remains debated but most of the studies consider that the eastern part of the Pyrenean-Cantabrian system underwent more shortening than the western part (e.g. Central Eastern Pyrenees: Mouthereau et al., 2014: 142 km; Macchiavelli et al., 2017: 125 km; Rosenbaum et al., 2002: 206 km, Canérot, 2016: 150 km; Muñoz, 1992: 147 km; Beaumont et al., 2000: 165 km; Grool et al., 2018: >111 km; Western Pyrenees: Teixell et al., 2016: 114 km; Rosenbaum et al., 2002: 144 km; Mattauer & Henry, 1974: 50 km; Central Cantabrian: Macchiavelli et al., 2017: 90 km; Quintana et al., 2015: 97<122 km; Pedrera et al., 2017: 34 km). However, the width of the hyperextended (or exhumed mantle) domain is difficult to constrain as it has been subducted (Grool et al., 2018; Mouthereau et al., 2014; Tugend et al., 2014). This led Chevrot et al. (2018) to propose that the apparent variation in the amount of shortening might reflect diffuse deformation toward the east and localised deformation in the west in relation with a variation in the width of the exhumed mantle domain prior to reactivation.

3.2.5.3 Key features and remaining questions

The formation of the orogenic belt led to the inversion of the Mesozoic rift basins in the BCB and the North Pyrenean Zone but no syn-convergence thermal overprint has been recorded by geothermometres, allowing to preserve the syn-rift HT/LP metamorphic event. Besides, the orogenic evolution has been widely studied via field observations and a large dataset of seismic, structural and thermochronological data. However, the first order architecture of the orogen has been challenged by recent seismic tomography showing along-strike variations (Chevrot et al., 2018). Moreover, rift-inheritance has been suggested to influence the architecture of the Pyrenean range (Jammes et al., 2014; Jourdon et al., 2019). However, the role of rift architecture in controlling the mode of contraction deformation (e.g. diffuse vs. localised; thin- vs. thick-skinned) remains poorly understood.

Figure I-18: *Cross-sections across the Pyrenean-Cantabrian system highlighting differences between recent lithospheric-scale models. Insert map after Teixell et al. (2018). Cross-section (a) after Tugend et al. (2014), (b) after Teixell et al. (2018), (c) after Pedrera et al. (2017), (d) after Quintana et al. (2015). Note the difference of subducted material between (a) and (b), and the difference in the orogenic architecture between (c) and (d).*



4. SCIENTIFIC QUESTIONS

The observation of rifted margins worldwide depicts a wide variety of architecture. This variation is due to syn-rift evolution but can be as well influenced by the inherited pre-rift architecture (see Figs. I-2 and I-3). The mode of lithospheric extension and its associated thermal evolution can vary with depth, along-dip and along-strike, and may result in a segmented margin (e.g. Lizarralde et al., 2007; Péron-Pinvidic et al., 2017). Following the Wilson cycle concept, these segmented rifted margins will be eventually reactivated and integrated in an orogenic system. The aim of this PhD is twofold: (1) understanding the role of inheritance and rift segmentation for rifting and reactivation, and (2) characterising the thermal evolution associated with hyperextension. In both cases, the Pyrenean-Cantabrian orogenic system will be used as a natural laboratory.

The evolution of rift systems is usually observed through dip sections and several models have been built based on natural examples and analogue modelling (see section I.2.1). Besides, the reactivation of rifted margins during the formation of a collisional orogen has been widely studied. However, despite being recognized in many passive margins worldwide, rift segmentation and related structures remain poorly understood features. As such, their fate and role during reactivation is unknown. The Pyrenean-Cantabrian collisional orogen has been described as a reactivated highly segmented rift system. However, no study attempted to characterise the evolution and the architecture associated with the most striking feature that is the Pamplona transform fault/transfer zone, at the boundary between the Pyrenean and Cantabrian segment. As such, two questions will be developed in **chapter II**:

- (A) What is the architecture of the inverted Pyrenean-Cantabrian junction?*
- (B) What was the pre-convergence architecture of the Pyrenean-Cantabrian junction?*

At a regional scale, rift inheritance and in particular rift domain boundaries (Sutra et al., 2013) have been suggested to control the reactivation and the architecture of the orogen (Mohn et al., 2014; Tugend et al., 2014). Yet, the lateral variation of rift domains in relation with rift segmentation might influence the reactivation pattern and the subsequent orogenic architecture. Therefore, main questions addressed in **chapter III** are:

- (C) Do rift domains influence the mode of deformation during reactivation? Does deformation vary through time in relation with inheritance?*
- (D) Do rift segment boundaries influence the reactivation pattern and the final orogenic architecture?*

Besides structural segmentation, the Pyrenean-Cantabrian system depicts an along-

strike variation of the distribution and grade of the syn-rift HT/LP metamorphic rocks. The thermal state of rift basins has been shown to depend on many parameters among which the upwelling of the asthenosphere represents the main source of heat during hyperextension. Yet, recent studies pointed out the decoupling between crustal thickness and location of the maximum top basement heat flow depending on the mode of lithospheric extension (see section I.2.3). As such, I will investigate in **chapter IV** the following two questions:

(E) *What is the influence of asymmetric rifting on the thermal evolution of a hyperextended domain?*

(F) *What do T_{max} values tell us about the thermal state of rift systems?*

5. STRUCTURE OF THE MANUSCRIPT

Chapter I introduces and summarizes the main scientific breakthroughs concerning inheritance and reactivation, the segmentation of rift systems and the thermal evolution during lithospheric extension. The principal results and remaining questions about the evolution of the Pyrenean-Cantabrian study case are then exposed, followed by the main questions addressed in this PhD. The following **chapters II, III and IV** correspond to the scientific papers answering these questions.

Chapter II investigates the architecture of the Pyrenean-Cantabrian junction and presents a new interpretation for the structural and kinematic evolution of the mid-Cretaceous rift system. This work, entitled “*Nature, origin and evolution of the Pyrenean – Cantabrian junction*”, will be submitted to the *International Journal of Earth Sciences*.

Chapter III explores the role of rift-inheritance and rift segmentation for the Pyrenean-Cantabrian orogenic architecture. Besides, it investigates the role of rift domains on the style of deformation during the reactivation and the influence of segmentation on the final orogenic architecture. This paper entitled “*Role of rift-inheritance and segmentation for orogenic architecture: example from the Pyrenean-Cantabrian system*” is in preparation for *Tectonics*.

Chapter IV deals with the thermal evolution associated with hyperextended rift systems. This study combines numerical modelling and data from the Arzacq-Mauléon study case to assess the role of rift asymmetry for the syn-rift thermal evolution. This work has been submitted to *Geochemistry, Geophysics, Geosystems* with the title “*Thermal evolution of asymmetric hyperextended magma-poor rift systems: results from numerical modelling and Pyrenean field observations*”.

Chapter V summarizes the main results and discuss their implications for the Pyrenean-Cantabrian system and for geological systems in general.

A final chapter includes the main conclusions of the work and an outlook discussing how the results of the PhD study can impact future research in the Pyrenean-Cantabrian system. Finally, the annexes show the supplementary materials of chapters II and IV, several field observations and cross-sections of the study area, seismic interpretations of the Basque-Cantabrian basin, new descriptions of the Ainhice borehole (Mauléon basin) and preliminary results from a UAV magnetic campaign on the Labourd massif.

CHAPTER II:

***NATURE, ORIGIN AND EVOLUTION OF THE
PYRENEAN-CANTABRIAN JUNCTION***

NATURE, ORIGIN AND EVOLUTION OF THE PYRENEAN-CANTABRIAN JUNCTION

International Journal of Earth Sciences, in prep.

Rodolphe Lescoutre¹, Gianreto Manatschal¹, Josep A. Muñoz²

¹*IPGS, EOST-CNRS, Université de Strasbourg, Strasbourg, France*

²*Grup de Geodinàmica i Anàlisi de Conques, Institut GEOMODELS, Departament de Geodinàmica i Geofísica, Facultat de Geologia, Universitat de Barcelona, Barcelona, Spain*

ABSTRACT

We investigate the present-day architecture of the Pyrenean-Cantabrian junction corresponding to a boundary between rift segments using seismic interpretation, field data and borehole information. This junction was formerly attributed to a major NNE-SSW striking Pamplona fault decoupling the Basque-Cantabrian and Mauléon rift systems. Cross-sections allow to characterize the architecture of former Late Triassic to mid-Cretaceous rift basins and to study their role during Late Cretaceous to Miocene convergence. We define two main phases of rifting corresponding to the ill-defined Late Jurassic to Barremian basins (Weald-Purbeck) and the Aptian to Cenomanian basins, the latter opening in a NNE-SSW direction bounded by WNW-ESE striking structures and coeval with mantle exhumation and high-temperature/low-pressure metamorphism. We show that the Aptian-Cenomanian rifting in the Basque-Cantabrian basin reactivated previous structures but formed an independent network of basins during hyperextension. Results show that no major E-W strike-slip movement may have occurred in the study area after Triassic time and that both the Mauléon and Basque-Cantabrian basins overlapped north and south of the Basque massifs, arguing against a major Pamplona fault and suggesting the existence of a relay system during Aptian to Cenomanian. During convergence, the thick evaporites decoupling horizon was responsible for the transport and allochthony of the former rift basins over large distance along the reactivated Leiza fault, the South Pyrenean Basal Thrust and the North Pyrenean Frontal Thrust (thin-skinned tectonics). Crustal-scale cross-section depicts the allochthony of the Basque massifs forming a crustal wedge over the Aquitaine and Ebro crusts. This study emphasizes the role of inheritance during rifting and reactivation, and provides a new syn-rift architecture which has implication for the Alpine reactivation. Finally, these results have strong implications for the Iberia-Eurasia plate boundary and the kinematics of the North Pyrenean basins.

1. INTRODUCTION

The kinematics of the Iberia-Eurasia plate boundary during Late Jurassic to Late Cretaceous is heavily debated due to the lack of reliable constrains and the ill-defined pre-chron 34 restoration of the southern North Atlantic (Barnett-Moore et al., 2016a; Nirrengarten et al., 2018). While some studies propose 400km of sinistral strike-slip and pull-apart basins in the Pyrenean domain (Canérot, 2017; Choukroune & Mattauer, 1978; Choukroune, 1992; Oliva-Urcia et al., 2010), others suggest limited and diffuse transtension followed by N-S extension (Jammes et al., 2009; Roca et al., 2011; Tugend et al., 2015). The absence of strong criteria from onshore geology makes it difficult to arbitrate between the different models and to constrain the timing of deformation between the two plates (e.g. Tavani et al., 2018; Teixell et al., 2018).

The Pyrenean-Cantabrian junction (Fig. II-1) represents a key area as it delimits two Mesozoic rift systems subsequently inverted during the Pyrenean orogeny. Moreover, Variscan to Alpine structures and rock sequences are exposed in the Basque Country, allowing to analyse the deformation and to study the role of inheritance during subsequent rifting and reactivation. However, apart from interpretations implying a so-called Pamplona transfer/transform fault (Rat, 1988; Razin, 1989; Richard, 1986), no studies integrating small and large-scale observations were carried out in order to understand the timing, nature and kinematics of this system and how far it is controlled by inheritance during its evolution. This study addresses questions such as:

- *How do the Pyrenean and Cantabrian systems connect? Do they interfere through time or do they evolve independently?*
- *How is the deformation partitioned in this area during both extensional and compressional events?*
- *What is the role of inheritances?*
- *How was reactivation controlled by the inherited rift system?*

In this study, new N-S and E-W striking cross-sections and a geological map integrating new and existing field data are presented in order to characterise the deformation affecting the Basque massifs and to discuss the nature, origin and evolution of the junction between the Cantabrian and Pyrenean systems. We describe the present-day architecture and define the role of inheritance in controlling the present-day architecture. Finally, we discuss the implications for the location and kinematics of the Iberia-Eurasia plate boundary.

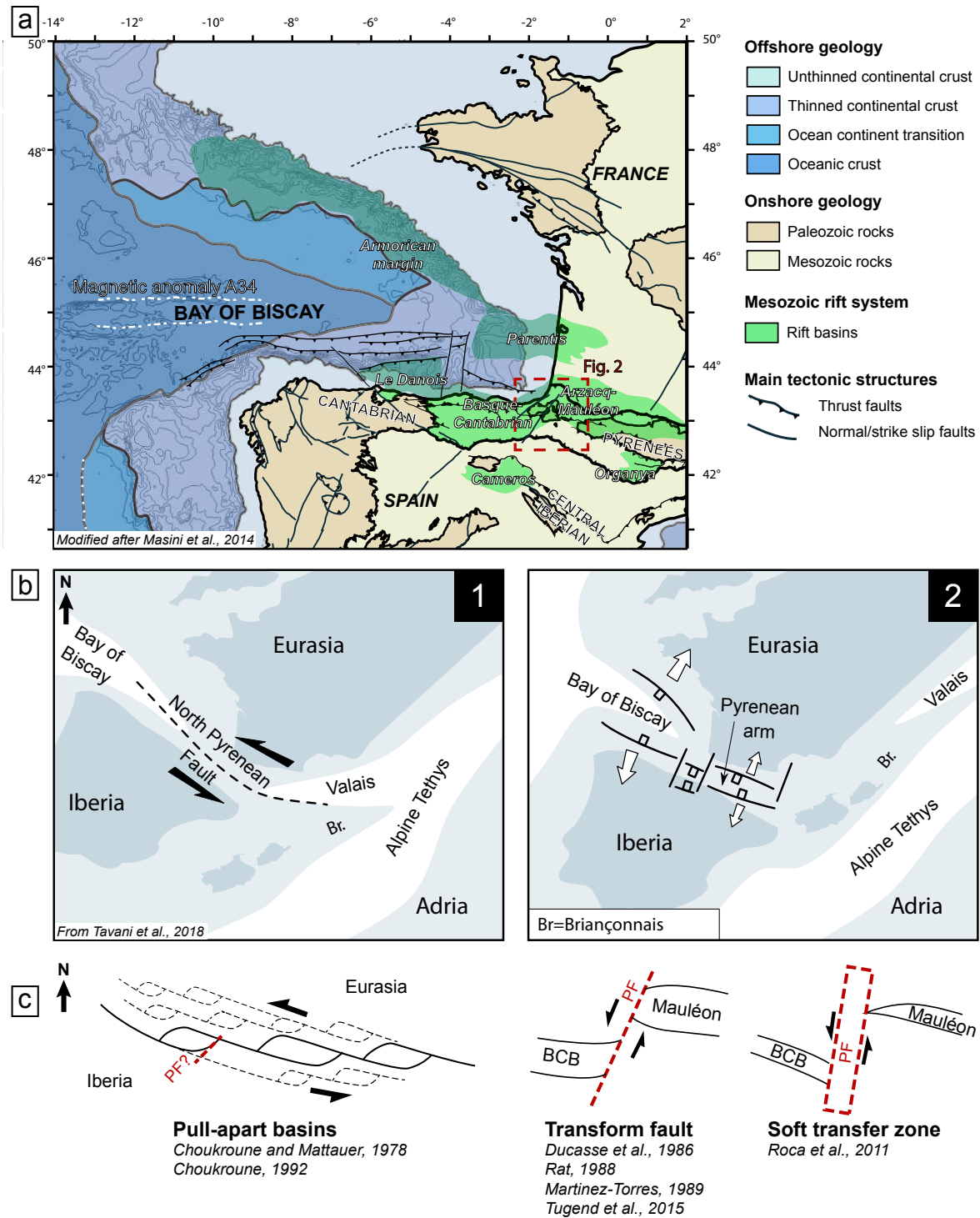


Figure II-1: a) Map of the Mesozoic rift basins between France and Spain. Location of the study area is indicated by the red square. Modified after Masini et al. (2014). b) Eurasia – Iberia kinematic scenarios at mid-Cretaceous time. Strike-slip scenario (1) after Stampfli & Borel (2002) and orthogonal rifting scenario (2) after Manatschal & Müntener (2009). Modified after Tavani et al. (2018). c) Models for the Pyrenean-Cantabrian junction during Aptian to Cenomanian. PF: Pamplona fault; BCB: Basque-Cantabrian basin.

2. GEOLOGICAL SETTING

2.1 Evolution of the Cantabrian and Pyrenean systems

2.1.1 Variscan and late to post Variscan phase

During the Variscan orogenic accretion, the future Pyrenean and Cantabrian systems are located in the foreland of the orogen (Ballèvre et al., 2014; Delvolvé et al., 1998) where flysch sediments (“Culm” facies) are deposited while granitic magmatism and HT/MP metamorphism took place in the hinterland (Catalán et al., 2007; Cochelin, 2016). The orogen is subsequently deformed and depicts an orocline formed by the present-day Iberian, Armorican and Central massifs (Ballèvre et al., 2014; Catalán et al., 2007). The Late Variscan stage is related to N-S to NW-SE compression (in present-day coordinates) associated with dextral strike-slip displacement and dome formation between Iberia-Corsica and European blocks (Arthaud & Matte, 1975; Cochelin, 2016). A Late Variscan to post-Variscan HT/LP event (300Ma according to Guitard et al., 1996) is responsible for granulite facies metamorphism affecting the pre-Carboniferous metasediments. This event is contemporaneous to or followed by Permian dextral transpression (Denèle et al., 2011) and associated with the deposition of a volcano-sedimentary sequence and related to the emplacement of intrusive rocks (Arthaud & Matte, 1975; Bixel & Lucas, 1987; Lago et al., 2004).

At the present-day Pyrenean – Cantabrian junction in the Basque Country (Figs. II-1 and II-2), various generations of Variscan folds and a major NE-SW trending thrust dipping toward the east between the Cinco Villas and Labourd massifs have been described (Campos, 1979; Heddebaut, 1973; Mohr & Pilger, 1965; Muller & Roger, 1977). Folded detritic flysch of the “Culm” facies of mid-Carboniferous age compose the major part of the Cinco Villas massif (Campos, 1979). Late to post-Variscan granulites are at present exposed within the Ursuya unit or as smaller blocks within the Cretaceous basins. The Aya granite pluton, emplaced at 267Ma within Devonian metasediments, is cropping out in the Cinco Villas massif together with its contact metamorphism (e.g. Denèle et al., 2011). On the Labourd massif, clay to red sandstone deposits of the N20 Bidarray basin have been attributed to the Permian transtensional event (Bixel & Lucas, 1987).

The post-Variscan, Permo-Triassic episode corresponds to an isostatically equilibrated lithosphere on which widespread Lower Triassic fluvial sandstones and Jurassic shallow marine sediments are deposited without showing evidence for major aggradation. However,

little is known about the crustal position of the Ursuya granulites prior to onset of rifting. While some studies (Cochelin, 2016; Ducasse et al., 1986a; Guitard et al., 1996; Vissers, 1992) propose a scenario in which the granulites are exhumed during Late Variscan to Permian, other studies propose a mid-Cretaceous age for the exhumation (Jammes et al., 2009; Masini et al., 2014). Moreover, a strong control of Variscan structures on the Mesozoic evolution of the Basque Country was suggested by Arthaud & Matte (1975), García-Mondéjar et al. (1996) and Muller & Roger (1977) based on their orientation. However, no reactivated Variscan structures have been evidenced in the study area, which question their role controlling Mesozoic rift structures.

2.1.2 Rifting episodes

The kinematics of the Pyrenean-Cantabrian system is ill-defined during Jurassic and Early Cretaceous rifting due to the lack of well-defined magnetic anomalies and pin points (Fig. II-1). After a poorly constrained Triassic transtensional event (e.g. Soula et al., 1979), the opening of the southern North Atlantic initiating in Late Jurassic involved a sinistral displacement of Iberia with respect to Eurasia. It led authors (Choukroune & Mattauer, 1978; Choukroune, 1992) to propose a sinistral strike-slip deformation between the Iberian and Eurasian plates resulting in the formation of pull-apart basins belonging to a Late Jurassic to Late Cretaceous single rift event based on the kinematic scenario of Olivet (1996). In contrast, based on field kinematic constraints, other studies (Jammes et al., 2009; Tugend et al., 2015) proposed a main Early to Late Cretaceous north-south extensional event that followed a first phase of transtensional deformation that may be responsible for the formation of Late Jurassic to Early Cretaceous basins. In this study, we will describe the different rifting events and discuss their kinematic evolution based on the description of the Cantabrian-Pyrenean junction (Figs. II-1 and II-2).

2.1.2.1 Triassic rifting

The Early to Middle Triassic is represented by the deposition of Lower Triassic continental detritic sandstones that are overlain by marine limestones belonging to the Muschelkalk Fm. This evolution can be observed throughout the Eurasian and Iberian plates. It is followed by the deposition of claystones and evaporites of the Keuper Fm. (Stevaux & Winnock, 1974) in confined basins. This rifting event, which remains ill-defined, is proposed to have formed along E-W to NW-SE directed transtensional systems related to the opening of the Neotethys and/or the Central and/or northern North Atlantic (Boess & Hoppe, 1986; Doré et al., 1999; Scotese & Schettino, 2017).

In the Pyrenean-Cantabrian system, these basins were controlled by N50-60, N80 and N110 to N140 normal faults in the Aquitaine basin (Curnelle, 1983; Muller & Roger, 1977;

Peybernès & Souquet, 1984; Puigdefàbregas & Souquet, 1986; Rat, 1988; Soula et al., 1979) and NW-SE faults in the Cantabrian system (García-Mondéjar et al., 1986) that may have been used as pathways for the Late Triassic alkaline magmatism (ophites).

The Lower Triassic sandstones and the Upper Triassic evaporites are wide spread in the Cantabrian and Pyrenean domains. However, the extent and importance of this extensional event remains poorly constrained as part of the Late Triassic evaporites have been remobilized during subsequent tectonic events. The wide spread transgressional carbonate platform of the Jurassic marks the transition to an open sea shelf environment during a period with little tectonic activity (Biteau et al., 2006).

2.1.2.2 Late Jurassic to Barremian rifting

This tectonic phase, which roughly takes place at the initiation of rifting along the western margin of the Iberian plate (Barnett-Moore et al., 2016b; Nirrengarten et al., 2018), corresponds to the deposition of the Purbeck-Weald shallow marine to continental deposits occurring in various locations of Western Europe and especially in Spain and France (e.g. BCB: Tavani et al., 2013, Ábalos, 2016, Ábalos et al., 2008; Cameros: Casas Sainz, 1993; Parentis: Ferrer et al., 2012; Pyrenees: Peybernès, 1982).

In the study area, Late Jurassic to Barremian basins have been described in the BCB (e.g. Amiot, 1982; Campos, 1979; Del Pozo, 1971; Lamare, 1936; Llanos, 1980; Pujalte, 1977; Soler, 1971) and in the Pyrenees (e.g. Canerot et al., 1978; Combes et al., 1998; Delfaud, 1970; Peybernes, 1978). In the Western Pyrenees, they appear as disconnected small basins (e.g. Delfaud, 1970) associated with the formation of bauxites on the Jurassic limestones at the southern margin of the basin (Chainons Béarnais), followed by formation of lignite and deposition of Wealdian carbonates (Canerot et al., 1978; Combes et al., 1998; Peybernes, 1978). A broader basin (central BCB) with marine deposits has been described in the BCB together with smaller basins (east of Hendaya fault) (e.g. Amiot, 1982; Soler, 1971). The depositional environment shows a high variability with marine to lagoonal or lacustrine deposits going from limestones to shale, anhydrite and sandstones (Campos, 1979; Delfaud, 1970; Peybernes, 1978; Soler, 1971). In the Arzacq and Mauléon basins, authors (Delfaud, 1970; Puigdefàbregas & Souquet, 1986; Richard, 1986) suggest that these basins were related to basement subsidence accommodated along N10 to N50 and N110 structures. In the BCB, Salomon et al. (1982) showed similar orientations and geometries associated with variations in depocenter thicknesses that they related to subsiding rotational blocks.

Because the kinematics and structures governing these marine to continental basins are poorly constrained, their importance for the subsequent tectonic events are difficult to estimate.

Yet, their sparse distribution in Western Europe seems to reveal a complex pre-Aptian diffuse Iberia-Eurasia plate boundary that needs, in detail, to be defined.

2.1.2.3 Aptian to Cenomanian rifting

This period corresponds to oceanic accretion in the Bay of Biscay and to the formation of deep E-W striking hyperextended basins within the Cantabrian and Pyrenean systems. This hyperextension event leads locally to mantle exhumation (Lagabrielle et al., 2010), alkaline magmatism (Azambre & Rossy, 1976; Montigny et al., 1986), and High Temperature – Low Pressure (HT/LP) metamorphism of the sedimentary cover (Albarède & Michard-Vitrac, 1978; Clerc et al., 2015; Cuevas & Tubía, 1999; Golberg & Leyreloup, 1990; Mendia & Ibarguchi, 1991; Montigny et al., 1986). The increase of accommodation space in the North Pyrenean Zone and in the BCB is expressed in the sedimentation by the transition from Aptian carbonate platform and marls to thick Albian turbidite sequences, referred to as the “Flysch Noir” (Rat, 1959; Souquet et al., 1985).

In the study area (Fig. II-2), this hyperextension is controlled by WNW-ESE striking normal and detachment faults such as the South and the North Mauléon Detachment faults (SMD and NMD, respectively) (Masini et al., 2014) or the reactivated Barbarin thrust fault, south of the BCB (Larrasoña et al., 2003a). Kinematic indicators and lateral ramps argue for a NNE-SSW displacement along these structures (Jammes et al., 2009; Masini et al., 2014). Several studies proposed that most of the present-day compressional structures (e.g. Amotz, Leiza, Sainte Barbe, Lakoura thrust faults) rooted on former extensional faults subsequently reactivated during the Cenozoic convergence (DeFelipe, 2017; Razin, 1989; Teixell, 1993). Moreover, N-S to NNE-SSW transfer faults (TF) have been recognized in both basins. In the Mauléon basin, they control the progressive westward opening toward the Late Albian to Cenomanian St-Jean-de-Luz basin (e.g. St-Jean-Pied-de-Port, Ayherre and Ibaron TF) (Claude, 1990; Razin, 1989; Fig. II-2). In the BCB, the Hendaya and Pamplona faults are considered to represent transfer faults, even though their role during Aptian to Cenomanian rifting is still poorly understood (e.g. Aller & Zeyen, 1996; Jammes et al., 2010). The Pamplona fault is usually considered as the eastern termination of the BCB basin (e.g. Cuevas & Tubía, 1999; Frankovic et al., 2016; García-Mondéjar et al., 1996; Pedreira et al., 2003). The location of the former rift axis is given by the occurrence of the granulite and mantle rocks such as observed along the E-W Chainons Béarnais and Leiza fault (e.g. Azambre & Monchoux, 1998; DeFelipe, 2017; DeFelipe et al., 2017; Lagabrielle et al., 2010; Lamare, 1936; Llanos, 1980; Mendia & Ibarguchi, 1991). This is supported by the HT/LP metamorphism of the Late Triassic to Albian rocks of the Nappe des Marbres (Lamare, 1936; Martínez-Torres, 1992) and Chainons Béarnais (Corre et al., 2018).

In the St-Jean-de-Luz basin, an enigmatic block of marmorised and scapolite-bearing Jurassic limestones is cropping out to the south of Biarritz (BRGM, 1963) suggesting that the mid-Cretaceous metamorphism could extent north of the Cinco Villas massif. In both systems, the Late Cenomanian could represent the end of fault-controlled subsidence and the transition to post-rift thermal subsidence (e.g. Teixell et al., 2018). This is suggested by the formation of carbonate platforms (“calcaire des Cañons”) on the margins of the Mauléon – St-Jean-de-Luz basins (e.g. Cuvillier et al., 1964; Floquet et al., 1988; Puigdefàbregas & Souquet, 1986; Razin, 1989) and on the southern margin of the BCB (e.g. Feuillée & Rat, 1971; Floquet, 1998; Gräfe, 1999) while deep water turbidites or marls are deposited above hyperextended domains (e.g. Puigdefàbregas & Souquet, 1986; Figs. II-2 and supplementary material S1 in annexes). During this time, the Basque massifs were considered to form a basement high with eventual episodes of emersion (Floquet et al., 1988; Mathey, 1986; Razin, 1989).

In contrast to the Late Jurassic – Barremian rift event, the Aptian – Cenomanian depositional environment is mostly deep marine and the distribution of the basins follows a roughly continuous E-W trend. The Aptian – Cenomanian rift event argues for a north-south extension direction as indicated by the existing kinematic data such as N20 transfer faults (Razin, 1989; Roca et al., 2011; Tavani et al., 2018), N110 detachments faults (DeFelipe et al., 2017; Jammes et al., 2009; Masini et al., 2014), and the continuous E-W stripe of HT/LP metamorphic rocks along the North Pyrenean Metamorphic Zone (e.g. Clerc et al., 2015). However, Late Jurassic – Barremian deformation is difficult to assess due to the lack of recognition of any pre-Aptian structures and to the significant amount of salt sealing basement faults. As such, the role of any Late Jurassic – Barremian structures on the evolution of the hyperextended rift event is unknown and likely underestimated. Moreover, the eastern termination of the BCB and the western termination of the Mauléon basin, although defined in studies by the Pamplona fault, have not been characterised. Finally, the Eurasian or Iberian affinity of the Basque massifs has been debated and remains until today unsolved (e.g. Engeser & Schwentke, 1986; Larrasoaña et al., 2003b; Peybernès & Souquet, 1984; Rat, 1988; Schott & Peres, 1988).

2.1.3 Convergence and collision

The convergence between the Iberian and Eurasian plates initiated at 83.5Ma due to the northward migration of the Africa plate with respect to Europe (e.g. Macchiavelli et al., 2017; McClay et al., 2004; Thinon et al., 2001). This led to the northward underthrusting of lithospheric rocks of Iberian affinity below the Eurasian crust in the Pyrenean system (e.g. Chevrot et al., 2018). This compressional event is associated with syn-orogenic flysch sedimentation that initiated during Santonian in the external part of the orogen (e.g. Boillot &

Capdevila, 1977; Capote et al., 2002). Main crustal thickening occurred from Eocene onward (Mouthereau et al., 2014; Muñoz, 1992; Teixell, 1990) resulting in a double asymmetric wedge-type crustal architecture (Ábalos, 2016; Camara, 1997; Seguret, 1972). In most parts of the Pyrenean and Cantabrian systems, tectonic inversion led to the inversion of hyperextended basins and reactivation of WNW-ESE rift structures such as the North Pyrenean Frontal Thrust (NPFT) and the South Pyrenean Basal Thrust (SPBT) (e.g. Lagabrielle et al., 2010; Mouthereau et al., 2014; Roca et al., 2011; Teixell, 1993; Tugend et al., 2014; Vacherat et al., 2017).

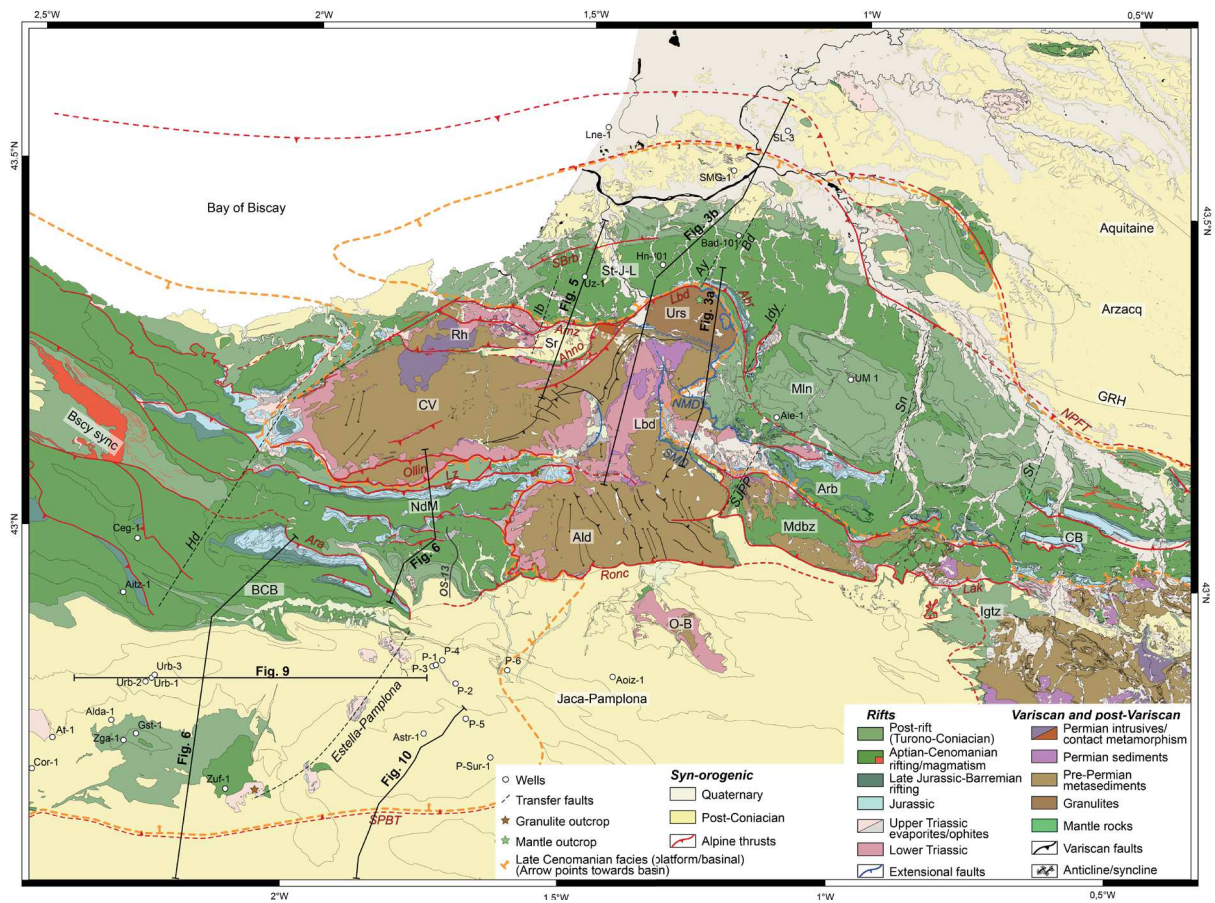


Figure II-2: Geological map of the Western Pyrenean – Eastern Cantabrian system. Location of boreholes, cross-sections and seismic interpretations presented in this study are shown on the map. Details on the distribution of the Late Cenomanian basinal vs. platform facies are provided in supplementary information (Fig. S1 in annexes). Massifs/basins: St-J-L: St-Jean-de-Luz basin; Rh: La Rhune massif; Sr: Sare basin; CV: Cinco Villas massif; Urs: Ursuya massif; Lbd: Labourd massif; Ald: Aldudes massif; Mln: Mauléon basin; Arb: Arbailles massif; Mdbz: Mendibelza massif; CB: Chainons Béarnais; GRH: Grand Rieu High; Igtz: Igoutze massif; O-B: Oroz-Betelu massif; NdM: Nappe des Marbres; BCB: Basque-Cantabrian basin; Bscy sync: Biscay synclorium. Thrusts: NPFT: North Pyrenean Frontal Thrust; SPBT: South Pyrenean Basal Thrust; SBrb: Ste-Barbe backthrust; Lbd: Labourd; Amz: Amotz; Ahno: Ainhoa; Abr: Arbéroue Croissant; Lak: Lakoura; Ronc: Roncesvalles; Lz: Leiza; Ara: Aralar. Extensional faults: NMD: North Mauléon Detachment; SMD: South Mauléon Detachment. Transfer faults: Ib: Ibarren; Ay: Ayherre; Bd: Bardos; Idy: Iholdy; SJPP: St-Jean-Pied-de-Port; Sn: Saison; Sr: Sarailé; Hd: Hendaya. Boreholes: Lne-1: Labenne-1; SMG-1: Ste-Marie-de-Gosse-1; SL-3: St-Lon-3; HN-101: Hasparren-101; UZ-1: Ustaritz-1; Bad-101: Bardos-101; UM-1: Uhart-Mixe-1; Aie-1: Ainhice-1; P-1/2/3/4/5/6: Pamplona-1/2/3/4/5/6; P-Sur-1: Pamplona Sur-1; Astr-1: Astrain-1; Zuf-1: Zufia-1; Gst-1: Gastiain-1; Zga-1: Zuñiga-1; At-1: Atauri-1; Cor-1: Corres-1; Urb-1/2/3: Urbasa-1/2/3; Aitz-1: Aitzgorry-1; Ceg-1: Cegama-1

At the Pyrenean – Cantabrian junction, the westward continuation of the north-directed Pyrenean subduction was debated (Ducasse et al., 1986b; Turner, 1996) but was recently confirmed by active and passive seismic imaging (Díaz et al., 2012; Pedreira et al., 2003). Reactivation of WNW-ESE rift structures and closure of hyperextended domains has been proposed in the Mauléon, BCB and St-Jean-de-Luz basins (e.g. DeFelipe et al., 2017; Ducoux, 2017; Johnson & Hall, 1989b; Lagabrielle et al., 2010; Larrasoña et al., 2003a; Razin, 1989; Teixell, 1993; Tugend et al., 2014). However, the timing of initiation of tectonic inversion in this area remains unconstrained. In these basins, shortening was partially accommodated by thin-skinned deformation (deformation of the Upper Triassic evaporites and the sedimentary cover above) occurring along the Triassic Keuper evaporite decollement level (e.g. Carola et al., 2013; Claude, 1990; Larrasoña et al., 2003a; Le Pochat, 1982; Razin, 1989) eventually rooting on thick-skinned (deformation of the Lower Triassic sandstones and below) crustal thrusts such as the Labourd thrust, the NPFT and the SPBT (e.g. Camara, 1997; Richard, 1986; Teixell, 1998; Teixell et al., 2018).

Despite the recognition of reactivated normal faults, the timing of reactivation and the role of thin- vs. thick-skinned deformation is unrevealed in the Basque Country. In particular, little is known about the role of both Late Jurassic – Barremian and Aptian – Cenomanian structures controlling the reactivation.

This geological setting highlights the remaining questions about the evolution of the Basque Country. The complex tectonic events and the occurrence of a decoupling salt level at the base of the Mesozoic sediments make it difficult to decipher the structural framework of the Pyrenean – Cantabrian junction. As such, authors often refer to a NE-SW striking crustal fault, referred to as the Pamplona fault, to accommodate the deformation between both systems.

2.2 The Pamplona fault: previous interpretations and kinematic implications

The N20 Pamplona fault (PF) has been initially defined to the south of the Basque massifs by: 1) the alignment of salt diapirs between the Jaca-Pamplona basin and the BCB, 2) the eastern termination of the Nappe des Marbres against the Aldudes massif, and 3) the opposite transport direction of the main thrusts on each side of the PF (Feuillée & Rat, 1971; Rat, 1988; Richard, 1986). The salt diapirs are usually referred to as the Estella – Elizondo (Feuillée & Rat, 1971) or “diapires Navarrais” (Richard, 1986) and concern a lineament that runs from Estella to the Basque massifs (Brinkmann & Logters, 1968). In this study, and in order to avoid overinterpretation, we will solely refer to the aligned, rounded-shape diapirs

observed on the map as the Estella – Pamplona diapirs (Fig. II-2). García-Mondéjar et al. (1996) proposed that the diapirs originated on an inherited NNE-SSW Variscan structure. In this area, the PF separates a western domain (BCB) composed of Jurassic to Turonian sediments from an eastern domain (Jaca-Pamplona basin) where Upper Jurassic to Lower Cretaceous sediments are either reduced or absent (eroded or never deposited) (Larrasoña et al., 2003a; Richard, 1986). To the north of the Basque massifs, Razin (1989) and Claude (1990) described a change of the deformation mode across the Bardos (and Ayherre) fault due to the absence of indurated Jurassic to Lower Cretaceous sediments on the western side of this fault. As such, and because of its NE-SW trend, this fault is sometimes considered as the northward continuation of the PF (Claude, 1990; Razin, 1989), even though some authors are shifting its trace east of the Labourd massif (e.g. Jammes et al., 2009; Larrasoña et al., 2003a; Martínez-Torres, 1992). An east to west rise of the Moho topography has been described across the Basque Country (near Bilbao) from seismic refraction data (Daignieres et al., 1982; Gallart et al., 1981; Pedreira et al., 2003) and a deepening of the top basement toward the west has been identified in the eastern BCB from seismic reflection data (e.g. Vergés, 2003). Díaz et al. (2012) proposed, based on receiver function analysis, that the European Moho is offset across the Pamplona fault. On the other hand, gravity anomaly maps highlight a shift of a shallow high-density anomaly toward the south-east in the Basque Country (Casas et al., 1997; Jammes et al., 2010), and (Chevrot et al., 2014) identified a strong P-wave velocity contrast at >50km depth in the Basque Country. The Pamplona fault was also considered to be responsible for a switch in the subduction direction between the Pyrenean and Cantabrian systems (Ducasse et al., 1986b; Turner, 1996). However, this idea was rebutted by recent geophysical data (see 2.1.3).

Because the orientation of the PF (N20) is similar to Variscan and Triassic structures and to the trend of the Bidarray Permian basin (see chapter 2.1.1), authors proposed a Variscan to Triassic and/or Jurassic age for this structure (e.g. Curnelle, 1983; García-Mondéjar et al., 1996; Martínez-Torres, 1992; Muller & Roger, 1977; Rat, 1988). However, the role of this structure in the Pyrenean evolution and kinematics is controversial and different authors proposed different scenarios depending on the position, age and extent of the PF. In summary, two competing models have been proposed (Fig. II-1): 1) Normal fault in a pull-apart setting due to E-W transtension (suggested by Choukroune & Mattauer, 1978; Choukroune, 1992; Larrasoña et al., 2003b); or 2) N20 transform/transfer fault (Rat, 1988; Roca et al., 2011; Tugend et al., 2015) segmenting the Mauléon basin and BCB. In the latter interpretation, the PF was either interpreted as a sharp or a soft transfer zone.

1) Based on a kinematic restoration between the Iberian and Eurasian plates and on the triangular shape of the rift basins north of the North Pyrenean Fault (NPF) (e.g. Debroas, 1987), Choukroune & Mattauer (1978) proposed a model of pull-apart basins (Fig. II-1). These basins developed across the actual Cantabrian and Pyrenean mountain chains due to the supposed eastward displacement and rotation of the Iberia plate relative to the Eurasian plate. In this model, the eastward displacement occurred along the NPF, defined as a Variscan to Alpine strike-slip fault defining the Iberian-Eurasian plate boundary. In the Eastern and Central Pyrenees, the NPF corresponds to a jump in the Moho topography (Arthaud & Matte, 1975; Choukroune & Mattauer, 1978; Choukroune et al., 1973; Daignieres, 1978; Roure et al., 1989). SE-NW directed kinematics have been supported by AMS measurement within Albian sediments of the Mauléon basin (Oliva-Urcia et al., 2010).

2) Alternative interpretations involve a N-S to N30 sinistral (or dextral, see review in Larrasoña et al., 2003a) Pamplona strike-slip fault in the Basque Country that follows Late Variscan structural trends (Arthaud & Matte, 1975; García-Mondéjar et al., 1996; Mattauer, 1968; Muller & Roger, 1977). A transfer/transform fault was used to explain the transfer of deformation from the Western Pyrenees to the eastern Basque-Cantabrian system during both Cretaceous extension and Cenozoic inversion (e.g. Roca et al., 2011; Tugend et al., 2015). These interpretations are based on geological and geophysical interpretations and the present-day observed offset of the mid-Cretaceous rift axis (BCB to Mauléon rift systems) (Fig. II-1).

It has to be noticed that all previous studies either describe the PF from a large-scale point of view (e.g. Richard, 1986) while field studies focused either on the eastern termination of the BCB (Larrasoña et al., 2003a) or the western termination of the Mauléon basin (Claude, 1990; Razin, 1989). In this study we focus on the evolution of both the BCB and Mauléon basin and their relation with inherited structures using large scale seismic data and field observations.

3. MAP DESCRIPTION OF THE CANTABRIAN-PYRENEAN JUNCTION

We generated a geological map of the Western Pyrenean – Eastern Cantabrian system based on previous geological maps, publications and our own observations (Fig. II-2). As such, the French part of the map is modified after the 50'000 harmonized geological map of the BRGM (Genna, 2007) and the Spanish part from the geological maps of IGME (Campos et al., 1972a, 1972b; Campos & García-Dueñas, 1972; Carbayo et al., 1972, 1977; Del Valle, 1972; Del Valle et al., 1972, 1973; Gabaldón et al., 1984a; 1984b; 1984c; Gabaldón et al., 1985; Juch et al., 1972; Knausse et al., 1972; Puigdefábregas et al., 1976; Ramírez et al., 1986; Ramírez Merino et al., 1984) and Ábalos (2016). The St-Jean-de-Luz and Sare basins are modified after

the work of Razin (1989) and the south-west region of the Mauléon basin is from Masini et al. (2014). The Oroz-Betelu massif area is constrained from Ciry et al. (1963) and the Variscan structures of the Basque massifs are taken from Heddebaut (1973), Mohr & Pilger (1965) and Campos (1979, and references therein).

On a map view, the Palaeozoic rocks are located within the Basque massifs where they show Variscan deformation mainly governed by NE-SW to NW-SE faults and folds. The Variscan structures are rather continuous throughout the massifs (e.g. main Variscan thrust; Schoeffler, 1982) and are truncated by Permian structures in the N20 Bidarray Permian basin (part of the Labourd massif) and magmatic intrusion within the Cinco Villas massif.

The Lower Triassic sandstones seal the Variscan and Permian structures, but they never crop out on top of the Ursuya granulitic unit. Moreover, no clasts of granulite rocks have been found within the Lower Triassic sandstones (Hart et al., 2016) suggesting a post-Triassic denudation of the granulites. At the scale of the Basque massifs, the Lower Triassic sandstones form a continuous and only slightly deformed rim that marks the tectonic or stratigraphic contact with the post-Lower Triassic sedimentary cover.

The Upper Triassic evaporites are well represented throughout the study area, where they mostly appear along compressional structures (e.g. Chainons Béarnais, Nappe des Marbres) and along N20 structures (e.g. Saison or Iholdy transfer faults in the Mauléon basin). They contain blocks and fragments of Palaeozoic and Mesozoic rocks as well as granulites and mantle rocks (e.g. Leiza faults and Chainons Béarnais). In the eastern BCB, the Upper Triassic evaporites crop out as rounded shaped diapirs (Estella – Pamplona diapirs) containing blocks of Mesozoic and Palaeozoic rocks. Moreover, garnet-biotite-sillimanite bearing paragneisses, which are typical for granulite facies metamorphism, and scapolite-bearing Jurassic blocks have been evidenced in the Estella diapir (Cincunegui et al., 1943; Pflug & Schöll, 1976).

The supra-evaporite sequence appears on a map view as tilted and folded by E-W to WNW-ESE trending structures within the BCB and Mauléon basin. The Jurassic rocks are very often associated with Triassic evaporites and Alpine thrusts. Interestingly, on the south-western part of the Aldudes massif, the Jurassic limestones and marls are missing and Aptian to Albian conglomerates and calcareous sandstones are overlaying directly Upper Triassic ophites, Middle Triassic limestones and Lower Triassic sandstones. No Jurassic rocks are observed within the Jaca-Pamplona basin and very few within the St-Jean-de-Luz basin.

Upper Jurassic to Barremian rocks corresponding to the Purbeck-Weald facies are observed in the Mauléon basin and BCB and behave similar to the Jurassic limestones in the present-day architecture. However, they are reduced or absent in both the Nappe des Marbres, the St-Jean-de-Luz basin and the Jaca-Pamplona basin.

The Aptian to Coniacian syn- to post-hyperextension sequences roughly follow a WNW-ESE trend at regional scale and depict a sigmoid shape across the Palaeozoic Basque massifs. WNW-ESE (N110) rift structures such as the SMD and NMD are well preserved in the south-west of the Mauléon basin and display a rotation toward the north when approaching the Labourd massif and especially the Bidarray Permian basin. In the St-Jean-de-Luz basin, the rift-inherited Amotz fault (Richard, 1986) shows a similar WNW-ESE orientation, while the reactivated Ste-Barbe back-thrust (Razin, 1989) shows a roughly WSW-ENE orientation. On figure II-2, we depict the limit between Late Cenomanian shelf and basinal facies deposits, corresponding to the sediments deposited at the end of rifting and at the beginning of thermal subsidence. Some areas display basinal facies characterized by marls or deep water turbidite deposits while others show shelf environment characterized by carbonate platform deposits, often onlapping onto the Palaeozoic basement.

The post-Coniacian (syn-convergence) rocks crop out mainly north of the NPFT and south of SPBT where they have been deformed along WNW-ESE oriented folds. Compressional structures show mainly an E-W to WNW-ESE orientation (e.g. NPFT, SPBT, Aralar and Amotz faults) except around the Basque massifs where various thrust fault orientations are observed (e.g. NNE-SSW Labourd thrust, SW-NE Roncesvalles thrust).

4. CROSS-SECTIONS AND SEISMIC INTERPRETATIONS ACROSS THE PYRENEAN-CANTABRIAN JUNCTION

In the following, we describe cross-sections and seismic interpretations that correspond to key areas to describe the architecture of the Basque Country. These cross-sections cover a N-S zone that follows the hypothetical trace of the Pamplona fault between the Mauléon – St-Jean-de-Luz basins, Labourd – Cinco Villas massifs and BCB – Jaca-Pamplona basins (see Fig. II-3). In order to project boreholes (at depth) on the seismic lines (in time), we apply a simple time-depth conversion to the seismic section with 4,5 seconds (TWT) corresponding to 10'000 meters.

4.1 Western Mauléon basin – Labourd massif

Figures II-3a and II-3b are N-S cross-sections across the Aldudes, Labourd and Ursuya massifs. Cross-section 3a runs in the eastern part of the Labourd massif, from the Aldudes massif to the Mauléon basin. The cross-section 3b runs in the western part of the Labourd massif, from the Aldudes massif to the Aquitaine platform via the St-Jean-de-Luz basin. The St-Jean-de-Luz

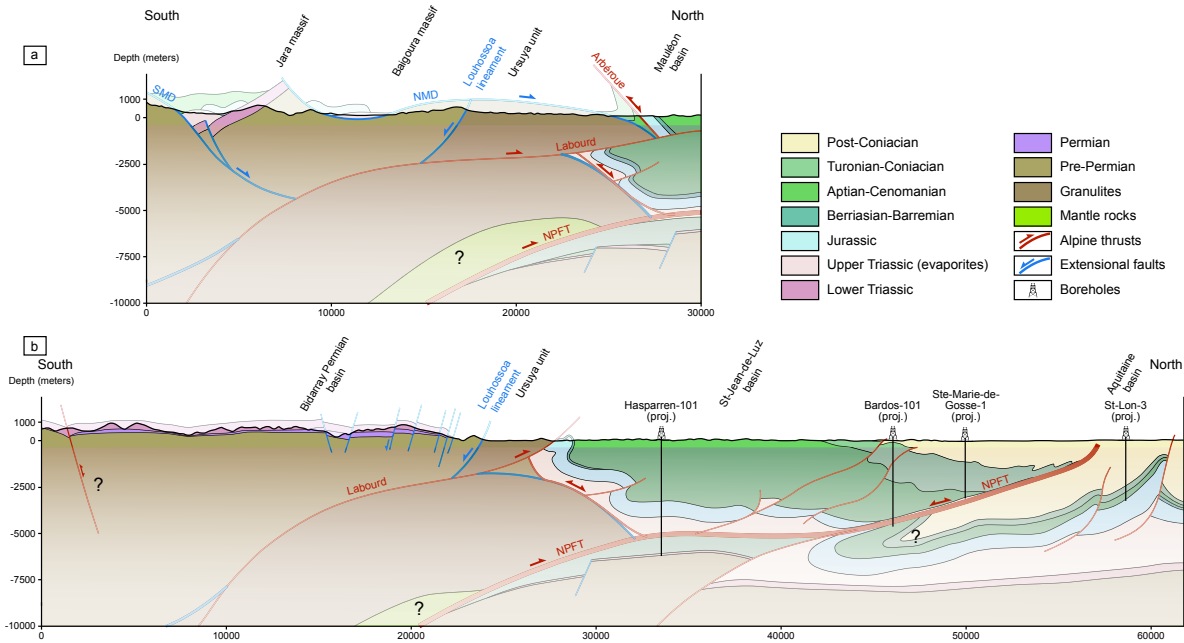


Figure II-3: N-S cross-sections across the eastern (a) and western (b) Labourd massif. Note the allochthony of the Labourd massif on the Aquitaine platform and the preservation of pre-Alpine structures on top of the Labourd basement. Location on figure II-2. Description of the figure is provided in the text.

basin and southern Aquitaine platform section is modified after the seismic interpretation of Serrano et al. (2006). The subsurface data are constrained by own field measurements (Fig. II-4) and observations and the BRGM geological maps (Genna, 2007). The location of mantle (or high density) rocks in depth is constrained by Wang et al. (2016).

The southern part of cross-section 3a shows the Palaeozoic rocks of the Aldudes massif and the Albian SMD (Hart et al., 2017; Masini et al., 2014). To the north, in the hanging-wall of the SMD, the Lower Triassic sandstones of the Jara massif are tilted toward the south. They are overlain by Late Triassic evaporites, Jurassic limestones and Albo-Cenomanian breccias and shales (Masini et al., 2014). The NMD and the allochthonous Mesozoic cover compose the northern face of the Jara massif. Further to the north, the NMD truncates the south-dipping Louhossoa lineament which juxtaposes the granulite facies metamorphic rocks of the Ursuya unit to the low to medium grade Palaeozoic rocks of the Baigoura massif. The northern tip of the Ursuya unit is capped by an overturned syncline composed of Albian to Turonian deposits and the tectono-sedimentary breccias of the Bonloc through (Jammes et al., 2009; Richard, 1986). The Late Triassic to mid-Cretaceous rocks of the Arbéroue Croissant are tilted toward the north along a south-vergent thrust and display about 200m of Neocomian deposits unconformably laying on Middle Jurassic sediments (Upper Jurassic eroded) (Richard, 1986).

Cross-section 3b is located to the west of the previous section, however, in this western section, no sedimentary cover is preserved on the Ursuya unit and the Labourd thrust is cropping out. Moreover, to the north, the Hasparren 101, Bardos 101 and Ste-Marie-de-Gosse 1 boreholes and the seismic interpretation (modified after Serrano et al., 2006) show that the Mesozoic cover is thrust on top of Late Cretaceous calcareous flysch and the Aquitaine platform along the NPFT, detached into the Upper Triassic salt. No Upper Jurassic (only Oxfordian) to mid-Albian sediments have been recorded in the Mesozoic cover of the Hasparren 101 borehole and in the allochthonous unit (above the NPFT) of the Bardos 101 borehole. To the south of the section, the Lower Triassic sandstones seal the Bidarray Permian basin and display a remarkably flat bedding that extends to the Aldudes massif, which depicts a large anticlinorium up to the Roncesvalles fault where Lower Triassic rocks crop out again (Fig. II-2). Near the Ursuya unit, the Lower Triassic sandstones are affected by south-vergent low offset normal faults and are abruptly dipping toward the NE in the proximity of the Louhossoa fault.

At depth, the occurrence of the autochthonous Aquitaine basement has been attested by the Hasparren 101 borehole, which highlights the stratigraphic contact of the Turono-Senonian calcareous turbidites onto the Lower Triassic sandstones at 6212m. In order to restore the allochthonous mid-Cretaceous Mauléon and St-Jean-de-Luz basins between the unstretched Labourd massif and the thick Aquitaine crust, Razin (1989) proposed a major thrust (“Chevauchement Pyrénéen”, or NPFT) that transported the Labourd and Cinco Villas massifs on top of the Aquitaine basement during Pyrenean convergence. The major, previously defined thin-skinned thrust can reasonably represent the thin-skinned prolongation of this crustal thrust. Such important loading is likely responsible for the general southward tilt of the Aquitaine basement observed on seismic sections (e.g. Serrano et al., 2006). On both sections, we display the north-vergent Labourd thrust (Hall & Johnson, 1986; Razin, 1989; Zolnaï, 1971), which has been suggested based on map relationships showing the Jurassic rocks of the St-Jean-de-Luz – Mauléon basins being overlain by the Ursuya unit on its north-western part, and by the large-scale folding of the Alpine structures in the basins that mimics the shape of the Labourd massif to the north. The location of the mantle at depth is extrapolated from the tomographic cross-section of Wang et al. (2016) that reveals a fast anomaly from about 10km depth below the eastern Labourd massif.

These cross-sections highlight the allochthony of both the Labourd massif (southern margin of the mid-Cretaceous basins) and the Mesozoic sediments that composed the Mauléon and St-Jean-de-Luz basins on top of the Aquitaine basin (northern margin of the St-Jean-de-Luz – Mauléon basins) via the thick-skinned and thin-skinned NPFT. These cross-sections also highlight the northward displacement of the Labourd massif along the Labourd thrust (>8 km

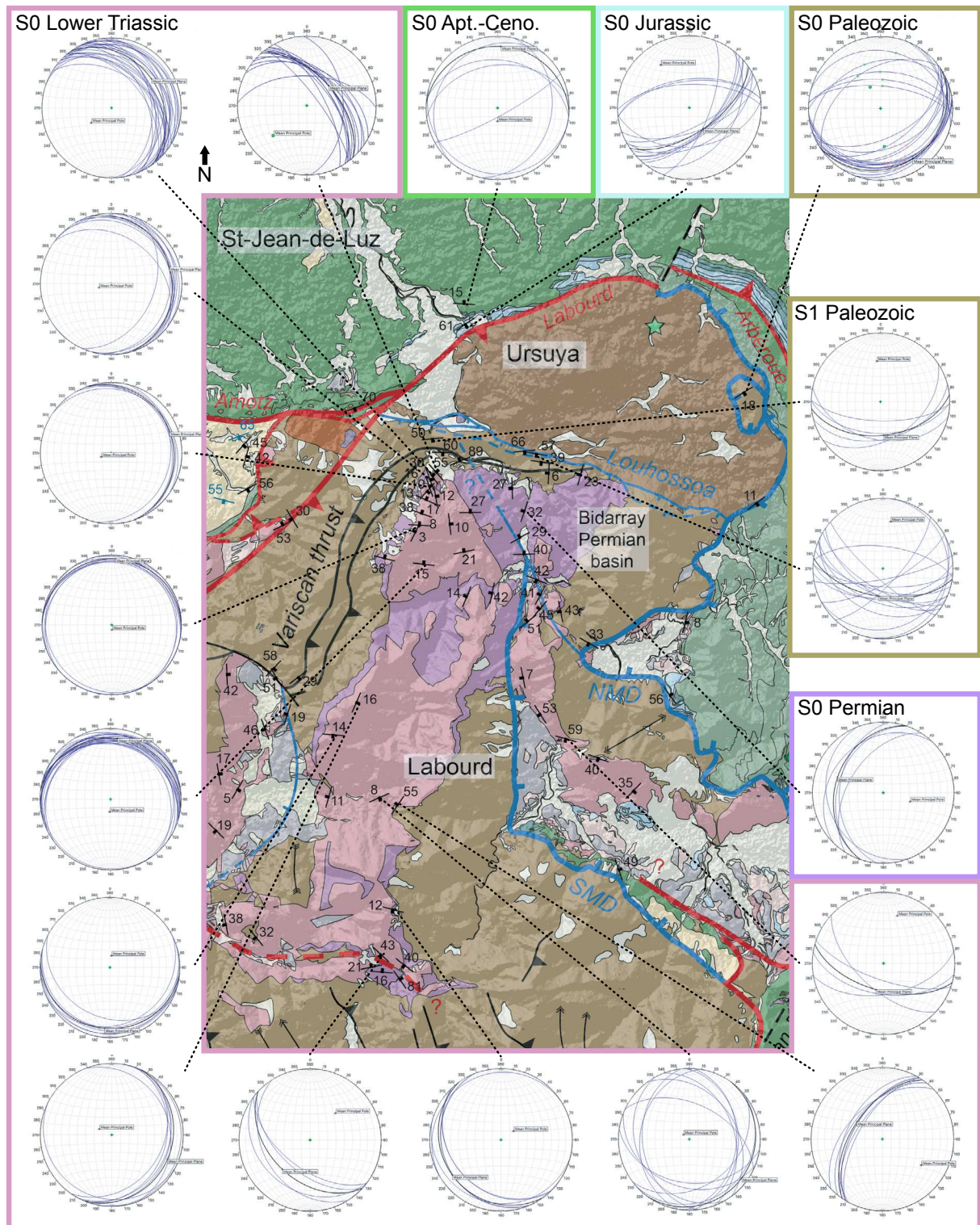


Figure II-4: Geological map of the Labourd – Ursuya area with structural data. For caption, see figure II-2.

according to Richard, 1986), which displaced the granulitic and Palaeozoic rocks of the massif on top of the Cretaceous sediments of the Mauléon and St-Jean-de-Luz basins. Interestingly, very little Alpine imprint is observed throughout the massif allowing a good preservation of the Cretaceous rift architecture and the Permian basin. Finally, the comparison of the Mauléon - St-Jean-de-Luz basins on both cross-sections shows a western domain where the Neocomian to mid-Albian deposits are very reduced or absent in comparison to the eastern section, suggesting that the Ayherre-Bardos faults (Figs. II-2 and II-3) might have represented the western termination of a basin during the Early Cretaceous such as proposed by Richard (1986).

4.2 St-Jean-de-Luz basin – northern Cinco Villas massif

Figure II-5 is a N-S cross-section across the St-Jean-de-Luz basin, north of the Cinco Villas massif, modified after Razin (1989). This cross-section runs through the Cinco Villas massif, the Sare basin and the St-Jean-de-Luz basin up to the Ste Barbe back-thrust (Fig. II-2). The subsurface data are taken from Razin (1989) and the geological maps from the BRGM (Genna, 2007). The Ustaritz 1 borehole provides information about the stratigraphy in the basin.

To the south of the section, the Lower Triassic sandstones are affected by strong contractional deformation and are unconformably overlain by the deltaic Zugarramurdi conglomerates and sandstones (Feuillée, 1964; Prave, 1986) deposited during the Late Albian to Early Cenomanian. On top, the Late Cenomanian to Coniacian Sare carbonate platform and Campanian calcareous flysch are steeply dipping toward the north and form the southern flank of the Sare basin syncline, which corresponds to the eastern continuation of La Rhune massif (Fig. II-2). The Sare basin is bounded to the north by the Amotz reactivated normal fault that corresponds to the southern margin of the St-Jean-de-Luz basin. Here, it has been observed clasts of Paleozoic to Mesozoic rocks belonging to the fault-related Amotz breccias which are time equivalent to the Ascain sandstones (or St Pée sandstones; Souquet et al., 1985) and to the deep facies turbidites of the Flysch Noir (or locally “Flysch de Mixe”). As such it suggests a Late Albian to Cenomanian age for this fault. At depth (Ustaritz borehole, interpretation of Teyssonnières, 1983), these sandstones and turbidites lie on about 50 meters of Upper Hettangian sediments. South-vergent thrust faults soling out into the Upper Triassic evaporites and reactivating paleo-normal faults (e.g. Ste Barbe thrust) have been described by Razin (1989). They are cross-cut and overturned by north-vergent thrust faults that used the same décollement level. Further to the north of this section, the Labenne 1 borehole displays the repetition of the Eocene deposits into the Lutetian décollement horizon Razin (1989).

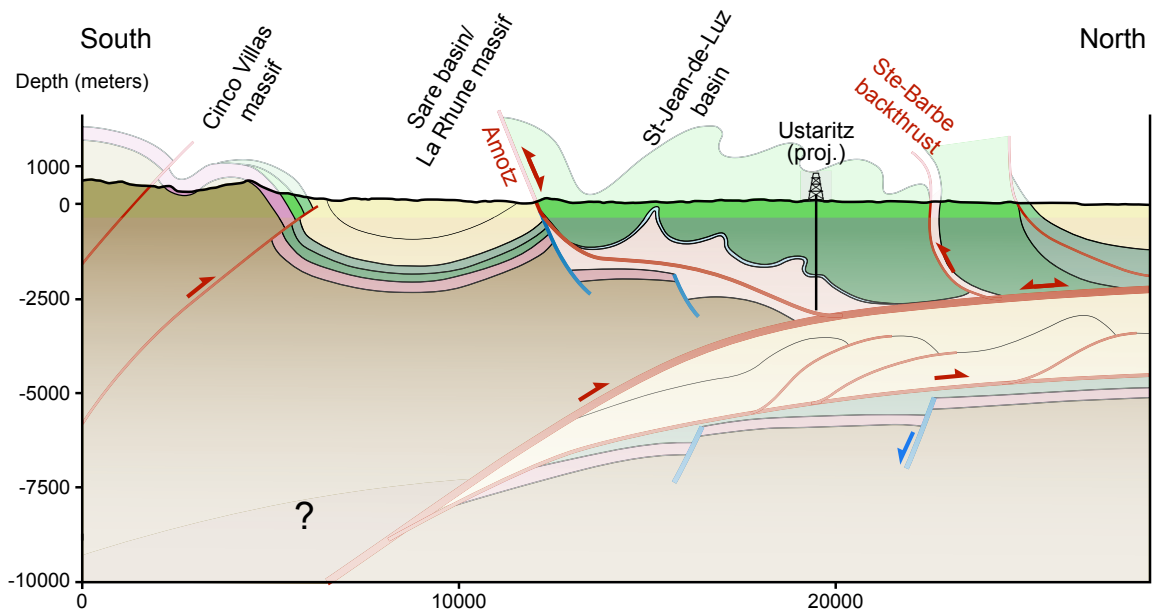


Figure II-5: N-S cross-section across the St-Jean-de-Luz basin. Modified after Razin (1989). Location on figure II-2. See caption in figure II-3 and description of the figure is provided in the text.

This section highlights the allochthony of the Late Albian to Cenomanian St-Jean-de-Luz basin that was controlled by WNW-ESE and WSW-ENE normal faults associated with the westward prolongation of the Mauléon basin. In the basin, Middle Jurassic to mid-Albian sediments have not been observed and were probably never deposited as only clasts of Lower Jurassic sediments have been observed in the Upper Albian deposits (Richard, 1986). The Upper Albian deltaic facies are overlain by up to 2000m of syn-rift turbidite deposits. From Late Cretaceous onwards, the basin was affected by thin-skinned thrusting toward the south that reactivated normal faults (e.g. Ste Barbe fault) and by north-vergent thin-skinned thrusts that transported the Mesozoic sequence on top of Eocene deposits (Razin, 1989). The basin shows a general tilt toward the north that reflects the crustal buttress involved by the thick-skinned northward displacement of the allochthonous Cinco Villas massif on top of the Aquitaine platform along the NPFT. The amount of shortening has been estimated to 60km by Razin (1989) based on structural considerations and basin reconstruction.

4.3 Eastern BCB – southern Cinco Villas massif

Figure II-6 represents a N-S cross-section across the BCB, south of the Cinco Villas massif. In order to avoid complexities raised by the Pamplona fault and associated diapirs, we split the cross-sections in 2 segments. The northern segment runs from the Cinco Villas massif to the Aralar thrust, where previous (Bodego et al., 2015) and new field measurements (Fig. II-7) together with the geological map (Del Valle et al., 1973) are used to constrain the upper part of the section. The line drawing and the suggestion of interpretation of the OS13 seismic line (projected, see location on figure II-2) is used to constrain the deeper part of the section (Figs. II-2 and II-6). The southern segment is located further to the west and runs from the Aralar thrust to the Ebro basin to the south. As such, the Aralar thrust can be used as a reference to extend the cross-section to the south-west, where seismic lines and boreholes are available. We used the RL40 and ALL2 seismic lines, Urbasa-2, Zuñiga-1 and Gastiain-1 boreholes, and subsurface data from IGME geological maps to constrain this segment.

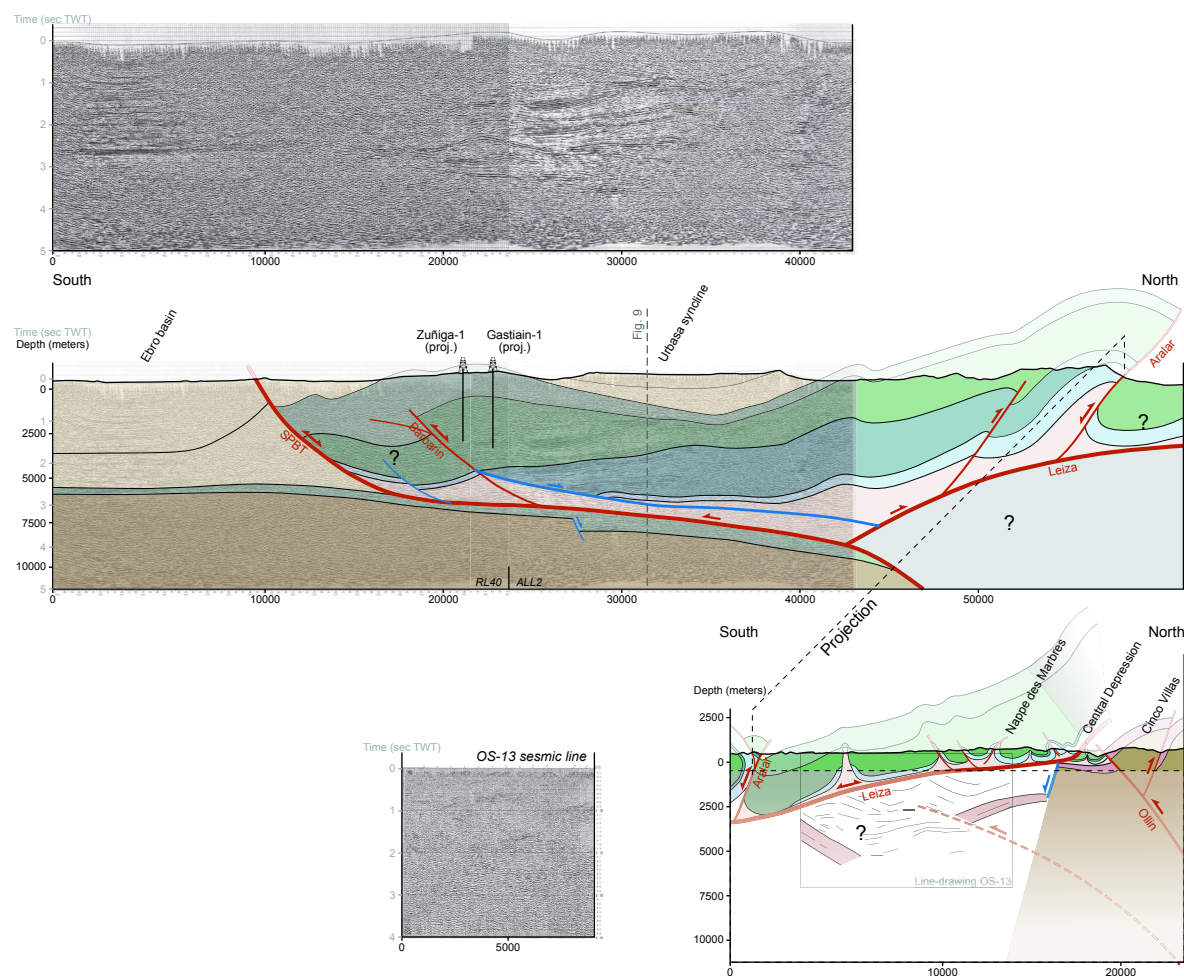


Figure II-6: N-S cross-section and seismic interpretation across the BCB. Location on figure II-2. See caption in figure II-3 and description of the figure is provided in the text.

On the northern segment, the north-dipping Ollin thrust, located at the southern edge of the Cinco Villas massif, places the Triassic and Paleozoic rocks of the massif on top of the Mesozoic sediments of the Central Depression. The Central Depression shows very reduced Upper Triassic, Jurassic and Albian sequences unconformably overlying Lower Triassic sandstones. Toward the south, the Nappe des Marbres displays a thicker Aptian (Urgonian platform facies) and Albian to Cenomanian (calcareous turbidites) sequences unconformably laying on top of either very reduced Purbeck-Weald sediments or more generally on Jurassic

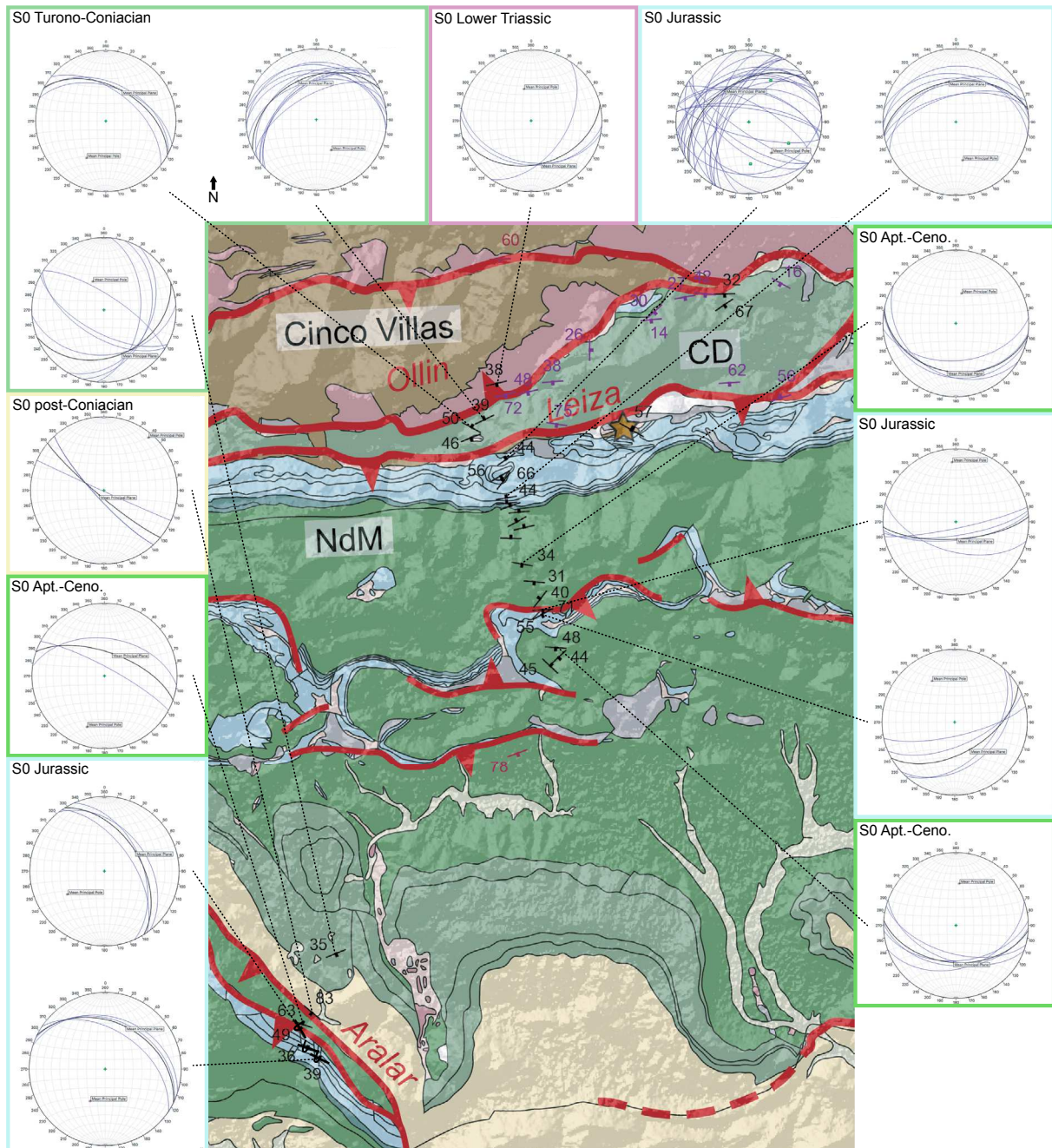


Figure II-7: Geological map of the northern BCB basin and associated structural data. Black dip data are own measurements, purple are from Bodego et al. (2015) and red are from IGME 1/50000 maps of Sumbilla (Del Valle et al., 1973) and Gulina (Carbayo et al., 1977). CD: Central Depression; NdM: Nappe des Marbres. For caption, see figure II-2.

limestones and marls (Lamare, 1936). The Mesozoic succession is underlain by the Upper Triassic evaporites, which represent the rooting horizon of thrusts. The Upper Triassic to Albian sediments of the Nappe des Marbres show recrystallisation and dypire formation related to the mid-Cretaceous HT/LP event. This metamorphism increases toward the north (Martínez-Torres, 1992) up to the Leiza fault, where metric-scale folds and quartz-rich fluid circulation are observed. On the OS-13 seismic line, which images below the Nappe des Marbres, we interpret a strong low-angle reflector dipping toward the south and rising up to the surface toward the north, corresponding to the trace of the Leiza fault at surface (Figs. II-6 and II-7). The southern boundary of the Nappe des Marbres is represented by the south-dipping Aralar thrust, which delimits a southern domain composed of thick (>300m) Late Jurassic to Barremian sediments deposited in a lagoonal to lacustrine environment. On the Aralar ridge, the mid-Cretaceous rocks are mostly represented by carbonate platforms (Feuillée, 1971; Mathey, 1986), contrasting with the deep water turbidites and flysch sediments of the Nappe des Marbres.

On the southern segment, the top Neocomian is projected from figure II-9 and the Urbasa-2 borehole. The Purbeck-Weald sequence forms a hanging-wall syncline basin, suggesting a decoupling along the Upper Triassic evaporites during deposition. We identified the continuous reflectors of the Urgonian facies (Aptian) and the reflective semi-continuous horizons of the sandstones and claystones of the Late Albian Utrillas formation (Carola, 2014). The Aptian to Cenomanian sequence is getting very thin below the Urbasa syncline and increases again against the Barbarin thrust. On the southernmost part of the section, underneath the Ebro basin, strong and remarkably flat reflectors located at 2,5 – 2,7 seconds (TWT) can be assigned to Upper Albian – Upper Cretaceous sediments (Carola et al., 2013; Carola, 2014) that occur over the seismic basement characterized by a chaotic reflection pattern (Gallastegui, 2000). These reflectors can be followed below the SPBT, where the deformed top basement (e.g. normal fault) is tilted toward the north. In the Ebro foreland basin, syn-convergence sediments are thickening and deformed toward the SPBT. Between the SPBT and the Barbarin thrusts, the seismic reflectors are unclear and do not allow to propose reliable interpretations. At depth, we involve a south-vergent crustal thrust below the Aralar thrust that would be responsible for the northward tilt of the Ebro basement and the rise of the top basement observed on the northern segment.

The cross-section and seismic interpretation highlight a strong decoupling and an allochthony of the post-salt Mesozoic cover. Indeed, these sections show that at least 20km of northward displacement has been accommodated by the Leiza fault in order to bring the thick metamorphic sedimentary sequence of the Nappe des Marbres above the thinned and unmetamorphosed sediments of the Central Depression (e.g. DeFelipe, 2017). This fault is

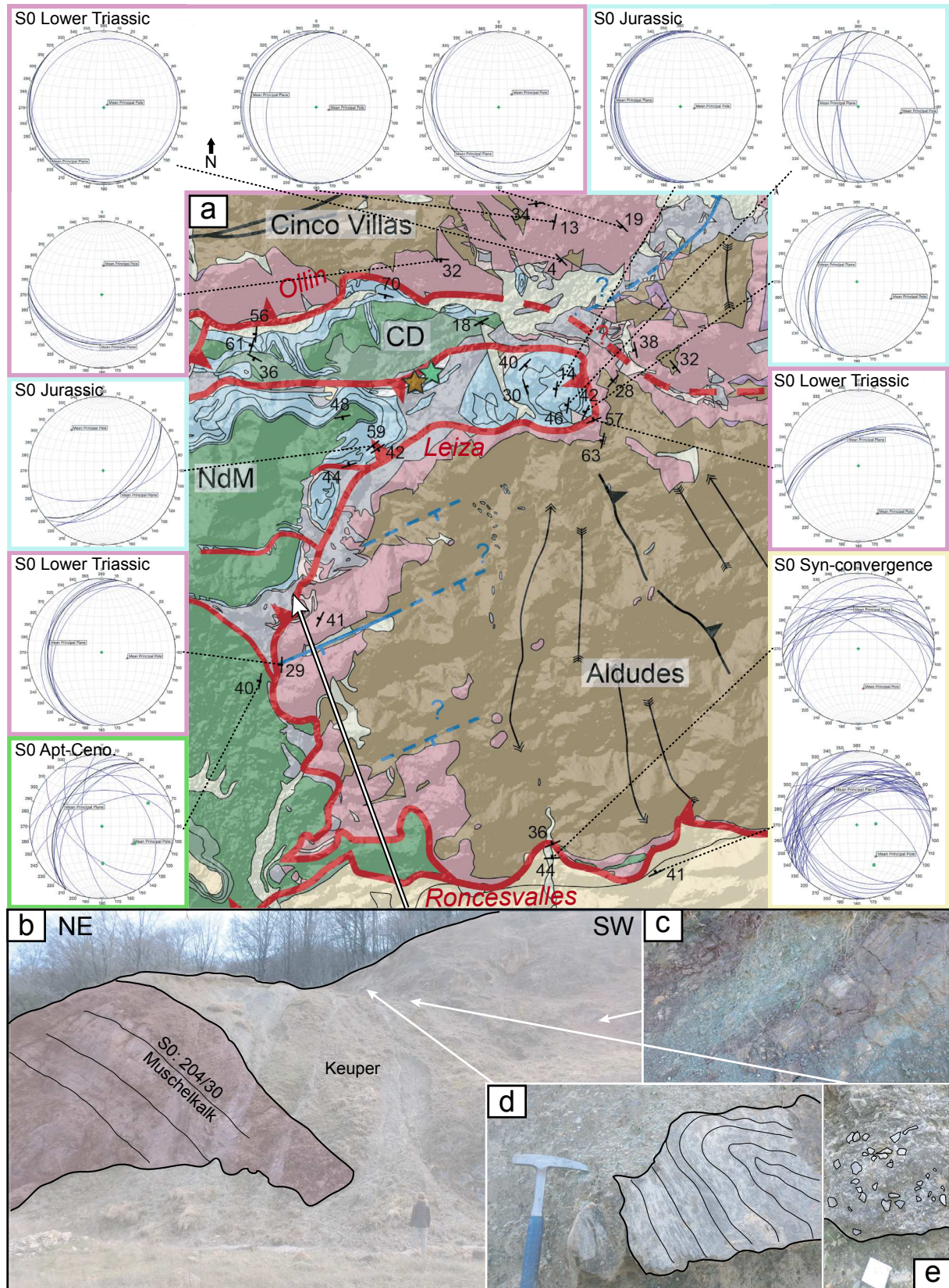
continuously observed toward the east, where it is associated with mantle rocks and granulites embedded in the Upper Triassic evaporites together with Jurassic marble clasts (DeFelipe et al., 2012, 2017). In the most eastern part, the trace of the Leiza fault follows a N-S orientation and juxtaposes the metamorphic Mesozoic sediments of the Nappe des Marbres above the west-dipping Lower Triassic sandstones of the Aldudes massif (Fig. II-8). This tectonic contact is always represented by the Upper Triassic evaporites and an unusual amount of ophites. Along this contact, we identified allochthonous clasts and blocks of folded Paleozoic basement embedded in the evaporites, attesting that this thrust has detached into an extensional decollement level that put the denuded Paleozoic basement in tectonic contact with the base of the Nappe des Marbres.

Similarly, more than 15km of displacement had to occur along the SPBT in order to restore back the Upper Cretaceous sediments of the hanging-wall with respect to their equivalent beds in the autochthonous Ebro foreland basin (Carola et al., 2013; Larrasoña et al., 2003a; Martínez-Torres, 1993). The Aralar thrust seems to reactivate a normal fault that defined the northern margin of a Late Jurassic - Barremian basin as evidenced by the very reduced continental deposits or even absence of deposition in its footwall (Nappe des Marbres). At mid-Cretaceous time, the Aralar ridge probably represented a transitional domain between a shallow environment, characterized by carbonate platform, and a deeper environment toward the north characterized by turbidites (Mathey, 1986). To the south, the seismic interpretation suggests that the Barbarin thrust reactivated a normal fault controlling the deposition of the Aptian to Cenomanian sediments (e.g. Larrasoña et al., 2003a). Interestingly, only little contractional deformation is observed in this allochthonous unit of the BCB except along the northern margin of the Purbeck-Weald basin (Aralar thrust).

4.4 BCB – Jaca-Pamplona basin

Figure II-9 is an E-W seismic interpretation across the eastern BCB and Jaca-Pamplona basin, crossing the Estella-Pamplona diapirs. We used the ALL7 and AN10 seismic lines and the Urbasa-2, Urbasa-3 and Pamplona-3 boreholes to constrain the interpretation.

On the western part, the section shows a >10km wide anticline composed of Jurassic to Cenomanian rocks and a core composed of Late Triassic evaporites. The Urbasa-2 borehole reports about 2000m of Berriasian to Barremian sediments (5842 to 3880m) affected by reverse faulting, which are likely responsible for the disrupted reflectors observed on the seismic line at the location of the well. These Berriasian to Barremian sediments are mainly marls, claystones



and sandstones, sometimes interbedded with claystones, anhydrites and lignite (e.g. from 4350 to 4100m). Lignite has also been described within the Neocomian sediments of the Chainons Béarnais associated with bauxites (see chapter 2.1.2.2). On top of them, about 1900m of Aptian to Cenomanian sandstones and marls are observed, followed by Turonian to Palaeocene marls and limestones. Toward the east, the Berriasian – Barremian deposits are thinning out and terminate along the location of the Estella – Pamplona salt diapirs such as evidenced by the Pamplona-3 borehole. On the same transect, the Aptian to Cenomanian sediments depict thickness variations up to the east of the diapirs where they reach 1400m and display a similar lithology. All along the section, the sedimentary cover is floored by the Upper Triassic salt that lays upon the rather thin Late Cretaceous to Cenozoic rocks of the Ebro basin, which successively shallows toward the east (7500m to 5000m).

This section highlights the eastern, present-day termination of the Late Jurassic to Barremian basin that corresponds to the trace of the Estella – Pamplona diapirs. Indeed, Aptian to Cenomanian sediments display similar thickness and facies on both sides of the diapirs (see Urbasa-2 and Pamplona-3 boreholes), arguing for an eastern prolongation of the BCB south of the Aldudes massif. However, Upper Jurassic to Barremian deposits, if deposited, have been eroded before Aptian east of the diapirs. As such, the change in Cretaceous sedimentary thickness on both sides of the Estella-Pamplona diapirs (see chapter 2.2) cannot be solely attributed to the Aptian – Cenomanian rifting event and might actually correspond to the eastern termination of a Late Jurassic to Barremian basin. Subsequent overburden could have sustained salt mobilization, which would be partly responsible for the thickness variation and onlap geometries observed within the Aptian – Cenomanian sequence of this E-W section.

On this section, the Mesozoic sedimentary cover is transported toward the south along the SBPT due to thin-skinned deformation controlled by the Late Triassic evaporites. Displacement was initiated within the deformed Late Triassic horizon and resulted in the formation of a structural relief once transported in the hanging-wall of the thrust. It led to the formation of a “hanging-wall drop fault” in the allochthonous unit and to the deposition of a thick syn-convergence sequence on the eastern part of the Estella – Pamplona diapirs such as proposed by (Larrasoña et al., 2003a).

Figure II-8: a) Structural data of the eastern part of the Nappe des Marbres. Note the Leiza fault delimiting the allochthonous Nappe des Marbres from the Aldudes and Cinco Villas massifs. CD: Central Depression, NdM: Nappe des Marbres. For caption, see figure II-3. b) Outcrop picture of the western border of the Aldudes massif (location: 43°03'51.6"N ; 1°37'04.0"W). A massive block of Muschelkalk is embedded in the Upper Triassic evaporites on top of the Lower Triassic sandstones (in the background, not visible). c) Typical varicolored Upper Triassic evaporites. d) Allochthonous block of folded Palaeozoic schist embedded in the evaporites. e) Allochthonous block of Palaeozoic polymictic breccias (detached from the outcrop).

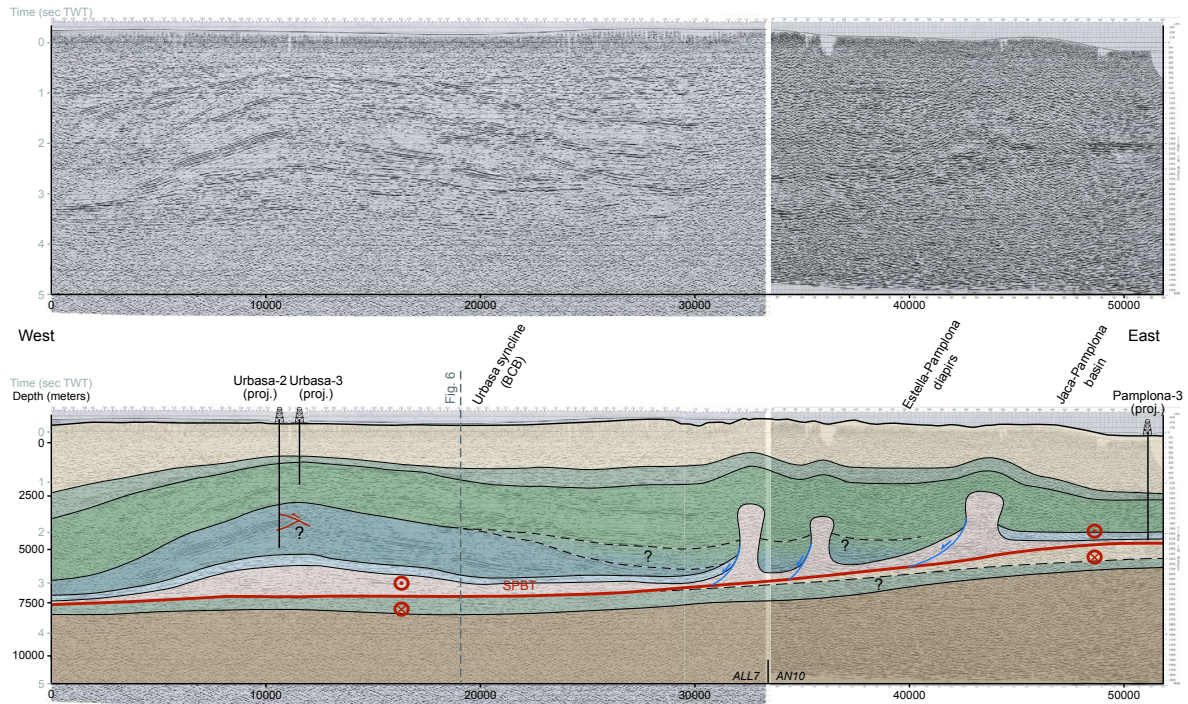


Figure II-9: E-W seismic interpretation across the Estella-Pamplona diapirs. Location on figure II-2. See caption in figure II-3 and description of the figure is provided in the text.

4.5 Jaca-Pamplona basin

Figure II-10 represents a N-S seismic interpretation across the southern part of the Jaca-Pamplona basin. We used the PP17V seismic line and the Astrain-1 and Pamplona-5 boreholes for this section.

On this section, the northern part shows about 1200m of Aptian to Cenomanian siltstones and sandstones (Astrain-1 well) laying on Jurassic marls and Late Triassic claystones and gypsum. This Mesozoic sequence overthrust the Late Cretaceous to Cenozoic sediments deposited on top of the Ebro basement. On top of the Aptian – Turonian succession, syn-convergence sediments are thickening toward the south, showing a syncline in the hanging-wall of the SPBT. In the footwall of the SPBT, the syn-convergence sediments (>4000m) of the Ebro basin display overturned beds and a syncline geometry and are detached from the lower autochthonous succession. Below, the basement of the Ebro basin slightly dips toward the north at about 5000m depth.

This section highlights the eastern prolongation of the Aptian – Cenomanian BCB in the Jaca – Pamplona basin with up to 1200m of deposits and the absence of Late Jurassic – Barremian sediments. Here again, the Mesozoic sediments have been transported toward

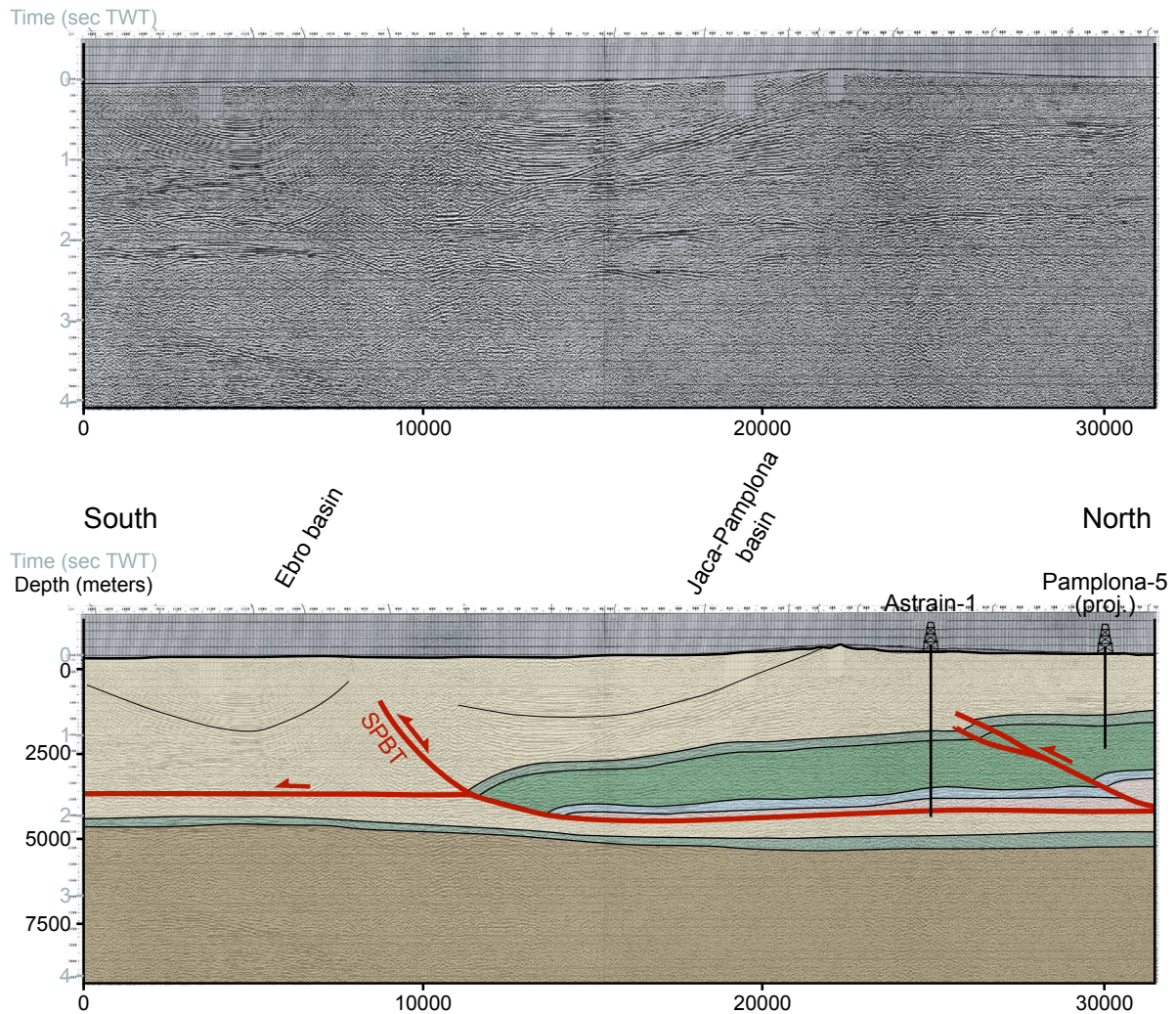


Figure II-10: N-S seismic interpretation across the Jaca – Pamplona basin. Location on figure II-2. See caption in figure II-3 and description of the figure is provided in the text.

the south along the SPBT. The Late Triassic salt controlled the thin-skinned deformation that carried the Aptian – Cenomanian basin above the Ebro foreland basin such as testified by the pre-convergence sedimentary pile on top of the Palaeozoic basement.

As such, the seismic interpretations across the BCB (Fig. II-6) and Jaca – Pamplona basins (Figs. II-9 and II-10) show that both basins have been synchronously transported on top of the Ebro/Duero basin along the SPBT and that no strike-slip movement occurred between them during convergence. This is testified by the preservation of the rounded shape Estella – Pamplona diapirs (Fig. II-2; Frankovic et al., 2016) and by the absence of any strike-slip deformation along the Estella-Pamplona diapirs during convergence (Larrasoña et al., 2003a). As a consequence, the SPBT represented the southern margin of the Aptian-Cenomanian BCB east and west of the Estella-Pamplona diapirs.

5. DISCUSSION

5.1 Role of inheritance for the architecture of the Pyrenean – Cantabrian junction

The role of inherited structures in shaping the present-day architecture of the Basque-Cantabrian junction is difficult to assess. Despite NNE-SSW oriented structures are very common in the study area, they cannot be linked to one particular tectonic event only. Indeed, it seems that this orientation guides the structural evolution of the Basque Country from Variscan to Alpine convergence (e.g. Variscan: García-Mondéjar et al., 1996; Permian: Lucas, 1987; Triassic: Curnelle, 1983; Late Jurassic – Barremian: Feuillée & Rat, 1971; Aptian – Cenomanian: Razin, 1989; Santonian to Miocene: Razin, 1989; see chapter 2.1). This is particularly well documented by the turning of the Albo-Cenomanian SMD and NMD from a WNW-ESE to NNE-SSW orientation along the preserved NNE-SSW Bidarray Permian basin (Fig. II-4). Moreover, this orientation is also observed in the Alpine structures as exemplified by the Oyarzun and Labourd lateral ramps, although in this case it is more difficult to identify the nature and age of the inherited structure that is at their origin. Thus, at this stage it is difficult to clearly define the role of inherited structures on the tectonic evolution of the Basque-Cantabrian junction. Nonetheless, we attribute an importance to inheritance in controlling the orientation and location of the Late Jurassic – Barremian basins (e.g. Delfaud, 1970; Feuillée & Rat, 1971; Razin, 1989) as observed along the Estella – Pamplona diapirs (Fig. II-9) or the Mena-Sedano-Poza de la Sal structure (western BCB) (e.g. Del Pozo, 1971; Feuillée & Rat, 1971), both of which depicting NNE-SSW aligned diapirs.

In this study, we identify the north-western and south-western limits of a Late Jurassic – Barremian basin in the BCB that corresponds to the reactivated Aralar thrust and SBPT, respectively (Fig. II-6). This basin probably also controlled the initiation and localisation of Aptian – Cenomanian hyperextended basins as indicated by the development of a thick sedimentary wedge against the former SPBT. However, the migration of the deformation into areas where no Late Jurassic – Barremian deposits are observed (i.e. Nappe des Marbres; Figs. II-6 and II-11) shows that, apart from inheritance, the rift propagation was controlled by other processes as well.

The occurrence of thick Upper Triassic evaporites in many places affected by subsequent Late Jurassic to Cenomanian extension shows that salt tectonics has significantly controlled the style of deformation during the multiple rifting episodes and the later convergence.

Indeed, throughout the study area it can be shown that the post-Triassic sedimentary cover was detached above a rather continuous and efficient decoupling level defined by the Upper Triassic evaporites. This is well documented by the occurrence of mantle and granulite clasts embedded within the Keuper at the base of the Jurassic to Cenomanian sedimentary cover (e.g. DeFelipe et al., 2017; Jammes et al., 2010b; Lagabrielle et al., 2010). This decollement horizon has been reactivated during the tectonic inversion resulting in a decoupling of the sedimentary cover (thin-skinned) from the shortening of the underlying basement (thick-skinned) (Fig. II-11). Our work highlights the importance of inheritance on controlling the thin- and thick-skinned deformation during extension and reactivation.

5.2 Structural evolution of the Aptian – Cenomanian rift basins

Based on field and seismic observations and integration of drill hole data, we propose a new model for the Aptian to Cenomanian rift architecture, which has strong implications for the paleogeographic, kinematic and reactivation history of the Pyrenean – Cantabrian junction.

Previous interpretations suggested the occurrence of a crustal scale NNE-SSW Pamplona fault that delimited the BCB and the Mauléon basin as either E-W directed transtensional pull-apart basins or as a transform/transfer fault in a N-S to NNE-SSW extensional direction (see Fig. II-1). In our study, we showed that the St-Jean-de-Luz basin represented the western continuation of the Mauléon basin from Late Albian onwards, as indicated by the occurrence of more than 2000 meters of deep water turbidites in this basin (Fig. II-5). Similarly, we identified the prolongation of the BCB east of the Estella-Pamplona diapirs (i.e. in the Jaca-Pamplona basin; Figs. II-9 and II-10) where up to 1400 meters of Aptian – Cenomanian sediments have been recorded. We suggest that the St-Jean-de-Luz and Jaca-Pamplona basins represent the western and eastern continuation of the Mauléon basin and BCB respectively (Figs. II-5, II-9 and II-10). The Aptian-Cenomanian BCB likely narrows toward the east and terminates along the Oroz-Betelu massif where Late Albian to Cenomanian conglomerates and sandstones have been observed (Ciry et al., 1963; Fig. II-2). The Late Albian to Cenomanian St-Jean-de-Luz basin probably tipped out against the Landes high or Biscay massifs (Voort, 1964) from where the basin was fed (Razin, 1989). The extend of the Aptian-Cenomanian hyperextended basin is well shown by the distribution of the post-rift upper Cretaceous facies distribution (Fig. II-2) to which the western Jaca-Pamplona and St-Jean-de-Luz basins belong.

In this study we also describe former WNW-ESE extensional faults (SPBT, SMD, NMD, NPFT and Amotz faults) that bounded the Aptian – Cenomanian BCB, Mauléon and St-Jean-de-Luz rift basins (Figs. II-2, II-3, II-5 and II-6). The orientation of these structures

corresponds to the trend of the HT/LP Albo-Cenomanian metamorphic rocks and exhumed mantle/granulite rocks in the BCB and Mauléon basins (e.g. Clerc et al., 2015). Moreover, several NNE-SSW trending transfer faults such as the Ibarra, Saison, or St-Jean-Pied-de-Port transfer faults have been described across the area. All these observations argue for a N-S to NNE-SSW direction of extension during Aptian to Cenomanian at the Pyrenean – Cantabrian junction as already suggested by Tugend et al. (2015), Tavani & Muñoz (2012) or Tavani et al. (2018). This is also in line with kinematic indicators described from the SMD and NMD (Masini et al., 2014) in the Mauléon basin.

As a consequence, we show that the mid-Cretaceous Cantabrian and Pyrenean rift systems display a spatial overlap characterized by a V-shape geometry south and north of the Basque massifs (previously suggested by Floquet & Mathey, 1984). One should note that overlapping rift systems have been shown to preferentially develop during orthogonal extension in contrast to transform faults that mostly develop in oblique systems (Acocella, 2008), giving additional credits for N-S direction of extension. This major observation enables to discard the existence of a NNE-SSW striking Pamplona transform fault during Aptian to Cenomanian extension linking the Aquitaine with the Ebro basins.

5.3 A new model for inheritance and reactivation at the Pyrenean-Cantabrian junction

These new results, implying overlapping WNW-ESE striking rift basins north and south of the Basque massifs and rebutting crustal decoupling between the Cantabrian and Pyrenean rift systems, suggest a new initial framework for the reactivation of this domain during Pyrenean convergence. In particular, little is known about how reactivation proceed in such system where weak rift basins overlap in the direction of shortening.

In the following, we identify and characterize the thin-skinned (supra-salt) and thick-skinned (crustal) deformation on a N-S crustal cross-section (Fig. II-11a) and on a map view (Fig. II-12a). In figures II-11 and II-12, we plot the thin-skinned and thick-skinned singular points (S point; e.g. Willett et al., 1993), which correspond to the location of the basal tip of the wedge formed by the post-salt unit (thin-skinned) and crustal unit (thick-skinned), respectively, during contractional deformation. As such, the location of the thin-skinned S points for the Mauléon – St-Jean-de-Luz and BCB – Jaca-Pamplona basins correspond to the intersection between the NPFT and Amotz – Arbéroue thrusts, and SPBT and Leiza thrusts, respectively. The location of the thick-skinned S point corresponds to the former wedge at reactivation

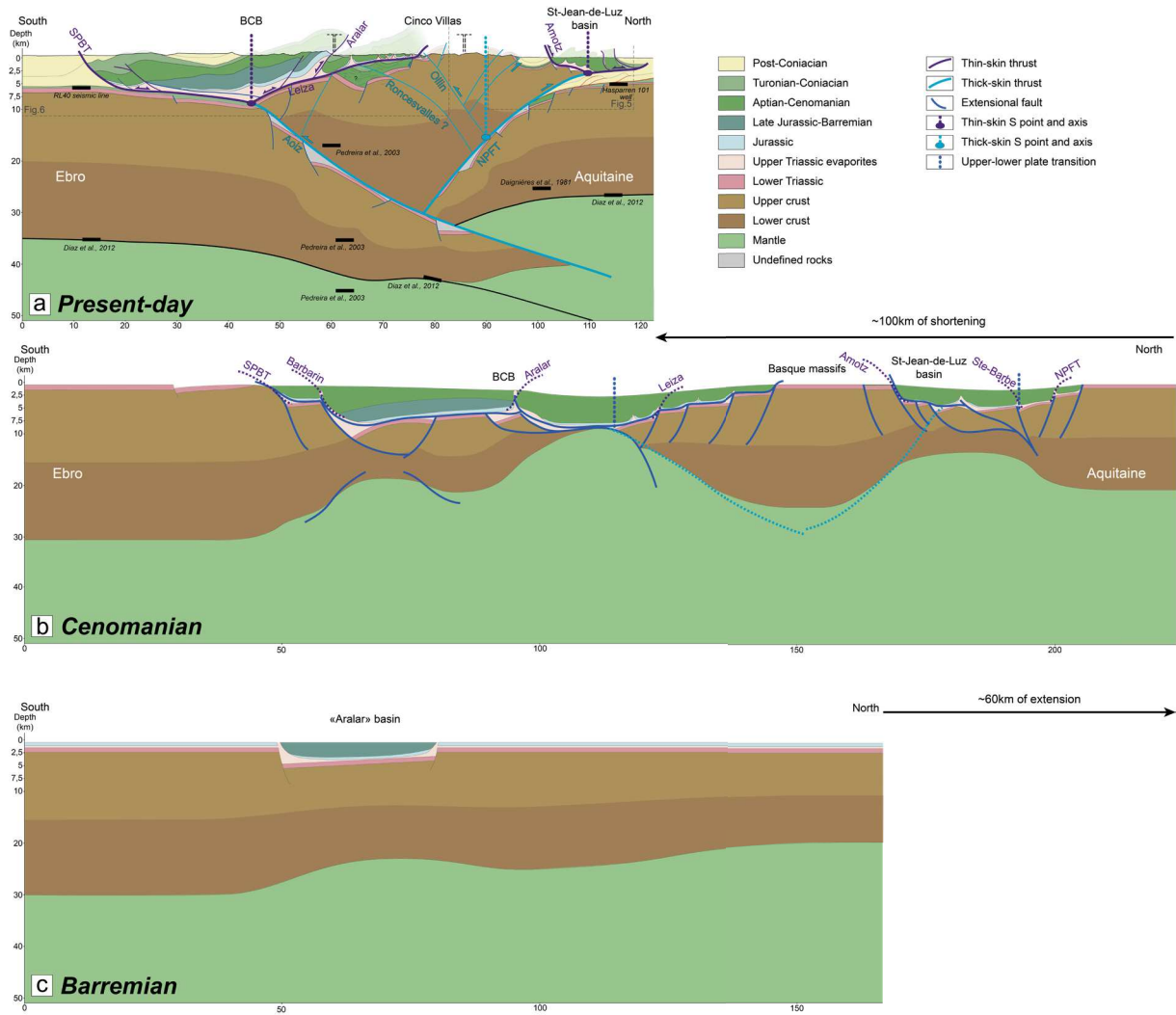


Figure II-11: a) Present-day crustal cross-section across the BCB to St-Jean-de-Luz basin. Note the juxtaposition of thin-skinned and thick-skinned thrusts of opposite vergence and the allochthony of the BCB and St-Jean-de-Luz basin on both sides of the crustal wedge. Moho depths are from Diaz et al. (2012) and Daignieres et al. (1982), and we plot the layer segments defined on seismic reflections from profile 1 of Pedreira et al. (2003). Location of cross-section on figure II-12. b) Restored cross-section at Cenomanian time depicting the architecture of the overlapped rift basins north and south of the Basque massifs. c) Restored crustal section at Barremian time. Variation of the Moho depth from south to north is based on present-day crustal thickness.

initiation and as such, corresponds at present-day to the axis between the north-vergent and south-vergent crustal thrusts.

On figure II-11a, we project the cross-sections of figures II-5 and II-6 on a crustal scale cross-section running from the Ebro basin to the Aquitaine basin via the BCB, the Cinco Villas massif and the St-Jean-de-Luz basin. The top basement is defined by seismic interpretations and the Hasparren 101 borehole, while the Moho depth is constrained by the study of Díaz et al. (2012) and Daignieres et al. (1982). We also propose a restoration of the cross-section at a late rifting stage (i.e. Cenomanian; Fig. II-11b) and a pre-Apto-Cenomanian stage (i.e.

Late Barremian; Fig. II-11c) taking into account crustal volume preservation using the ImageJ software (<https://imagej.nih.gov/ij/>). Based on these cross-sections and our study, we propose a general map (Fig. II-12a) highlighting the main thin-skinned and thick-skinned structures of our study area.

Thin-skinned thrust faults south of the Basque massifs correspond to the SPBT (and the Barbarin thrust fault that is part of the splay faults), the Leiza fault and the Aralar thrust (Fig. II-6). At least 15 km of southward displacement have been accommodated along the SPBT and minimum 20km have been estimated along the north-directed Leiza fault (Figs. II-6 and II-11). Both reactivated Aptian – Cenomanian detachment faults and transport the supra-salt sedimentary cover above the thick crusts of the Ebro and Basque massifs, respectively. The internal part of the BCB shows only minor north-vergent thrust faults mainly reactivating inherited structures such as the Late Jurassic – Barremian Aralar paleo-normal fault or the E-W striking squeezed salt extrusion observed in the Nappe des Marbres. North of the Basque massifs, the north-vergent NPFT represents the thin-skinned reactivation of an Aptian (or Late Albian in the St-Jean-de-Luz basin) to Cenomanian extensional fault (Razin, 1989). The NPFT is responsible for a significant northward transport of the Mesozoic basin as highlighted by figures II-3 and II-5 where it unconformably overlies the Cenozoic deposits on top of the Aquitaine platform. Most of the thin-skinned thrusts that crop out at the surface at present-day are dipping toward the north such as the Arbéroue, Amotz and St-Barbe thrusts, which reactivated north-dipping Aptian – Cenomanian and Late Albian – Cenomanian detachment faults. The Chainons Béarnais display a similar architecture as observed in the Nappe des Marbres, with E-W striking squeezed salt extrusions that are affected by minor south-vergent thrusts.

The thick-skinned deformation can be defined by surface geology and by deep imaging of the crust. In our study, we identified and summarized major north-vergent thick-skinned thrusts such as the Labourd, Ainhoa and the NPFT (e.g. Razin, 1989; Teixell, 1998) that are located on the northern part of the Basque massifs (Figs. II-2 and II-12). The NPFT, which accommodated a significant amount of crustal shortening, is relayed northward from east to west across the Saison transfer fault (Masini et al., 2014) and has been identified in both the Mauléon and St-Jean-de-Luz basins. This structure can be continuous toward the west and correspond to the North Iberian/Pyrenean Front located at the south of the Landes High (e.g. Roca et al., 2011). South-vergent crustal thrusts such as the Roncesvalles, Ollin and Lakoura thrusts are observed on the southern border of the Basque massifs (DeFelipe, 2017; Ruiz et al., 2006; Teixell, 1990, 1998). Moreover, seismic interpretation across the BCB argues for a south-vergent crustal thrust below the Urbasa syncline (see chapter 4.3). Based on receiver

function analysis, Díaz et al. (2012) imaged a continuous north-dipping “slab” from east to west below the Basque massifs, connecting the Cantabrian and Pyrenean segments. The WSW-ESE striking orientation of Roncesvalles thrust, which differs from the general WNW-ESE striking contractional structures, might correspond to the trend of the “slab” at depth.

These observations suggest a decoupling between the thin-skinned and thick-skinned deformation at the scale of the orogen. The entire BCB – western Jaca-Pamplona basin has been transported and uplifted along the thin-skinned SPBT and Leiza faults on top of the colliding Ebro and Basque crustal blocks (Figs. II-9, II-11 and II-13) and leading to the formation of a sedimentary wedge at the front of the allochthonous Basque massifs (Figs. II-6 and II-11). Similarly, the Mauléon and St-Jean-de-Luz basins have been transported along the thin-skinned NPFT and Arbéroue – Amotz faults during the crustal shortening that brought the Basque massifs above the Aquitaine basin (Figs. II-3, II-5 and II-11). Independently, the crustal deformation appears to be continuous from the Pyrenean to the Cantabrian systems. Indeed, crustal thrusts do not show a change in vergence or any major offset across the Basque Country (Fig. II-12). As such, change in thrust vergences previously attributed to the Pamplona fault (see chapter 2.2) actually correspond to the present-day juxtaposition of the thin-skinned and thick-skinned deformations (Fig. II-13). Moreover, on a map view (Fig. II-12), the crustal faults depict a sigmoid shape across the Pyrenean to Cantabrian systems and do not argue in favor of a crustal

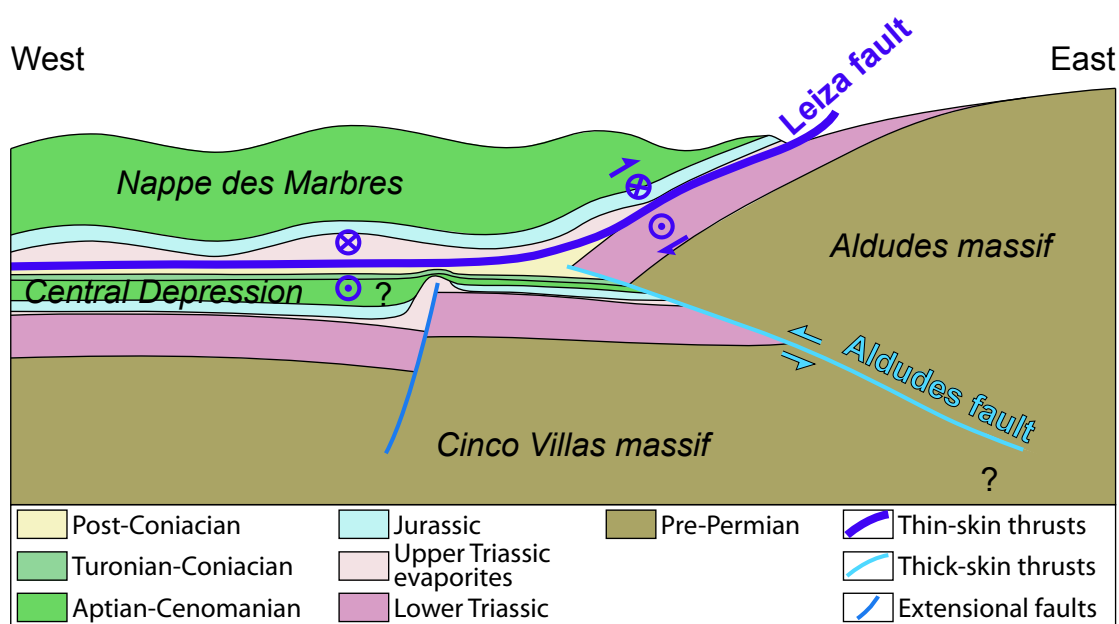


Figure II-13: Schematic cross-section across the eastern Nappe des Marbres to the Aldudes massif showing the allochthony of the Nappe de Marbres above the Cinco Villas and Aldudes massifs (Basque massifs). See location on figure II-12a.

decoupling between both systems. Complexities on the cylindric reactivation pattern are brought by the Labourd, Aldudes or Oyarzun lateral ramps that we can eventually attribute to oblique N-S to NW-SE convergence direction (Macchiavelli et al., 2017) with respect to the inherited NNE-SSW trend in the area. In this context, the existence of a regional scale NNE-SSW crustal fault decoupling the reactivation between the Pyrenean and the Cantabrian systems is unlikely.

Our mapping and field data evidence a good preservation from the Alpine deformation of the Labourd and the Basque massifs in general such as represented by the Bidarray Permian basin, the SMD and NMD rift structures and the distribution of the Lower Triassic sandstones. Moreover, previous authors (Masini et al., 2014; Teixell, 1998; Teixell et al., 2016) suggested that in the western Mauléon basin, a larger amount of basement was involved in the orogenic prism that formed on top of the NPFT, and along which a piece of lower crustal or subcontinental mantle was transported and responsible for the present-day positive gravity anomaly (Casas et al., 1997).

We suggest that this peculiar structural framework results from the reactivation of the overlapped, weak Pyrenean and Cantabrian hyperextended rift basins and the inability to deform the intermediate crustal block formed by the Basque massifs. Indeed, hyperextended domains have been shown to localize the initiation of reactivation and the northward underthrusting of the Iberian crust (e.g. DeFelipe, 2017; Jammes et al., 2009; Masini et al., 2014; Mouthereau et al., 2014; Quintana et al., 2015; Vacherat et al., 2017). However, in this area, the western Mauléon basin and the eastern BCB rift systems might compete during reactivation. As a consequence, geophysical data reflect this structural complexity that we can barely observe in the field. We believe that the interpretation of Díaz et al. (2012) should be revised in the light of our study and new investigations about the crustal architecture of the Basque country should be undertaken.

5.4 Implications for kinematics of the Western Pyrenees

The kinematics between Iberia and Europe and the location of the plate boundary have been widely debated in the Pyrenean community (see Fig. II-1). At a plate kinematic scale, geodynamic reconstructions involve a significant strike-slip component from Valanginian to Santonian between Iberia and Eurasia (Stampfli & Borel, 2002). At the scale of the Pyrenean – Cantabrian systems, previous kinematic scenarios imply either a Late Jurassic to Late Cretaceous E-W strike-slip deformation associated with formation of pull-apart basins or a N-S extension associated with offset rift segments along transform faults from either Early Cretaceous or Aptian (see 2.2). However, none of these scenarios satisfy geophysical or geological observations

(Barnett-Moore et al., 2016a; Nirrengarten et al., 2018). Based on geological and geophysical constrains, Nirrengarten et al. (2018) propose that the Iberia and Eurasia plate kinematics can imply a more diffuse boundary with the interplay of a Landes High and an Ebro block, where transtensional deformation might be distributed between the Central Iberian rift system and the Pyrenean system.

In our study, we showed that the Aquitaine and Ebro basement were connected via the Basque massifs from Aptian onward and that Aptian – Cenomanian rift systems opened along a N-S direction of extension (Fig. II-12b). Furthermore, we did not observe evidence for major strike-slip deformation (E-W or N-S) or rotation from Triassic onward within the Basque massifs, neither at larger scale such as suggested by the redundancy of the NNE-SSW Variscan to Triassic inherited trend on both the Aquitaine and Ebro blocks (e.g. Ebro: Feuillée & Rat, 1971; Basque massifs: Lucas, 1987; Aquitaine: Curnelle, 1983). Moreover, similar orientations of Permo-Triassic structures (e.g. Teruel fault) have been described in the south-eastern part of the Ebro basin (Arche & López-Gómez, 1996; Vargas et al., 2009; Fig. II-1).

As a consequence, the Ebro block can hardly be displaced and rotated by 400km from Europe during the Jurassic and Cretaceous. In this context, the existence of the NPF, on which most of the sinistral strike-slip movement was supposedly accommodated, seems unlikely in the Western Pyrenees (e.g. Chevrot et al., 2014; Mattauer & Séguret, 1971). Furthermore, the western prolongation of the NPF across the Aldudes – Labourd massifs and at the location of the Leiza fault (e.g. Arthaud & Matte, 1977; Combes et al., 1998; Floquet & Mathey, 1984; Hall & Johnson, 1986; Martínez-Torres, 1992; Mathey et al., 1999; Mendia & Ibarguchi, 1991; Muller & Roger, 1977; Rat, 1988) is not corroborated by our study and would imply an even greater offset as we need to restore back the Leiza fault south of its present-day situation. As such, questions remain about the accommodation of the sinistral strike-slip movement. Although we cannot exclude that part of the movement was accommodated along NNE-SSW transfer faults in the BCB and Mauléon basin (e.g. Canérot, 2017; Iriarte & García-Mondéjar, 2001; Tavani et al., 2018), such structures certainly do not account for the proposed 400km of eastward displacement of Iberia with respect to Eurasia during Aptian to Albian extension.

As a consequence, we suggest that the strike-slip deformation took place, if it existed, either outside from the present-day Pyrenean – Cantabrian junction or along a diffuse plate boundary. The lateral component had to be accommodated during the Late Jurassic to Late Barremian/Early Aptian (i.e from about M0 to C34 magnetic anomalies) associated with the formation of sparse and confined pull-apart basins. Finally, these results suggest that affecting an Iberian or Eurasian affinity to the Palaeozoic basement on both sides of the NPF or in the Basque massifs is misleading as the Ebro block could be part of Eurasia since the Triassic.

6. CONCLUSION

The aim of this study was to define the nature and the evolution of the Pyrenean – Cantabrian junction with particular emphasis on the role of inheritance. We used field cross-sections and seismic interpretations combined with drill hole data to describe the present-day architecture of the eastern and western termination of the BCB and Mauléon basin, respectively, that correspond to the trace of the formerly defined Pamplona fault. Our results show that:

1) Aptian – Cenomanian rifting took place along a N-S direction of extension controlled by WNW-ESE striking detachment faults and NNE-SSW transfer zones, associated with mantle exhumation and HT/LP metamorphism in WNW-ESE oriented V-shaped basins. The Late Jurassic – Barremian rift episode was eventually controlled by similar WNW-ESE and NNE-SSW structures. In our study area, we showed that Aptian – Cenomanian rifting initiated but did not propagate at the location of Late Jurassic – Barremian basins.

2) The Aptian to Cenomanian BCB and the Mauléon basin propagated further eastward and westward respectively, than the trace of the so-called suggested Pamplona fault. As a consequence, we discard the occurrence of any transform fault to transfer the deformation from the BCB to the Mauléon rift systems.

3) No major strike-slip or rotational deformation has been observed in the Basque Country as argued by the conspicuous Variscan to Triassic inherited NNE-SSW trend across the Aquitaine and Ebro basement.

4) Thin-skinned and thick-skinned structures display a contrasting architecture in the study area. Thin-skinned deformation reactivated and transported the former Aptian – Cenomanian rift basins while thick-skinned deformation seems to shortcut the Basque area, eventually responsible for the preservation of the pre-Alpine structures in the Basque massifs.

These results have major implications for the kinematics of the Basque Country and for the architecture of the Pyrenean – Cantabrian junction:

1) The architecture of the Basque Country at Cenomanian time results in two overlapping rift systems north and south of the Basque massifs. As such, the tectonic evolution of the Cantabrian – Pyrenean junction cannot be explained by crustal decoupling between both systems.

2) The Ebro block could be part of the Eurasia plate since Triassic and therefore undermines any important strike-slip displacement along the NPF during Jurassic and Cretaceous.

3) The Iberia – Eurasia plate boundary has to be located outside the study area or had to occur over a more diffuse area during Late Jurassic to Barremian.

CHAPTER III:

***ROLE OF RIFT-INHERITANCE AND
SEGMENTATION FOR OROGENIC
ARCHITECTURE: EXAMPLE FROM THE
PYRENEAN-CANTABRIAN SYSTEM***

ROLE OF RIFT-INHERITANCE AND SEGMENTATION FOR OROGENIC ARCHITECTURE: EXAMPLE FROM THE PYRENEAN-CANTABRIAN SYSTEM

Tectonics, in prep.

Rodolphe Lescoutre¹, Gianreto Manatschal¹

¹IPGS, EOST-CNRS, Université de Strasbourg, Strasbourg, France

ABSTRACT

The Basque Country corresponds to an inverted rift accommodation zone at the junction between the hyperextended Pyrenean and Cantabrian rift segments. The recognition of an inherited rift segment boundary allows for the first time to investigate the reactivation associated with large-scale rift segmentation in an orogenic system. We use field and seismic observations to propose a new map of rift domains and we provide balanced cross-sections in order to define the along-strike architecture associated with segmentation during rifting and subsequent Alpine reactivation. This study aims to characterize and identify reactivated and newly formed structures during inversion of two rift segments and its intermitted segment boundary. During convergence, two phases have been recognized within rift segment (eastern Mauléon basin). The Late Cretaceous to Paleocene underthrusting/subduction phase, mostly governed by thin-skinned deformation that reactivated the former hyperextended domains and the supra-salt sedimentary cover. The Eocene to Miocene collisional phase, controlled by thick-skinned deformation that took place once necking domains collided and formed an orogenic wedge. At the rift segment boundary, the underthrusting/subduction phase was already controlled by thick-skin deformation due to the formation of shortcutting thrust faults at the termination of overlapping V-shaped rift segments. Therefore, a proto-wedge composed of the Basque massifs formed since the initiation of reactivation in this area, where the pro- and retro-wedges correspond to the Cantabrian and Pyrenean segments, respectively. We suggest that this proto-wedge is responsible for the preservation of pre-Alpine structures on the Basques massifs and for the emplacement of subcontinental hyperextended mantle rocks at crustal level beneath the western Mauléon basin. These results argue for a first order cylindrical orogenic architecture from the Central Pyrenean segment to the Cantabrian segment despite rift segmentation. They also highlight the relative control of 3D rift-inheritance for the evolution and the local architecture of orogenic systems.

1. INTRODUCTION

In most collisional orogens worldwide, the restoration of the pre-collisional stage and the role of rift-inheritance have been investigated in the external, fold and thrust belt domains by the help of 2D balanced cross-sections. Few studies attempted to restore the internal parts, where the pre-collisional architecture has been intensively reactivated or subducted. A further difficulty is that internal parts of collisional orogens generally correspond to former distal parts of rifted margins, domains that are yet poorly understood and from which fate and behaviour during reactivation remain little investigated. Of particular importance to understand the structural evolution of internal parts of orogenic systems are the boundaries between rift domains (Sutra et al., 2013), where changes in mechanical and rheological properties occur (Chenin et al., 2017; Mohn et al., 2014; Tugend et al., 2015). These studies stressed in particular the role of the “coupling point” defined as the boundary between the necking and hyperextended domains, corresponding to the limit between crust thicker than 10km showing ductile levels in the crust; and crust thinner than 10km where the residual continental crust is brittle and the top of the mantle is serpentized and can act as an efficient decoupling horizon during reactivation (Péron-Pinvidic et al., 2008). Due to a major change in bulk rheology, crustal thickness and mechanical coupling between mantle and crust, the coupling point may play an important role in separating domains with different deformation style during tectonic inversion. In 2D sections, the coupling point may separate domains that can be subducted (hyperextended domain) from domains that can act as buttress and form the abutments of the future orogen (e.g. Lacombe & Bellahsen, 2016). While the role of the coupling point has been investigated in 2D sections (e.g. role of necking zone in Tugend et al., 2014), the role of the along-strike evolution of the coupling point/line has not yet been considered in the orogenic evolution. Yet, the present-day architecture of rift systems reveals a significant along-strike variability associated with transfer zones or relay zones (e.g. Belgarde et al., 2015; Péron-Pinvidic et al., 2017). As a consequence, integrating 3D inheritance in the reactivation of rift domains can complexify the reactivation pattern or lead to the formation of new structures that might explain the regional non cylindricality of collisional orogens (Chevrot et al., 2018; Jammes et al., 2014). Such 3D implications might account for some of the complexities encountered when dealing with 2D restorations and explain geological anomalies observed in orogenic systems.

In this study, we investigate the onshore Pyrenean – Cantabrian junction (Western Pyrenees), which corresponds to an overlapping rift relay system subsequently reactivated during Pyrenean convergence (Lescoutre et al., chapter II). This area preserves the first order rift architecture and therefore allows to study the 3D reactivation of a segmented hyperextended system.

This study aims to answer to the following questions:

- *How does 3D rift-inheritance control the orogenic architecture?*
- *How does a rift segment boundary behave during reactivation?*
- *Do coupled vs. decoupled rift domains and rift domain boundaries control the reactivation?*

2. GENERALITIES ABOUT THE PYRENEES, RIFT ARCHITECTURE, SEGMENTATION AND REACTIVATION

2.1 The Pyrenean-Cantabrian case study

The Pyrenean and Cantabrian orogenic systems are striking WNW-ESE between France and Spain and can be described as two segments of the same orogenic event separated by the Basque massifs, which represent as such, the Cantabrian-Pyrenean junction (Fig. III-1). The present-day architecture of the Pyrenean and Cantabrian orogenic systems corresponds to an asymmetric double-verging crustal wedge with a north-dipping underthrust/subducted “slab” (Alonso et al., 1996; Beaumont et al., 2000; Chevrot et al., 2018; Choukroune, 1989; Muñoz, 1992; Pedreira et al., 2003; Pulgar et al., 1996; Roure et al., 1989; Teixell, 1998). The slab formed during the Late Cretaceous to Miocene N-S convergence (e.g. Macchiavelli et al., 2017; Mouthereau et al., 2014) reactivating and inverting the former Cantabrian and Pyrenean mid-Cretaceous rift basins, and forming the present-day mountain chain and fossil Eurasian and Iberian plate boundary. These rift systems, which opened in a N-S to NNE-SSW direction of extension (e.g. Jammes et al., 2009; Tavani et al., 2018), reached mantle exhumation (e.g. Lagabrielle et al., 2010) and were associated with syn-rift High-Temperature/Low-Pressure metamorphism of the pre- to syn-rift sedimentary succession (Albarède & Michard-Vitrac, 1978; Clerc et al., 2015; Montigny et al., 1986; Ravier, 1959). The latter were detached above the Upper Triassic evaporites, representing a prominent decoupling horizon during both the rifting and compressional events (Lagabrielle et al., 2010; Vergés & García-Senz, 2001). No oceanic crust (ophiolite) or subduction-related features (e.g. arc volcanism, back-arc basin) have been evidenced in or around the inverted Cantabrian or Pyrenean basins, suggesting that the slab is only composed of continental and serpentinized mantle rocks.

On a map view, the Pyrenean orogenic system can be divided in 5 structural domains bounded by major WNW-ESE striking structures: the Axial Zone, the North Pyrenean Zone, the South Pyrenean Zone, the Aquitaine foreland basin (and Landes High), and the Ebro/Duero foreland basins (see details in Mattauer & Henry, 1974). The Axial Zone corresponds to the hinterland of the orogen and is composed of Palaeozoic rocks that represent the tectonic basement

that was marginally affected by several rift events and final Late Cretaceous to Miocene orogeny. It is bounded to the north by the North Pyrenean Zone, the latter corresponding to the former mid-Cretaceous hyperextended basins that have been subsequently inverted (e.g. Lagabrielle et al., 2010). They are bounded to the north by the North Pyrenean Frontal Thrust (NPFT) and the Aquitaine basin, which lies over European crust. Note that, towards the west of the Pyrenees, the Palaeozoic Basque massifs have been either attributed to the Axial Zone or to the North Pyrenean Zone, i.e. to belong either to the European or Iberian plates (e.g. Rat et al., 1983; Schott & Peres, 1988). To the south of the Axial Zone, the South Pyrenean Zone corresponds to piggyback basins (Puigdefàbregas et al., 1992) bounded to the south by the South Pyrenean Frontal Thrust (SPFT) and the Ebro foreland basin, which lies over Iberian crust.

In the Cantabrian segment, the Palaeozoic massifs of the Axial Zone are not observed anymore and therefore the South Pyrenean and North Pyrenean Zones cannot be defined. Instead, this terminology is replaced by WNW-ESE striking structural domains such as the Bilbao anticlinorium or the Biscay synclinorium, which are part of the Basque-Cantabrian basin (BCB) (Fig. III-1). However, similarly to the Pyrenean segment, the lateral continuation of the NPFT juxtaposes the inverted BCB and the Landes High, the latter corresponding to the westward prolongation of the Aquitaine foreland. Toward the south, the SPFT juxtaposes the BCB and the Ebro/Duero foreland basin such as observed in the Pyrenean segment.

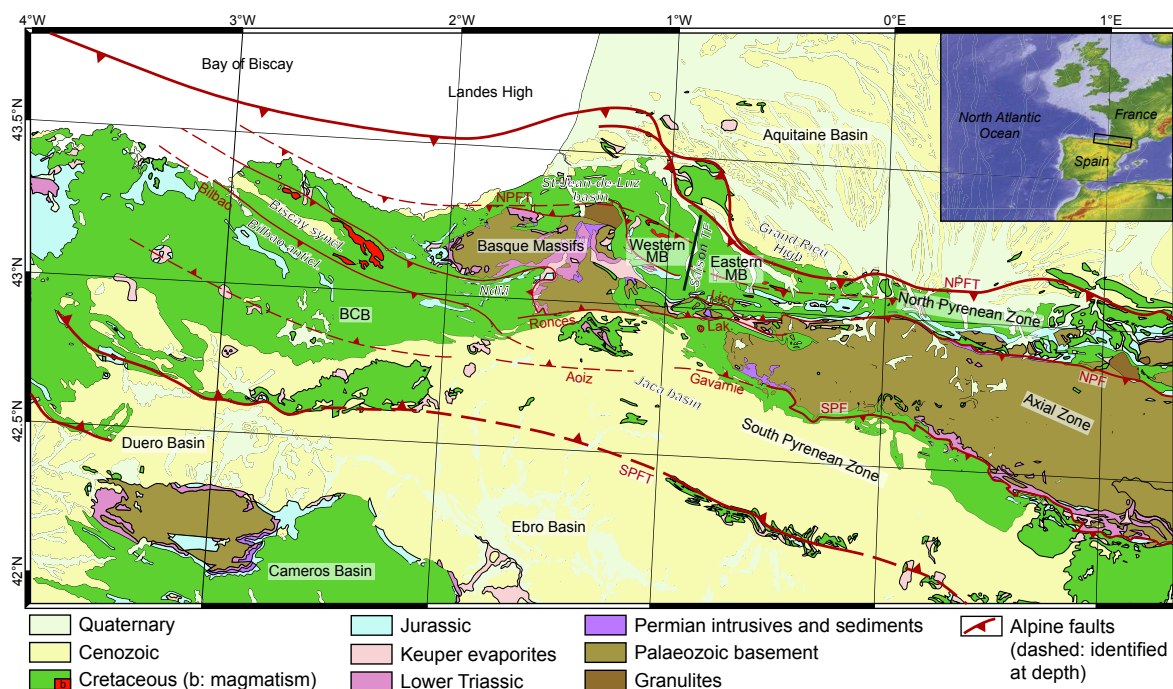


Figure III-1: Geological map of the Pyrenean-Cantabrian systems with the main domains and structural units. BCB: Basque-Cantabrian basin; NdM: Nappe des Marbres; Ronces: Roncesvalles fault ; Lak : Lakora fault ; SPFT : South Pyrenean Frontal Thrust ; NPFT: North Pyrenean Frontal Thrust; NPF: North Pyrenean Fault; SPF: South Pyrenean Fault; MB: Mauléon basin. Insert shows the location of the map.

2.2 Formation and reactivation of rift domains

The crustal architecture of rifted margins, together with the thermal state at onset of convergence, are likely to control the evolution of orogenic systems (Chenin et al., 2017; Erdős et al., 2014; Jammes & Huisman, 2012; Mohn et al., 2011; Vacherat et al., 2016). Sutra et al. (2013) and Péron-Pinvidic et al. (2013) proposed that magma-poor rifted margins can be characterized by 4 domains, each one characterized by a different crustal architecture and rheology (Fig. III-2).

The proximal domain corresponds to a 30 ± 5 km thick crust composed of brittle upper and ductile lower crusts and exhibiting local fault bounded basins and minor accommodation space outside these basins. At outcrop scale, this domain is characterized by thin, shallow marine and/or continental sediments deposited over partly eroded pre-rift upper crust.

The necking domain corresponds to an increase of the accommodation space related to oceanward crustal thinning (e.g. Osmundsen & Redfield, 2011). This domain preserves ductile levels in the crust and exhibits top-basement detachment faults that can exhume mid-crustal rocks. At outcrop scale, this domain is represented by slope to bathyal depositional environments onlapping onto either detachment surfaces characterized by gouges, cataclasites, tectono-sedimentary breccias or allochthonous crustal blocks.

The hyperextended domain shows a very large accommodation space and can be divided in two sub-domains, the hyper-thinned sub-domain corresponding to a <10 km thick, often hydrated crust and the exhumed mantle domain, which corresponds to a basement floored by serpentinized mantle. At outcrop scale, this domain is characterized by deep marine sediments downlapping onto detachment surfaces floored by either crustal or serpentinized mantle rocks.

This rifting stage ultimately leads to the accretionary stage with the formation of a ~ 6 km thick magmatic oceanic crust consisting of tholeiitic magmatic material (Anonymous, 1972).

During rifting, once the crust and the mantle are coupled (e.g. coupling point separating necking and hyperextended domains; Fig. III-2), rift evolution can develop asymmetrically and an upper plate and a lower plate can be distinguished, the former presenting the hangingwall and the latter the footwall of the main exhumation fault (e.g. Brune, 2014; Lister et al., 1986; Péron-Pinvidic et al., 2017; Sutra et al., 2013). Note that oceanic crust did not develop in the Pyrenean-Cantabrian rift systems, as shown by the absence of tholeiitic basalts and therefore will not be discussed in this paper.

Initiation of convergence should be expected to occur in the weakest part of the margin (e.g. Erdős et al., 2014). Péron-Pinvidic et al. (2008) and Lundin & Doré (2011) showed for the N-Atlantic margins that convergence initiated in the exhumed and hyper-thinned domains, i.e. oceanward of the coupling point. It appears that the compressional structures tend to use existing structures (e.g. top basement eventually composed of serpentinized mantle) and low-angle detachment faults (e.g. Epin et al., 2017; Jammes et al., 2014; Stern, 2004; Tugend et al., 2014). The underthrust of the hyper-thinned and exhumed domains is favored and sustained by low frictional slip surfaces composed of hydrated material (serpentine, talc, clays etc.) (Beltrando et al., 2014; Hilairet et al., 2007). Since the hyperextended domain can exceed 100km in width (Chenin et al., 2017), it is wide enough to be pulled down into the eclogite facies, as indicated by the occurrence of ultra-high pressure rocks in orogenic domains. During this underthrusting/subduction stage, part of these domains can eventually be scraped and accreted within the accretionary wedge or transported within nappes (e.g. Andersen et al., 2012; Beltrando et al., 2014; Epin et al., 2017). Collisional processes initiate when the necking zone is entering subduction, i.e. when the conjugate coupling points meet. At this stage, the >10km thick crust of the necking domain can form a buttress (Mohn et al., 2014; Tugend et al., 2014) and a crustal wedge related to continental collision starts to develop (Mouthereau et al., 2014). At this stage, the singular point (S point), which corresponds to the location where one plate slides below the other (e.g. basal tip of the wedge; Beaumont et al., 2000; Willett et al., 1993), may coincide with the coupling point inherited from the former margin structure. Note that the occurrence of an effective decoupling layer in the crust or within the sedimentary cover can lead to the formation of a secondary S point (e.g. Roure et al., 1990). In the final collisional episode, rift-related high-angle normal faults of the proximal margin are reactivated (e.g. Buitter & Pfiffner, 2003; Butler et al., 2006; Carrera et al., 2006) leading to the formation of the thrust-and-fold belt forming the external part of the orogen.

The previously described 2D inversion of a hyperextended rift system might be hampered in case of non-cylindrical along-strike variation of the rift architecture. In particular, the V-shaped basin architecture or transfer zones might precursory lead to the collisional stage along-strike and impede subduction to nucleate and can complexify the orogenic framework at former rift segment terminations. In this study, we aim to study the role of segmentation and along-strike rift-inheritance on the 3D orogenic architecture using the example of the Western Pyrenees.

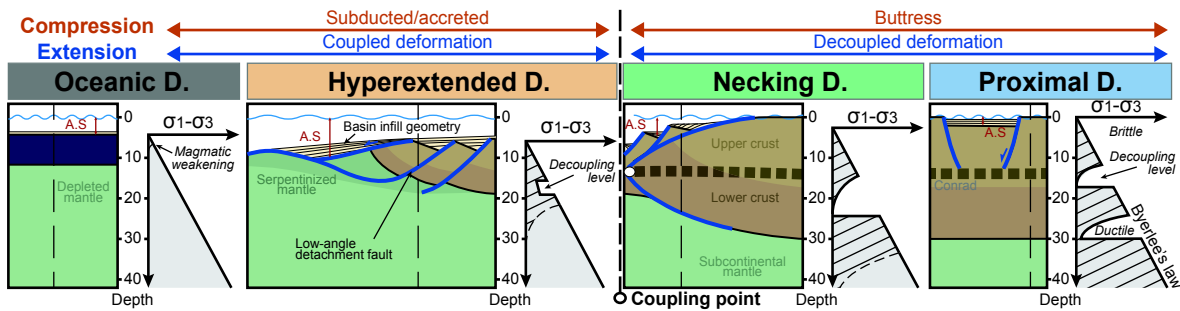


Figure III-2: Diagnostic structural and sedimentary relationships and rheological profiles characterizing the different rift domains. Note that the total accommodation space (A.S.; water plus sediments) can either be characterized by thickness (if subsidence rates equal sedimentation rates, in which case depositional environment remains shallow), or by a deepening of the depositional environment, in which case subsidence rates are higher than sedimentation rates. Thus, the proximal domain is formed by either continental or shallow marine sediments that remain thin; while the hyperextended domain is formed by either deep water facies and/or very thick shallow marine to continental sequences. The rheological profiles show the strength profile both at the end of rifting (hatched area) and after thermal relaxation (grey). The location of the rheological profiles is indicated by the vertical dashed lines in the sections. The main observation is that each rift domain is characterized by a different pre- and post- thermal relaxation rheological section with different locations for the potential crustal/mantle decoupling levels.

2.3 Along-strike segmentation

The along-strike architecture of rift systems has been shown to be highly variable in most present-day margins (Nonn et al., 2017; Péron-Pinvidic et al., 2017), very often controlled by pre-rift inheritance (e.g. Belgarde et al., 2015; Mercier de Lépinay et al., 2016). Junction between rift segments can occur via a transform fault (see review of Basile, 2015), a transfer zone (Faulds & Varga, 1998) or an accommodation zone associated with relay ramps (Acocella et al., 2005; Bubeck et al., 2017; Faulds & Varga, 1998). However, the 3D architecture of such junctions remains poorly-understood with respect to the 2D dip architecture of rifted margins.

In an accommodation zone, rift systems overlap parallel or slightly oblique to the direction of extension (Corti, 2012; Wilson, 1990; Zwaan et al., 2016). This overlapping geometry is favoured by orthogonal rifting and by a large offset between rift segments (Le Calvez & Vendeville, 2002; Zwaan et al., 2016), providing that the total length of the rift segments is much greater than the distance between the overlapping rift axis (Acocella, 2008). In detail, segment rotation or second order transfer zones and relay zones can accommodate the termination of rift segments (e.g. Faulds & Varga, 1998; Le Calvez & Vendeville, 2002; Tapponnier et al., 1990).

The reactivation of transfer zones during tectonic inversion has been only little investigated (e.g. Calassou et al., 1993; Konstantinovskaya et al., 2007; Ustaszewski et al., 2005), whilst the reactivation of overlapped rift systems and their implication for the orogenic architecture has yet to be explored.

3. THE PYRENEAN-CANTABRIAN STUDY CASE

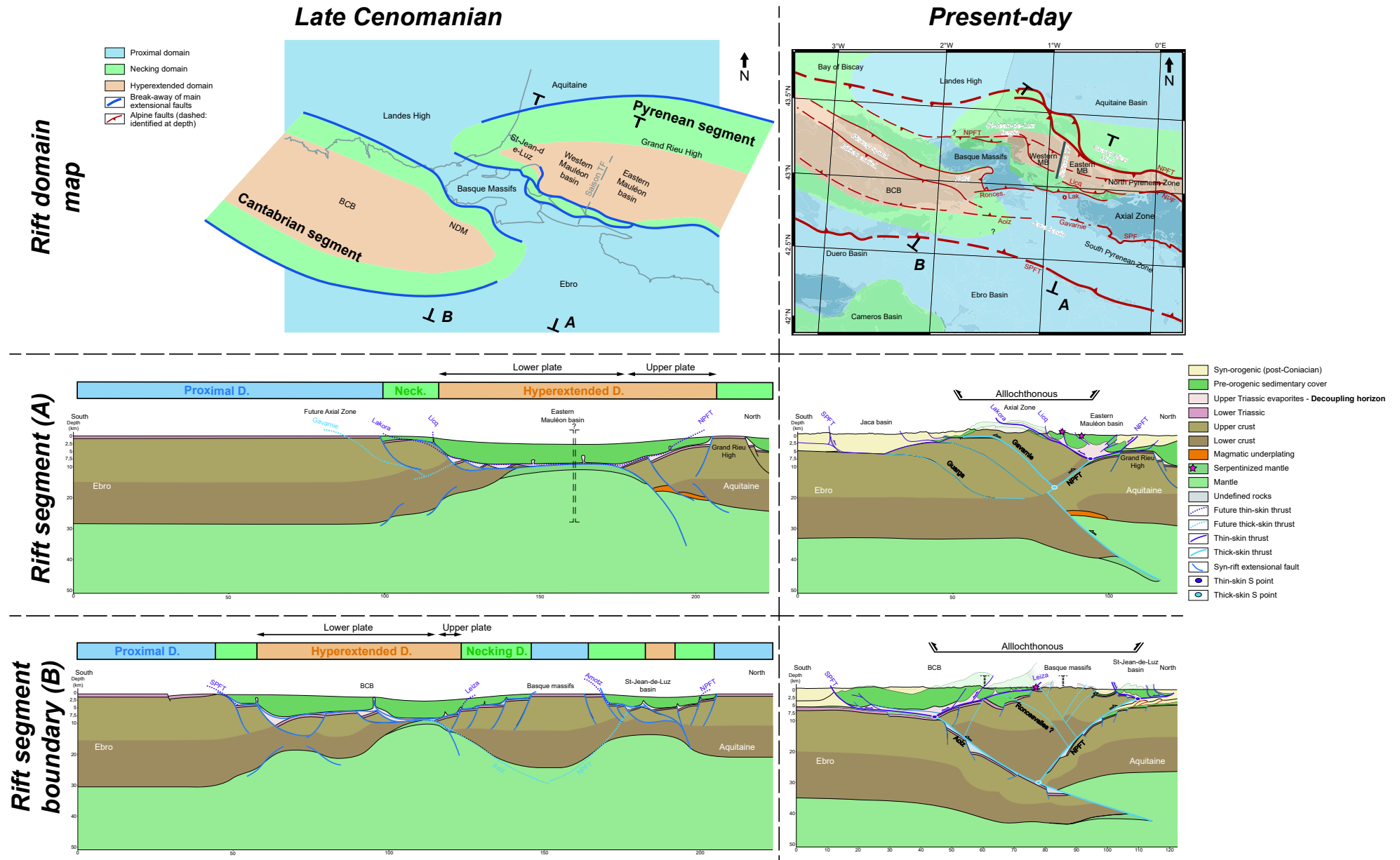
3.1 Identification of former rift domains

Tugend et al. (2014) identified and mapped former rift domains of the study area based on gravity inversion, seismic interpretation and field observations. However, the transition between the Pyrenean and Cantabrian rift systems was attributed by the authors to a crustal-scale transform fault (Pamplona fault) and, as a consequence, the termination of rift domains along-strike was assumed to end abruptly. In a recent study, Lescoutre et al. (chapter II) showed that the paleogeography of the area actually corresponds to overlapping rift basins, the Mauléon basin propagating westward in the St-Jean-de-Luz basin whilst the BCB propagated eastward in the Jaca-Pamplona basin. These results require a re-mapping of the rift domains in this area (Fig. III-3) based on the criteria presented in the previous chapter and ask for an evaluation of the consequences for the subsequent convergence.

Proximal domain: The Aquitaine, Landes High and Ebro/Duero units correspond to domains with a >20km thick crust (Bois et al., 1997; Fernández-Viejo et al., 2000; Pedreira et al., 2003; Tugend et al., 2014), which is compatible with the occurrence of upper-Cretaceous erosional surfaces or thin, shallow water sedimentary sequences (García-Mondéjar, 1986; García-Mondéjar et al., 1996; Vergés & García-Senz, 2001). The Axial Zone, the South Pyrenean Zone and the Basque massifs correspond during the upper Cretaceous to shallow marine and/or emerged areas suggesting that these domains were also formed over crust >20km (Bodego & Agirrezabala, 2017; Casteras, 1949; Feuillée & Sigal, 1965; Razin, 1989; Vacherat et al., 2017).

Necking domain: In the Pyrenean segment, transitional slope facies associated with detachment faulting have been observed over the Mendibelza massif (Boirie & Souquet, 1982) and more generally on the northern margin of the Basque massifs (Johnson & Hall, 1989a, 1989b; Masini et al., 2014; Razin, 1989; Vacherat et al., 2017). In the Cantabrian segment, these transitional facies have been retrieved north of the Biscay synclinorium, south of the Basque massifs and north of the SPFT (Bodego et al., 2015; Fernandez-Mendiola & García-Mondejar, 1990; García-Mondejar, 1989; Gräfe, 1999; Mathey et al., 1999; Meschede, 1987).

Figure III-3: Rift domain maps and cross-sections across the eastern Mauléon basin (rift segment) and the eastern BCB and St-Jean-de-Luz basin (rift segment boundary) at late rifting stage (Late Cenomanian) and after Alpine collision (present-day). For description and discussion of the figure see text.



Reactivation of major basin bounding faults has been proposed to occur along the NPFT based on structural reconstruction in both the Pyrenean and Cantabrian segments (Baby et al., 1988; Gómez et al., 2002; Lagabrielle et al., 2010; Razin, 1989). In the Pyrenees, the thinned crust of the Grand Rieu represented a topographic high between the Arzacq basin to the north and the Mauléon basin to the south (Masini et al., 2014). As such, we assume that the necking domain extended from the north of the Arzacq basin up to the southern margin of the Grand Rieu High.

Hyperextended domain: This domain corresponds to thick turbidite sequences deposited during Albian to Cenomanian in the BCB, western Jaca-Pamplona basin, St-Jean-de-Luz basin and Mauléon basin (e.g. Rat, 1988; Souquet et al., 1985) associated with serpentized mantle rocks (Lagabrielle et al., 2010; Mendia & Ibarguchi, 1991), syn-rift HT/LP metamorphic rocks (Clerc et al., 2015 and references therein) and sometimes alkaline magmatic rocks (Azambre & Rossy, 1976; Montigny et al., 1986).

3.2 Present-day architecture

3.2.1 Rift segments

In the Pyrenean segment, the Grand Rieu High is located in the footwall of the NPFT, which transports the Mauléon basin and part of the upper crust of the Axial Zone (Ebro basement) towards the north (Biteau et al., 2006; Daignieres et al., 1982; Teixell, 1998). Towards the south, the reactivated thin-skinned Licq fault and the basement-involved thin-skinned Lakora thrust emplace the basin over the Axial Zone (Masini et al., 2014; Teixell, 1990; Teixell et al., 2016). Between the NPFT and the Licq fault, the Mauléon basin is affected by WNW-ESE striking folds and thrusts, the latter detached in the Upper Triassic horizon. The Axial Zone corresponds to the north-dipping Gavarnie and Guarga imbricate thrust system (Teixell, 1990) responsible for the flysch deposits in the South Pyrenean Zone (Labaume et al., 1985).

As such, the thin-skinned S point corresponds to the base of the wedge formed by the supra-salt basin (i.e. intersection between the thin-skinned Licq and NPFT). At depth, the indentation of the Aquitaine crust at mid-crustal level within the Ebro crust led to a crocodile-shape architecture (Teixell, 1998). As such, the former hyperextended domain and lower crust of the Ebro lower plate represent the underthrust material, while the upper crust of the necking domain (Mendibelza/Igountze) has been thrust onto the indentor. In this segment, the Gavarnie and NPFT form the pro-wedge and retro-wedge respectively, of the orogenic wedge (Beaumont et al., 2000).

In the Cantabrian segment, i.e. the central BCB, the thin-skinned SPFT juxtaposes the supra-salt BCB above the Ebro/Duero foreland basin (Camara, 1997; Carola et al., 2013; Martínez-Torres, 1993). North of the basin, the reactivated NPFT (Gómez et al., 2002) put the BCB and its para-autochthonous sedimentary cover over the Landes High (Pedreira et al., 2007; Quintana et al., 2015; Roca et al., 2011). Between these two major faults, the BCB shows internal deformation mainly governed by WNW-ESE striking folds and thrusts (e.g. Ábalos et al., 2008), the latter detached along the Upper Triassic decoupling horizon. At depth, a high density, magnetic body attributed to lower crustal or mantle rocks has been described in the hangingwall of the NPFT (e.g. Aller & Zeyen, 1996; Pedreira et al., 2007).

In the section, the thin-skinned S point can be defined, which corresponds to the base of the wedge formed by the supra-salt basin. The crustal wedge (and related thick-skinned S point) formed between the NPFT and the SPFT (e.g. Roca et al., 2011), whilst the underthrust slab is composed, in the section, by crust derived from the former southern margin of the BCB.

As such, the SPFT/Licq and NPFT represent prominent structures for the Pyrenean and Cantabrian orogenic systems as they delimit the allochthonous units of the orogenic wedge from the autochthonous units (Ebro/Duero and Grand Rieu/Landes Highs) (Beaumont et al., 2000). Moreover, the NPFT and the SPFT have been shown to reactivate rift structures of the former necking domains in the Pyrenean and Cantabrian systems. This suggests that the limits of the orogenic structural units correspond at a first order to the limits of the former rift domains at rift segments.

3.2.2 Rift segment boundary

At the segment boundary, the inverted eastern BCB and St-Jean-de-Luz basin represent the southern and northern branch respectively, of two overlapping rift basins with the Basque massifs as the intermediate block (Fig. III-3; Lescoutre et al., chapter II). Here, the BCB and St-Jean-de-Luz basin are passively transported above the Basque massifs and the Ebro and Aquitaine foreland basins via the thin-skinned NPFT, SPFT, Leiza and Amotz reactivated structures detached in the evaporite horizon (see Fig. III-3 for location; Lescoutre et al., chapter II; DeFelipe, 2017; Martínez-Torres, 1993; Razin, 1989; Serrano et al., 2006). The basement shows north-dipping thrusts south of the Basque massifs and south-dipping thrusts north of the Basque massifs. Southward, the Aoiz thrust (Cámara & Klimowitz, 1985; Lescoutre et al., chapter II) juxtaposes the Basque massifs over the Ebro basement (4247 meters deep in the Aoiz borehole; Instituto Geológico y Minero de España (IGME), 1990) whilst toward the north, the NPFT put the Basque massifs over the Aquitaine crust (Razin, 1989; Serrano et al., 2006). The NPFT is continuous toward the east in the western Mauléon basin up to the NNE-SSW Saison

transfer fault, along which the NPFT is shifted toward the south (Masini et al., 2014). Masini et al. (2014) noted that, in contrast to the eastern Mauléon basin (rift segment), the hyperextended basement of the western Mauléon basin, together with the subcontinental mantle responsible for the gravity anomaly were thrust above the Aquitaine crust along the NPFT (Casas et al., 1997; Jammes et al., 2010a; Wang et al., 2016). Interestingly, at the south-western termination of the Mauléon basin, the South and North Mauléon Detachments (lateral equivalent to the Licq detachment fault) show no major Alpine overprint (Masini et al., 2014), which is also true for the Permian basin located on the Basque massifs (Lucas, 1987; Lescoutre et al., chapter II).

In the eastern continuation of the BCB, the E-W striking and north-dipping Roncesvalles thrust fault (or “*faille de Bigorre*” in Souquet et al., 1977) seems to link the southern branch with the Pyrenean rift segment and strikes parallel to the Lakora thrust. In the western continuation of the northern branch, the strike of the NPFT changes from WNW-ESE to NE-SW and finally seems to link with the Cantabrian segment (e.g. Gómez et al., 2002; Rat, 1988; Roca et al., 2011).

At depth, the seismic profiles obtained from receiver function analysis (Díaz et al., 2012) suggest that the underthrust/subducted slab at the rift segment junction formed from the underthrusting of the southern margin of the BCB basin and is continuous toward the east, i.e. in the Jaca-Pamplona basin up to the Mauléon basin. In contrast, no slab is observed associated with the northward underthrusting of the Aquitaine crust in the northern Pyrenean branch (St-Jean-de-Luz) and the crustal thickness is about 20 to 30km at present-day (Daignières et al., 1982; Pedreira et al., 2003; Tugend et al., 2014), suggesting that it nearly returned to initial crustal thickness during Pyrenean convergence.

At this segment boundary, the location of the thick-skinned S point is located at the intersection between the north-dipping slab (Aoiz fault) and the south-dipping NPFT identified below the St-Jean-de-Luz basin. As a consequence, and in contrast to the rift segments, the thick-skinned S point is not located below the inverted rift basin and the orogenic wedge is formed by the entire Basque massifs. Moreover, two thin-skinned S points are identified corresponding to the allochthonous BCB and St-Jean-de-Luz overlapping rift basins.

3.3 Rift architecture

3.3.1 Rift segments

The restoration of the Pyrenean and Cantabrian rift segments at the end of rifting depicts the same first order architecture (e.g. Masini et al., 2014; Roca et al., 2011; Tugend et al., 2014).

In the Pyrenean segment (eastern Mauléon), the northern part of the Igountze-Mendibelza unit corresponds to the WNW-ESE striking north-dipping Licq detachment fault (or South Mauléon Detachment fault in Masini et al., 2014) (Johnson & Hall, 1989a, 1989b; Masini et al., 2014) over which conglomerates have been deposited (Boirie & Souquet, 1982). This fault belongs to a set of extensional detachment faults that exhumed basinward serpentized mantle rocks underneath the detached supra-salt sedimentary cover (Corre et al., 2016; Lagabrielle et al., 2010) associated with deposition of deep water turbidites within the basin (Debroas, 1990; Souquet et al., 1985). The mantle exhumation led to a syn-rift HT/LP metamorphism of the pre- to syn-rift sequence toward the northern margin of the basin (Hart et al., 2017; Lescoutre et al., chapter IV) associated with magmatism (Genna, 2007). Northward, the south-dipping NPFT extensional fault controlled the northern margin of the basin (south of the Grand Rieu High) and was detached in the decoupling horizon made of evaporites.

In the BCB, the basement-sediment interface is hidden by a thick Mesozoic to Cenozoic sedimentary cover. However, and similarly to the Pyrenean segment, the tectono-stratigraphic reconstructions suggest north-dipping detachment faults (SPFT) that exhumed lower crustal levels and serpentized mantle rocks (Carola et al., 2013; Roca et al., 2011). Hydrothermal mineralisations (Cuevas & Tubía, 1999) and high vitrinite reflectance values (6-7%VR; Robert, 1971) have been described in the Lower Cretaceous sediments of the northern Bilbao anticline, suggesting that syn-rift HT/LP metamorphism also occurred in the BCB. Moreover, syn- to post-rift volcanism has been described in the Biscay synclinorium (Azambre & Rossy, 1976; Castañares et al., 2001). The dense and magnetic body defined in the central BCB could represent such underplating magmatic rocks (Aller & Zeyen, 1996; Casas et al., 1997; Pedreira et al., 2007).

All these observations suggest an asymmetry of the rift system, with a lower plate setting on the southern margin and an upper plate on the northern margin limited by north-dipping detachment faults in both the BCB and Mauléon basin. In both basins, the pre- to syn-rift sedimentary cover has been detached from the underlying basement along the Upper Triassic evaporite horizon.

3.3.2 Rift segment boundary

The eastern BCB (southern branch) architecture is similar to the BCB rift segment described above with the north-dipping SPFT detachment fault and mantle exhumation. However, the hyperthinned domain appears to be wider, eventually taking over the large exhumed mantle domain suggested in the central segment. This exhumed mantle domain is overlain by the Nappe des Marbres unit (Lamare, 1936; Martínez-Torres, 1992), forming the hangingwall of the Leiza fault that is detached in the Upper Triassic evaporites (Mathey et al., 1999; Mendia & Ibarra, 1991). The northern margin of the basin corresponded to the present-day location of the Ollin thrust (Bodego et al., 2015), which is an E-W striking structure located on the southern border of the Basque massifs. The BCB propagated and narrowed eastward (i.e. the western Jaca-Pamplona basin; Lescoutre et al., chapter II) as suggested by the thinning of the syn-rift sequence (Astrain-1 borehole; Instituto Geológico y Minero de España (IGME), 1990) and the apparent absence of syn-rift metamorphism (Lescoutre et al., chapter IV; Robert, 1971). The Cantabrian segment probably wedged out south of the Roncesvalles fault as suggested by the deposition of shallow water sandstones and conglomerates over the Oroz-Betelu massif (Ciry et al., 1963).

The Late Albian to Cenomanian St-Jean-de-Luz basin probably suffered of less extension as suggested by the 2000m thick syn-rift succession (Razin, 1989) that is significantly thinner than that in the main depocenter of the Mauléon basin that can be up to 4km (Masini et al., 2014; Vacherat et al., 2014) and the very low-grade syn-rift metamorphism (see Lescoutre et al., chapter II for details). The geometry of the basin can be defined by the E-W striking Amotz fault on the southern border of the basin, whilst the geometry of the northern border could roughly correspond to the present-day orientation of the reactivated WSW-ENE striking Ste-Barbe back-thrust, as suggested by Razin (1989). This basin was fed by siliciclastic sediments derived from the south and the west (Razin, 1989), suggesting that the basin terminated north-west of the Basque massifs. This suggests a V-shape, westward termination of the Mauléon basin.

3.4 Time constraints on the contractional deformation

The timing of the contractional deformation is difficult to assess in the north-western Pyrenees due to ill-recorded syn-orogenic sediments. Field evidence for inversion is provided by the Lower Eocene flysch sediments (Hecho group) associated with the Gavarnie and Guarga thrusts (Labaume et al., 1985; Teixell, 1996). Cooling ages measured on this imbricate thrust

system yield a Late Eocene to Miocene age of exhumation (Fitzgerald et al., 1999; Bosch et al., 2016), coeval with the main subsidence episode recorded in the southern Aquitaine basin (Desegaulx & Brunet, 1990). The timing of fault activity along the Lakora thrust is ill-constrained (Teixell, 1990, 1996) but could have initiated already in the Late Cretaceous, as suggested by the flexure of the Upper Cretaceous Carbonate platform in the footwall of the thrust (Teixell, 1996; Teixell et al., 2016). Note that in the Central-Eastern Pyrenees, Grool et al. (2018) identified the first phase of deformation at Late Santonian-Early Campanian in the North Pyrenean basins associated with the NPFT, while Boillot & Capdevila (1977) described the onset of flysch sedimentation in the South Pyrenean Zone at Late Santonian.

The timing of deformation is also ill-constrained in the BCB (e.g. Camara, 1997; Gómez et al., 2002). Syn-tectonic conglomerates along the SPBT suggest that this thrust was active at least from Oligocene onwards (Carola et al., 2013; Portero et al., 1979). Analysis of the tectonic subsidence on the Landes High suggests that the major subsidence on the northern margin of the basin occurred during the Early to Late Eocene (Gómez et al., 2002), eventually related with the NPFT.

In the northern branch (Pyrenean segment), the NPFT initiated at mid-Eocene according to Razin (1989) based on the age of the first syn-folding sediments in the Aquitaine basin. Late Eocene to Early Miocene ages have been defined based on seismic for a thrust fault attributed to the NPFT in the offshore Bay of Biscay (Ferrer et al., 2008). Fission tracks analyses on apatite and zircons on the Ursuya massif (north Basque massifs) yield ages at 48.3Ma and 81.8Ma, respectively (Vacherat et al., 2014), suggesting exhumation between Late Cretaceous to Eocene. Note that the Eocene cooling ages are common throughout the Pyrenean and Cantabrian systems (e.g. DeFelipe, 2017; Fitzgerald et al., 1999; Jolivet et al., 2007; Bosch et al., 2016; Vacherat et al., 2014). Additional thermochronological data from the Cinco Villas and Aldudes massifs suggest that the exhumation of these massifs occurred already from the Late Cretaceous (80-60Ma) to present with a more rapid exhumation from Eocene onward (DeFelipe et al., 2019).

In the southern branch (Cantabrian segment), the age of the SPBT could be similar to the Cantabrian rift segment (i.e. Oligocene or older; Carola et al., 2013) while thermochronological data on a sample located along the Leiza fault suggests rapid cooling prior to 40Ma (DeFelipe et al., 2019). To the east, the Roncesvalles thrust fault put the Santonian limestones over the late Upper Cretaceous mudstones in which it seems to vanish, probably sealed by the Paleocene sediments (Del Valle et al., 1972). This suggests that the Roncesvalles fault could be Late Cretaceous in age and thus potentially coeval to the E-W striking Lakora thrust located in its eastern prolongation.

It results that the Eocene to Miocene collisional episode is very well dated throughout the Palaeozoic massifs, both from syn-orogenic sediments and thermochronological data. However, convergence already initiated at Late Santonian to Early Campanian in the Pyrenees as attested by plate kinematic considerations (Macchiavelli et al., 2017). This suggests that the underthrusting of the hyperextended crust corresponds to a phase that cannot be easily recognized from the stratigraphy and since the lithosphere was not thermally equilibrated at the onset of convergence (Vacherat et al., 2014), the use of isostasy and/or thermochronology to date onset of convergence is difficult. At this stage, the underthrusting/subduction stage seems to be best recorded in the Basques massifs by thermochronological data (DeFelipe et al., 2019) and along the Roncesvalles fault, i.e. at the termination of rift segments, which may, as discussed below, be related to the reactivation history of the segment boundary.

4. DISCUSSION

4.1 Role of rift-inheritance at the Pyrenean-Cantabrian junction

4.1.1 Structural evolution and implications for the present-day architecture

In the following, we will refer to the figures III-4 and III-5 to depict the structural evolution at the Pyrenean-Cantabrian junction from the initiation of reactivation to the present-day situation. For convenience, the Landes High, Grand Rieu High and Aquitaine will be refer to the Eurasian plate in the following, whilst the Ebro and Duero will be refer to the Iberian plate.

4.1.1.1 Underthrusting stage

In the Pyrenean and Cantabrian segments, the hyperextended domains from the Iberian plate were underthrust below the Eurasian plate from the Santonian to the Early Eocene. Meanwhile, the thin-skinned Licq, SPFT and NPFT as well as intra-basin folding likely accommodated the shortening of the supra-salt sedimentary cover (Figs. III-4 and III-5; Grool et al., 2018; Mouthereau et al., 2014).

At the segment boundaries corresponding to the V-shaped terminations, besides the evaporite decoupling horizon, there was no inherited weak structure (e.g. serpentinized level) available to be reactivated. As such, new structures had to develop in order to accommodate the shortening in these domains. In the northern branch of the overlapping rift system, the north-

vergent WNW-ESE striking NPFT transferred the deformation from the western termination of the Pyrenean segment to the Cantabrian segment, whilst in the southern branch, the south-vergent E-W striking Roncesvalles thrust fault transferred the deformation between the eastern termination of the Cantabrian segment to the Pyrenean segment (Figs. III-4 and III-5). Based on the geographic link and the similarities between the basement-involved Roncesvalles and Lakora thrusts, i.e. the E-W orientation and syn-underthrusting stage activity, we propose that the Lakora thrust might represent the eastward prolongation of the shortcutting Roncesvalles thrust. Note that the formation of new thrust faults that shortcut external domains to connect offset rift structures has been described in analogue sandbox models of transfer zones by Konstantinovskaya et al. (2007).

At this segment boundary, and in contrast to the rift segments, the Eurasian plate underthrust the Basque massifs and the dip of the underthrusts are in opposite direction between the eastern Mauléon basin (rift segment) and the western Mauléon basin (segment boundary) (Fig. III-4). As a consequence, in the eastern Mauléon segment, the former lower plate (Iberia) underthrust the upper plate (Eurasia), whereas in the western Mauléon the lower plate (Basque massifs/Iberia) and its subcontinental mantle overrode the upper plate (Eurasia). This structural evolution allowed to emplace the subcontinental mantle at a crustal level (Fig. III-4, cross-section C) such as observed at present-day on seismic refraction profiles and on gravity anomaly maps (Casas et al., 1997; Wang et al., 2016). Moreover, it allowed to keep the hyperextended basement of the western Mauléon basin (Masini et al., 2014) and related pre-Alpine features (e.g. South and North Mauléon detachments, Bidarray Permian basin) in a pop-up structure similar to an orogenic wedge since the initiation of convergence. This change in tectonic style probably occurred across the NNE-SSW striking Saison transfer fault (Fig. III-5; Le Pochat et al., 1976; Masini et al., 2014).

These observations suggest that this initial stage of reactivation was mainly controlled by rift-inheritance within rift segments (Jammes et al., 2009; Lagabrielle et al., 2010; Quintana et al., 2015; Roca et al., 2011; Teixell et al., 2016; Tugend et al., 2014) whereas new structures formed at segment boundaries by shortcutting the area, initiating a proto-crustal wedge at the location of the Basque massifs (Fig. III-5) where the onset of exhumation has been proposed to occur during the Late Cretaceous (DeFelipe et al., 2019). These new structures involved thick-skinned deformation of the necking and proximal domains at the termination of rift segment. Since such zones can preserve embryonic stages of convergence, they represent critical domains to date the initiation of reactivation.

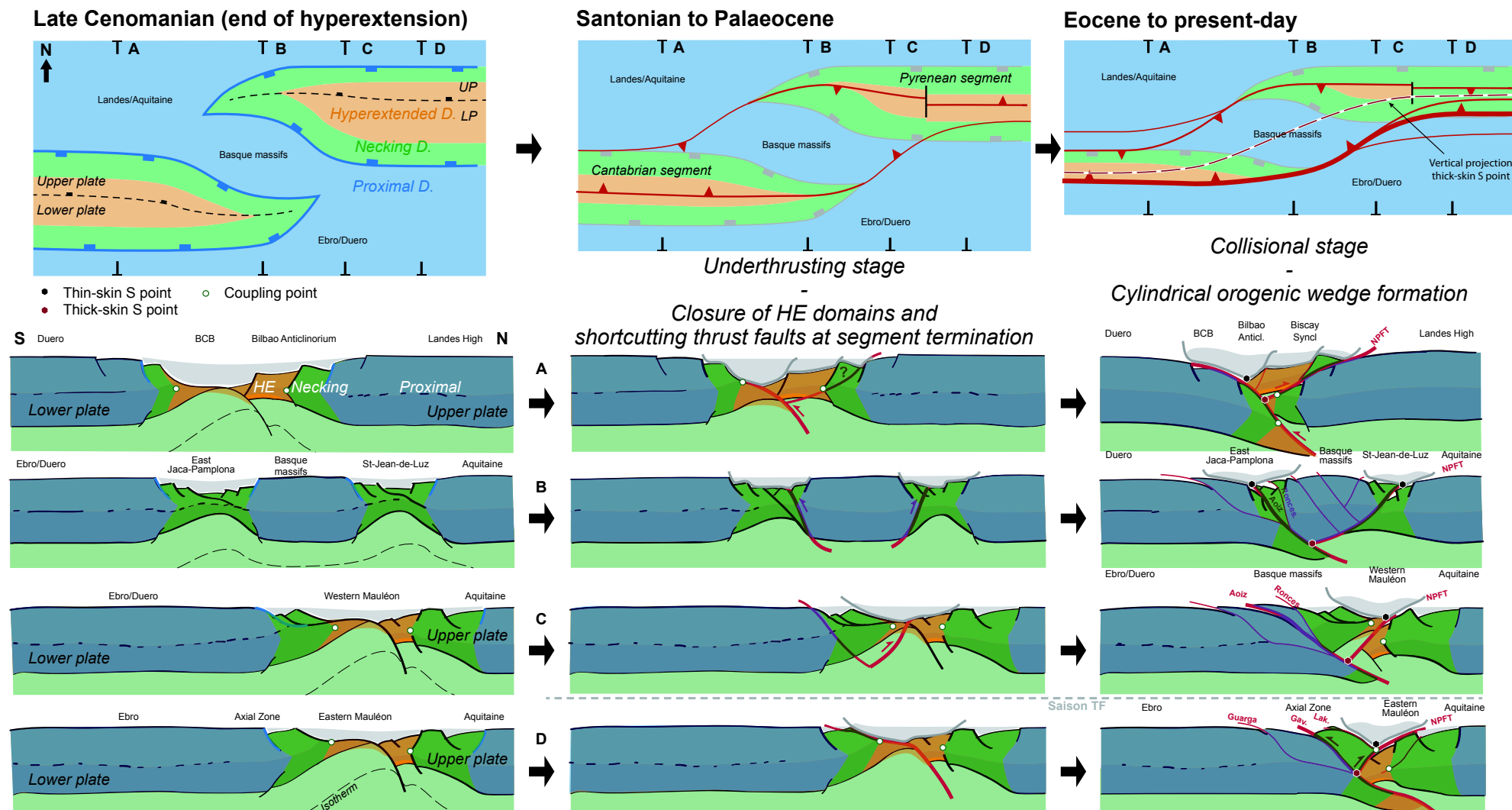


Figure III-4: Schematic evolution of the Pyrenean-Cantabrian systems from Late Cenomanian to present-day. Note that maps do not represent the sedimentary infill but show the crustal rift domain distribution. Note in particular the variation in the style of deformation on both sides of the Saison TF between sections C and D, in relation with the early proto-wedge at rift segment boundary. Description of the figure is provided in the text.

4.1.1.2 Collisional stage

The collisional stage corresponds to the thickening of the crust at Eocene time related to the development of thick-skinned thrusts such as the imbricated north-dipping Gavarnie and Guarga thrusts (Figs. III-4 and III-5) and associated with an episode of subsidence of the southern Eurasian plate. This stage corresponds to the collision of the conjugate necking domains that initiated when the coupling points intersected. It was also synchronous with the onset of the formation of the orogenic wedge (Mouthereau et al., 2014; Sinclair et al., 2005), whose pro- and retro-wedge structures correspond to the Gavarnie fault and NPFT respectively. The wedge is formed by the former upper crust of the necking domain. Note that the related S point will migrate through time due to the progressive indentation of the Eurasian crust at a mid-crustal level (i.e. ductile-brittle transition) within the Iberian crust (Fig. III-4). At depth, the former hyperextended domain and the lower crust of the necking domain of the Iberian plate form the underthrusting slab. In the Cantabrian segment, the thick-skinned deformation is controlled by the NPFT and SPFT and the orogenic wedge is formed by the former hyperextended and necking domains of the Eurasian plate. The underthrusting slab is formed by the hyperextended and necking domains of the Iberian plate.

Towards the segment boundaries, the entire Basque massifs form an orogenic wedge bounded by the Aoiz fault (pro-wedge) and the NPFT (retro-wedge) and the underthrusting slab is composed of the necking to proximal domains of the Iberian plate. The Aoiz thrust could correspond to the westward continuation of the Gavarnie thrust. As such, the width of the crustal wedge is increasing at the segment boundary, defined by the distance between the overlapping rift systems (Figs. III-3 and III-5).

Our study shows that, despite a complex inherited structural pattern during the initiation of reactivation, a unique orogenic wedge formed ultimately on top of a north-dipping underthrusting/subducting slab from the central Pyrenean segment to the Cantabrian segment (Chevrot et al., 2018). These observations reveal a cylindricity of the first order architecture from the Western Pyrenean to Cantabrian segments once the collisional stage began (Fig. III-5).

4.1.2 Role of structural and thermal inheritance at segment boundaries

The mid-Cretaceous rift structural inheritance has shown to control both the location and the evolution of the contractional deformation in the Pyrenean and Cantabrian rift segments. Toward rift segment boundaries, structural anomalies such as shallow mantle emplacement and preservation of pre-Alpine structures have been described (Jammes et al., 2009; Masini et al., 2014; Wang et al., 2016). Moreover, we identify an along-strike change of the main

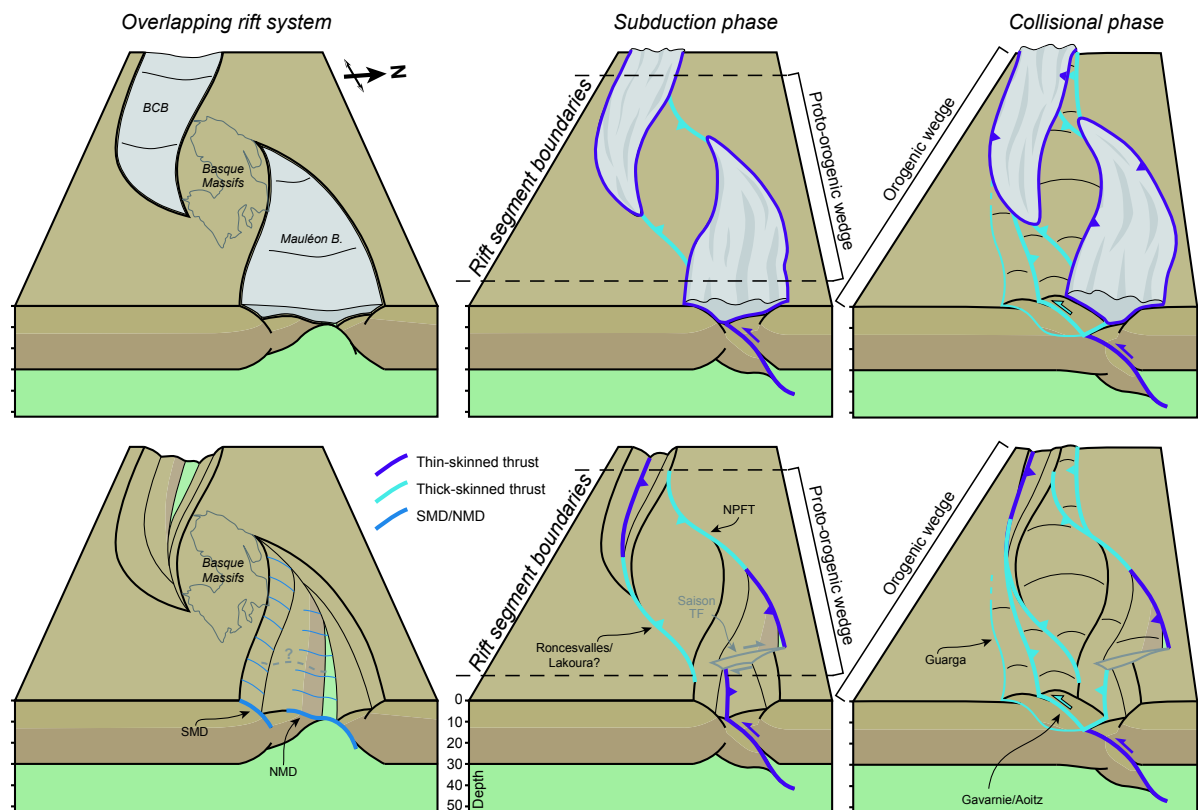


Figure III-5: Schematic 3D evolution of the Pyrenean-Cantabrian junction highlighting the structural evolution during the subduction (Santonian – Paleocene) and collisional (Eocene – Miocene) phases. The uppermost 3D block diagrams show the evolution with the decoupled sedimentary basins while the lowermost diagrams show the crustal architecture only. Saison TF: Saison Transfer Fault; SMD; South Mauléon Detachment; NMD: North Mauléon Detachment.

underthrust dip direction during the initiation of reactivation related to segmentation. This structural change cannot be easily explained by reactivation of former rift structures as it did not reactivate the north-dipping detachments associated with mantle exhumation (e.g. North Mauléon Detachment). One can partly argue with the deformation associated with soft transfer zones. In the latter, Konstantinovskaya et al. (2007) showed that during tectonic inversion, new thrusts can emerge between shifted reactivated extensional faults in the transfer zone. However, to our knowledge, the tectonic inversion has not been tested for overlapping rift systems in which extensional faults of opposite dip direction could complexify the reactivation pattern. Besides the structural control, one can suggest that the thermal state related to hyperextension and not yet equilibrated at the onset of convergence (Vacherat et al., 2014) could have had a role on the reactivation of this system. Indeed, the thermal inheritance involved by the two overlapping, thinned lithospheres might influence the reactivation at the junction between rift segments. However, in order to make prediction on the control of the thermal structure at onset of convergence, 3D thermo-mechanical models are needed.

4.2 Implications for the reactivation of hyperextended rift systems

4.2.1 Role of 3D rift-inheritance for the 2D architecture of orogenic systems

The Pyrenean-Cantabrian study case shows that the dip evolution and architecture of reactivated hyperextended rift systems are strongly controlled by 3D rift-inheritance. Rift-structures might be preserved whilst new structures might form in order to accommodate along-strike complexities. Dealing with 2D balanced cross-sections in these areas without considering the lateral evolution may lead to unpredicted reactivation patterns. In particular, sampling of mantle or lower crustal rocks in orogenic systems might be favoured by along-strike structural reorganisation related to segment boundaries as suggested in this study (Fig. III-4).

Present-day analogues showing substantial along-strike rift segmentation have been recognized worldwide (Orphan: Skogseid, 2010; East African rift system: Corti, 2012; Australia: Belgarde et al., 2015; Central Atlantic: Péron-Pinvidic et al., 2017). Yet, only few studies working on orogenic systems have considered the role of rift segmentation to account for the orogenic architecture (e.g. Beauchamp, 2004; Likerman et al., 2013; Thomas, 2006).

We believe that further studies are needed to better investigate the role and importance of rift-inheritance (structural, compositional and thermal) associated to rift segment boundaries (transfer/transform fault, overlapping rift systems) in controlling the 3D architecture of orogenic systems.

4.2.2 Relative control of inheritance on the contractional deformation through time

Our study shows that during the first stage of rift inversion (i.e. closure of hyperextended domains) rift segment evolution is controlled by the reactivation of the hyperextended domain, i.e. oceanward of the coupling point, where the crust and upper mantle deformation is governed by brittle rheology. The decoupling level at this stage corresponds to lithological contrast, e.g. serpentinized mantle (Fig. III-2; Péron-Pinvidic et al., 2008). However, once conjugate necking domains collide (i.e. coupling points overlap) ductile rheology is implemented to the system and the upper crust and mantle are decoupled in the ductile lower crust. At this stage, rift inheritance is not anymore the main parameter controlling the orogenic evolution. New contractional structures, perpendicular to the shortening direction are created following the classical Coulomb wedge theory (e.g. Davis et al., 1983). This suggests that two main processes can be distinguished during contractional deformation, i.e. a first “subduction” stage, which is controlled by rift-inheritance, and a second “collisional” stage governed by orogenic processes.

Interestingly, this correlation between inheritance and coupled/decoupled structural evolution is opposite to that described during extension. Indeed, during rifting the formation

of the proximal and necking domains have been shown to be mainly controlled by pre-rift inheritance, whereas the formation of the hyperextended and oceanic domains represent new real estate domains that are mostly controlled by large-scale rift-induced processes such as hydration and magmatic processes (Manatschal et al., 2015).

5. CONCLUSION

The aim of our study was to investigate the reactivation of segmented hyperextended rift systems based on the Pyrenean-Cantabrian example. Based on restored cross-sections and an updated map of the rift domains, we identified the structures and their relative timing in order to characterise the reactivation of the overlapped Pyrenean and Cantabrian rift basins.

We showed that reactivation can be divided in two phases controlled by rift inheritance in rift segments, the underthrusting/subduction phase and the collisional phase. On the one hand, the hyperextended domain is underthrust during the Santonian to Late Paleocene, eventually reactivating top basement detachment faults, locally flooring exhumed serpentized mantle. Supra-salt rift basins are inverted via the reactivation of the evaporite decoupling horizon. On the other hand, when conjugate necking domains meet, the contraction is governed by thick-skinned deformation as testified by the formation of the Eocene to Miocene Gavarnie and Guarga thrusts. This phase is responsible for the formation of an orogenic wedge in between the Eurasian (Landes) and Iberian (Ebro) plates.

This evolution is complexified at a rift segment boundary, i.e. where the Pyrenean and Cantabrian rift segments overlapped (Basque massifs area). At the tip of V-shaped basins, the lack of hyperextended domains and therefore weak decoupling levels (e.g. serpentized levels) impeded reactivation to proceed. As such, new, shortcutting structures such as the NPFT and Roncesvalles faults were created in order to transfer the deformation to rift segments. These thick-skinned NPFT and Roncesvalles thrust faults led to the formation of a precursor orogenic wedge at the rift junction that corresponds to the Basques massifs. At this stage, we suggest that the E-W striking basement-involved thin-skinned Lakora thrust might represent the eastern continuation of the shortcutting Roncesvalles thrust. Moreover, we propose that this precursor pop-up structure (orogenic wedge) is responsible for the preservation of pre-Alpine structures and the emplacement of subcontinental mantle rocks at a crustal level at the southern margin of the western Mauléon basin (north-western Basque massifs).

The final architecture results in a continuous E-W striking orogenic wedge overlaying a north-dipping underthrust/subducted slab throughout the entire Pyrenean and Cantabrian systems. This study highlights a first contractional phase dominated by rift-inheritance followed by a second collisional phase controlled by orogenic processes.

CHAPTER IV:

***THERMAL EVOLUTION OF ASYMMETRIC
HYPEREXTENDED MAGMA-POOR RIFT SYSTEMS:
RESULTS FROM NUMERICAL MODELLING AND
PYRENEAN FIELD OBSERVATIONS***

THERMAL EVOLUTION OF ASYMMETRIC HYPEREXTENDED MAGMA-POOR RIFT SYSTEMS: RESULTS FROM NUMERICAL MODELLING AND PYRENEAN FIELD OBSERVATIONS

Submitted to Geochemistry, Geophysics, Geosystems

Rodolphe Lescoutre¹, Julie Tugend^{1,2,3}, Sascha Brune^{4,5}, Emmanuel Masini³,
Gianreto Manatschal¹

¹*IPGS, EOST-CNRS, Université de Strasbourg, Strasbourg, France*

²*Sorbonne Université, CNRS-INSU, Institut des Sciences de la Terre Paris, ISTeP UMR 7193, F-75005 Paris, France.*

³*Total R&D, CSTJF, Pau, France*

⁴*GFZ Potsdam, German Research Centre for Geosciences, Potsdam, Germany*

⁵*Institute of Earth and Environmental Sciences, University of Potsdam, Germany*

KEY POINTS

- Numerical modelling and field observations of asymmetric rifts show an asymmetric thermal evolution during hyperextension.
- Asymmetric rift basins can record diachronous heat peaks resulting from different successive thermal events (formation of allochthons).
- Determination of thermal gradients from peak temperatures is misleading as the thermal architecture results from a diachronous evolution.

ABSTRACT

We investigate the thermal and structural evolution of asymmetric rifted margin formation using numerical modelling and geological observations derived from the Western Pyrenees. Our numerical model provides a self-consistent physical evolution of the top basement heat flow during asymmetric rifting. Maximum top basement heat flow occurs at the upper-lower plate transition resulting in a strong thermal asymmetry during rifting. Results of this dynamic model reveal a diachronism in the record of maximum heat flow related to rift migration in basal rift sequences. The Mauléon-Arzacq basin (W-Pyrenees) corresponds to a mid-Cretaceous asymmetric hyperextended rift basin. New vitrinite reflectance data in addition to existing data sets from this basin reveal a strong asymmetry in the distribution of peak heat

(T_{\max}), where highest values are located at the former upper to lower plate transition. This data set from the Arzacq-Mauléon field study confirms for the first time the thermal asymmetry predicted by numerical models. Furthermore, numerical modelling results also suggest that complexities in T_{\max} distribution could arise when hanging-wall derived extensional allochthons become part of the lower plate and are transported away from the upper-lower plate transition. More generally, we discuss the relative control of thermal processes such as burial and heat flow on the evolution and thermal architecture of hyperextended rift systems. This study emphasizes the limitations of integrating punctual thermal data from pre- to syn-rift sedimentary sequences, which is often done in order to describe the rift-related thermal evolution and paleothermal gradients at the scale of a rift basin or margin.

1. INTRODUCTION

Over the past decade, our understanding of hyperextended rift systems greatly improved thanks to the combination of geological observations and numerical experiments (Duretz et al., 2016; Huismans & Beaumont, 2014; Lavier & Manatschal, 2006). On the one hand, seismic interpretations from present-day rifted margins (e.g. Autin et al., 2010; Osmundsen & Ebbing, 2008; Reston & McDermott, 2011) and field observations from fossil analogues (e.g. Clerc et al., 2016; Frasca et al., 2016; Masini et al., 2014) brought new constraints on their tectonic and sedimentary evolution. On the other hand, numerical models (Huismans & Beaumont, 2014; Lavier & Manatschal, 2006) helped to decipher some of the physical processes that control hyperextension.

The first order architecture of rifted margins has been widely defined (Péron-Pinvidic et al., 2013, 2017; Sutra et al., 2013; Tugend et al., 2015) and subdivided into ‘structural’ rift domains, one of which being referred to as the “hyperextended domain”. Hyperextended rift systems have been reproduced in various numerical experiments, which demonstrated that these systems show an overall asymmetry of the conjugate margin architecture and a shift of the rising asthenosphere (Brune et al., 2014; Jammes & Lavier, 2016; Svartman Dias et al., 2015; Tetreault & Buitier, 2017). The diachronous evolution is also observed in the overlying sedimentary sequence as indicated by the migration of the syn-tectonic sequence towards the exhumation point (Hart et al., 2016; Masini et al., 2014; Mohn et al., 2010; Péron-Pinvidic & Manatschal, 2010).

Previous studies explored the distribution of heat within present-day (Leroy et al., 2010; Lucazeau et al., 2008) and fossil rift systems (Beltrando et al., 2015; Chelalou et al., 2016; Clerc et al., 2015; Hart et al., 2016, 2017; Vacherat et al., 2014) to define the thermal

architecture of hyperextended rift basins. However, despite these recent studies, the thermal evolution and architecture of rifted margins and especially the consequence of asymmetric rifting remain poorly understood. Notably, the spatial and temporal evolution of rift systems is shown to be complex (Alves et al., 2009; Mohn et al., 2015; Naliboff et al., 2017; Savva et al., 2014; Tugend et al., 2015) and its control on the rift-related thermal evolution remains at present unconstrained. Simple correlations between isolated, punctual observations within a rift system and the overall thermal architecture and evolution of the entire basin are not straightforward. This is particularly important for rifted margins where several heat sources with different thermal amplitudes and durations are recognized (Ungerer et al., 1990) and where the structural evolution is shown to be complex through time (e.g. Péron-Pinvidic et al., 2013). All these complexities do not favour 3D extrapolation from local thermal measurements only and ask for a better understanding of the processes controlling the thermal evolution during rifting and particularly during extreme crustal thinning and mantle exhumation. From an industrial perspective, understanding the processes controlling the thermal evolution of basins is fundamental to model and predict petroleum systems that could be in asymmetric rift systems extremely different along conjugate pairs (e.g. maturation and timing of migration of hydrocarbons). Thus, progress on this topic has strong impact on the exploration potential of ultra-deep offshore settings. In that aspect, the former Arzacq-Mauléon hyperextended rift basin preserved in the Western Pyrenees represents a unique opportunity to assess the entire pre- to syn-rift sedimentary sequence, which is a prerequisite to unravel the thermal evolution of these systems during their formation.

In this study, we use a 2D numerical model to analyse top basement heat flow evolution and define the first order heat distribution during asymmetric lithospheric thinning. In parallel, we investigate the thermal structure of the fossil asymmetric Arzacq-Mauléon rift basin for which we present unpublished vitrinite reflectance data (proxy for T_{\max}) acquired by Elf Aquitaine (now Total) in the 80's from boreholes. This study allows us to test the numerical model predictions and to discuss some geological and thermal complexities using a natural example. We then emphasize implications of the numerical model concerning the thermal evolution of extensional allochthons, or more generally of allochthonous extensional units. Through this work, we emphasize the necessity of understanding the rift evolution to better constrain the crustal/lithospheric thermal architecture of hyperextended rift basins. Note that we explicitly focus in this study on the syn-rift evolution and do not aim to predict the final thermal architecture of the whole basin, which depends also on the post rift infill history of the basin.

2. ASYMMETRIC RIFTED MARGINS: OBSERVATIONS AND CONCEPTS

Numerous examples of conjugate asymmetric rift systems have been observed and described worldwide across the North and South Atlantic margins (e.g. Chian et al., 1995; Blaich et al., 2011; Péron-Pinvidic et al., 2013; 2017) or the Australia-Antarctica margins (e.g. Espurt et al., 2012; Gillard et al., 2016). This asymmetry is noticeable from a crustal and structural point of view (Fig. IV-1; Nirrengarten et al., 2016). One of the margins shows a generally wider crustal taper, mainly exhibiting oceanward dipping detachment faults rooting onto the Moho (Fig. IV-1, right side: Iberia, Labrador and Celtic platform margins). The conjugate margin generally shows a sharper crustal taper and a complex structural pattern with ocean- and continentward dipping high-angle normal faults (Fig IV-1, left side: Newfoundland, West Greenland and Porcupine High). This asymmetry was classically interpreted as related to different geometries between lower and upper plate margins respectively based on the concept first introduced by Lister et al. (1986). As such, upper and lower plate margins can be defined relatively to a major (or a succession of) detachment fault system(s), respectively corresponding to the hanging wall and footwall of the major active detachment fault.

Recent studies suggest that this asymmetry is mainly acquired during the formation of the hyperextended domain (e.g. Nirrengarten et al. 2016), bounded landward by the necking domain and seaward by the exhumed domain and/or oceanic domain (e.g. Péron-Pinvidic et al., 2013; Sutra et al., 2013). Numerical models suggest that the asymmetry of a rifted margin is mainly controlled by the extensional rate and the rheology (Huisman & Beaumont, 2002). In the hyperextended domain, the crust is sufficiently thinned so that brittle behavior prevails and deformation is largely coupled at the scale of the crust (Nirrengarten et al., 2016; Pérez-Gussinyé & Reston, 2001). The formation of upper and lower plates in the hyperextended domain is associated with progressive rift migration and sequential normal faulting (Brune et al., 2014; Hauptert et al., 2016; Lister et al., 1986; Ranero & Pérez-Gussinyé, 2010; Svartman Dias et al., 2015). Furthermore, applying the critical Coulomb wedge theory to predict deformation in hyperextended domains, Nirrengarten et al. (2016) show that extensional allochthons can form and migrate from the upper to the lower plate. The exhumed mantle domain may show a more complex structural evolution with out-of-sequence faulting (Gillard et al., 2016).

Coincident with this asymmetric crustal structure, the overlying stratigraphic architecture differs between upper and lower plates. The first order stratigraphic architecture of the lower and upper plate margins is schematically shown in figure IV-2 together with the terminology used to describe the syn-hyperextension (syn-HE) stratigraphic sequence (Masini et al., 2013). Most of the crustal thinning in the upper plate is interpreted as accommodated by intra-crustal extension associated with simultaneous detachment faulting on the conjugate

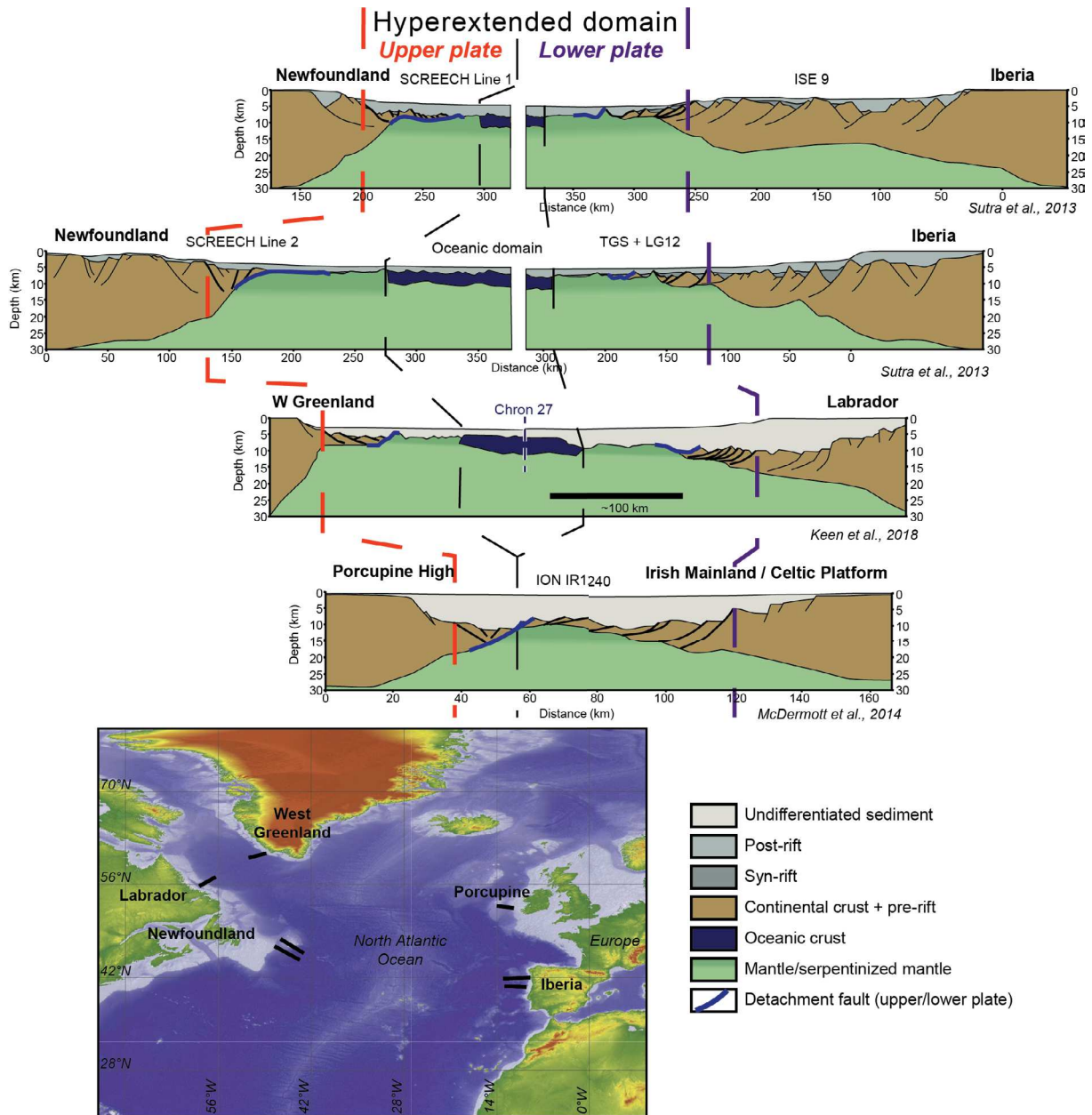


Figure IV-1: Examples of asymmetric rifted margins and basins from the Northern Atlantic. The asymmetry is interpreted as related to differences between lower and upper plate architectures formed during hyperextension. Iberia-Newfoundland after Sutra et al. (2013); Labrador-West Greenland after Keen et al. (2018); Porcupine basin after McDermott et al. (2014). The hyperextended domain includes the coupled domain as defined by Sutra et al. (2013).

lower plate. This leads to the preservation of an upper crustal block with a generally more continuous/preserved pre-rift stratigraphy (Hauptert et al., 2016; Péron-Pinvidic et al., 2017). As such, sediments deposited onto the upper plate are progressively stacked and include pre- to post- tectonic sediments. On the lower plate, progressive in-sequence detachment faults result in complex stratigraphic architectures combining classical growth strata and subhorizontal deposition of syn-hyperextension sediments (e.g. Masini et al., 2011; Tugend et al., 2015) onto

exhumed deep crustal and mantle rocks. The sediments deposited onto the active exhumation fault are younging towards the hanging-wall (i.e. upper plate) and are mainly syn- to post-tectonic. During the exhumation process, crustal blocks can be pulled out from the upper plate and loaded onto the lower plate (Nirrengarten et al., 2016). Thus, such blocks change from a upper to a lower plate position. The stratigraphic architecture associated to these so-called extensional allochthons is complex (e.g. Masini et al., 2011) as they can preserve pre- to syn-rift sediments over exhumed surfaces and they are often overlain passively by post-rift sediments.

These structural and stratigraphic observations allow the identification of key criteria to discriminate upper and lower plates. To summarize, the lower plate shows a complex structure and abundant accommodation space, generally associated with a wider zone of exhumed deep basement rocks capped by a detachment surface and extensional allochthons (Péron-Pinvidic et al., 2017). The architecture of the upper plate shows preserved upper crustal rocks overlain by typical syn-tectonic sedimentary wedges associated with tilted blocks and little syn-tectonic accommodation space compared to the lower plate margin (Péron-Pinvidic et al., 2017).

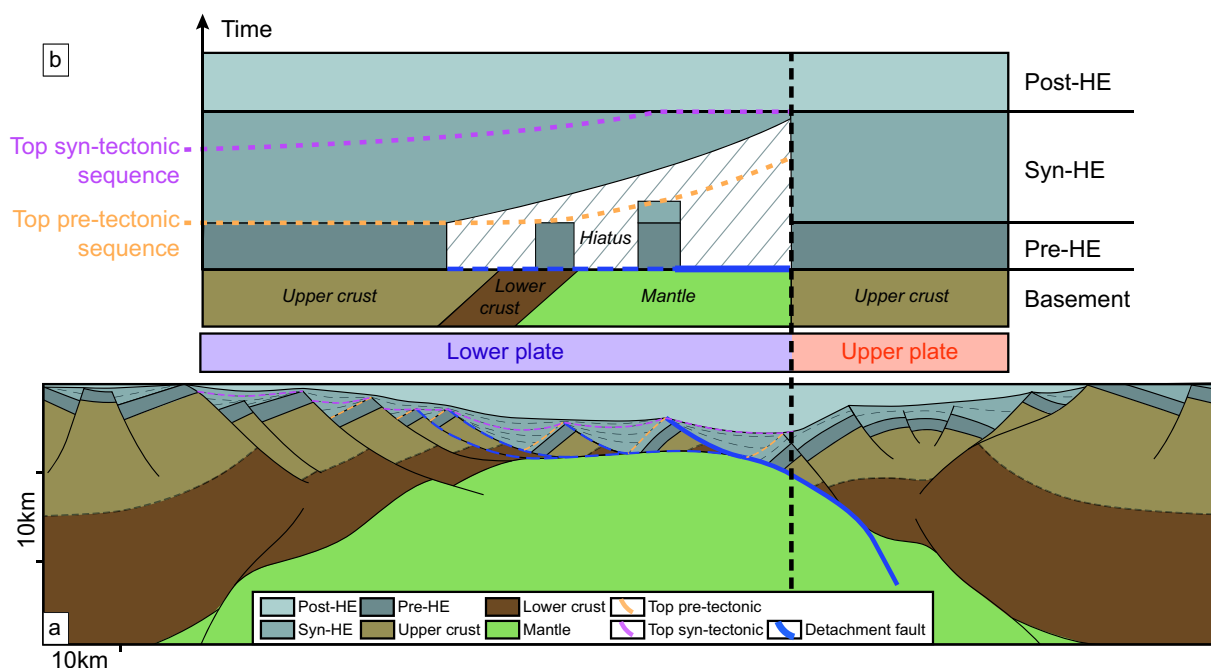


Figure IV-2: a: Concept of upper/lower plate showing the related asymmetric crustal and sedimentary architecture. In this model, no decoupling level is considered between the sediments and the basement. Deep crustal rocks can be exhumed in the footwall of detachment faults on the lower plate. Allochthonous blocks are progressively delaminated and migrate from the upper to the lower plate (Nirrengarten et al., 2016). b: Wheeler diagram showing the expected stratigraphic architecture of pre-, syn- and post-hyperextension (HE) sediments. The top of the pre-tectonic sequence delimits sediments that are not affected by extensional deformation. The top of the syn-tectonic sequence corresponds to the limit between sediments deposited during active faulting and those deposited during the post-tectonic “sag” phase (as defined in Masini et al., 2014). Note the younging of the syn-tectonic sequences toward the active exhumation fault.

3. NUMERICAL MODEL OF ASYMMETRIC RIFTING

3.1 Setup, inputs and updates

The numerical model presented here provides a dynamic description of an asymmetric rift system, which captures the first order rift architecture and evolution of the hyperextended basins such as described in the previous section. The simulation is based on the Iberia-Newfoundland model presented in Brune et al. (2014; 2017) and employs the finite element code SLIM3D (Popov & Sobolev, 2008). This code captures visco-elasto-plastic deformation processes of the lithosphere such as ductile flow in the lower crust (Clift et al., 2015) and the asthenosphere (Brune et al., 2013; Koopmann et al., 2014), normal faulting (Brune, 2014), and associated evolution of lithospheric stress (Brune et al., 2012, 2016). Brittle deformation is represented through Mohr-Coulomb plasticity and localisation of faults is further facilitated via the standard approach of strain-dependent friction softening (Huisman & Beaumont, 2003). All model parameters are provided in the supplementary Table S1.

The computed 2D model is 500km wide, 150km deep and uses 4 distinct layers and flow laws: upper crust (22km thick, wet quartzite flow law of Gleason & Tullis, 1995); lower crust (11km thick; wet anorthite flow law of Rybacki & Dresen, 2000); strong lithospheric mantle (dry olivine flow law of Hirth & Kohlstedt, 2003), weak asthenospheric mantle (wet olivine flow law, Hirth & Kohlstedt, 2003). The lithosphere-asthenosphere boundary (set to 1300°C) is initially located at 105km depth. The employed values for pre-rift layer thicknesses lie within the possible range suggested by geophysical models of neighbouring less-deformed areas (Díaz & Gallart, 2009; Tesauro et al., 2009; Torne et al., 2015), however it has to be noted that layer thicknesses at rift onset and associated rheological flow laws are amongst the most poorly constrained model parameters.

The surface temperature is set to 0°C and the bottom temperature to 1300°C. Between these top and bottom boundary conditions, the initial thermal state is controlled by heat advection, radiogenic heat production, and heat conductivity of each specific layer. As such, the initial Moho temperature corresponds to 600°C and the initial surface heat flow to 67 mW/m². Heat flow at the top of the model is then defined by the evolution of these parameters during crustal and lithospheric thinning and is derived from the vertical thermal gradient at each location.

The setup reproduces a passive rift where the rise of the lithosphere-asthenosphere boundary is controlled by lithospheric thinning due to a prescribed full extension velocity of 8 mm/yr. The asymmetry of the model develops self-consistently and is controlled by crustal rheology, thermal configuration, and strain-dependent softening. A randomly distributed small amount of initial strain is used to break the symmetry such that the fault orientation and distribution is not predetermined by the model and asymmetric rifting can freely proceed. Evolution of topography is allowed via a free surface boundary condition and the isostatic equilibrium at the bottom boundary is controlled by the Winkler foundation including in and out-flow of material (Egan, 2012; Popov & Sobolev, 2008).

In order to keep the model as transparent and simple as possible and to stay general rather than focusing on specific rift settings, we do not account for some processes that are generally thought to affect the dynamics of rift systems. For instance, magmatic additions are not included in the model, as their volumes are highly limited in magma-poor rift systems. Also, the role of fluids on local heat flow variations is not represented as it is probably of subordinate importance at the scale (time and space) of the model. The reference model does not take into account sedimentary infill and related loading blanketing by the sedimentary infill, nor the burial-related thermal history. However, a model with sediment infill has also been performed (Fig. S2 in annexes), but the results show that including a realistic sedimentary infill does not affect our conclusions on the basal heat flow evolution. In order to avoid the strong thermal impulse involved by the formation of oceanic crust and to consider only the thermal evolution associated to rifting, the modelled extension stops shortly prior to lithospheric breakup inducing thermal relaxation that lasts until the end of the model run. In the following, we describe the heat flow as well as its evolution at different locations at the base of the basin (top basement).

3.2 Thermal evolution of rifted margins: numerical model results

The model (Fig. IV-3 and Movie S3 in annexes) illustrates that the deformation quickly localises onto major asymmetric border faults while shearing occurs in the ductile layers of the model. It should be noted that the top of the crust always displays an elasto-plastic behaviour in the model. Rapid rheological coupling accounts for the formation of in-sequence faulting associated with upwelling of the lithosphere-asthenosphere boundary at the tip of the active fault. Antithetic normal faults control the deformation of the brittle upper crust in the hanging-wall of the active extensional fault, while a low-viscosity pocket forms in the lower crust (Fig. IV-3, stage 2). As highlighted in Brune et al. (2014), rift migration is caused by the lateral strength gradient between the low-viscosity pocket (exhumation channel) and the cooling

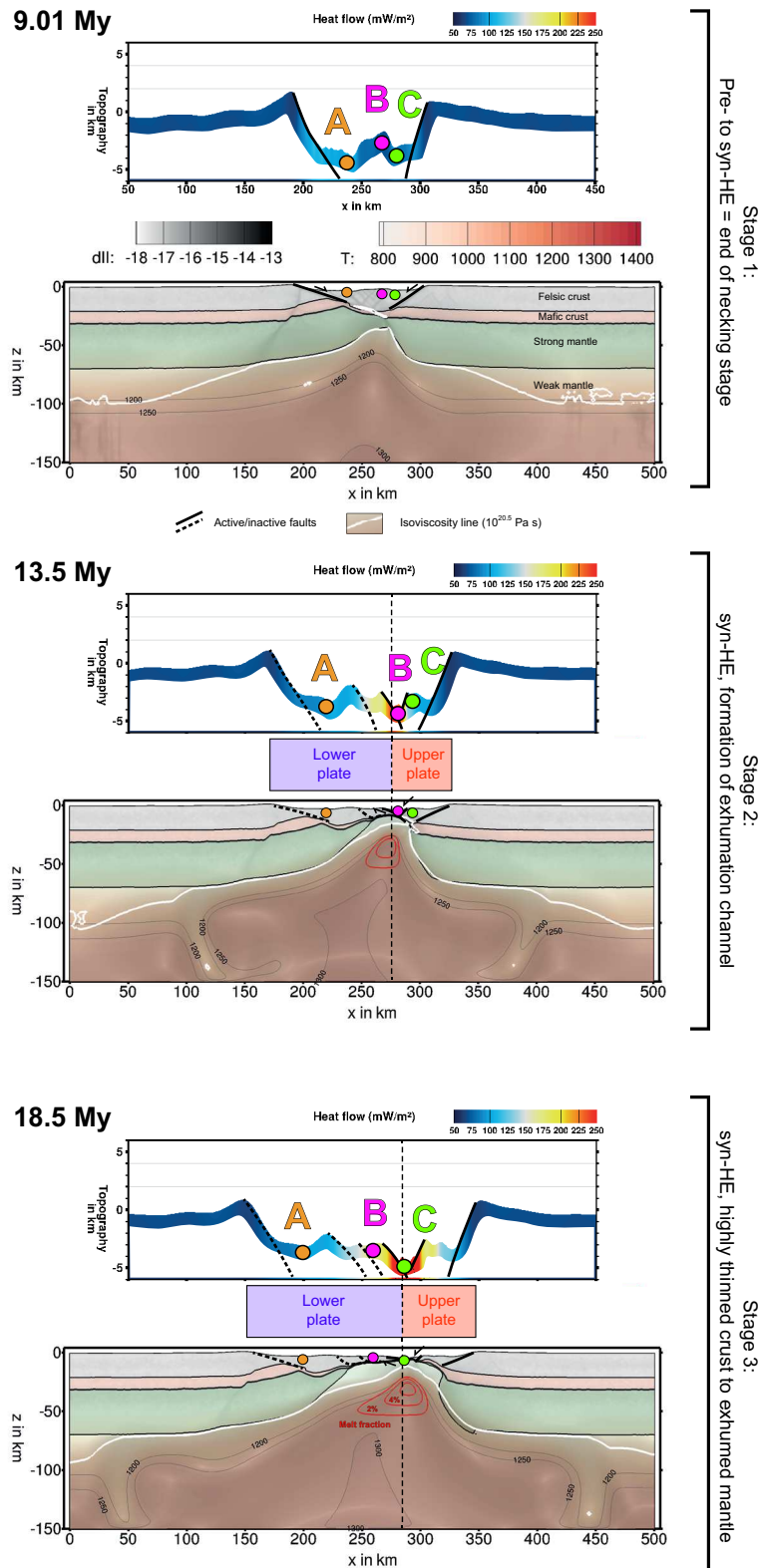


Figure IV-3: Snapshots of the dynamic model (see supplementary material: Movie S3) at 9.01 My (stage 1: early HE), 13.5 My (stage 2: intermediate stage of HE) and 18.5 My (stage 3: end of HE). The deformation of the different lithospheric layers is displayed in terms of semi-transparent strain rate (dll) at each time step together with the temperature field and selected isotherms. The evolution of the topography and the distribution of heat flow at the top of the basement are also shown. Markers A, B and C within the crust illustrate the formation of extensional allochthons due to the migration of the deformation toward the upper plate via in-sequence detachment faulting. Note the position of the maximum heat flow at the upper-lower plate transition during hyperextension.

mantle at the footwall of the active fault. As a consequence, the rift shows a typical upper-lower plate architecture and a crustal scale detachment that is well expressed on the 13.5 My snapshot (Fig. IV-3, stage 2). On the lower plate (left side), detachment faults thin the crust to a thickness <10km at the centre of the basin.

The overall geometry reveals a wide lower plate and a relatively sharp upper plate margin configuration once hyperextension begins (i.e. at about 12 My). From that moment on, the maximum heat flow at each time step is shifted toward the right side (upper plate) of the model and is not in the middle of the rift shoulders anymore (Fig. IV-3, stages 2 and 3). Regarding the displacement of markers A, B and C, we can see that A is moving toward the left (with the lower plate) from $X=240$ km to $X=220$ km between stages 1 and 2, while B and C slightly move toward the right during this time. From stage 2 to stage 3, markers A and B move for about 25 km toward the left while C is only slightly displaced.

We extract the evolution of heat flow experienced by each marker (A, B, C) through time (Fig. IV-4). We find that marker A records heat flow, which starts at 70 mW/m², reaches 110 mW/m² at about 10 My and then slowly decreases to 90 mW/m². The heat flow at marker B is at first almost constant at 70 mW/m² and from 10 My on it increases to reach a maximum of about 225 mW/m² at 13.5 My. The heat flow quickly decreases even before the end of rifting at 19 My to a value of 165 mW/m². Similarly, marker C shows a rapid increase from 12 My to a maximum of 325 mW/m² at 19 My.

These data evidence a strong diachronism (Fig. IV-4) in the record of maximum heat flow for the 3 markers in the asymmetric rift model. Moreover, maximum heat flow at the base of the basin is constantly increasing with time due to the successive thinning of the lithosphere. Such basal heat flow trend is similar for the model with sediments (Fig. S2 in annexes) except that the heat flow value remains high for much longer. Note the diachronous migration of markers from the right side of the main detachment fault to the left (i.e. from upper to lower plate) due to rift migration. This shows that rocks from the upper plate at the beginning of rifting are eventually transferred to the lower plate where they form extensional allochthons (Brune et al., 2014; Nirrengarten et al., 2016). Maximum heat flow (Fig. IV-3, stages 2 and 3) occurs above the location of maximum strain rate, i.e. at the immediate hanging wall of the detachment fault system along which deep crustal and mantle rocks are exhumed. It is important to note that, at 13.5 My (stage 2), the location of the maximum heat flow (250 mW/m²) is very close (less than 50 km) to the rift shoulder of the upper plate, where heat flow is less than 70 mW/m². This generates a horizontal gradient for heat flow of about 3,5 mW/m² per km for the upper plate and of about 1,4 mW/m² per km for the lower plate (distance of 125 km).

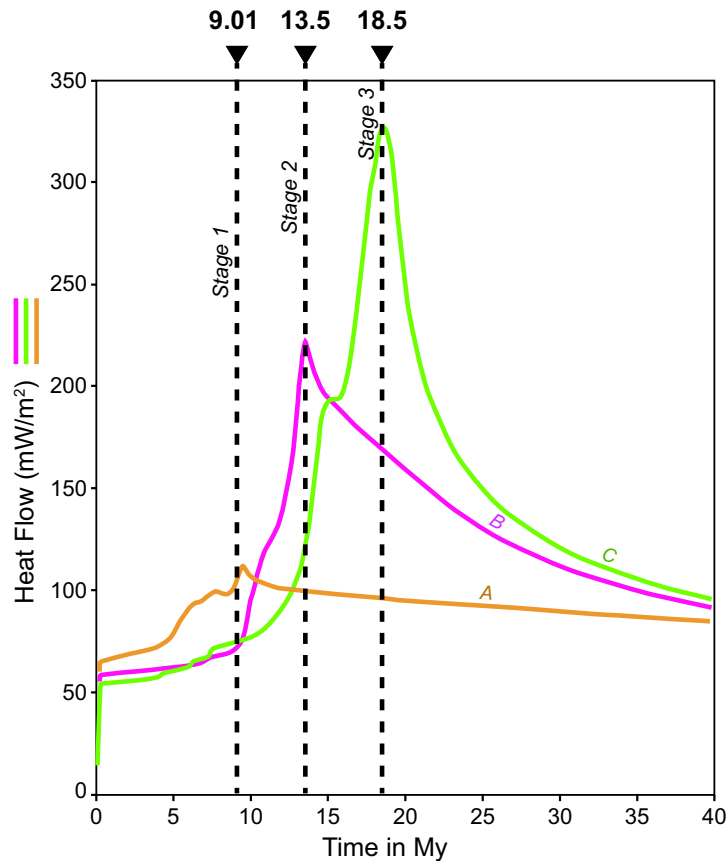


Figure IV-4: Heat flow evolution for the 3 markers A, B and C during rifting (see Fig. IV-3 for location). A general increase of the maximum heat flow through time is highlighted. Maximum heat flow for each marker A, B and C is diachronous.

In summary, numerical modelling illustrates a strong asymmetry on the distribution of maximum basal heat flow during asymmetric rifting, independent from the sedimentation rate (Figs. IV-3 and S2 in annexes). Indeed, the maximum heat flow is located above the active exhumation fault (exhumation front), which corresponds to the upper-lower plate transition in our interpretation (Fig. IV-2). This results in an asymmetric temperature configuration with a sharp horizontal variation in heat flow on the upper plate and a significantly smoother variation on the lower plate. This relationship mirrors the crustal architecture of the model with a sharp upper plate and a wide lower plate margin. As expressed in the graph in figure IV-4, a consequence of this model is the migration of upper plate rocks undergoing very high heat flow onto the lower plate, where heat flow is quickly decreasing leading to a diachronous evolution of the thermal structure.

4. FOSSIL EXAMPLE OF ASYMMETRIC RIFT: OBSERVATIONS FROM THE ARZACQ-MAULÉON BASIN

4.1 Geological context

Few examples exist where the thermal record of asymmetric rifted margins can be accessed and compared to results from numerical modelling experiments. Here, we focus on an onshore fossil example of an asymmetric hyperextended rift system: the Arzacq-Mauléon basin, located in the Western Pyrenees. This basin mainly formed during Aptian to Cenomanian time as part of the Pyrenean rift system, simultaneous to the opening of the Bay of Biscay. Its southern part was subsequently inverted and integrated in the Pyrenean orogen during Late Cretaceous to Miocene convergence (Puigdefàbregas & Souquet, 1986).

The inversion of the Arzacq-Mauléon basin as a pop-up structure (Daignières et al., 1994; Seguret, 1972) enabled the exposure of rift-related sedimentary and basement rocks and partial preservation of several rift structures, allowing the restoration of the former asymmetric rift structure (Masini et al. 2014). The southern boundary of the basin includes a series of Palaeozoic massifs (Fig. IV-5, Aldudes, Mendibelza, Igountze) that are thrust toward the south (Daignières et al., 1994; Muñoz, 1992; Teixell, 1990, 1998). The Mauléon basin is bounded to the west by the Labourd massif and by the Pamplona fault zone (Claude, 1990; Jammes et al., 2009; Masini et al., 2014; Razin, 1989; Schoeffler, 1982). To the north, the Mauléon basin is thrust onto the Arzacq basin along the north-vergent North Pyrenean Frontal Thrust system (NPFT), consisting of the St Palais and the Ste Suzanne thrusts (Fig. IV-5b). The presence of exhumed granulites (Ursuya Massif, Fig. IV-5) and mantle rocks in the basin are interpreted as fingerprints of extreme crustal thinning of this basin (Jammes et al., 2009; Lagabrielle et al., 2010; Lagabrielle & Bodinier, 2008; Masini et al., 2014; Tugend et al. 2014; 2015). The end of rifting was associated with an alkaline magmatic activity (Montigny et al., 1986) and a HT/LP metamorphism of Mesozoic pre- and early syn-rift sediments (Albarède & Michard-Vitrac, 1978; Azambre & Monchoux, 1998; Azambre & Rossy, 1976; Golberg & Maluski, 1988; Montigny et al., 1986; Thiébaud et al., 1988).

The occurrence of this rift-related HT-LP metamorphism resulted in the acquisition of an increasing amount of data aiming to investigate the rift-related thermal structure of this basin and more generally of the Pyrenean rift system (Clerc et al., 2015; Hart et al., 2017; Vacherat et al., 2014). Clerc et al. (2015) provided new constraints on peak temperatures (T_{\max}) from Raman Spectroscopy on Carbonaceous Material (RSCM) from the Mauléon basin (Fig. IV-5a and fig.

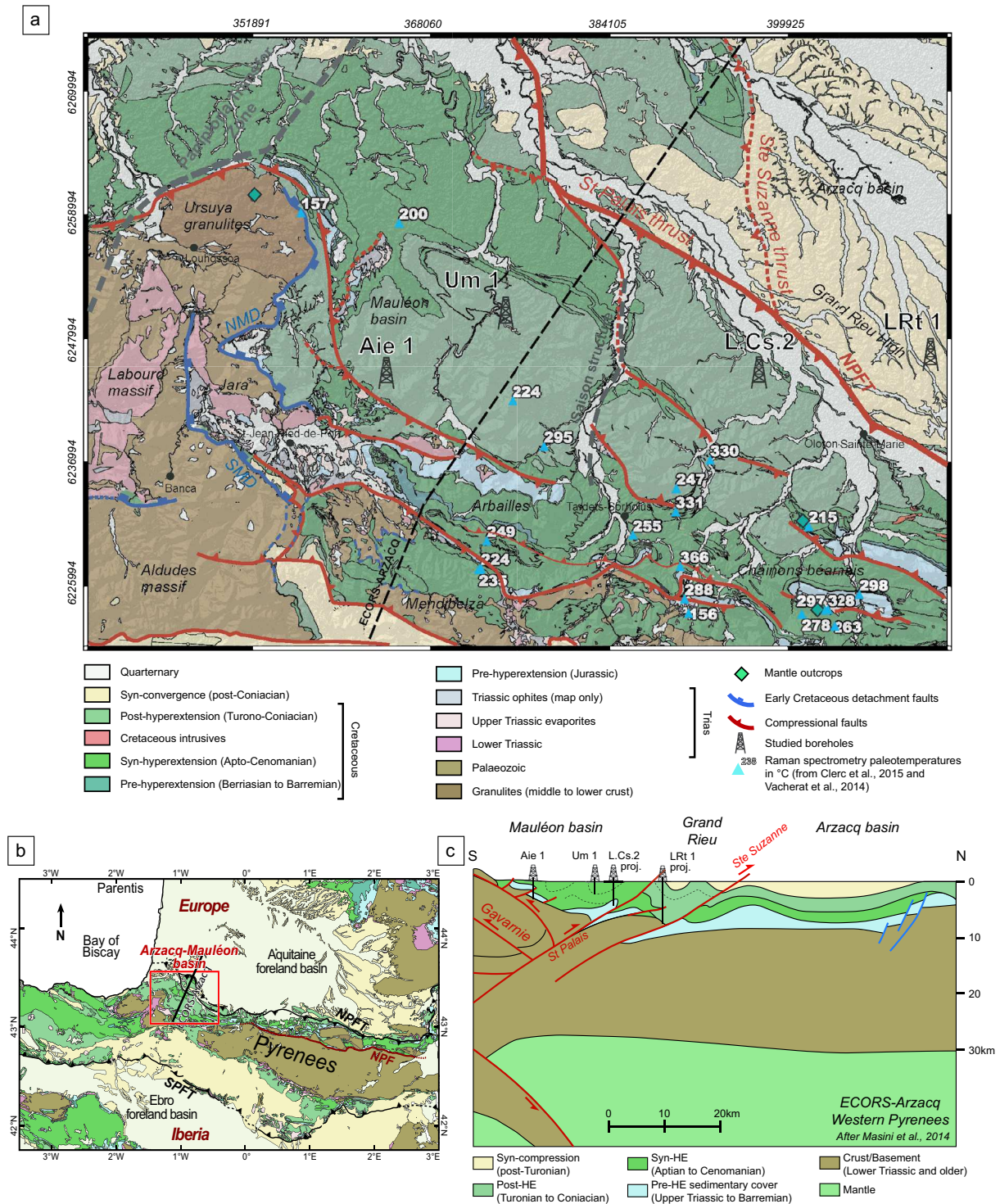


Figure IV-5: a: Geological map of the Mauléon-Arzacq basin (compiled from Genna (2007) and own observations). The locations of RSCM data (T_{max}) from subsurface rocks (Fig. S4 in annexes) and selected boreholes of this study are indicated. Coordinates are in meters (Lambert 93 projection). b: Geological map of the Pyrenees with location of the study area. Coordinates are in decimal degrees (WGS84 projection). c: Interpreted ECORS Arzacq-Western Pyrenees seismic profile, modified after Masini et al. (2014). Note that part of the pre-HE sedimentary cover is composed of the Late Triassic evaporites responsible for the thickness variation.

S4 in annexes). The authors showed that relatively high temperatures in sedimentary rocks are systematically associated with the occurrence of mantle rocks and granulites. They interpreted medium to high geothermal gradients associated with mantle exhumation and a thick pre-HE (Upper Triassic to Barremian) to syn-HE (Apto-Cenomanian) sedimentary cover acting as a thermal blanket. Vacherat et al. (2014) and Hart et al. (2017) performed detrital zircon fission-track and (U-Th-Sm)/He, and detrital zircon (U-Th)/He thermochronology, respectively, in order to define the paleo-thermal gradient. Their results show a thermal gradient ranging between 80 to 100°C/km for rifting in the hyperextended domain of the basin.

4.2 Rift evolution and former architecture

Based on previous studies (e.g. Ducasse et al., 1986a; Jammes et al., 2009; Johnson & Hall, 1989b; Velasque et al., 1989) and new field data, Masini et al. (2014) argued that the Arzacq-Mauléon basin developed asymmetrically via north-dipping detachment faults, implying the formation of a upper-lower plate architecture. Masini et al. (2014) evidenced two main detachment faults along the southern border of the Mauléon basin, referred to as the South and the North Mauléon Detachment faults (SMD and NMD, respectively; Fig. IV-5a). They are associated with cataclasites, gouges and tectono-sedimentary breccias affecting and reworking the Paleozoic basement (Fig. IV-6). The sedimentary architecture and facies evolution from Upper Aptian to Albian sediments record the progressive creation of accommodation space. Masini et al. (2014) proposed, based on the migration of the syn-tectonic sedimentary facies tracts, a northward migration of the deformation associated with these north-dipping detachment faults delimiting tilted blocks (Jara-Arbailles, Fig. IV-6) (see also Hart et al., 2016).

The detailed architecture of the northern Mauléon basin, floored by the NMD, is hardly accessible due to the thick Albo-Cenomanian cover. However, Jammes et al. (2009) and Masini et al. (2014) suggested that the Labourd massif might represent the western lateral prolongation of the basement located below the northern Mauléon basin. In this area, the authors described evidence for fluid and reaction assisted brittle fault rocks and associated tectono-sedimentary breccias, diagnostic of extensional detachment faults in hyperextended settings (Jammes et al., 2009; Pinto et al., 2015; Tugend et al., 2015). The description of depositional contacts between Albo-Cenomanian sediments and exhumed mid crustal granulites (Jammes et al., 2009) and the reworking of these granulites in the overlying sediments argue for laterally discontinuous and allochthonous pre-rift cover sequences separated by exhumation windows (Fig. IV-6). These observations have been interpreted as evidence for extensional detachment faulting leading to

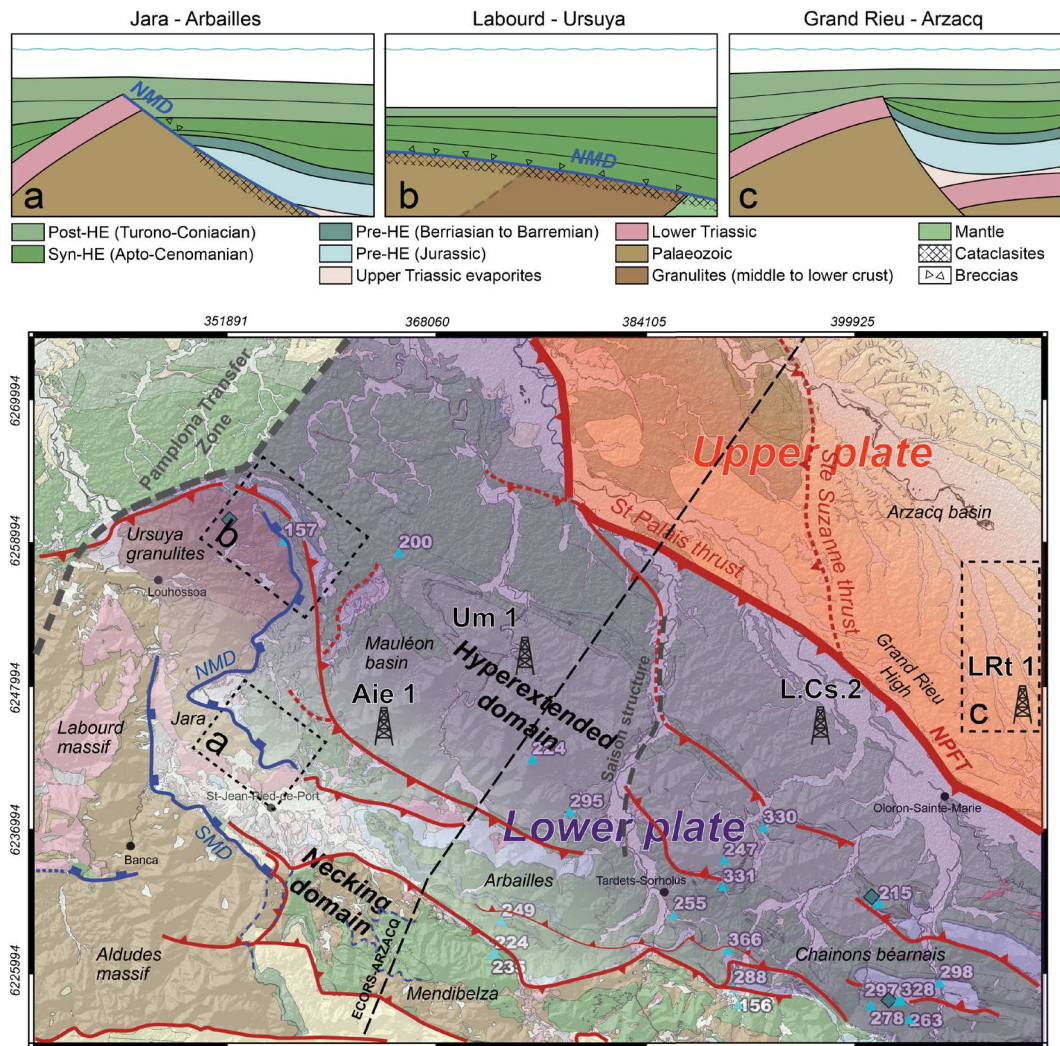


Figure IV-6: Key field observations, map of rift domains (after Tugend et al., 2014) and plate polarity in the inverted hyperextended Arzacq-Mauléon basin. Square (a) and (b) correspond to key observations illustrating the main rift geometries preserved for the lower plate and square (c) for the upper plate.

exhumation of deeper crustal and mantle levels in the Mauléon basin (Jammes et al., 2009). The cooling ages of the footwall (i.e. Ursuya granulites, Ar/Ar on biotite: 200Ma > ZHe: 51Ma) (Hart et al., 2016; Masini et al., 2014; Vacherat et al., 2014) may correspond to the age of the sub-horizontal syn-exhumation deposits of the Bonloc trough (Albo-Cenomanian). The occurrence, at present-day, of a positive gravimetric anomaly in the Mauléon basin, attributed to a high density body at shallow depth below the basin, has been interpreted by some authors (Casas et al., 1997; Chevrot et al., 2015; Jammes et al., 2010a; Pedreira et al., 2007; Wang et al., 2016) as the evidence for extreme crustal thinning and likely mantle exhumation during rifting. Moreover, magmatism within Albo-Cenomanian sediments in the northern part of the Mauléon basin (Fig. IV-5 and IV-7) attests for major lithospheric thinning in the hanging-wall of the NMD. In summary, the overall first order architecture of the Mauléon basin, i.e. the creation

of accommodation space and the exhumation of crustal and mantle rocks linked to basinward dipping faults, is compatible with a lower plate setting (Fig. IV-2; Jammes et al., 2009; Masini et al., 2014; Tugend et al., 2014).

Crustal extension factors below the Arzacq basin, i.e. β -factors of ~ 2 have been estimated from subsidence analysis (Brunet, 1984), suggesting that the crust beneath the Arzacq basin has been less thinned than the Mauléon basin (Masini et al., 2014), the latter reaching mantle exhumation. Drill holes located between the Arzacq and the Mauléon basins (e.g. Le Rouat, Fig. IV-7) document a major unconformity between basement rocks (especially Lower Triassic sandstones) and sub-horizontal, late syn- to post-HE Cretaceous sediments (Fig. IV-6). This suggests that the Grand Rieu was a relative topographic high until late stages of rifting (Masini et al., 2014; Tugend et al., 2014) and created a topographic boundary between the Arzacq and Mauléon basins. This also reveals that the basement is not capped by a major detachment fault at this place, as it is the case for basement highs in the southern Mauléon basin (e.g. Labourd massif, Jara tilted block, Aldudes exhumed basement, Fig. IV-5). It also points out the role of Late Triassic evaporites during mid-Cretaceous extension decoupling extension between the sub- and supra-evaporite sedimentary cover (i.e. from Jurassic to Aptian) (Jammes, Manatschal, et al., 2010; Lagabrielle et al., 2010; Masini et al., 2014). However, the overall preservation of the pre-HE stratigraphy, together with little, observable rift deformation and minor crustal thinning suggests a typical upper plate architecture for the northern margin of the Mauléon basin (Fig. IV-2).

4.3 Vitrinite reflectance data (proxy for T_{\max})

4.3.1 Data set and method

We provide unpublished vitrinite reflectance data (courtesy of Total) from sedimentary rocks of selected boreholes from the Mauléon-Arzacq basin (Fig. IV-7 and fig. S5 in annexes). These 4 boreholes are located along the dip direction with respect to the former rift orientation and provide information about the sedimentary and basement architecture of both the upper and lower plates. Thus, these boreholes can represent a section through the basin, from proximal to distal in the hyperextended domain that has not been strongly inverted during convergence and that are documenting structural levels that are not outcropping at present. The vitrinite reflectance (in %) measures the thermal maturation of organic components. It can be used as a proxy for source rock maturation and maximum temperature history (T_{\max}) of sedimentary rocks (Taylor et al., 1998). The evolution of vitrinite reflectance values (%VR) in boreholes provides a constraint on the relative T_{\max} reached by the samples within the stratigraphic log

within the inverted basin. Figure IV-7a shows the four simplified stratigraphic logs from the Mauléon (Ainhice 1, Uhart-Mixe 1, Les Cassières 2) and Arzacq basins (Le Rouat 1). Le Rouat 1 is located on the Grand Rieu High. Wells are not significantly deviated and thus we can assume that distance corresponds, in a first approximation, to vertical depth.

4.3.2 Borehole description

The Ainhice 1 borehole (Aie 1) shows 1700 meters of Cenomanian flysch noir to Lower Jurassic Calcareous marls with a major erosional unconformity between the Oxfordian and the Middle-Albian. This sequence is duplicated below a thrust fault with %VR values reaching 4,43%VR in the Middle-Albian and 4,57%VR in the Jurassic. This sequence lies onto a 400m thick chaotic evaporitic layer composed of shales, evaporites and ophites, unconformably lying above a 640m thick sequence of quartzites and black shales (4,42%VR) attributed to the Palaeozoic, with the omission of Lower Triassic sandstones and conglomerates.

The Uhart-Mixe 1 borehole (Um 1) reaches 1868m depth. The top of the sequence is composed of Turonian limestones, less than 300m thick, followed by Cenomanian to probably Albian flysch and marls at the bottom. The %VR go from 3,75 to 5,09 with a general increase of the value with depth even though strong variations are observed within the log (Um 1 on Fig. IV-7a).

The Les Cassières 2 borehole (L.Cs.2) penetrated down to 5692m depth. The upper part of the drill hole is composed of about 1200m of Turonian to Campanian flysch (shales, sandstones, marls) with %VR of 2,13 to 2,55. A very thick Cenomanian Flysch Noir sequence (1700m) is represented with the occurrence of an episyenite sill at its base. Vitrinite reflectance values range from 2,6 at the top to 3,51 at the base. The top Albian (%VR of 4,09) is also composed of magmatic dykes. The underlying Albo-Aptian marls show evidence for an intense fluid circulation that may be responsible for the silicification of limestone beds and, toward the base, an increase of dolomitized fractures and marly beds. Available VR values are about 5,40%VR. Neocomian limestones (Lower Cretaceous) display VR values of 5,15 to 5,83 and are unconformably lying over Lower Jurassic limestones (5,77%VR).

The Le Rouat 1 borehole (LRt 1) is composed of Eocene sandstones and mudstones that overlie Upper Cretaceous marly flysch. The base of the Upper Cretaceous unit (~5000m) is characterized by rounded clasts of dolostones, limestones and red mudstones attributed to Lower Jurassic, Upper Jurassic and Permo-Triassic, respectively. This 5000m thick sequence shows a value of 2,67%VR at the base. This sequence is unconformably deposited onto Permo-Triassic sandstones (2,35%VR) that are unconformably lying onto black schists attributed to the Devonian.

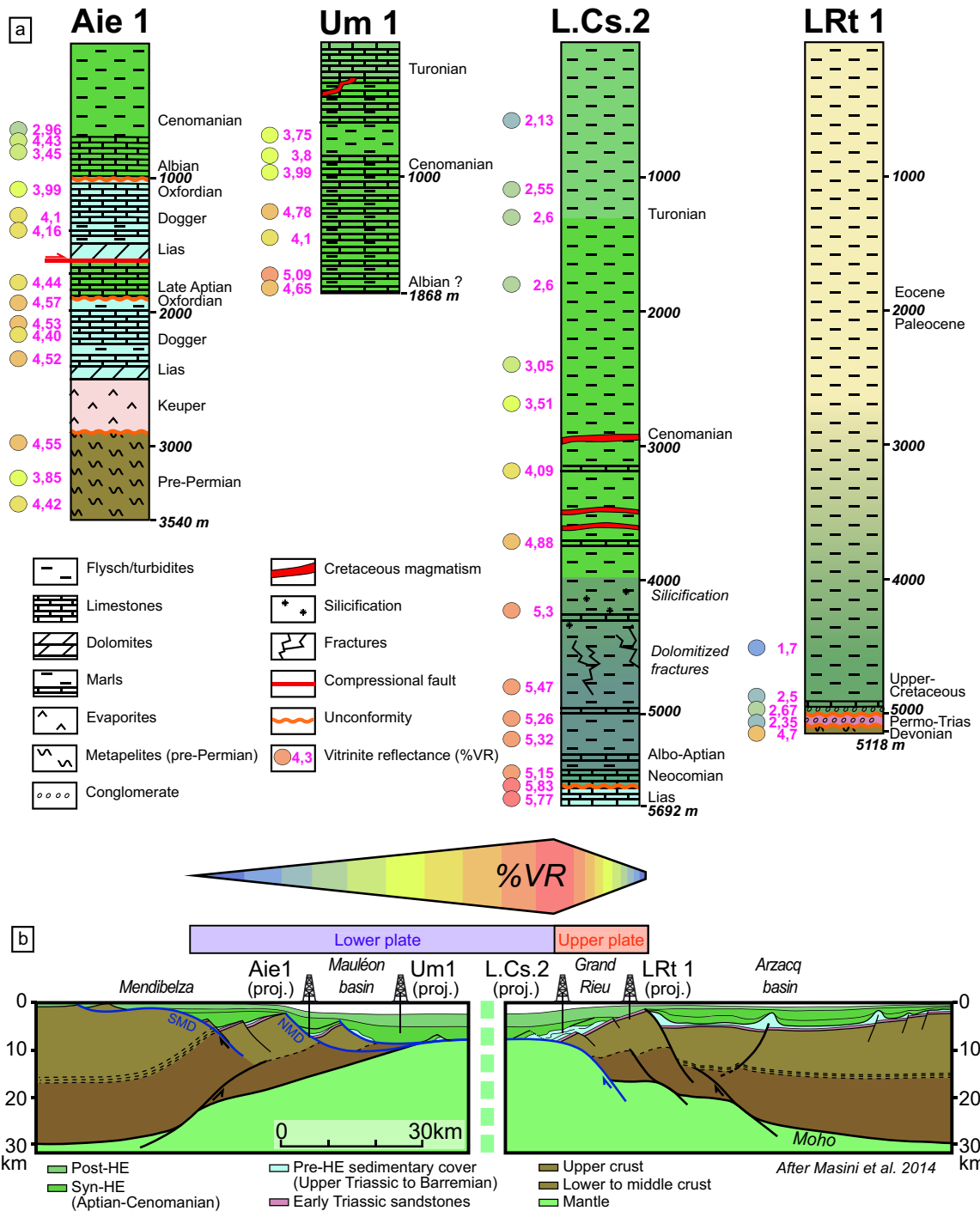


Figure IV-7: a: Synthetic well logs shown for the Arzacq-Mauléon basin: Ainhice (Aie 1), Uhart-Mixe (Um 1), Les Cassières (L.Cs.2) and Le Rouat (LRT 1) (location in Fig. IV-5). See caption in Fig. IV-5 for the colour code of sedimentary sequences. b: Restored cross-section of the Arzacq-Mauléon basin before the compression (i.e. before Santonian), with approximate location of the boreholes.

4.3.3 Results

From south to north, we observe a deepening of the Mauléon basin associated with crustal thinning and mantle exhumation. Likewise, vitrinite reflectance (or T_{\max}) shows a downward and northward increase south of the St Palais thrust. In detail, Aie 1 shows high %VR (3,44 to 4,44%VR) in Albo-Cenomanian and Jurassic marls and limestones, suggesting the erosion of quite thick post-rift sequences during Pyrenean convergence. Moreover, duplication of the sedimentary sequence at the base of the Early Jurassic is due to a northward thrust fault located at about 1700 meters and may control the overlying erosion. At the bottom of the borehole, below the Triassic Keuper, there is no evidence for the Permo-Triassic red beds. This supports the existence of an extensional contact north of the Jara block, which can be related to the NMD (Masini et al., 2014). We suggest that the heterogeneity of %VR values in the Um 1 borehole might be related to multiple small-scale thrusts due to Pyrenean convergence. Northward, the L.Cs.2 borehole displays intense silicification and dolomitized fractures, which attest for fluid migration in Apto-Albian sediments. It is important to note that the %VR steadily increases from the surface to 3200 meters (i.e. Late Albian) and that they reach a maximum value of 5,15 to 5,83%VR from 5000 to 5692 meters in the Apto-Albian to Lower Jurassic units. This %VR trend between post-Albian (depth-dependent %VR) and pre-Albian (maximum constant %VR) rocks has been observed in few boreholes from the Mauléon basin (e.g. Moncayolle).

On the LRt 1 borehole, in the Arzacq basin, the thick (about 5km) Late Cretaceous to Eocene sedimentary sequence displays a constant increase from top to bottom but merely reach 2,67%VR. Additionally, the Permo-Triassic conglomerates reach values of 2,35%VR, which evidence a relative low T_{\max} that has not been overprinted by the mid-Cretaceous thermal event. Thus, we can infer that the Late Cretaceous sediments did not experienced significant heat flow. Interestingly, a quite high and abrupt change in %VR is observed in the Devonian meta-sediments below the Triassic conglomerate, arguing for a Variscan thermal imprint.

These observations evidence a progressive deepening of the Mauléon basin from south to north as expected for a lower plate, associated with a general increase of T_{\max} (in this study %VR) and first occurrence of magmatism. The highest T_{\max} are observed at the transition between the lower plate and the upper plate (Fig. IV-7b, L.Cs.2 borehole). North of the St Palais thrust (i.e. upper plate), the rift-related crustal thickness abruptly changes and the recorded T_{\max} are very low in the syn- to post-HE sediments (LRt 1 borehole). This structural and thermal relationship points to a general asymmetry of the Arzacq-Mauléon rift system that is not consistent with symmetrical rifting.

5. DISCUSSION

5.1 First order rift-related thermal structure and evolution of hyperextended systems

5.1.1 Thermal asymmetry

The numerical model shows that due to the asymmetric rift evolution, the maximum heat flow location at the base of the basin tends to migrate toward and to stabilize over the upper-lower plate transition (Fig. IV-3). The location of the maximum heat flow in the model is controlled by the upwelling of hot asthenospheric mantle as a consequence of asymmetric lithospheric thinning due to major detachment fault activity (Brune et al., 2014). Note that such structural control on the asthenosphere/lithosphere boundary depth cannot be captured by depth uniform models (e.g. McKenzie, 1978). The evolution of heat flow during extension from markers A to C (Fig. IV-4) shows that the maximum value is increasing during rifting due to lithospheric thinning and asthenospheric upwelling.

In the Arzacq-Mauléon basin, the asymmetry is also well expressed in the distribution of T_{\max} , once restored back into their former rift context (Fig. IV-7b). The highest T_{\max} values were located at the upper and lower plate transition, associated with deep crustal and mantle rocks. They were later transported during convergence onto the upper plate along the St Palais thrust and juxtaposed to sediments showing lower T_{\max} values.

Both the numerical model and field observations show an asymmetric heat distribution with respect to the upper-lower plate transition (Figs. IV-3 and IV-7b). This strongly suggests a control of rift asymmetry on the location of highest basal heat flow and T_{\max} in rift basins, which cannot be explained by pure shear depth uniform thinning. This asymmetric evolution during rifting may be applicable to the heat flow evolution of other asymmetric magma-poor rift systems such as the Parentis basin (Jammes et al., 2010a), the Newfoundland-Iberia conjugate margins, the Labrador Sea, the Porcupine Basin (Fig. IV-1), the Central South Atlantic magma-poor segments (Péron-Pinvidic et al., 2017), the Australia-Antarctica margins (Direen et al., 2013), the Australian North West Shelf (Karner & Driscoll, 1999) or the East Australia – Lord Howe rise conjugates (Gaina et al., 1998).

these two thermal events can be juxtaposed on the lower plate and result in very sharp limits between high and low T_{max} values occurring over short distances (Fig. IV-8 and IV-9).

In case of low sedimentation rates during rifting, the T_{max} values recorded by syn- to post-tectonic sediments are expected to be much lower than T_{max} values recorded in the extensional allochthons (pre-tectonic). In this case, a strong contrast between the T_{max} recorded in the allochthon and in the overlying sedimentary sequence is expected. As a consequence, paleothermal gradients determined from such data sets might not be representative and may provide unrealistic values (Fig. IV-9).

In case of high sedimentation rates, the burial related thermal event might eventually overprint or obliterate the former thermal event due to the basal heat flow (Fig. IV-9). As a consequence, the pre- to syn-HE sedimentary sequences that floor the basin of lower plates might display complex and diachronous high T_{max} values (Fig. IV-8 and IV-9). This can result in erroneous determinations of paleothermal gradients and the overestimation of the global heat flow at the base of the basin. Sedimentation can either reveal or obliterate these diachronous thermal events (heat flow vs. burial dominated) and further work will be necessary to model these extreme cases.

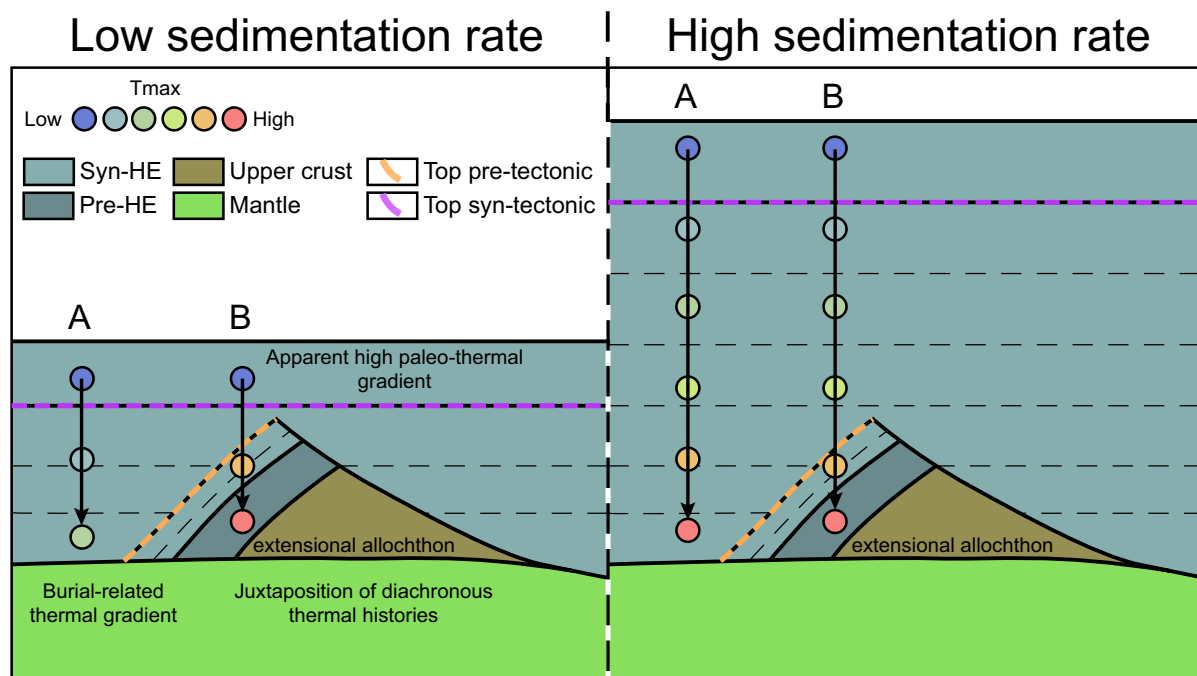


Figure IV-9: Role of sedimentation rates on the thermal architecture of hyperextended domains at the end of rifting. T_{max} in the pre-tectonic sediments (extensional allochthon) have been recorded at the upper-lower plate transition and transported onto the lower plate. T_{max} within the syn- to post-tectonic sediments are diachronous and depend on sedimentation rate (burial) during hyperextension. Gradient A show a typical burial-related thermal gradient under moderate heat flow on the lower plate (late HE). Gradient B juxtaposes two diachronous thermal histories. In low sedimentation rate systems, the determination of the paleothermal gradient using T_{max} can be misleading. In high sedimentation rate systems, the apparent paleothermal gradient is similar but can result from two different thermal histories.

5.1.3 T_{max} , thermal gradient and heat flow: general implications

Thermal parameters such as T_{max} , thermal gradient and surface heat flow are commonly used to define the thermal architecture of rift basins with the assumption that crustal thinning is the main controlling factor. However, data from numerical models imply a more complex architecture, where diachronous thermal and tectonic histories might be juxtaposed on a single vertical section.

Indeed, the thermal gradient and top basement heat flow values are increasing during rifting but their locations might vary due to rift migration. Especially in asymmetrical rift basins, a strong variation of the thermal gradient from the lower to the upper plate must be expected. Moreover, this first-order thermal structure can be modified by fluid circulation (e.g. Person et al., 1996; Souche et al., 2014; Boulvais, 2016) or magmatic additions at various time leading to local perturbations of the T_{max} values. Type and rate of sedimentation can also affect the surface and top basement heat flow, such as evidenced by the thermal blanketing effect (e.g. Hutchison, 1985; Souche et al., 2017). However, in low sedimentation rate systems, the top basement heat flow can slightly decrease with respect to models without sedimentation (e.g. Theissen & Rüpke, 2009; Souche et al., 2017) but follows a trend that is similar to our model (Fig. IV-4). In this study, we only investigated the basal heat flow that is best recorded in the pre-tectonic sequence, future work is necessary to isolate the thermal evolution of the post-HE sequence, taking into account fluids, sedimentation rates and syn- to post-HE magmatic activity.

T_{max} is commonly used to constrain paleothermal gradient and thermal architecture of fossil rift basins. However, our analysis highlights that the maximum temperature reached by a rock does not reflect the complete thermal history of the rock and is hence prone to misinterpretation (Fig. IV-9). This is exemplified in the diachronous tectonic and thermal histories of our study, where rocks with T_{max} acquired at different moments and in different thermal contexts have been juxtaposed (see Figs. IV-8 and IV-9). The resulting paleothermal gradient extracted with these two values might be unrealistically high and does not represent a real paleothermal gradient at any time of the rift evolution.

From this study, we can assume that the thermal asymmetry observed in pre- to syn-HE sequences may be a good indicator to define the polarity (upper vs. lower plate) of hyperextended rift systems. Moreover, abrupt changes of T_{max} values could suggest the occurrence of an allochthonous extensional unit on top of a detachment fault in a lower plate setting.

5.2 Implications and limitations derived from the Pyrenean case

New vitrinite reflectance data from the Arzacq-Mauléon basin show an asymmetry of the T_{\max} distribution within the pre- to syn-HE sequence of the basin, likely due to asymmetric heat flow evolution associated with northward migration of the north-dipping Mauléon detachment faults (Masini et al., 2014). Despite a well constrained metamorphic zone (NPMZ) in the eastern Pyrenees and in the Basque-Cantabrian basin, its continuation in the Mauléon basin was questioned (Albarède & Michard-Vitrac, 1978; Golberg & Leyreloup, 1990). Based on this new thermal data set derived from boreholes, we can suggest that the so-called NPMZ, and consequently rocks with highest T_{\max} are not exposed but are buried deeper in the northern part of the Mauléon basin. Its south-western shift within the Basque-Cantabrian basin is probably controlled by the Pamplona transfer zone.

Although we demonstrate a structural and thermal asymmetry of the Arzacq-Mauléon rift system similar to the numerical model, the complexity raised by allochthons has not been evidenced in our study area. We suggest that gravity gliding and migration of the pre-HE sedimentary cover on Upper Triassic evaporites might result in additional complexity to the tectonic and thermal history. Such a process has been recently proposed by Lagabrielle et al. (2010) and Corre et al. (2016) for symmetric rifting in the eastern and western Pyrenees, respectively. However, the field observations and the existing data set do not enable to resolve the impact of such allochthony on the thermal architecture of the basin. Moreover, fluid circulation might have played a role in the distribution of T_{\max} in the basin by homogenisation of the temperature field such as proposed by Boulvais (2016) in the Eastern Pyrenees.

6. CONCLUSIONS

Both numerical model and field study show a thermal asymmetry with the maximum heat flow and the highest T_{\max} located at the upper-lower plate transition. Numerical model results also highlight a strong diachronism in the record of the maximum heat flow for each extensional allochthon in hyperextended domains. These results might apply to all asymmetric, hyperextended magma-poor rifted margins.

We suggest that the peak heat in sedimentary rift basins is controlled by the relative importance of two processes:

- A local and short-lived thermal event located above the focus of hot asthenospheric upwelling at the upper-lower plate transition that leads to very high heat flow, which is likely amplified by fluid circulation. Upper plate blocks made of pre-tectonic material recording very

high T_{\max} values might be transferred during rift migration from the upper to the lower plate. Once this transfer is completed, heat flow within these blocks is rapidly decreasing as the upper-lower plate transition migrates further away.

- A regional event affecting the entire basin and related to basin infill and burial. The resulting thermal gradient in these sediments notably depends on the timing and rate of sedimentation, the lithology and the basal heat flow.

Both thermal events can be juxtaposed on the lower plate after the formation of allochthons and may lead to unrealistic or not representative paleothermal gradients in case of low sedimentation rates. Such a diachronous and asymmetrical evolution of the thermal parameters (T_{\max} , heat flow, thermal gradient) in asymmetric rift systems leads to a complex final thermal architecture that cannot be understood through depth uniform modelling (McKenzie, 1978) or extrapolation of 1D T_{\max} values.

ACKNOWLEDGMENTS

We thank M. Nirrengarten for helpful information regarding vitrinite reflectance data and Total for providing us with the data. All the data used are listed in the references or in the supporting information. This study was funded by the Orogen project, a tripartite joint academic-industry research program between the CNRS, BRGM and Total R&D Frontier Exploration program. J.T. was funded through the MM4 consortium. S.B. was funded through the Helmholtz Young Investigators Group CRYSTALS (VH-NG-1132). Supporting information related to this article are included as two tables (S1 and S4), two figures (S2 and S5) and one movie (S3).

CHAPTER V:
GENERAL DISCUSSION

The aim of this study was to investigate the role of inheritance and rift segmentation during rifting and reactivation, as well as the thermal evolution associated with hyperextension.

The Pyrenean-Cantabrian system has been characterised as a very segmented rift system, from both a structural and thermal point of view, that has been subsequently reactivated during the Alpine orogeny (e.g. Clerc et al., 2015; Roca et al., 2011; Tugend et al., 2015). However, the architecture and evolution of these rift segment boundaries have never been carefully studied and little is known about how they formed and the deformation during the different rift events and subsequent convergence. As such, the role of inheritance of rift segment boundaries and adjacent rift segments during the subsequent orogenic evolution remains ill-constrained, despite along-strike structural and thermal changes have been recognized (Chevrot et al., 2018; Clerc et al., 2015; Teixell et al., 2018). Moreover, although the McKenzie model has been proven to fail in predicting the thermal state of hyperextended domains (e.g. Callies et al., 2018), the recently proposed thermo-mechanical lithospheric models have not been rigorously tested to account for the Pyrenean-Cantabrian thermal evolution and for hyperextended rift systems in general.

These questions have been especially addressed to the onshore Basque Country, which remarkably preserves the syn-rift architecture of the rift segment boundary and benefits from a large dataset. The study of the tectono-sedimentary architecture combined with seismic interpretation allowed to define the structural evolution of this domain and to replace it in the general kinematic framework of the Iberia-Eurasia plate boundary. Moreover, the comparison between the rift segment architecture and their lateral terminations permits to analyse the mode of deformation that occurred during the reactivation as well as the influence of rift segment boundaries and the role of rift domains on the orogenic architecture. Finally, the restoration of the thermal state of the asymmetric Mauléon basin coupled to a numerical model allow to assess the influence of asymmetric rifting on the thermal evolution of hyperextended rift systems.

In the following, the main questions defined in the introduction of this PhD are discussed using the main results that came out of the study.

1. WHAT IS THE PRESENT-DAY ARCHITECTURE OF THE PYRENEAN-CANTABRIAN JUNCTION? (CHAPTER II – QUESTION A)

Previous studies used to investigate the architecture of the Basque Country via detailed descriptions of the inverted eastern BCB (DeFelipe, 2017; Lamare, 1936; Llanos, 1980; Martínez-Torres, 1992; Rat, 1988), the Mauléon basin (Claude, 1990; Jammes et al., 2009; Masini et al., 2014; Tugend et al., 2014) and the St-Jean-de-Luz basin (Razin, 1989). However, besides recent large-scale studies (Díaz et al., 2012; Pedreira et al., 2003, 2007), the study and the integration of results and observations from both the eastern Cantabrian and western Pyrenean segments in a coherent tectonic framework was lacking. As such, no study attempted to propose a restorable crustal cross-section of the entire Pyrenean-Cantabrian junction.

This study shows that, despite the apparent complexity of the surface geology, a N-S cross-section across the Basque massifs (Fig. V-1) depicts a typical orogenic wedge overriding the Ebro and Aquitaine foreland basins such as observed in the Eastern to Western Pyrenees (Muñoz, 1992; Teixell, 1998). Complexities are brought by the Upper Triassic evaporites, which decoupled the deformation between the sedimentary cover and the underlying basement. As such, the allochthonous BCB and St-Jean-de-Luz basin were passively uplifted and transported in front of the pro- and retro-wedge formed by the Basque massifs. These results reveal the role of the inherited evaporites as well as the strong decoupling between thin-skinned (supra-salt) and thick-skinned (infra-salt) deformation for the evolution of the Pyrenean-Cantabrian junction.

The Upper Triassic evaporites are particularly well represented in the study area (e.g. Brinkmann & Logters, 1968; James & Canérot, 1999). However, whether the Pyrenean-Cantabrian junction already represented a main depocenter during Upper Triassic, or the evaporites have been displaced toward the area during the Late Jurassic to Cretaceous tectonic evolution, is questioned.

2. WHAT WAS THE PRE-CONVERGENCE ARCHITECTURE OF THE PYRENEAN-CANTABRIAN JUNCTION? (CHAPTER II – QUESTION B)

The rift segmentation between the BCB and the Mauléon basin at mid-Cretaceous time was previously ascribed to the NNE-SSW Pamplona transform fault, which was defined by indirect observations such as the alignment of salt diapirs, the change in thrust vergence, the thickness variation of the Cretaceous basins or the offset of mantle and HT/LP metamorphic rocks (e.g. Larrasoña et al., 2003a; Martínez-Torres, 1992; Rat, 1988; Richard, 1986; Roca et al., 2011; Tugend et al., 2015). This fault was then supposedly decoupling the deformation

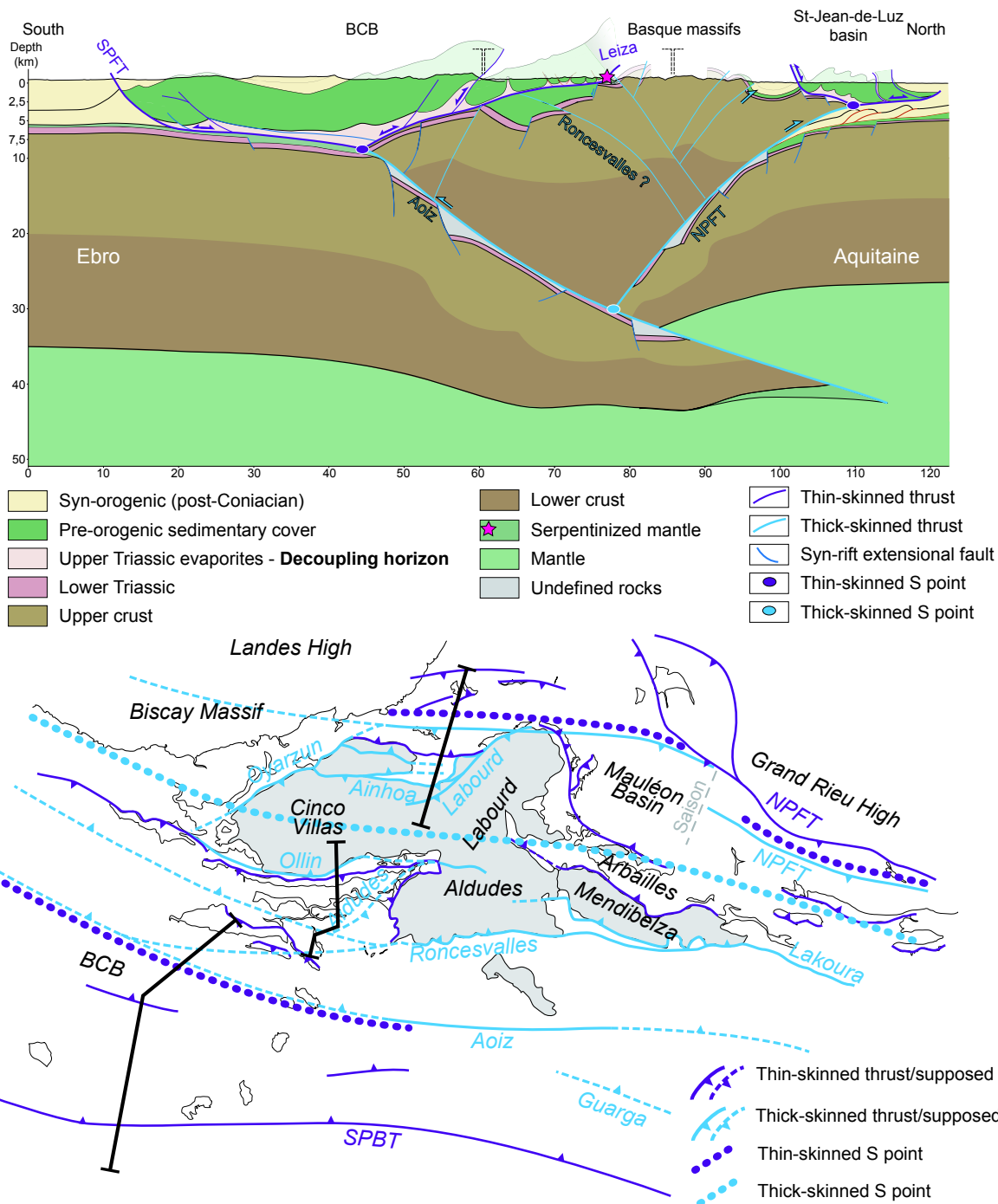


Figure V-1: Equilibrated crustal cross-section and structural map of the present-day Pyrenean-Cantabrian junction. Note the difference between the thin- and thick-skinned deformations and the influence on the orogenic architecture.

between the Cantabrian segment and the Pyrenean segment. However, no studies were conducted to identify such structures in detail on the field.

Detailed field observations and seismic interpretations discard the existence of the Pamplona transform fault at mid-Cretaceous time at the Pyrenean-Cantabrian junction. In contrast, it shows that Pyrenean and Cantabrian rift segments overlapped north and south of the Basque massifs, respectively, and that no strike-slip deformation may have occurred in the Basque massifs. As such, the geometry of the area corresponded to an accommodation zone such as observed, for example, in the East African rift system at present-day (e.g. Corti, 2012; Zwaan et al., 2016) or at oceanic spreading centres (e.g. Acocella, 2008; Bubeck et al., 2017). What hampered the rift segments to link is however unknown. One may postulate that structural (NNE-SSW Permian basin) and compositional (magmatic underplating from Permian and Late Triassic events) inheritance could have prevented fault linkage to occur or deviate rift structures such as observed for the South and North Mauléon detachments at the vicinity of the Labourd massif (see Fig. II-2).

3. HOW DID REACTIVATION PROCEED IN THE SEGMENTED PYRENEAN-CANTABRIAN SYSTEM? (CHAPTER III – QUESTIONS C AND D)

The convergence in the Pyrenean-Cantabrian system is considered to form from the reactivation of hyperextended domains followed by the collision of the thick crust of the proximal domains from Eocene time onwards (e.g. Mouthereau et al., 2014; Teixell et al., 2016; Tugend et al., 2014). At the Pyrenean-Cantabrian junction, the convergence was usually assumed to reactivate the Pamplona transform fault and as such, the contractional deformation was decoupled between the Pyrenean and Cantabrian segments (e.g. Canérot, 2017; Engeser & Schwentke, 1986; Muller & Roger, 1977; Tugend et al., 2015; Turner, 1996). Former studies also interpreted this zone to accommodate a flip in the direction of nappe transport (Engeser & Schwentke, 1986) and in the dip of the subduction (Turner, 1996).

This work shows that no decoupling occurred across the Basque Country and that deformation at the junction of rift segments was accommodated by the formation of new shortcutting structures around the Basque massifs. As such, a proto-orogenic wedge formed at the Pyrenean-Cantabrian junction during the Santonian to Palaeocene, while rift segments (western BCB and eastern Mauléon basin) were facing subduction of the hyperextended domains (Fig. V-2). It was followed by an Eocene to Miocene collisional phase, which determined the final orogenic architecture of the Pyrenean-Cantabrian system. The change from subduction to collision can be defined as the moment when the conjugate coupling points meet, which

corresponds to a major change in the rheological profile in dip direction (Fig. III-2). Since the coupling points merge along strike toward the V-shaped rift segment boundaries, the collisional stage will occur earlier in these locations or may even occur right at the initiation of convergence. These results reveal the importance of rift-inheritance for the evolution of orogenic systems. While it may be important during the early subduction and transition to the collision phase, it may be of lesser importance during the final stage of collision.

The formation of the proto-orogenic wedge and related shortcutting structures in the Basque Country was responsible for the emplacement of subcontinental mantle at a mid-crustal level as attested by the gravity anomaly and the seismic anisotropy underneath the western Mauléon basin (Casas et al., 1997; Jammes et al., 2010a; Wang et al., 2016). Moreover, it is also responsible for the preservation of the pre-Alpine architecture west of the Saison transfer fault (Fig. V-2) such as the Bidarray Permian basin and the South and North Mauléon detachments. These observations reveal that rift segment boundaries may represent anomalous areas for reactivation. However, they may not be easily recognizable due to the subsequent

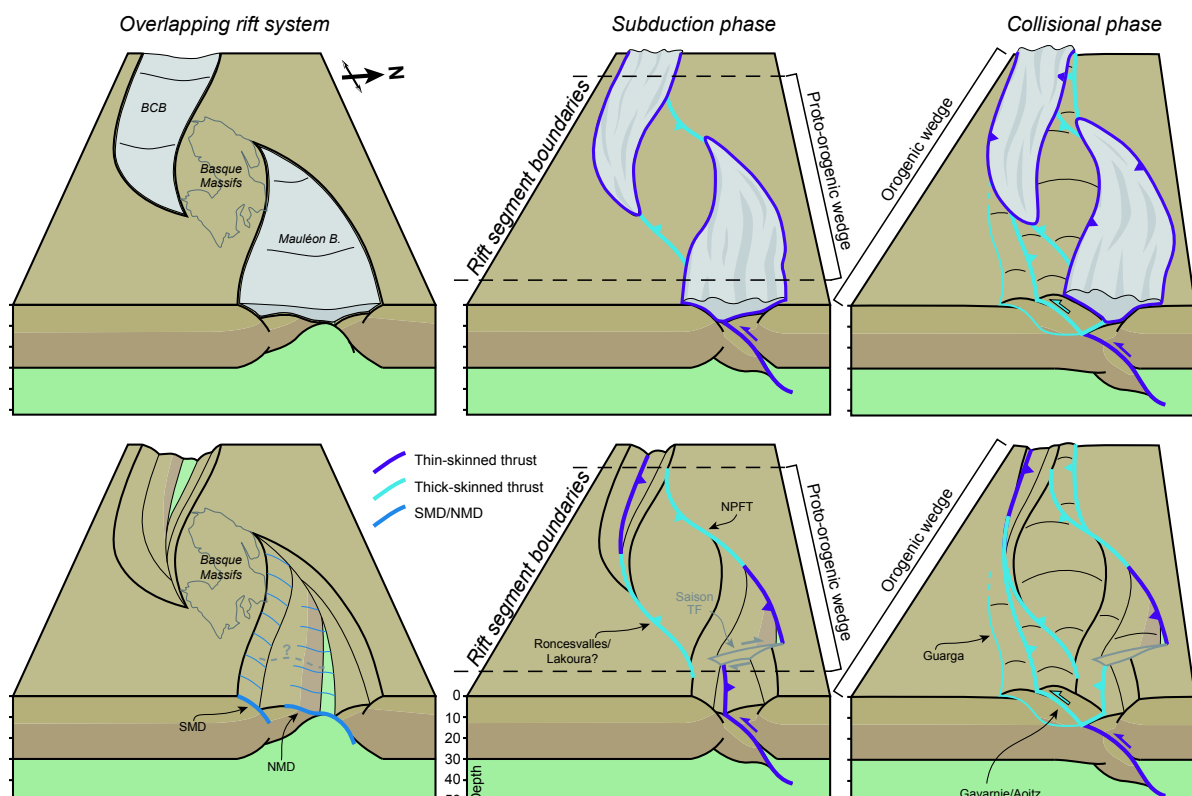


Figure V-2: Schematic 3D evolution of Cantabrian-Pyrenean junction with and without sediments, highlighting the formation of shortcutting structures at rift segment boundaries and the two phases of convergence at rift segments.

contractional imprint or because they may be obliterated by second-order structures such as the allochthonous supra-salt sedimentary cover in the Western Pyrenees. Besides, we may lack criteria to recognize them as segmentation can exhibit a multitude of types of architectures (Fig. I-IV). As such, reactivated rift segments in the Pyrenean-Cantabrian systems should not be regarded as a unique N-S decoupling structure but as a complex, anomalous areas. Possible candidates in the Central Eastern Pyrenees are the southern continuation of the Toulouse fault (Chevrot et al., 2018), or in the Santander area, at the western termination of the BCB.

Throughout the Pyrenees, the Eocene contractional event is well recorded by thermochronological data (e.g. Fitzgerald et al., 1999; Bosch et al., 2016) and syn-orogenic flysch sedimentation (Labaume et al., 1985). In contrast, the Santonian to Palaeocene convergence is well defined from plate tectonics and magnetic anomalies (Macchiavelli et al., 2017 and references therein) but is merely recorded in the Pyrenean-Cantabrian system as it reactivated domains that have been subsequently subducted. It appears that this phase can be preferentially recorded at the Pyrenean-Cantabrian junction due to the formation of new shortcutting structures. It provides as such a unique opportunity to date the initiation of convergence.

4. WHAT IS THE THERMAL EVOLUTION DURING HYPEREXTENSION? (CHAPTER IV – QUESTION E)

The extensional depth-uniform McKenzie model is widely used to assess the top basement heat flow evolution of rift basins. However, mantle exhumation can occur in hyperextended systems and as such, the crustal thickness dependent McKenzie model does not apply anymore. As such, the exhumed mantle domain is often assumed to have experienced the highest maximum temperatures (T_{\max}) and highest thermal gradient such as proposed in the North Pyrenean basins (e.g. Clerc et al., 2015; Clerc & Lagabrielle, 2014; Lagabrielle et al., 2016). However, the syn-rift lithospheric evolution is rarely considered to account for the thermal evolution in these models.

Numerical models show that in case of asymmetric lithospheric hyperextension, the McKenzie model is not able to predict the observations and that maximum heat flow is asymmetric, i.e. not necessarily related to the exhumed mantle domain. An asymmetric rift model satisfies both the structural and thermal architecture described in the Mauléon basin. However, future work is needed to see if such an asymmetric model is also able to predict observations made in other rift segments of the Pyrenean-Cantabrian system, such as the Aulus/Camarade basins in the Ariège area (e.g. Cochelin et al., 2018; Vacherat et al., 2016) or the BCB (Ducoux, 2017; Roca et al., 2011).

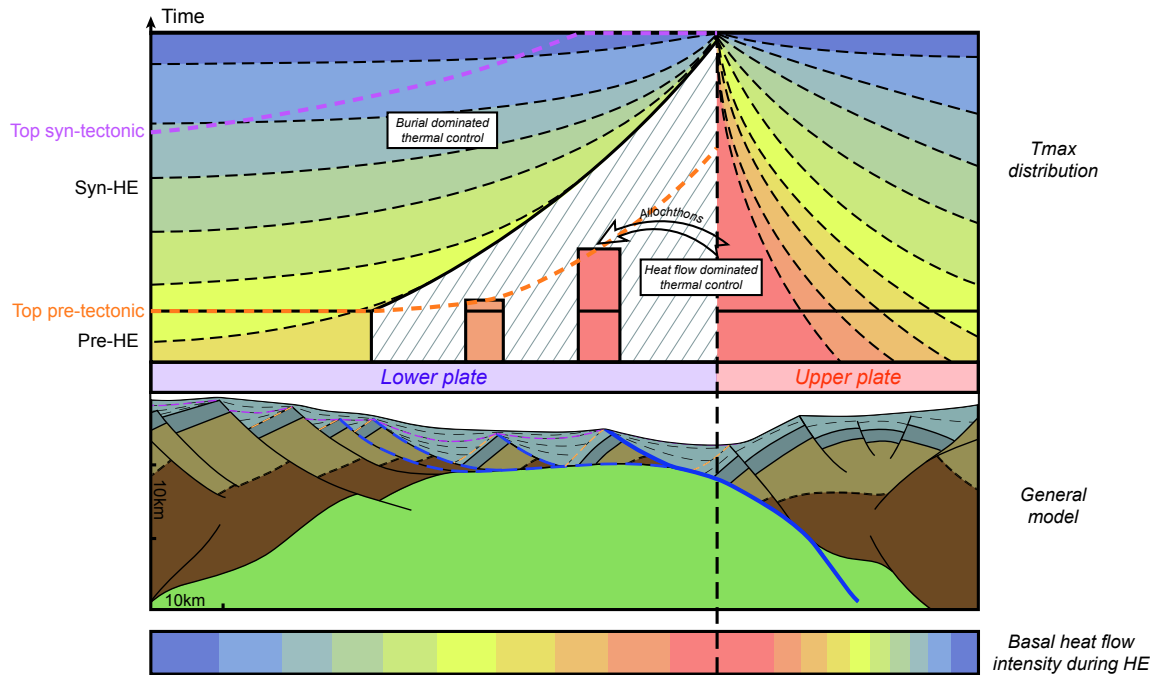


Figure V-3: First order thermal evolution associated with asymmetric hyperextended rifting. Note the expected T_{max} associated with extensional allochthons.

Another key observation is that asymmetric rift models show the migration of the thermal peak, resulting in a complex and diachronous thermal evolution of the distal parts of these basins. Indeed, rift migration implies that extensional allochthons may form successively and migrate from the upper to the lower plate during hyperextension (Fig. V-3). However, the maximum top basement heat flow remains located at the upper-lower plate transition during the rift evolution. As a consequence, each extensional allochthon may diachronously suffer and record a punctual thermal event. This diachronous thermal evolution predicted by the model has not been observed in the Pyrenean-Cantabrian system, either because of poor data resolution or because the evaporite decoupling layer impeded allochthons to migrate.

5. KINEMATIC IMPLICATION FOR THE IBERIA-EURASIA PLATE BOUNDARY (CHAPTER II)

5.1 Aptian to Cenomanian

The variety of geodynamic models for the Iberia-Eurasia plate boundary involves different kinematic scenarios for the Pyrenean-Cantabrian tectonic evolution, a problem that has not been solved so far (Fig. I-14). The rift architecture of the Pyrenean-Cantabrian junction strongly argues in favour of a NNE-SSW direction of extension from Aptian (or Late Aptian?) to Cenomanian. Indeed, rift basin depocenters and associated HT/LP metamorphic zones are aligned along a WNW-ESE orientation (Clerc et al., 2015) in relation with WNW-ESE striking rift structures such as the north-dipping South and North Mauléon detachments, Amotz fault and Barbarin/SPFT detachment faults (e.g. DeFelipe, 2017; Jammes et al., 2009; Masini et al., 2014; Razin, 1989). Moreover, the overlapping rift geometry can provide constrains for kinematics as suggested by analogue and numerical models. Indeed, the structural architecture at offset rift segments has been shown to be dependent on the obliquity of extension and therefore, overlapping systems preferentially develop in case of orthogonal or slightly oblique extension (Acocella, 2008; Zwaan et al., 2016).

This NNE-SSW direction of extension for the Aptian to Cenomanian rift event is in opposition with kinematic models constrained by restoration of the N-Atlantic margins based on the use of the M series magnetic anomalies (e.g. Nirrengarten et al., 2018) and argues against the strike-slip model proposed by Stampfli & Borel (2002). Moreover, this is in contradiction with the occurrence of any left-lateral displacements along the NPF at this time (Choukroune & Mattauer, 1978) or with lozenge-shaped or pull-apart Albo-Cenomanian basins such as proposed by authors (e.g. Canérot, 2017; Debroas, 1987; García-Mondejar, 1989; García-Mondéjar et al., 1996; Larrasoña et al., 2003b; Peybernès & Souquet, 1984).

5.2 Late Jurassic to Barremian

The kinematics of the Late Jurassic to Aptian rift event remains unconstrained. No clear basin bounding structures have been recognized in this work, except potentially the WNW-ESE to E-W Aralar and Barbarin reactivated faults. The NNE-SSW aligned salt diapirs (Estella-Pamplona and Mena-Poza de la Sal diapirs) might also belong to a set of fractures in relation with these basins as suggested in chapter II or by Feuillée & Rat (1971), but further

studies are necessary to investigate if these aligned diapirs initiated because they correspond to former Late Triassic depocenters, and/or if they are related to the Late Jurassic-Barremian or Aptian-Cenomanian rift structures.

Beyond local considerations, the analysis of the distribution of the Late Jurassic-Barremian basins between France and Spain depicts a very wide area perforated by non-connected basins and characterised by complex geometries (e.g. Cameros, Parentis, Columbret, Maestrat, Asturian). These basins are generally composed of a very thick syn-rift sedimentary successions deposited in shallow marine to continental environments (e.g. ~7km in Cameros, Omodeo-Salè et al., 2014; ~7km in the Asturian basin, Cadenas & Fernández-Viejo, 2017), which underwent no to low-grade syn-rift metamorphism (Omodeo-Salé et al., 2017). These characteristics are strongly contrasting with the Aptian-Cenomanian deep marine sediments deposited in narrow basins mostly located along the Pyrenean-Cantabrian corridor and affected by a syn-rift HT/LP metamorphism (Clerc et al., 2015; Ravier, 1959). Such a contrasting tectonic pattern might reflect a different kinematic framework during the Late Jurassic to Aptian, potentially in relation with the left-lateral motion of Iberia.

6. GENERAL IMPLICATIONS (CHAPTERS II, III AND IV)

6.1 Reactivation of segmented rift systems

The analysis of the deformation in the Pyrenean-Cantabrian system reveals that two phases can be distinguished during the reactivation of hyperextended rift systems in general (e.g. Mohn et al., 2014; Mouthereau et al., 2014). The subduction phase reactivates the hyperextended domain, i.e. basinward of the coupling point, while the collisional phase corresponds to the collision of conjugate necking and proximal domains located landward of the coupling point, and leading to the formation of an orogenic wedge. The latter is mostly governed by orogenic processes resulting in the formation of new structures, well recorded in collisional systems. However, the subduction phase consists of the reactivation and inversion of rift structures and to the subduction of former distal domains. As such, this phase might not be identifiable nor recorded in orogens. This overall evolution shows that inheritance is important during the first phase of deformation but becomes marginal once the system becomes mature. Such relative control of inheritance through time has also been suggested during extension in relation with the formation of the hyperextended domain, i.e. basinward of the coupling point (Manatschal et al., 2015).

Nevertheless, this evolution is likely to be hampered when dealing with 3D systems where the along-strike architecture can juxtapose different rift domains. At these rift segment boundaries, tectonic inversion may lead to anomalous architecture in relation with shortcutting structures (e.g. Likerman et al., 2013). Moreover, structures identified in 2D rift segments can laterally evolve due to structural reorganisation (e.g. thin- to thick-skinned thrust faults), making difficult their recognition in the field. Furthermore, in mature orogenic systems, segmentation and inheritance can be overprinted by collisional structures leading, at a first order, to a cylindrical orogenic architecture. This final orogenic architecture is very well reproduced by numerical models even for those assuming pre-convergence rift-inheritance (e.g. Jammes et al., 2014). However, they fail in representing intermediate stages where inheritance and along-strike segmentation can strongly influence the deformation such as proposed at the Pyrenean-Cantabrian junction for the subduction phase.

6.2 Thermal state of hyperextended rift systems (Question F)

The McKenzie model predicts that the top basement heat flow can be defined by a crustal stretching factor (β). However, when mantle is exhumed to the seafloor (Boillot et al., 1987), the β -factor is infinite and as such the McKenzie model cannot be used for hyperextended domains. Besides, results of this manuscript show that lithospheric evolution can be strongly asymmetric, so is the maximum top basement heat flow, located at the upper-lower plate transition. During rift migration (Brune et al., 2014), extensional allochthons and associated pre- to syn-tectonic sediments will be transported from the upper to the lower plate and as such may diachronously record T_{\max} associated with this transient thermal event. Once on the lower plate, syn- to post-tectonic sediments can be deposited onto the extensional allochthon and may lead to the juxtaposition of diachronous and abrupt variation of T_{\max} values. As such, an asymmetric thermal and structural evolution may lead to a complex thermal architecture, especially in sediment starved systems, where sediment burial is less likely to overprint the syn-rift thermal history. T_{\max} from various thermal events can eventually be superposed on a vertical section in relation with extensional allochthons and may lead to define erroneous paleo-thermal gradients in 1D models. As such, single T_{\max} values should not be extrapolated to assess the syn-rift thermal gradient of a basin, and the evolution of the base lithosphere (the 1300°C isotherm) has to be taken into account to understand the thermal evolution of a hyperextended rift basin.

CONCLUSION

The aim of this PhD was to investigate: 1) the architecture of the Pyrenean-Cantabrian junction, 2) the orogenic evolution associated with the reactivation of rift segment boundaries, and 3) the thermal evolution of asymmetric hyperextended rift systems. The Pyrenean-Cantabrian system represents a natural laboratory to explore the questions of segmentation, reactivation and thermal evolution in rift systems as it benefits from datasets collected over decades and active ongoing research in the Pyrenees.

The main results of this PhD thesis can be summarized as follow:

1. ARCHITECTURE OF THE PYRENEAN-CANTABRIAN JUNCTION

- Geological cross-sections and seismic interpretations across the Pyrenean-Cantabrian junction allow to discard the existence of a major NNE-SSW Pamplona transform fault across the Basque massifs. Instead, the structural pattern depicts a wide accommodation zone characterised by overlapping rift systems north and south of the Basque massifs during Aptian to Cenomanian time.
- The WNW-ESE striking extensional structures and depocenters, together with the overlapping geometry, strongly argue for NNE-SSW direction of extension during Aptian (or Late Aptian?) to Cenomanian, providing kinematic constrains for the Iberia-Eurasia plate boundary at mid-Cretaceous. In the same time, it undermines any displacement along the NPF for this time laps.
- The Upper Triassic evaporites strongly decoupled the deformation between the crust (thick-skinned) and the supra-salt sedimentary cover (thin-skinned), allowing to transport the basins over the thick proximal domains.
- The overall N-S crustal architecture across the Pyrenean-Cantabrian junction depicts an orogenic wedge, represented by the Basque massifs, overlying the Eurasian and Iberian (Ebro) plates, and a subducting slab composed of the hyperextended domain of the former BCB.

2. REACTIVATION OF THE PYRENEAN AND CANTABRIAN RIFT SEGMENT BOUNDARIES

- Rift domain and structural mapping as well as geological cross-sections from the Cantabrian to the Pyrenean segments allow to characterise the transfer of the deformation from one segment to the other. At rift segments (eastern Mauléon and central BCB), two phases of deformation have been recognized. The subduction phase (Santonian to Paleocene),

controlled by rift inheritance, reactivated the rift structures via the northward subduction of the hyperextended domain (thin-skin tectonics). Once the conjugate coupling points meet (necking domains), the collisional phase initiated (Eocene to Miocene), governed by orogenic processes, and led to the formation of new thick-skinned structures and to the development of an orogenic wedge.

- At the V-shaped termination of rift segment boundaries, new shortcutting faults (thick-skinned) formed during the subduction phase to transfer the shortening from one segment to the other (Roncesvalles fault and NPFT). They are responsible for the formation of a proto-orogenic wedge composed of the Basque massifs. The Saison transfer fault is assumed to accommodate the change from north-dipping underthrusting in the Eastern Mauléon basin to south-dipping in the Western Mauléon basin.

- The formation of a precursor orogenic wedge is proposed to be responsible for the emplacement at crustal level of subcontinental mantle rocks and the preservation of pre-Alpine structures at the Pyrenean-Cantabrian junction.

- Despite a strongly segmented syn-rift architecture, the final orogenic architecture depicts an unique orogenic wedge from the Central Pyrenean to the Central Cantabrian segments.

3. THERMAL EVOLUTION OF ASYMMETRIC HYPEREXTENDED RIFT SYSTEMS

- Thermo-mechanical model of asymmetric rifting and thermal data (%VR) from the Mauléon basin allow to investigate the thermal evolution of asymmetric hyperextended systems. Both the Pyrenean analogue and the numerical model show that asymmetric rifting led to asymmetric heat distribution, the highest T_{\max} and maximum top basement heat flow being located at the upper-lower plate transition.

- Numerical models show that the peak top basement heat flow is diachronous for extensional allochthons as they migrate from the upper to the lower plate during rift migration. It suggests that high T_{\max} can be recorded at the upper-lower plate transition and transported onto the lower plate.

- This study shows that the use of single T_{\max} values to define the thermal architecture (e.g. paleo-thermal gradient) may lead to erroneous results in complex diachronous and allochthonous extensional settings.

This manuscript shows that the thermal state of rift systems may be influenced by the structural evolution. Such results would require to be tested in present-day asymmetric rifted margins such as the Iberia-Newfoundland or the Labrador-West Greenland passive margins.

Besides, this study highlights the role of rift segmentation for the reactivation pattern. The reactivation of accommodation and transfer zones should be tested in numerical models in order to constrain the timing of deformation and the implication for the orogenic architecture. It could allow to identify criteria that are representative of inverted rift segments and help recognise them in field analogues (e.g. Alps, Taiwan, Caledonides).

OUTLOOKS

The following sections indicate some of the questions and research projects that come out from the results of my PhD and that will be undertaken during my postdoctoral research.

1. ARCHITECTURE OF THE CANTABRIAN-PYRENEAN RIFT JUNCTION FROM SEISMIC TOMOGRAPHY

This study partly highlights how along-strike deformation was accommodated across the Pyrenean-Cantabrian junction based on N-S seismic sections together with subsurface data and field observations. However, further and deeper constrains on the lateral continuation of structures identified at the surface could help understand their role for the orogenic evolution and their relationship with inheritance. Seismic tomography has revealed to represent a powerful tool to study the crustal architecture of the Pyrenees (e.g. Chevrot et al., 2015, 2018; Wang et al., 2016) thanks to the deployment of a dense network of seismological stations (PYROPE and IBERARRAY; Chevrot et al., 2014). As such, new profiles and/or map sections across the Basque Country may provide outcomes on the crustal architecture between the Pyrenean and Cantabrian segments.

2. FORMATION AND REACTIVATION OF OVERLAPPING RIFT SYSTEMS: STRUCTURAL AND THERMAL RESULTS FROM NUMERICAL MODELLING?

This manuscript highlights an anomalous structural and compositional architecture towards rift segment boundaries such as the emplacement of subcontinental mantle at crustal levels and the switch in the dip of the underthrusting direction during the subduction phase responsible for the preservation of the pre-orogenic structures. However, the processes going on during extension and reactivation of overlapping rift systems remain poorly known and might not be understood from field analysis alone. Numerical models testing the formation of overlapping rift systems have shown that various structural evolutions can occur in accommodation/transfer zones (Allken et al., 2013; Le Pourhiet et al., 2017; Zwaan et al., 2016). In particular, Le Pourhiet et al. (2017) showed that for weak lower crustal rocks (e.g. sedimentary rocks), the lower crust can be re-mobilized at transfer zones and may spread to accommodate hyperextension. Such models provide new thermal and structural constrains on the evolution of rift segments and should be tested for reactivation in order to determine the role of thermal and structural inheritance for the architecture of subsequent orogenic belts. This might also provide new models to explain the present-day architecture of the Basque Country and the exhumation of the granulite rocks.

3. COMBINING GEOPHYSICAL METHODS AND GEOLOGICAL OBSERVATIONS TO ASSESS THE ROLE OF RIFT SEGMENTATION AND RIFT POLARITY ON THE PYRENEAN OROGENIC ARCHITECTURE (IN PREP.)

The chapters II and III highlight the role of rift segmentation for the reactivation while chapter IV shows the importance of rift asymmetry on the rift architecture with the development of a wide lower plate and a sharp upper plate (rift polarity). However, little is known about how the along-strike change in the rift polarity may influence the reactivation pattern and the final orogenic architecture. The Pyrenean-Cantabrian system has been shown to represent such along-strike variation of the rift polarity (Tugend et al., 2014) as well as along-strike variation of the orogenic architecture (Chevrot et al., 2018) where both seem to occur in the Central Pyrenees. Combining tomographic and magnetic methods (see Annexes 6) together with geological cross-sections might help decipher the role of upper-lower plate architecture on the orogenic architecture.

4. GEODYNAMIC EVOLUTION OF IBERIA, EBRO AND EURASIA DURING THE MESOZOIC

The structural evolution of the Basque-Cantabrian junction provides kinematic constrains for the Iberia – Eurasia plate boundary, arguing for NNE-SSW direction of extension during the Aptian to Cenomanian. This implies that part of the lateral displacement of Iberia has to occur before Aptian or away from the Pyrenean and Cantabrian segments. The latter solution has been partly proposed by Nirrengarten et al. (2018) who suggested that part of the strike-slip component was accommodated along the Iberian range, i.e. south of the Ebro block. The former solution, proposed by Jammes et al. (2009) and Tugend et al. (2015), involves either localised or diffuse deformation from Late Jurassic to Barremian in relation with the opening of the southern North Atlantic. Considering the recent work of Tavani et al. (2018), involving mostly NNE-SSW extension from Late Jurassic to Cenomanian, the left-lateral displacement would have occurred before Late Jurassic (Late Triassic rifting?) or not at all. In any case, these results need to be integrated in geodynamic models and be confronted again to geological observations.

5. THERMAL STATE OF RIFT SYSTEMS PRIOR TO REACTIVATION

The chapter IV highlights the asymmetric top basement heat flow evolution in relation with asymmetric hyperextension. The results show that the crust of the upper plate can suffer high geothermal gradient and can behave ductile in comparison to the lower plate. In case of

tectonic inversion, this thermal and rheological state might control the reactivation pattern and the architecture of the subsequent orogen. As such, future models should be performed in order to test the role of asymmetric structural and thermal evolution during reactivation and their influence on the final orogenic architecture.

6. CRUSTAL THINNING DURING MID-CRETACEOUS RIFTING: WHAT IS THE CONTROLLING FACTOR?

Restored cross-sections of chapter III indicate that the syn-rift architecture of the BCB and Mauléon basin was characterised by abrupt crustal thinning resulting in a zone of necking and hyperextension that was about 60km wide, which is short in comparison to the world average of magma-poor passive margins that is ~170km wide (Chenin et al., 2017). However, the reasons for such abruptness have been only little investigated (Jammes et al., 2009; 2010b). As such, future research should focus on scenarios to explain such abrupt crustal thinning:

- Oblique extension has been shown to strongly localised deformation during extension (Brune et al., 2012). This manuscript shows that only little strike-slip component may have occurred during Albo-Cenomanian hyperextension at the Pyrenean-Cantabrian junction. However, little is known about the pre-Aptian kinematics.

- Thin and brittle crust favours rheological coupling and as such mantle exhumation (e.g. Jammes et al., 2014). This brittle-governed mode of deformation contrasts with models for the Pyrenees involving ductile-governed crustal extension (e.g. Clerc & Lagabrielle, 2014; Corre, 2017; Lagabrielle et al., 2016). Indeed, the latter implies very wide crustal domains and can barely reach mantle exhumation (Brune et al., 2017). However, despite brittle deformation has been attested in the study area, the large occurrence of meta-sediments constituting the Pyrenean-Cantabrian crust would rather favor intra-crustal decoupling in weak horizons (e.g. Silurian black schists; Clerc et al., 2016) and as such cannot solely explain the narrow Pyrenean basins.

- Inheritance has been shown to weaken the crust and localize the deformation (Ziegler & Cloetingh, 2004). In the Pyrenees, inherited features such as the Late Variscan NPF or related strike-slip structures have been proposed to represent such weakness that could be used to localize deformation during Albo-Cenomanian hyperextension (e.g. Cochelin et al., 2018; Jammes et al., 2010a). However, such structure may not have existed in the eastern BCB or in some parts of the North Pyrenean Zone where the NPF or pre-Aptian structures have not been clearly identified.

REFERENCES

A

- Ábalos, B. (2016). Geologic map of the Basque-Cantabrian Basin and a new tectonic interpretation of the Basque Arc. *International Journal of Earth Sciences*, 1–28. <https://doi.org/10.1007/s00531-016-1291-6>
- Ábalos, B., Alkorta, A., & Iríbar, V. (2008). Geological and isotopic constraints on the structure of the Bilbao anticlinorium (Basque–Cantabrian basin, North Spain). *Journal of Structural Geology*, 30(11), 1354–1367. <https://doi.org/10.1016/j.jsg.2008.07.008>
- Acocella, V. (2008). Transform faults or Overlapping Spreading Centers? Oceanic ridge interactions revealed by analogue models. *Earth and Planetary Science Letters*, 265(3–4), 379–385. <https://doi.org/10.1016/j.epsl.2007.10.025>
- Acocella, V., Morvillo, P., & Funicello, R. (2005). What controls relay ramps and transfer faults within rift zones? Insights from analogue models. *Journal of Structural Geology*, 27(3), 397–408. <https://doi.org/10.1016/j.jsg.2004.11.006>
- Aguilar, C., Liesa, M., Castiñeiras, P., & Navidad, M. (2014). Late Variscan metamorphic and magmatic evolution in the eastern Pyrenees revealed by U–Pb age zircon dating. *Journal of the Geological Society*, 171(2), 181–192. <https://doi.org/10.1144/jgs2012-086>
- Albarède, F., & Michard-Vitrac, A. (1978). Age and significance of the North Pyrenean metamorphism. *Earth and Planetary Science Letters*, 40(3), 327–332. [https://doi.org/10.1016/0012-821X\(78\)90157-7](https://doi.org/10.1016/0012-821X(78)90157-7)
- Aller, J., & Zeyen, H. J. (1996). A 2.5-D interpretation of the Basque country magnetic anomaly (northern Spain): geodynamical implications. *Geologische Rundschau*, 85(2), 303–309. <https://doi.org/10.1007/BF02422236>
- Allken, V., Huismans, R. S., & Thieulot, C. (2012). Factors controlling the mode of rift interaction in brittle-ductile coupled systems: A 3D numerical study. *Geochemistry Geophysics Geosystems*, 13. <https://doi.org/10.1029/2012GC004077>
- Allken, V., Huismans, R. S., Fossen, H., & Thieulot, C. (2013). 3D numerical modelling of graben interaction and linkage: a case study of the Canyonlands grabens, Utah. *Basin Research*, 25(4), 436–449. <https://doi.org/10.1111/bre.12010>
- Alonso, J., Pulgar, J., García-Ramos, J., & Barba, P. (1996). W5 Tertiary basins and Alpine tectonics in the Cantabrian Mountains (NW Spain). *Tertiary Basins of Spain: The Stratigraphic Record of Crustal Kinematics*.
- Alves, T. M., Moita, C., Cunha, T., Ullnaess, M., Myklebust, R., Monteiro, J. H., & Manuppella, G. (2009). Diachronous evolution of Late Jurassic–Cretaceous continental rifting in the northeast Atlantic (west Iberian margin). *Tectonics*, 28(4), n/a-n/a. <https://doi.org/10.1029/2008TC002337>
- Amiot, M. (1982). El Cretácico superior de la región Navarro-Cántabra. *El Cretácico de España*, 88–111.
- Andersen, T. B., Corfu, F., Labrousse, L., & Osmundsen, P.-T. (2012). Evidence for hyperextension along the pre-Caledonian margin of Baltica. *Journal of the Geological Society*, 169(5), 601–612. <https://doi.org/10.1144/0016-76492012-011>
- Anonymous. (1972). Penrose field conference on ophiolites. *Geotimes*, 17(12), 24–25.
- Arche, A., & López-Gómez, J. (1996). Origin of the Permian-Triassic Iberian Basin, central-eastern Spain. *Tectonophysics*, 266(1–4), 443–464. [https://doi.org/10.1016/S0040-1951\(96\)00202-8](https://doi.org/10.1016/S0040-1951(96)00202-8)
- Arthaud, F., & Matte, P. (1975). Les décrochements tardi-hercyniens du sud-ouest de l'Europe. *Geometrie et essai de reconstitution des conditions de la deformation*. *Tectonophysics*, 25(1–2), 139–171. [https://doi.org/10.1016/0040-1951\(75\)90014-1](https://doi.org/10.1016/0040-1951(75)90014-1)
- Arthaud, F., & Matte, P. (1977). Late Paleozoic strike-slip faulting in southern Europe and northern Africa: Result of a right-lateral shear zone between the Appalachians and the Urals. *GSA Bulletin*, 88(9), 1305–1320. [https://doi.org/10.1130/0016-7606\(1977\)88<1305:LPSFIS>2.0.CO;2](https://doi.org/10.1130/0016-7606(1977)88<1305:LPSFIS>2.0.CO;2)
- Aurell, M., Robles, S., Bádenas, B., Rosales, I., Quesada, S., Meléndez, G., & García-Ramos, J. (2003). Transgressive–regressive cycles and Jurassic palaeogeography of northeast Iberia. *Sedimentary Geology*, 162(3–4), 239–271. [https://doi.org/10.1016/S0037-0738\(03\)00154-4](https://doi.org/10.1016/S0037-0738(03)00154-4)
- Autin, J., Leroy, S., Beslier, M.-O., D'Acremont, E., Razin, P., Ribodetti, A., et al. (2010). Continental break-up history of a deep magma-poor margin based on seismic reflection data (northeastern Gulf of Aden margin, offshore Oman). *Geophysical Journal International*, 180(2), 501–519. <https://doi.org/10.1111/j.1365-246X.2009.04424.x>
- Autran, A., Carreras, J., Durand-Delga, M., & Laumonier, B. (1996). Le cycle Hercynien dans les Pyrénées. *Réflexions géodynamiques finales*. *Synthèse Géologique et Géophysique Des Pyrénées*, 1, 679–693.

- Azambre, B., & Monchoux, P. (1998). Métagabbros amphiboliques et mise en place crustale des lherzolites des Pyrénées (France). *Comptes Rendus de l'Académie Des Sciences - Series IIA - Earth and Planetary Science*, 327(1), 9–15. [https://doi.org/10.1016/S1251-8050\(98\)80012-8](https://doi.org/10.1016/S1251-8050(98)80012-8)
- Azambre, B., & Rossy, M. (1976). Le magmatisme alcalin d'âge cretace, dans les Pyrenees occidentales et l'Arc basque; ses relations avec le metamorphisme et la tectonique. *Bulletin de La Societe Geologique de France*, S7-XVIII(6), 1725. <https://doi.org/10.2113/gssgfbull.S7-XVIII.6.1725>

B

- Baby, P., Crouzet, G., Specht, M., Déramond, J., Bilotte, M., & Debroas, E. (1988). Rôle des paléostructures albo-cénomaniennes dans la géométrie des chevauchements frontaux nord-pyrénéens. *Comptes Rendus de l'Académie Des Sciences. Série 2, Mécanique, Physique, Chimie, Sciences de l'univers, Sciences de La Terre*, 306(4), 307–313.
- Ballèvre, M., Martínez Catalán, J. R., López-Carmona, A., Pitra, P., Abati, J., Fernández, R. D., et al. (2014). Correlation of the nappe stack in the Ibero-Armorican arc across the Bay of Biscay: a joint French–Spanish project. *Geological Society, London, Special Publications*, 405(1), 77–113. <https://doi.org/10.1144/SP405.13>
- Barnett-Moore, N., Hosseinpour, M., & Maus, S. (2016a). Assessing discrepancies between previous plate kinematic models of Mesozoic Iberia and their constraints. *Tectonics*, 35(8), 1843–1862. <https://doi.org/10.1002/2015TC004019>
- Barnett-Moore, Nicholas, Müller, D. R., Williams, S., Skogseid, J., & Seton, M. (2016b). A reconstruction of the North Atlantic since the earliest Jurassic. *Basin Research*. <https://doi.org/10.1111/bre.12214>
- Barnolas, A., & Pujalte, V. (2004). La Cordillera Pirenaica. *Geología de España*, 233–241.
- Barr, T. D., & Dahlen, F. A. (1989). Brittle frictional mountain building: 2. Thermal structure and heat budget. *Journal of Geophysical Research: Solid Earth*, 94(B4), 3923–3947. <https://doi.org/10.1029/JB094iB04p03923>
- Basile, C. (2015). Transform continental margins — part 1: Concepts and models. *Tectonophysics*, 661, 1–10. <https://doi.org/10.1016/j.tecto.2015.08.034>
- Bassi, G. (1991). Factors controlling the style of continental rifting: insights from numerical modeling. *Earth and Planetary Science Letters*, 105(4), 430–452. [https://doi.org/10.1016/0012-821X\(91\)90183-I](https://doi.org/10.1016/0012-821X(91)90183-I)
- Bassi, G., Keen, C. E., & Potter, P. (1993). Contrasting styles of rifting: Models and examples from the Eastern Canadian Margin. *Tectonics*, 12(3), 639–655. <https://doi.org/10.1029/93TC00197>
- Beauchamp, W. (2004). Superposed folding resulting from inversion of a synrift accommodation zone, Atlas Mountains, Morocco. In *Thrust tectonics and hydrocarbon systems* (Vol. 82, pp. 635–646). McClay, K.R.
- Beaumont, C., Muñoz, J. A., Hamilton, J., & Fullsack, P. (2000). Factors controlling the Alpine evolution of the central Pyrenees inferred from a comparison of observations and geodynamical models. *Journal of Geophysical Research: Solid Earth*, 105(B4), 8121–8145. <https://doi.org/10.1029/1999JB900390>
- Belgarde, C., Manatschal, G., Kuszniir, N., Scarselli, S., & Ruder, M. (2015). Rift processes in the West-Australian Superbasin, North West Shelf, Australia: insights from 2D deep reflection seismic interpretation and potential fields modelling. *The APPEA Journal*, 55(2), 400. <https://doi.org/10.1071/AJ14035>
- Bellahsen, N., Leroy, S., Autin, J., Razin, P., d'Acremont, E., Sloan, H., et al. (2013). Pre-existing oblique transfer zones and transfer/transform relationships in continental margins: New insights from the southeastern Gulf of Aden, Socotra Island, Yemen. *Tectonophysics*, 607, 32–50. <https://doi.org/10.1016/j.tecto.2013.07.036>
- Beltrando, M., Manatschal, G., Mohn, G., Dal Piaz, G. V., Vitale Brovarone, A., & Masini, E. (2014). Recognizing remnants of magma-poor rifted margins in high-pressure orogenic belts: The Alpine case study. *Earth-Science Reviews*, 131, 88–115. <https://doi.org/10.1016/j.earscirev.2014.01.001>
- Beltrando, M., Stockli, D. F., Decarlis, A., & Manatschal, G. (2015). A crustal-scale view at rift localization along the fossil Adriatic margin of the Alpine Tethys preserved in NW Italy. *Tectonics*, 34(9), 1927–1951. <https://doi.org/10.1002/2015TC003973>
- Benmakhlof, M., Galindo-Zaldívar, J., Chalouan, A., Sanz de Galdeano, C., Ahmamou, M., & López-Garrido, A. C. (2012). Inversion of transfer faults: The Jebha–Chrafate fault (Rif, Morocco). *Journal of African Earth Sciences*, 73–74, 33–43. <https://doi.org/10.1016/j.jafrearsci.2012.07.003>
- Bernus Maury, C. (1984). Etude des paragéneses caractéristiques du métamorphisme mésozoïque dans

- la partie orientale des Pyrénées.
- Biteau, J.-J., Le Marrec, A., Le Vot, M., & Masset, J.-M. (2006). The Aquitaine Basin. *Petroleum Geoscience*, 12(3), 247–273. <https://doi.org/10.1144/1354-079305-674>
- Bixel, F., & Lucas, C. (1983). Magmatisme, tectonique et sédimentation dans les fossés stéphano-permiens des Pyrénées occidentales. *Revue de Géologie Dynamique et de Géographie Physique*, 24(4), 329–342.
- Bixel, F., & Lucas, C. (1987). Approche géodynamique du Permien et du Trias des Pyrénées dans le cadre du Sud-Ouest Européen. *Cuadernos de Geología Ibérica= Journal of Iberian Geology: An International Publication of Earth Sciences*, (11), 57–82.
- Bixel, François. (1984). Le volcanisme stéphano-permien des Pyrénées. Université Paul Sabatier, Département de Géologie, Petrologie, Géologie
- Blaich, O. A., Faleide, J. I., & Tsikalas, F. (2011). Crustal breakup and continent-ocean transition at South Atlantic conjugate margins. *Journal of Geophysical Research: Solid Earth*, 116(B1).
- Bodego, A., & Agirrezabala, L. M. (2017). The Andatza coarse-grained turbidite system (westernmost Pyrenees): Stratigraphy, sedimentology and structural control. *Estudios Geológicos*, 73(1), 3.
- Bodego, Arantxa, Iriarte, E., Agirrezabala, L. M., García-Mondéjar, J., & López-Horgue, M. A. (2015). Synextensional mid-Cretaceous stratigraphic architecture of the eastern Basque–Cantabrian basin margin (western Pyrenees). *Cretaceous Research*, 55(Supplement C), 229–261. <https://doi.org/10.1016/j.cretres.2015.01.006>
- Boess, J., & Hoppe, A. (1986). Mesozoischer Vulkanismus in Nordspanien: Rifting im Keuper und Kreide-Vulkanismus auf Transform-Störungen? *Geologische Rundschau*, 75(2), 353–369. <https://doi.org/10.1007/BF01820617>
- Boillot, G. (1984). Some remarks on the continental margins in the Aquitaine and French Pyrenees. *Geological Magazine*, 121(05), 407. <https://doi.org/10.1017/S0016756800029939>
- Boillot, G., & Capdevila, R. (1977). The Pyrenees: Subduction and collision? *Earth and Planetary Science Letters*, 35(1), 151–160. [https://doi.org/10.1016/0012-821X\(77\)90038-3](https://doi.org/10.1016/0012-821X(77)90038-3)
- Boillot, G., Recq, M., Winterer, E. L., Meyer, A. W., Applegate, J., Baltuck, M., et al. (1987). Tectonic denudation of the upper mantle along passive margins: a model based on drilling results (ODP leg 103, western Galicia margin, Spain). *Tectonophysics*, 132(4), 335–342. [https://doi.org/10.1016/0040-1951\(87\)90352-0](https://doi.org/10.1016/0040-1951(87)90352-0)
- Boirie, J., & Souquet, P. (1982). Les poudingues de Mendibelza: dépôts de cônes sous-marins du rift albien des Pyrénées. *Bull. Cent. Rech. Explor. Prod. Elf Aquitaine*, 6(2), 405–435.
- Bois, C., Gariel, O., Lefort, J.-P., Rolet, J., & Brunet, F. (1997). Geologic contribution of the Bay of Biscay deep seismic survey: a summary of the main scientific results, a discussion of the open questions.
- Bosch, G., Teixell, A., Jolivet, M., Labaume, P., Stockli, D., Domènech, M., & Monié, P. (2016). Timing of Eocene–Miocene thrust activity in the Western Axial Zone and Chaînon Béarnais (west-central Pyrenees) revealed by multi-method thermochronology. *Comptes Rendus Geoscience*, 348(3–4), 246–256. <https://doi.org/10.1016/j.crte.2016.01.001>
- Boulvais, P. (2016). Fluid generation in the Boucheville Basin as a consequence of the North Pyrenean metamorphism. *From Rifting to Mountain Building: The Pyrenean Belt*, 348(3), 301–311. <https://doi.org/10.1016/j.crte.2015.06.013>
- Bouroullac, J., Delfaud, J., & Deloffre, R. (1979). Organisations sédimentaire et paléocologique de l’Aptien supérieur à faciès urgonien dans les Pyrénées occidentales et l’Aquitaine méridionale. *Geobios*, 12, 25–43. [https://doi.org/10.1016/S0016-6995\(79\)80048-0](https://doi.org/10.1016/S0016-6995(79)80048-0)
- BRGM. (1963). Notice explicative de la feuille Bayonne à 1/50 000 (1001). Éditions Du Bureau de Recherches Géologiques et Minières, Orléans, 1–16.
- Brinkmann, R., & Logters, H. (1968). Diapirs in Western Pyrenees and Foreland, Spain, 153, 275–292.
- Bronner, A., Sauter, D., Manatschal, G., Péron-Pinvidic, G., & Munschy, M. (2011). Magmatic breakup as an explanation for magnetic anomalies at magma-poor rifted margins. *Nature Geoscience*, 4, 549.
- Brune, S. (2014). Evolution of stress and fault patterns in oblique rift systems: 3-D numerical lithospheric-scale experiments from rift to breakup. *Geochemistry, Geophysics, Geosystems*, 15(8), 3392–3415. <https://doi.org/10.1002/2014GC005446>
- Brune, S., Popov, A. A., & Sobolev, S. V. (2012). Modeling suggests that oblique extension facilitates rifting and continental break-up: OBLIQUE EXTENSION FACILITATES RIFTING AND BREAK-UP. *Journal of Geophysical Research: Solid Earth*, 117(B8), n/a-n/a. <https://doi.org/10.1029/2011JB008860>

- Brune, S., Popov, A. A., & Sobolev, S. V. (2013). Quantifying the thermo-mechanical impact of plume arrival on continental break-up. *Progress in Understanding the South Atlantic Margins*, 604(Supplement C), 51–59. <https://doi.org/10.1016/j.tecto.2013.02.009>
- Brune, S., Heine, C., Pérez-Gussinyé, M., & Sobolev, S. V. (2014). Rift migration explains continental margin asymmetry and crustal hyper-extension. *Nature Communications*, 5, 4014. <https://doi.org/10.1038/ncomms5014>
- Brune, S., Williams, S. E., Butterworth, N. P., & Müller, R. D. (2016). Abrupt plate accelerations shape rifted continental margins. *Nature*, 536, 201.
- Brune, S., Heine, C., Clift, P. D., & Pérez-Gussinyé, M. (2017). Rifted margin architecture and crustal rheology: Reviewing Iberia-Newfoundland, Central South Atlantic, and South China Sea. *Marine and Petroleum Geology*, 79(Supplement C), 257–281. <https://doi.org/10.1016/j.marpetgeo.2016.10.018>
- Brune, S., Williams, S. E., & Müller, R. D. (2018). Oblique rifting: the rule, not the exception. *Solid Earth*, 9(5), 1187–1206. <https://doi.org/10.5194/se-9-1187-2018>
- Brunet, M.-F. (1984). Subsidence history of the Aquitaine basin determined from subsidence curves. *Geological Magazine*, 121(5), 421–428.
- Bubeck, A., Walker, R. J., Imber, J., Holdsworth, R. E., MacLeod, C. J., & Holwell, D. A. (2017). Extension parallel to the rift zone during segmented fault growth: application to the evolution of the NE Atlantic. *Solid Earth*, 8(6), 1161–1180. <https://doi.org/10.5194/se-8-1161-2017>
- Buck, W. R., Martinez, F., Steckler, M. S., & Cochran, J. R. (1988). Thermal consequences of lithospheric extension: Pure and simple. *Tectonics*, 7(2), 213–234. <https://doi.org/10.1029/TC007i002p00213>
- Buiter, S. J. H., & Pfiffner, O. A. (2003). Numerical models of the inversion of half-graben basins: INVERSION OF HALF-GRABEN BASINS. *Tectonics*, 22(5), n/a-n/a. <https://doi.org/10.1029/2002TC001417>
- Burbank, D. W., Puigdefàbregas, C., & Muñoz, J. A. (1992). The chronology of the Eocene tectonic and stratigraphic development of the eastern Pyrenean foreland basin, northeast Spain. *Geological Society of America Bulletin*, 104(9), 1101–1120. [https://doi.org/10.1130/0016-7606\(1992\)104<1101:TCOTET>2.3.CO;2](https://doi.org/10.1130/0016-7606(1992)104<1101:TCOTET>2.3.CO;2)
- Burg, J.-P., & Gerya, T. V. (2005). The role of viscous heating in Barrovian metamorphism of collisional orogens: thermomechanical models and application to the Lepontine Dome in the Central Alps. *Journal of Metamorphic Geology*, 23(2), 75–95. <https://doi.org/10.1111/j.1525-1314.2005.00563.x>
- Burg, J.-P., Van Den Driessche, J., & Brun, J.-P. (1994). Syn- to post-thickening extension: mode and consequences. *Comptes Rendus de l'Académie Des Sciences. Série 2. Sciences de La Terre et Des Planètes*, 319(9), 1019–1032.
- Busch, J. P., Mezger, K., & van der Pluijm, B. A. (1997). Suturing and extensional reactivation in the Grenville orogen, Canada. *Geology*, 25(6), 507. [https://doi.org/10.1130/0091-7613\(1997\)025<0507:SAERIT>2.3.CO;2](https://doi.org/10.1130/0091-7613(1997)025<0507:SAERIT>2.3.CO;2)
- Butler, R. W. H., Tavarnelli, E., & Grasso, M. (2006). Structural inheritance in mountain belts: An Alpine–Apennine perspective. *Journal of Structural Geology*, 28(11), 1893–1908. <https://doi.org/10.1016/j.jsg.2006.09.006>

C

- Cadenas, P., & Fernández-Viejo, G. (2017). The Asturian Basin within the North Iberian margin (Bay of Biscay): seismic characterisation of its geometry and its Mesozoic and Cenozoic cover. *Basin Research*, 29(4), 521–541. <https://doi.org/10.1111/bre.12187>
- Calassou, S., Larroque, C., & Malavieille, J. (1993). Transfer zones of deformation in thrust wedges: An experimental study. *Tectonophysics*, 221(3), 325–344. [https://doi.org/10.1016/0040-1951\(93\)90165-G](https://doi.org/10.1016/0040-1951(93)90165-G)
- Callies, M., Filleaudeau, P.-Y., Lorant, M., & Peters, F. (2018). How to predict thermal stress in hyperextended margins: Application of a new lithospheric model on the Iberia margin. *AAPG Bulletin*, 102(04), 563–585. <https://doi.org/10.1306/07111716116>
- Camara, P. (1997). The Basque-Cantabrian basin's Mesozoic tectono-sedimentary evolution. *Mémoires de La Société Géologique de France*, 171, 187–191.
- Cámara, P., & Klimowitz, J. (1985). Interpretación geodinámica de la vertiente centro-occidental surpirenaica (cuencas de Jaca-Tremp). *Estudios Geológicos*, 41(5–6), 391. <https://doi.org/10.3989/egeol.85415-6720>
- Campos, J. (1979). Estudio geológico del Pirineo vasco al W del río Bidasoa. *Munibe*, SC Aranzadi,

- 31(1–2), 3–139.
- Campos, J., & García-Dueñas, V. (1972). Mapa geológico de España E. 1:50.000, Serie MAGNA(Hoja de San Sebastián, 64).
- Campos, J., García-Dueñas, V., Lamolda, M. A., & Pujalte, V. (1972a). Mapa geológico de España E. 1:50.000, Serie MAGNA(Hoja de Irún, 41).
- Campos, J., García-Dueñas, V., Lamolda, M. A., & Pujalte, V. (1972b). Mapa geológico de España E. 1:50.000, Serie MAGNA(Hoja de Jaizquibel, 40).
- Canérot, J. (2016). The Iberian plate: myth or reality? *Boletín Geológico y Minero de España*, 127(2/3), 557–568.
- Canérot, J. (2017). The pull apart-type Tardets-Mauléon Basin, a key to understand the formation of the Pyrenees. *Bulletin de La Société Géologique de France*, 188(6), 35. <https://doi.org/10.1051/bsgf/2017198>
- Canerot, J., Peybernes, B., & Ciszak, R. (1978). Presence d'une marge meridionale a l'emplacement de la zone des chainons bearnais (Pyrenees basco-bearnaises). *Bulletin de La Société Géologique de France*, S7-XX(5), 673–676. <https://doi.org/10.2113/gssgfbull.S7-XX.5.673>
- Capote, R., Muñoz, J., Simón, J., Liesa, C., & Arlegui, L. (2002). Alpine tectonics I: the Alpine system north of the Betic Cordillera. *The Geology of Spain*, 367–400.
- Carbayo, A., del Valle, J., León, L., & Villalobos, L. (1972). Mapa geológico de España E. 1:50.000, Serie MAGNA(Hoja de Garralda, 116).
- Carbayo, A., León, L., & Villalobos, L. (1977). Mapa geológico de España E. 1:50.000, Serie MAGNA(Hoja de Gulina, 115).
- Carola, E., Tavani, S., Ferrer, O., Granado, P., Quintà, A., Butillé, M., & Muñoz, J. A. (2013). Along-strike extrusion at the transition between thin- and thick-skinned domains in the Pyrenean Orogen (northern Spain). *Geological Society, London, Special Publications*, 377(1), 119–140. <https://doi.org/10.1144/SP377.3>
- Carola i Molas, E. (2014). The transition between thin-to-thick-skinned styles of deformation in the Western Pyrenean Belt.
- Carrera, N., Muñoz, J. A., Sàbat, F., Mon, R., & Roca, E. (2006). The role of inversion tectonics in the structure of the Cordillera Oriental (NW Argentinean Andes). *Tectonic Inversion and Structural Inheritance in Mountain Belts*, 28(11), 1921–1932. <https://doi.org/10.1016/j.jsg.2006.07.006>
- Carreras, J., & Capella, I. (1994). Tectonic levels in the Palaeozoic basement of the Pyrenees: a review and a new interpretation. *Journal of Structural Geology*, 16(11), 1509–1524. [https://doi.org/10.1016/0191-8141\(94\)90029-9](https://doi.org/10.1016/0191-8141(94)90029-9)
- Casas, A., Kearey, P., Rivero, L., & Adam, C. R. (1997). Gravity anomaly map of the Pyrenean region and a comparison of the deep geological structure of the western and eastern Pyrenees. *Earth and Planetary Science Letters*, 150(1), 65–78. [https://doi.org/10.1016/S0012-821X\(97\)00087-3](https://doi.org/10.1016/S0012-821X(97)00087-3)
- Casas Sainz, A. M. (1993). Oblique tectonic inversion and basement thrusting in the Cameros Massif (Northern Spain). *Geodinamica Acta*, 6(3), 202–216. <https://doi.org/10.1080/09853111.1993.11105248>
- Castañares, L., & Robles, S. (2004). El vulcanismo del Albiense-Santonense en la Cuenca Vasco-Cantábrica. *Geología de España*, 306–308.
- Castañares, L. M., Robles, S., Gimeno, D., & Bravo, J. C. V. (2001). The Submarine Volcanic System of the Errigoiti Formation (Albian-Santonian of the Basque-Cantabrian Basin, Northern Spain): Stratigraphic Framework, Facies, and Sequences. *Journal of Sedimentary Research*, 71(2), 318–333. <https://doi.org/10.1306/080700710318>
- Casteras, M. (1949). Observations sur la structure du revêtement crétacé et nummulitique de la zone primaire axiale au sud de Larrau et de Sainte-Engrâce (Basses-Pyrénées). *Annales Hébert et Haug (Laboratoire Géologique de Paris)*, 7, 45–59.
- Chelalou, R., Nalpas, T., Bousquet, R., Prevost, M., Lahfid, A., Poujol, M., et al. (2016). New sedimentological, structural and paleo-thermicity data in the Boucheville Basin (eastern North Pyrenean Zone, France). *From Rifting to Mountain Building: The Pyrenean Belt*, 348(3), 312–321. <https://doi.org/10.1016/j.crte.2015.11.008>
- Chenin, P. (2016). Unravelling the impact of inheritance on the Wilson Cycle: A combined mapping and numerical modelling approach applied to the North Atlantic rift system.
- Chenin, P., Manatschal, G., Picazo, S., Müntener, O., Karner, G., Johnson, C., & Ulrich, M. (2017). Influence of the architecture of magma-poor hyperextended rifted margins on orogens produced by the closure of narrow versus wide oceans. *Geosphere*, 13(2), 559–576. <https://doi.org/10.1130/GES01363.1>

- Chevrot, S., Villaseñor, A., Sylvander, M., Benahmed, S., Beucler, E., Cougoulat, G., et al. (2014). High-resolution imaging of the Pyrenees and Massif Central from the data of the PYROPE and IBERARRAY portable array deployments. *Journal of Geophysical Research: Solid Earth*, 119(8), 6399–6420. <https://doi.org/10.1002/2014JB010953>
- Chevrot, S., Sylvander, M., Diaz, J., Ruiz, M., Paul, A., & Group, the P. W. (2015). The Pyrenean architecture as revealed by teleseismic P-to-S converted waves recorded along two dense transects. *Geophysical Journal International*, 200(2), 1096–1107. <https://doi.org/10.1093/gji/ggu400>
- Chevrot, S., Sylvander, M., Diaz, J., Martin, R., Mouthereau, F., Manatschal, G., et al. (2018). The non-cylindrical crustal architecture of the Pyrenees. *Scientific Reports*, 8(1), 9591. <https://doi.org/10.1038/s41598-018-27889-x>
- Chian, D., Loudon, K. E., & Reid, I. (1995). Crustal structure of the Labrador Sea conjugate margin and implications for the formation of nonvolcanic continental margins. *Journal of Geophysical Research: Solid Earth*, 100(B12), 24239–24253.
- Childs, C., Watterson, J., & Walsh, J. J. (1995). Fault overlap zones within developing normal fault systems. *Journal of the Geological Society*, 152(3), 535–549. <https://doi.org/10.1144/gsjgs.152.3.0535>
- Chorowicz, J. (1989). Transfer and transform fault zones in continental rifts: examples in the Afro-Arabian Rift System. Implications of crust breaking. *Journal of African Earth Sciences (and the Middle East)*, 8(2–4), 203–214. [https://doi.org/10.1016/S0899-5362\(89\)80025-9](https://doi.org/10.1016/S0899-5362(89)80025-9)
- Choukroune, P. (1989). The Ecore Pyrenean deep seismic profile reflection data and the overall structure of an orogenic belt. *Tectonics*, 8(1), 23–39. <https://doi.org/10.1029/TC008i001p00023>
- Choukroune, P., & Mattauer, M. (1978). Tectonique des plaques et Pyrenees; sur le fonctionnement de la faille transformante nord-pyreneenne; comparaisons avec des modeles actuels. *Bulletin de La Societe Geologique de France*, S7-XX(5), 689–700. <https://doi.org/10.2113/gssgfbull.S7-XX.5.689>
- Choukroune, Pierre. (1972). Relations entre tectonique et metamorphisme dans les terrains secondaires de la zone nord-pyreneenne centrale et orientale. *Bulletin de La Societe Geologique de France*, S7-XIV(1–5), 3–11. <https://doi.org/10.2113/gssgfbull.S7-XIV.1-5.3>
- Choukroune, Pierre. (1992). Tectonic evolution of the Pyrenees. *Annual Review of Earth and Planetary Sciences*, 20(1), 143–158.
- Choukroune, Pierre, Seguret, M., & Galdeano, A. (1973). Caracteristiques et evolution structurale des Pyrenees; un modele de relations entre zone orogenique et mouvement des plaques. *Bulletin de La Societe Geologique de France*, S7-XV(5–6), 600–611. <https://doi.org/10.2113/gssgfbull.S7-XV.5-6.600>
- Cincunegui, M., Mendizabal, J., & Valle, A. (1943). Mapa geológico de España 1: 50.000. Explicación de la hoja núm. 172 (Allo). IGME. Madrid.
- Ciry, R., Amiot, M., & Feuillée, P. (1963). Les transgressions cretacees sur le massif d'Oroz-Betelu (Navarre espagnole). *Bulletin de La Société Géologique de France*, 7(5), 701–707.
- Claude, D. (1990). Étude stratigraphique, sédimentologique et structurale des dépôts mésozoïques au nord du massif du Labourd: rôle de la faille de Pamplona, Pays Basque.
- Clerc, C., Lagabrielle, Y., Neumaier, M., Reynaud, J.-Y., & de Saint Blanquat, M. (2012). Exhumation of subcontinental mantle rocks: evidence from ultramafic-bearing clastic deposits nearby the Lherz peridotite body, French Pyrenees. *Bulletin de La Societe Geologique de France*, 183(5), 443–459. <https://doi.org/10.2113/gssgfbull.183.5.443>
- Clerc, Camille, & Lagabrielle, Y. (2014). Thermal control on the modes of crustal thinning leading to mantle exhumation: Insights from the Cretaceous Pyrenean hot paleomargins. *Tectonics*, 33(7), 1340–1359.
- Clerc, Camille, Lahfid, A., Monié, P., Lagabrielle, Y., Chopin, C., Poujol, M., et al. (2015). High-temperature metamorphism during extreme thinning of the continental crust: a reappraisal of the North Pyrenean passive paleomargin. *Solid Earth*, 6(2), 643.
- Clerc, Camille, Lagabrielle, Y., Labaume, P., Ringenbach, J.-C., Vauchez, A., Nalpas, T., et al. (2016). Basement – Cover decoupling and progressive exhumation of metamorphic sediments at hot rifted margin. Insights from the Northeastern Pyrenean analog. *Tectonophysics*, 686(Supplement C), 82–97. <https://doi.org/10.1016/j.tecto.2016.07.022>
- Clerc, Camille, Ringenbach, J.-C., Jolivet, L., & Ballard, J.-F. (2018). Rifted margins: Ductile deformation, boudinage, continentward-dipping normal faults and the role of the weak lower crust. *Gondwana Research*, 53, 20–40. <https://doi.org/10.1016/j.gr.2017.04.030>
- Clift, P. D., Brune, S., & Quinteros, J. (2015). Climate changes control offshore crustal structure at South China Sea continental margin. *Earth and Planetary Science Letters*, 420(Supplement C), 66–72. <https://doi.org/10.1016/j.epsl.2015.03.032>

- Cochelin, B. (2016). Champ de déformation du socle paléozoïque des Pyrénées.
- Cochelin, B., Chardon, D., Denèle, Y., Gumiaux, C., & Le Bayon, B. (2017). Vertical strain partitioning in hot Variscan crust: Syn-convergence escape of the Pyrenees in the Iberian-Armorican syntax. *Bulletin de La Société Géologique de France*, 188(6), 39. <https://doi.org/10.1051/bsgf/2017206>
- Cochelin, B., Lemirre, B., Denèle, Y., de Saint Blanquat, M., Lahfid, A., & Duchêne, S. (2018). Structural inheritance in the Central Pyrenees: the Variscan to Alpine tectonometamorphic evolution of the Axial Zone. *Journal of the Geological Society*, 175(2), 336–351. <https://doi.org/10.1144/jgs2017-066>
- Cohen, C. R. (1982). Model for a passive to active continental margin transition: implications for hydrocarbon exploration. *AAPG Bulletin*, 66(6), 708–718.
- Combes, P.-J., Peybernes, B., & Leyreloup, A. F. (1998). Altérites et bauxites, témoins des marges européenne et ibérique des Pyrénées occidentales au Jurassique supérieur — Crétacé inférieur, à l'ouest de la vallée d'Ossau (Pyrénées-Atlantiques, France). *Comptes Rendus de l'Académie Des Sciences - Series IIA - Earth and Planetary Science*, 327(4), 271–278. [https://doi.org/10.1016/S1251-8050\(98\)80085-2](https://doi.org/10.1016/S1251-8050(98)80085-2)
- Corre, B., Boulvais, P., Boiron, M. C., Lagabrielle, Y., Marasi, L., & Clerc, C. (2018). Fluid circulations in response to mantle exhumation at the passive margin setting in the north Pyrenean zone, France. *Mineralogy and Petrology*, 112(5), 647–670. <https://doi.org/10.1007/s00710-018-0559-x>
- Corre, Benjamin. (2017). La bordure nord de la plaque ibérique à l'Albo-Cénomanién: architecture d'une marge passive de type ductile (Chaînons Béarnais, Pyrénées Occidentales).
- Corre, Benjamin, Lagabrielle, Y., Labaume, P., Fourcade, S., Clerc, C., & Ballèvre, M. (2016). Deformation associated with mantle exhumation in a distal, hot passive margin environment: New constraints from the Sarailé Massif (Chaînons Béarnais, North-Pyrenean Zone). *From Rifting to Mountain Building: The Pyrenean Belt*, 348(3), 279–289. <https://doi.org/10.1016/j.crte.2015.11.007>
- Corti, G. (2012). Evolution and characteristics of continental rifting: Analog modeling-inspired view and comparison with examples from the East African Rift System. *Tectonophysics*, 522–523, 1–33. <https://doi.org/10.1016/j.tecto.2011.06.010>
- Corti, G., van Wijk, J., Cloetingh, S., & Morley, C. K. (2007). Tectonic inheritance and continental rift architecture: Numerical and analogue models of the East African Rift system: INHERITANCE AND RIFT ARCHITECTURE. *Tectonics*, 26(6), n/a-n/a. <https://doi.org/10.1029/2006TC002086>
- Cuevas, J., & Tubía, J. m. (1999). The discovery of scapolite marbles in the Biscay Synclinorium (Basque–Cantabrian basin, Western Pyrenees): geodynamic implications. *Terra Nova*, 11(6), 259–265. <https://doi.org/10.1046/j.1365-3121.1999.00255.x>
- Curnelle, R. (1983). Evolution structuro-sédimentaire du Trias et de l'Infra-Lias d'Aquitaine. *Bull. Cent. Rech. Explor. Prod. Elf-Aquitaine*, 7(1), 69–99.
- Cuvillier, J., Henry, J., Ribis, R., & Villanova, M. (1964). Microfaunes cenomaniennes et santoniennes dans le “calcaire des canons” (vallee d'Aspe, Sainte-Engrace, Basses-Pyrenees). *Bulletin de La Société Géologique de France*, S7-VI(2), 273–277. <https://doi.org/10.2113/gssgfbull.S7-VI.2.273>

D

- Dahlstrom, C. D. A. (1969). Balanced cross sections. *Canadian Journal of Earth Sciences*, 6(4), 743–757. <https://doi.org/10.1139/e69-069>
- Daignières, M. (1978). Géophysique et faille nord-pyréenne. *Bulletin de La Société Géologique de France*, S7-XX(5), 677–680. <https://doi.org/10.2113/gssgfbull.S7-XX.5.677>
- Daignières, M., Gallart, J., Banda, E., & Hirn, A. (1982). Implications of the seismic structure for the orogenic evolution of the Pyrenean Range. *Earth and Planetary Science Letters*, 57(1), 88–100. [https://doi.org/10.1016/0012-821X\(82\)90175-3](https://doi.org/10.1016/0012-821X(82)90175-3)
- Daignières, M., Séguret, M., & Specht, M. (1994). The Arzacq-Western Pyrenees ECORS Deep Seismic Profile. In A. Mascle (Ed.), *Hydrocarbon and Petroleum Geology of France* (pp. 199–208). Berlin, Heidelberg: Springer Berlin Heidelberg. https://doi.org/10.1007/978-3-642-78849-9_15
- Dauteuil, O., & Ricou, L.-E. (1989). Hot-fluid circulation as an origin for the North Pyrenean cretaceous metamorphism. *Geodinamica Acta*, 3(3), 237–249. <https://doi.org/10.1080/09853111.1989.11105190>
- Davis, D., Suppe, J., & Dahlen, F. A. (1983). Mechanics of fold-and-thrust belts and accretionary wedges. *Journal of Geophysical Research*, 88(B2), 1153. <https://doi.org/10.1029/JB088iB02p01153>
- Davis, M., & Kusznir, N. (2004). Depth-dependent lithospheric stretching at rifted continental margins. *Proceedings of NSF Rifted Margins Theoretical Institute*, 136, 92–137.

- Debroas, E., Canérot, J., & Bilotte, M. (2010). Les brèches d'Urdach, témoins de l'exhumation du manteau pyrénéen dans un escarpement de faille vraconnien-cénomancien inférieur (Zone nord-pyrénéenne, Pyrénées-Atlantiques, France). *Géologie de La France*, 2(2), 53–64.
- Debroas, E. J. (1978). Evolution de la fosse du flysch ardoisier de l'Albien supérieur au Senonien inférieur (zone interne métamorphique des Pyrénées navarro-languedociennes). *Bulletin de La Société Géologique de France*, S7-XX(5), 639–648. <https://doi.org/10.2113/gssgfbull.S7-XX.5.639>
- Debroas, E. J. (1987). Modèle de bassin triangulaire à l'intersection de décrochements divergents pour le fosse albo-cénomancien de la Ballongue (zone nord-pyrénéenne, France). *Bulletin de La Société Géologique de France*, III(5), 887. <https://doi.org/10.2113/gssgfbull.III.5.887>
- Debroas, E. J. (1990). Le flysch noir albo-cénomancien témoin de la structuration albienne à senonienne de la Zone nord-pyrénéenne en Bigorre (Hautes-Pyrénées, France). *Bulletin de La Société Géologique de France*, VI(2), 273–285. <https://doi.org/10.2113/gssgfbull.VI.2.273>
- DeFelipe, I. (2017). Crustal structure and alpine tectonic evolution of the eastern border of the Basque-Cantabrian Zone. Universidad de Oviedo.
- DeFelipe, I., Pedreira, D., Pulgar, J., Iriarte, E., & Mendia, M. (2012). Petrography and C and O stable isotope composition of ophicalcites in the Western Pyrenees/Eastern Cantabrian Mountains: Geodynamic implications (Vol. 14). Presented at the Geophys. Res. Abstr.
- DeFelipe, I., Pedreira, D., Pulgar, J. A., Iriarte, E., & Mendia, M. (2017). Mantle exhumation and metamorphism in the Basque-Cantabrian Basin (NSpain): Stable and clumped isotope analysis in carbonates and comparison with ophicalcites in the North-Pyrenean Zone (Urdach and Lherz). *Geochimistry, Geophysics, Geosystems*, 18(2), 631–652. <https://doi.org/10.1002/2016GC006690>
- DeFelipe, I., Pedreira, D., Pulgar, J. A., van der Beek, P. A., Bernet, M., & Pik, R. (2019). Alpine exhumation history of the eastern Basque-Cantabrian Zone–western Pyrenees from low-temperature thermochronology (Vol. 21, p. 16670). Presented at the EGU General Assembly Conference Abstracts.
- Del Pozo, J. R. (1971). Bioestratigrafía y microfácies del Jurásico y Cretácico del norte de España (región cantábrica) (Vol. 78). Departamento de Publicaciones.
- Del Valle, J. (1972). Mapa geológico de España E. 1:50.000, Serie MAGNA(Hoja de Pamplona, 141).
- Del Valle, J., Adler, R. E., de Boer, H. F., Jordan, H., Klarr, K., Krausse, H. ., et al. (1972). Mapa geológico de España E. 1:50.000, Serie MAGNA(Hoja de Valcarlos, 91).
- Del Valle, J., Villalobos, L., Bornhorst, H. U., de Boer, H. F., Krausse, K., Mohr, R., et al. (1973). Mapa geológico de España E. 1:50.000, Serie MAGNA(Hoja de Sumbilla, 90).
- Delfaud, J. (1970). Résumé d'une recherche sur la dynamique du domaine aquitano-pyrénéen durant le Jurassique et le Crétacé inférieur. Société linnéenne de Bordeaux.
- Delvolvé, J.-J., Vachard, D., & Souquet, P. (1998). Stratigraphic record of thrust propagation, Carboniferous foreland basin, Pyrenees, with emphasis on Pays-de-Sault (France/Spain). *Geologische Rundschau*, 87(3), 363–372. <https://doi.org/10.1007/s005310050215>
- Denèle, Y., Olivier, P., Gleizes, G., & Barbey, P. (2009). Decoupling between the middle and upper crust during transpression-related lateral flow: Variscan evolution of the Aston gneiss dome (Pyrenees, France). *Tectonophysics*, 477(3–4), 244–261. <https://doi.org/10.1016/j.tecto.2009.04.033>
- Denèle, Y., Paquette, J.-L., Olivier, P., & Barbey, P. (2011). Permian granites in the Pyrenees: the Aya pluton (Basque Country). *Terra Nova*, 24(2), 105–113. <https://doi.org/10.1111/j.1365-3121.2011.01043.x>
- Denèle, Y., Laumonier, B., Paquette, J.-L., Olivier, P., Gleizes, G., & Barbey, P. (2014). Timing of granite emplacement, crustal flow and gneiss dome formation in the Variscan segment of the Pyrenees. *Geological Society, London, Special Publications*, 405(1), 265–287. <https://doi.org/10.1144/SP405.5>
- Dercourt, J., Gaetani, M., & Vrielynck, B. (2000). Atlas Peri-Tethys Palaeogeographical Maps. CCGM.
- Desegaulx, P., & Brunet, M. F. (1990). Tectonic subsidence of the Aquitaine Basin since Cretaceous times. *Bulletin de La Société Géologique de France*, VI(2), 295. <https://doi.org/10.2113/gssgfbull.VI.2.295>
- Dewey, J. F., & Bird, J. M. (1970). Mountain belts and the new global tectonics. *Journal of Geophysical Research*, 75(14), 2625–2647. <https://doi.org/10.1029/JB075i014p02625>
- Díaz, J., & Gallart, J. (2009). Crustal structure beneath the Iberian Peninsula and surrounding waters: A new compilation of deep seismic sounding results. *Physics of the Earth and Planetary Interiors*, 173(1), 181–190. <https://doi.org/10.1016/j.pepi.2008.11.008>
- Díaz, J., Pedreira, D., Ruiz, M., Pulgar, J. A., & Gallart, J. (2012). Mapping the indentation between the Iberian and Eurasian plates beneath the Western Pyrenees/Eastern Cantabrian Mountains

- from receiver function analysis. *Tectonophysics*, 570–571, 114–122. <https://doi.org/10.1016/j.tecto.2012.07.005>
- Direen, N. G., Stagg, H. M. J., Symonds, P. A., & Colwell, J. B. (2011). Dominant symmetry of a conjugate southern Australian and East Antarctic magma-poor rifted margin segment: SOUTHERN RIFT SYSTEM CONJUGATE MARGINS. *Geochemistry, Geophysics, Geosystems*, 12(2), n/a–n/a. <https://doi.org/10.1029/2010GC003306>
- Direen, N. G., Stagg, H. M. J., Symonds, P. A., & Norton, I. O. (2013). Variations in rift symmetry: cautionary examples from the Southern Rift System (Australia–Antarctica). *Geological Society, London, Special Publications*, 369(1), 453–475. <https://doi.org/10.1144/SP369.4>
- Doré, A. G., Lundin, E. R., Fichler, C., & Olesen, O. (1997). Patterns of basement structure and reactivation along the NE Atlantic margin. *Journal of the Geological Society*, 154(1), 85–92. <https://doi.org/10.1144/gsjgs.154.1.0085>
- Doré, A. G., Lundin, E. R., Jensen, L. N., Birkeland, Ø., Eliassen, P. E., & Fichler, C. (1999). Principal tectonic events in the evolution of the northwest European Atlantic margin. In *Petroleum Geology of Northwest Europe: Proceedings of the 5th Conference* (pp. 41–61). Geological Society of London. <https://doi.org/10.1144/0050041>
- Ducasse, L., Velasque, P.-C., & Muller, J. (1986a). Glissement de couverture et panneaux basculés dans la région des Arbailles (Pyrénées occidentales): Un modèle évolutif créacé de la marge nord-ibérique à l'Est de la transformante de Pamplona. *Comptes Rendus de l'Académie Des Sciences. Série 2, Mécanique, Physique, Chimie, Sciences de l'univers, Sciences de La Terre*, 303(16), 1477–1482.
- Ducasse, L., Muller, J., & Velasque, P.-C. (1986b). La chaîne pyrénéo-cantabrique: subduction hercynienne, rotation créacée de l'Ibérie et subductions alpines différentielles. *Comptes Rendus de l'Académie Des Sciences. Série 2, Mécanique, Physique, Chimie, Sciences de l'univers, Sciences de La Terre*, 303(5), 419–424.
- Ducoux, M. (2017). Structure, thermicité et évolution géodynamique de la Zone Interne Métamorphique des Pyrénées. Retrieved from <http://www.theses.fr/2017ORLE2026/document>
- Duretz, T., Petri, B., Mohn, G., Schmalholz, S. M., Schenker, F. L., & Müntener, O. (2016). The importance of structural softening for the evolution and architecture of passive margins. *Scientific Reports*, 6. <https://doi.org/10.1038/srep38704>

E

- Egan, S. (2012). T. Gerya 2010. *Introduction to Numerical Geodynamic Modelling*. xvii + 345. Cambridge University Press. Price £40.00, US\$70.00 (HB). ISBN 978 0 521 88754 0. *Geological Magazine*, 149(01), 174. <https://doi.org/10.1017/S0016756811000604>
- Engeser, T., & Schwentke, W. (1986). Towards a new concept of the tectogenesis of the Pyrenees. *Tectonophysics*, 129(1–4), 233–242. [https://doi.org/10.1016/0040-1951\(86\)90253-2](https://doi.org/10.1016/0040-1951(86)90253-2)
- England, P. C., & Thompson, A. B. (1984). Pressure--Temperature--Time Paths of Regional Metamorphism I. Heat Transfer during the Evolution of Regions of Thickened Continental Crust. *Journal of Petrology*, 25(4), 894–928. <https://doi.org/10.1093/petrology/25.4.894>
- Epin, M.-E., Manatschal, G., & Amann, M. (2017). Defining diagnostic criteria to describe the role of rift inheritance in collisional orogens: the case of the Err-Platta nappes (Switzerland). *Swiss Journal of Geosciences*, 110(2), 419–438. <https://doi.org/10.1007/s00015-017-0271-6>
- Erdős, Z., Huismans, R. S., van der Beek, P., & Thieulot, C. (2014). Extensional inheritance and surface processes as controlling factors of mountain belt structure: Inherited structural control on orogens. *Journal of Geophysical Research: Solid Earth*, 119(12), 9042–9061. <https://doi.org/10.1002/2014JB011408>
- Espurt, N., Callot, J.-P., Roure, F., Totterdell, J. M., Struckmeyer, H. I. M., & Vially, R. (2012). Transition from symmetry to asymmetry during continental rifting: an example from the Bight Basin–Terre Adélie (Australian and Antarctic conjugate margins). *Terra Nova*, 24(3), 167–180. <https://doi.org/10.1111/j.1365-3121.2011.01055.x>

F

- Faulds, J. E., & Varga, R. J. (1998). The role of accommodation zones and transfer zones in the regional segmentation of extended terranes. In *Special Paper 323: Accommodation zones and transfer zones; the regional segmentation of the Basin and Range Province* (Vol. 323, pp. 1–45). Geological Society of America. <https://doi.org/10.1130/0-8137-2323-X.1>

- Fernandez-Mendiola, P. A., & García-Mondejar, J. (1990). Mid-cretaceous palaeogeographical evolution of the central Basque-Cantabrian basin (northern Spain). *Palaeogeography, Palaeoclimatology, Palaeoecology*, 81(1–2), 115–126. [https://doi.org/10.1016/0031-0182\(90\)90043-7](https://doi.org/10.1016/0031-0182(90)90043-7)
- Fernández-Viejo, G., Gallart, J., Pulgar, J. A., Córdoba, D., & Dañobeitia, J. J. (2000). Seismic signature of Variscan and Alpine tectonics in NW Iberia: Crustal structure of the Cantabrian Mountains and Duero basin. *Journal of Geophysical Research: Solid Earth*, 105(B2), 3001–3018. <https://doi.org/10.1029/1999JB900321>
- Ferrer, O., Roca, E., Benjumea, B., Muñoz, J. A., Ellouz, N., & MARCONI Team. (2008). The deep seismic reflection MARCONI-3 profile: Role of extensional Mesozoic structure during the Pyrenean contractional deformation at the eastern part of the Bay of Biscay. *Marine and Petroleum Geology*, 25(8), 714–730. <https://doi.org/10.1016/j.marpetgeo.2008.06.002>
- Ferrer, O., Jackson, M. P. A., Roca, E., & Rubinat, M. (2012). Evolution of salt structures during extension and inversion of the Offshore Parentis Basin (Eastern Bay of Biscay). *Geological Society, London, Special Publications*, 363(1), 361–380. <https://doi.org/10.1144/SP363.16>
- Feuillée, P. (1964). Sur l'âge cénomanien des calcaires à Caprines des Pyrénées basques occidentales. *Compt. Rend. Soc. Géol. France*, 2, 90–93.
- Feuillée, P., & Rat, P. (1971). Structures et paléogéographies pyrénéo-cantabriques. Ed. Technip.
- Feuillée, P., & Sigal, J. (1965). La transgression du Cretace superieur ('flysch nord-pyreneen') sur le massif des Cinco-Villas (Pyrenees basques). *Bulletin de La Société Géologique de France*, S7-VII(1), 45. <https://doi.org/10.2113/gssgfbull.S7-VII.1.45>
- Feuillée, Pierre. (1971). Les calcaires biogéniques de l'Albien et du Cénomanién pyrénéo-cantabrique: Problèmes d'environnement sédimentaire. *Palaeogeography, Palaeoclimatology, Palaeoecology*, 9(4), 277–311. [https://doi.org/10.1016/0031-0182\(71\)90004-6](https://doi.org/10.1016/0031-0182(71)90004-6)
- Fillon, C., Gautheron, C., & van der Beek, P. (2013). Oligocene–Miocene burial and exhumation of the Southern Pyrenean foreland quantified by low-temperature thermochronology. *Journal of the Geological Society*, 170(1), 67–77. <https://doi.org/10.1144/jgs2012-051>
- Fillon, C., Pedreira, D., van der Beek, P. A., Huismans, R. S., Barbero, L., & Pulgar, J. A. (2016). Alpine exhumation of the central Cantabrian Mountains, Northwest Spain: ALPINE EXHUMATION OF THE CANTABRIANS. *Tectonics*, 35(2), 339–356. <https://doi.org/10.1002/2015TC004050>
- Fitzgerald, P. ., Muñoz, J. ., Coney, P. ., & Baldwin, S. . (1999). Asymmetric exhumation across the Pyrenean orogen: implications for the tectonic evolution of a collisional orogen. *Earth and Planetary Science Letters*, 173(3), 157–170. [https://doi.org/10.1016/S0012-821X\(99\)00225-3](https://doi.org/10.1016/S0012-821X(99)00225-3)
- Floquet, M., & Mathey, B. (1984). Evolution sédimentologique, paléogéographique et structurale des marges ibérique et européenne dans les régions basco-cantabrique et nord-ibérique au Crétacé moyen et supérieur. *Act. Lab. Sédim. Paléont. Univ. Sabatier*, 1, 129–136.
- Floquet, M., Mathey, B., Rosse, P., & Vadot, J. P. (1988). Age cenomanien et turono-coniacien des calcaires de Sare (Pays Basque, France-Espagne); conséquences paleomorphologiques et tectogenetiques pour les Pyrenees occidentales. *Bulletin de La Société Géologique de France*, IV(6), 1021–1027. <https://doi.org/10.2113/gssgfbull.IV.6.1021>
- Floquet, Marc. (1998). Outcrop cycle stratigraphy of shallow ramp deposits: the Late Cretaceous Series on the Castillian ramp (northern Spain).
- Fossen, H. (2016). *Structural geology*. Cambridge University Press.
- Frankovic, A., Eguiluz, L., & Martínez-Torres, L. M. (2016). Geodynamic evolution of the Salinas de Añana diapir in the Basque-Cantabrian Basin, Western Pyrenees. *Journal of Structural Geology*, 83, 13–27. <https://doi.org/10.1016/j.jsg.2015.12.001>
- Frasca, G., Gueydan, F., Brun, J.-P., & Monié, P. (2016). Deformation mechanisms in a continental rift up to mantle exhumation. Field evidence from the western Betics, Spain. *Marine and Petroleum Geology*, 76(Supplement C), 310–328. <https://doi.org/10.1016/j.marpetgeo.2016.04.020>
- Fréchengues, M. (1993). Stratigraphie séquentielle et micropaléontologie du Trias moyen-supérieur des Pyrénées franco-espagnoles.
- Froitzheim, N., & Eberli, G. P. (1990). Extensional detachment faulting in the evolution of a Tethys passive continental margin, Eastern Alps, Switzerland. *Geological Society of America Bulletin*, 102(9), 1297–1308. [https://doi.org/10.1130/0016-7606\(1990\)102<1297:EDFITE>2.3.CO;2](https://doi.org/10.1130/0016-7606(1990)102<1297:EDFITE>2.3.CO;2)

G

- Gabaldón, V., Hernández Samaniego, A., Ramírez del Pozo, J. J., Carbaya Olivares, A., Castiella Muruzábal, J., & Solé Sedo, J. (1984a). Mapa geológico de España E. 1:50.000, Serie MAGNA(Hoja de Allo, 172).

- Gabaldón, V., Hernández Samaniego, A., Ramírez Merino, J. J., & Ramírez del Pozo, J. (1984b). Mapa geológico de España E. 1:50.000, Serie MAGNA(Hoja de Tafalla, 173).
- Gabaldón, V., Ramírez Merino, J. J., Olivé Davo, A., Villalobos Vilches, L., León González, L., & Carbayo Olivares, A. (1984c). Mapa geológico de España E. 1:50.000, Serie MAGNA(Hoja de Alsasua, 114).
- Gabaldón, V., Hernández Samaniego, A., & Simó Marja, A. (1985). Mapa geológico de España E. 1:50.000, Serie MAGNA(Hoja de Sangüesa, 174).
- Gaina, C., Müller, D. R., Royer, J.-Y., Stock, J., Hardebeck, J., & Symonds, P. (1998). The tectonic history of the Tasman Sea: A puzzle with 13 pieces. *Journal of Geophysical Research: Solid Earth*, 103(B6), 12413–12433. <https://doi.org/10.1029/98JB00386>
- Gallart, J., Banda, E., & Daignières, M. (1981). Crustal structure of the Paleozoic Axial Zone of the Pyrenees and transition to the North Pyrenean Zone (Vol. 37, pp. 457–480). Presented at the *Annales de Geophysique*, Editions CNRS 20/22 Rue St. Amand, 75015 Paris, France.
- Gallastegui, G., Heredia, N., Rodríguez Fernández, L., & Cuesta, A. (1990). El «stock» de Peña Prieta en el contexto del magmatismo de la unidad de Pisuerga-Carrion (Zona Cantábrica, N de España).
- Gallastegui, J. (2000). Estructura cortical de la cordillera y margen continental cantábricos: perfiles ESCI-N. *Trabajos de Geología*, 22(22), 3–234.
- García-Mondéjar, J. (1986). The Aptian—Albian Carbonate Episode of the Basque—Cantabrian Basin (Northern Spain): General Characteristics, Controls and Evolution. In M. E. Tucker, J. L. Wilson, P. D. Crevello, J. Rick Sarg, & J. F. Read (Eds.), *Carbonate Platforms* (pp. 257–290). Oxford, UK: Blackwell Publishing Ltd. <https://doi.org/10.1002/9781444303834.ch10>
- García-Mondejar, J. (1989). Strike-slip subsidence of the Basque-Cantabrian basin of northern Spain and its relationship to Aptian-Albian opening of Bay of Biscay. In *Extensional tectonics and stratigraphy of the North Atlantic margins* (Vol. 46, pp. 395–409). American Association of Petroleum Geologists Memoir.
- García-Mondéjar, J., Pujalte, V., & Robles, S. (1986). Características sedimentológicas, secuenciales y tectoestratigráficas del Triásico de Cantabria y norte de Palencia: Cuadernos de Geología Iberica, (10), 151–172.
- García-Mondéjar, J., Agirrezabala, L., Aranburu, A., Fernández-Mendiola, P., Gómez-Pérez, I., López-Horgue, M., & Rosales, I. (1996). Aptian—Albian tectonic pattern of the Basque—Cantabrian Basin (Northern Spain). *Geological Journal*, 31(1), 13–45.
- García-Mondéjar, J. G. (1979). El complejo urgoniano del sur de Santander.
- García-Sansegundo, J., Poblet, J., Alonso, J. L., & Clariana, P. (2011). Hinterland-foreland zonation of the Variscan orogen in the Central Pyrenees: comparison with the northern part of the Iberian Variscan Massif. *Geological Society, London, Special Publications*, 349(1), 169–184. <https://doi.org/10.1144/SP349.9>
- Garrido-Megias, A., & Rios-Aragues, L. M. (1972). Síntesis geológica del Secundario y Terciario entre los ríos Cinco y Segre. *Boletim. Geol. Min.*, 93, 1–47.
- Gawthorpe, R. L., & Hurst, J. M. (1993). Transfer zones in extensional basins: their structural style and influence on drainage development and stratigraphy. *Journal of the Geological Society*, 150(6), 1137–1152. <https://doi.org/10.1144/gsjgs.150.6.1137>
- Genna, A. (2007). Carte géologique harmonisée au 1/50 000 du département des Pyrénées-Atlantiques, (BRGM/RP-55408-FR).
- Gibbs, A. D. (1984). Structural evolution of extensional basin margins. *Journal of the Geological Society*, 141(4), 609–620. <https://doi.org/10.1144/gsjgs.141.4.0609>
- Gillard, M., Autin, J., & Manatschal, G. (2016). Fault systems at hyper-extended rifted margins and embryonic oceanic crust: Structural style, evolution and relation to magma. *Marine and Petroleum Geology*, 76, 51–67. <https://doi.org/10.1016/j.marpetgeo.2016.05.013>
- Gillcrist, R., Coward, M., & Mugnier, J.-L. (1987). Structural inversion and its controls : examples from the Alpine foreland and the French Alps. *Geodinamica Acta*, 1(1), 5–34. <https://doi.org/10.1080/09853111.1987.11105122>
- Gleason, G. C., & Tullis, J. (1995). A flow law for dislocation creep of quartz aggregates determined with the molten salt cell. *Tectonophysics*, 247(1), 1–23. [https://doi.org/10.1016/0040-1951\(95\)00011-B](https://doi.org/10.1016/0040-1951(95)00011-B)
- Gleizes, G., Leblanc, D., & Bouchez, J. L. (1997). Variscan granites of the Pyrenees revisited: their role as syntectonic markers of the orogen. *Terra Nova*, 9(1), 38–41. <https://doi.org/10.1046/j.1365-3121.1997.d01-9.x>
- Golberg, J. M., & Leyreloup, A. F. (1990). High temperature-low pressure Cretaceous metamorphism

- related to crustal thinning (Eastern North Pyrenean Zone, France). *Contributions to Mineralogy and Petrology*, 104(2), 194–207. <https://doi.org/10.1007/BF00306443>
- Golberg, J. M., Maluski, H., & Leyreloup, A. F. (1986). Petrological and age relationship between emplacement of magmatic breccia, alkaline magmatism, and static metamorphism in the North Pyrenean Zone. *Tectonophysics*, 129(1–4), 275–290. [https://doi.org/10.1016/0040-1951\(86\)90256-8](https://doi.org/10.1016/0040-1951(86)90256-8)
- Golberg, J.-M., & Maluski, H. (1988). Données nouvelles et mise au point sur l'âge du métamorphisme pyrénéen. *Comptes Rendus de l'Académie Des Sciences. Série 2, Mécanique, Physique, Chimie, Sciences de l'univers, Sciences de La Terre*, 306(6), 429–435.
- Gómez, M., Vergés, J., & Riaza, C. (2002). Inversion tectonics of the northern margin of the Basque Cantabrian Basin. *Bulletin de La Societe Geologique de France*, 173(5), 449–459. <https://doi.org/10.2113/173.5.449>
- Gräfe, K.-U. (1999). Sedimentary cycles, burial history and foraminiferal indicators for systems tracts and sequence boundaries in the Cretaceous of the Basco-Cantabrian Basin (northern Spain). *Neues Jahrbuch Fur Geologie Und Palaontologie-Abhandlungen*, 212(1), 85–130.
- Granado, P., Tavani, S., Carrera, N., & Muñoz, J. A. (2018). Deformation pattern around the Conejera fault blocks (Asturian Basin, North Iberian Margin). *Geologica Acta*, 16(4), 0357–0373.
- Grandjean, G. (1994). Etude des structures crustales dans une portion de chaîne et de leur relation avec les bassins sédimentaires. Application aux Pyrénées occidentales. *Bull. Cent. Rech. Explor. Prod. Elf Aquitaine*, 18, 391–420.
- Gretter, N., Ronchi, A., López-Gómez, J., Arche, A., De la Horra, R., Barrenechea, J., & Lago, M. (2015). The Late Palaeozoic-Early Mesozoic from the Catalan Pyrenees (Spain): 60 Myr of environmental evolution in the frame of the western peri-Tethyan palaeogeography. *Earth-Science Reviews*, 150, 679–708. <https://doi.org/10.1016/j.earscirev.2015.09.001>
- Grool, A. R., Ford, M., Vergés, J., Huismans, R. S., Christophoul, F., & Dielforder, A. (2018). Insights Into the Crustal-Scale Dynamics of a Doubly Vergent Orogen From a Quantitative Analysis of Its Forelands: A Case Study of the Eastern Pyrenees. *Tectonics*, 37(2), 450–476. <https://doi.org/10.1002/2017TC004731>
- Guitard, G., Vielzeuf, D., Martinez, F., Barnolas, A., & Chiron, J. (1996). Métamorphisme hercynien. *Synthèse Géologique et Géophysique Des Pyrénées*, 1, 501–584.

H

- Hall, C. A., & Johnson, J. A. (1986). Apparent western termination of the North Pyrenean Fault and tectonostratigraphic units of the western north Pyrenees, France and Spain. *Tectonics*, 5(4), 607–627. <https://doi.org/10.1029/TC005i004p00607>
- Hart, N. R., Stockli, D. F., & Hayman, N. W. (2016). Provenance evolution during progressive rifting and hyperextension using bedrock and detrital zircon U-Pb geochronology, Mauléon Basin, western Pyrenees. *Geosphere*, 12(4), 1166–1186. <https://doi.org/10.1130/GES01273.1>
- Hart, N. R., Stockli, D. F., Lavier, L. L., & Hayman, N. W. (2017). Thermal evolution of a hyperextended rift basin, Mauléon Basin, western Pyrenees. *Tectonics*, 36(6), 1103–1128. <https://doi.org/10.1002/2016TC004365>
- Hauptert, I., Manatschal, G., Decarlis, A., & Unternehr, P. (2016). Upper-plate magma-poor rifted margins: Stratigraphic architecture and structural evolution. *Marine and Petroleum Geology*, 69(Supplement C), 241–261. <https://doi.org/10.1016/j.marpetgeo.2015.10.020>
- Heddebaut, C. (1973). Etudes géologiques dans les massifs paléozoïques basques.
- Hilaret, N., Reynard, B., Wang, Y., Daniel, I., Merkel, S., Nishiyama, N., & Petitgirard, S. (2007). High-Pressure Creep of Serpentine, Interseismic Deformation, and Initiation of Subduction. *Science*, 318(5858), 1910–1913. <https://doi.org/10.1126/science.1148494>
- Hirth, G., & Kohlstedt, D. (2003). Rheology of the upper mantle and the mantle wedge: A view from the experimentalists. In J. Eiler (Ed.), *Geophysical Monograph Series (Vol. 138, pp. 83–105)*. Washington, D. C.: American Geophysical Union. <https://doi.org/10.1029/138GM06>
- Huismans, R., & Beaumont, C. (2011). Depth-dependent extension, two-stage breakup and cratonic underplating at rifted margins. *Nature*, 473(7345), 74–78. <https://doi.org/10.1038/nature09988>
- Huismans, R. S., & Beaumont, C. (2007). Roles of lithospheric strain softening and heterogeneity in determining the geometry of rifts and continental margins. *Geological Society, London, Special Publications*, 282(1), 111–138. <https://doi.org/10.1144/SP282.6>
- Huismans, Ritske S., & Beaumont, C. (2002). Asymmetric lithospheric extension: The role of frictional plastic strain softening inferred from numerical experiments. *Geology*, 30(3), 211–214. [https://doi.org/10.1130/0091-7613\(2002\)030<0211:ALETRO>2.0.CO;2](https://doi.org/10.1130/0091-7613(2002)030<0211:ALETRO>2.0.CO;2)

- Huismans, Ritske S., & Beaumont, C. (2003). Symmetric and asymmetric lithospheric extension: Relative effects of frictional-plastic and viscous strain softening: SYMMETRIC AND ASYMMETRIC EXTENSION. *Journal of Geophysical Research: Solid Earth*, 108(B10). <https://doi.org/10.1029/2002JB002026>
- Huismans, Ritske S., & Beaumont, C. (2014). Rifted continental margins: The case for depth-dependent extension. *Earth and Planetary Science Letters*, 407(Supplement C), 148–162. <https://doi.org/10.1016/j.epsl.2014.09.032>
- Hutchison, I. (1985). The effects of sedimentation and compaction on oceanic heat flow. *Geophysical Journal International*, 82(3), 439–459. <https://doi.org/10.1111/j.1365-246X.1985.tb05145.x>
- Hyndman, R. D., Currie, C. A., & Mazzotti, S. P. (2005). Subduction zone backarcs, mobile belts, and orogenic heat. *GSA Today*, 15(2), 4–10.

I

- Innocent, C., Briquieu, L., & Cabanis, B. (1994). Sr-Nd isotope and trace-element geochemistry of late Variscan volcanism in the Pyrenees: Magmatism in post-orogenic extension? *Tectonophysics*, 238(1–4), 161–181. [https://doi.org/10.1016/0040-1951\(94\)90054-X](https://doi.org/10.1016/0040-1951(94)90054-X)
- Instituto Geológico y Minero de España (IGME). (1990). Documentos sobre la Geología del subsuelo de España.
- Iriarte, E. (2004). La Depresión Intermedia entre Leitza y Elizondo (Pirineo Occidental): Estratigrafía y relaciones tectónica-sedimentación durante el Cretácico. Unpublished Ph. D. Thesis, Universidad Del País Vasco, Euskal Herriko Unibertsitatea.
- Iriarte, E., & García-Mondéjar, J. (2001). Flysch siliciclástico y flysch carbonatado en el relleno del graben cretácico de Latsaga (“Depresión Intermedia”, Navarra). *Geogaceta*, (30), 207–210.
- Issler, D., McQueen, H., & Beaumont, C. (1989). Thermal and isostatic consequences of simple shear extension of the continental lithosphere. *Earth and Planetary Science Letters*, 91(3–4), 341–358. [https://doi.org/10.1016/0012-821X\(89\)90008-3](https://doi.org/10.1016/0012-821X(89)90008-3)

J

- Jackson, J. A. (1980). Reactivation of basement faults and crustal shortening in orogenic belts. *Nature*, 283, 343.
- James, V., & Canérot, J. (1999). Diapirisme et structuration post-triasique des Pyrénées occidentales et de l’Aquitaine méridionale (France). *Eclogae Geologicae Helveticae*, 92(1), 63–72.
- James, V., Canérot, J., & Biteau, J. (1996). Données nouvelles sur la phase de rifting atlantique des Pyrénées occidentales au Kimméridgien: la masse glissée d’Ouzous (Hautes Pyrénées). *Géologie de La France*, 3, 60–66.
- Jammes, S., & Lavier, L. L. (2019). Effect of contrasting strength from inherited crustal fabrics on the development of rifting margins. *Geosphere*. <https://doi.org/10.1130/GES01686.1>
- Jammes, Suzon, & Huismans, R. S. (2012). Structural styles of mountain building: Controls of lithospheric rheologic stratification and extensional inheritance: CRUSTAL STRENGTH AND MOUNTAIN BUILDING. *Journal of Geophysical Research: Solid Earth*, 117(B10). <https://doi.org/10.1029/2012JB009376>
- Jammes, Suzon, & Lavier, L. L. (2016). The effect of biminerale composition on extensional processes at lithospheric scale. *Geochemistry, Geophysics, Geosystems*, 17(8), 3375–3392. <https://doi.org/10.1002/2016GC006399>
- Jammes, Suzon, Manatschal, G., Lavier, L., & Masini, E. (2009). Tectonosedimentary evolution related to extreme crustal thinning ahead of a propagating ocean: Example of the western Pyrenees. *Tectonics*, 28(4), TC4012. <https://doi.org/10.1029/2008TC002406>
- Jammes, Suzon, Tiberi, C., & Manatschal, G. (2010a). 3D architecture of a complex transcurrent rift system: The example of the Bay of Biscay–Western Pyrenees. *Tectonophysics*, 489(1–4), 210–226. <https://doi.org/10.1016/j.tecto.2010.04.023>
- Jammes, Suzon, Lavier, L., & Manatschal, G. (2010b). Extreme crustal thinning in the Bay of Biscay and the Western Pyrenees: From observations to modeling: MODELIZATION OF EXTREME CRUSTAL THINNING. *Geochemistry, Geophysics, Geosystems*, 11(10), n/a-n/a. <https://doi.org/10.1029/2010GC003218>
- Jammes, Suzon, Manatschal, G., & Lavier, L. (2010c). Interaction between prerift salt and detachment faulting in hyperextended rift systems: The example of the Parentis and Mauléon basins (Bay of Biscay and western Pyrenees). *AAPG Bulletin*, 94(7), 957–975. <https://doi.org/10.1306/12090909116>

- Jammes, Suzon, Huismans, R. S., & Muñoz, J. A. (2014). Lateral variation in structural style of mountain building: controls of rheological and rift inheritance. *Terra Nova*, 26(3), 201–207. <https://doi.org/10.1111/ter.12087>
- Johnson, J. A., & Hall, C. A. (1989a). Tectono-stratigraphic model for the Massif D'Igountze–Mendibelza, western Pyrenees. *Journal of the Geological Society*, 146(6), 925. <https://doi.org/10.1144/gsjgs.146.6.0925>
- Johnson, J. A., & Hall, C. A. (1989b). The structural and sedimentary evolution of the Cretaceous North Pyrenean Basin, southern France. *Geological Society of America Bulletin*, 101(2), 231–247.
- Jolivet, M., Labaume, P., Monié, P., Brunel, M., Arnaud, N., & Campani, M. (2007). Thermochronology constraints for the propagation sequence of the south Pyrenean basement thrust system (France-Spain): PROPAGATION OF THE SOUTH PYRENEAN PRISM. *Tectonics*, 26(5), n/a–n/a. <https://doi.org/10.1029/2006TC002080>
- Jourdon, A., Le Pourhiet, L., Mouthereau, F., & Masini, E. (2019). Role of rift maturity on the architecture and shortening distribution in mountain belts. *Earth and Planetary Science Letters*, 512, 89–99. <https://doi.org/10.1016/j.epsl.2019.01.057>
- Juch, D., Krausse, H., Müller, D., Requadt, H., Schafer, D., Solé, J., & Villalobos, L. (1972). Mapa geológico de España E. 1:50.000, Serie MAGNA(Hoja de Maya de Baztán, 66).
- Julivert, M. (1971). Decollement tectonics in the Hercynian Cordillera of Northwest Spain. *American Journal of Science*, 270(1), 1–29. <https://doi.org/10.2475/ajs.270.1.1>

K

- Karner, G. D., & Driscoll, N. W. (1999). Style, timing and distribution of tectonic deformation across the Exmouth Plateau, northwest Australia, determined from stratal architecture and quantitative basin modelling. *Geological Society, London, Special Publications*, 164(1), 271–311. <https://doi.org/10.1144/GSL.SP.1999.164.01.14>
- Keen, C. E., Dickie, K., & Dafoe, L. T. (2018). Structural characteristics of the ocean-continent transition along the rifted continental margin, offshore central Labrador. *Marine and Petroleum Geology*, 89, 443–463. <https://doi.org/10.1016/j.marpetgeo.2017.10.012>
- Knausse, H. F., Müller, D., Requadt, H., Campos, J., García-Dueñas, V., Garrote, A., et al. (1972). Mapa geológico de España E. 1:50.000, Serie MAGNA(Hoja de Vera de Bidasoa, 65).
- Konstantinovskaya, E. A., Harris, L. B., Poulin, J., & Ivanov, G. M. (2007). Transfer zones and fault reactivation in inverted rift basins: Insights from physical modelling. *Tectonophysics*, 441(1–4), 1–26. <https://doi.org/10.1016/j.tecto.2007.06.002>
- Koopman, A., Speksnijder, A., & Horsfield, W. T. (1987). Sandbox model studies of inversion tectonics. *Tectonophysics*, 137(1–4), 379–388. [https://doi.org/10.1016/0040-1951\(87\)90329-5](https://doi.org/10.1016/0040-1951(87)90329-5)
- Koopmann, H., Brune, S., Franke, D., & Breuer, S. (2014). Linking rift propagation barriers to excess magmatism at volcanic rifted margins. *Geology*, 42(12), 1071–1074. <https://doi.org/10.1130/G36085.1>
- Krabbendam, M., & Barr, T. D. (2000). Proterozoic orogens and the break-up of Gondwana: why did some orogens not rift? *Journal of African Earth Sciences*, 31(1), 35–49. [https://doi.org/10.1016/S0899-5362\(00\)00071-3](https://doi.org/10.1016/S0899-5362(00)00071-3)

L

- Labaume, P., Séguret, M., & Seyve, C. (1985). Evolution of a turbiditic foreland basin and analogy with an accretionary prism: Example of the Eocene South-Pyrenean Basin. *Tectonics*, 4(7), 661–685. <https://doi.org/10.1029/TC004i007p00661>
- Lacombe, O., & Bellahsen, N. (2016). Thick-skinned tectonics and basement-involved fold–thrust belts: insights from selected Cenozoic orogens. *Geological Magazine*, 153(5–6), 763–810. <https://doi.org/10.1017/S0016756816000078>
- Lagabrielle, Y., & Bodinier, J.-L. (2008). Submarine reworking of exhumed subcontinental mantle rocks: field evidence from the Lherz peridotites, French Pyrenees. *Terra Nova*, 20(1), 11–21. <https://doi.org/10.1111/j.1365-3121.2007.00781.x>
- Lagabrielle, Y., Labaume, P., & de Saint Blanquat, M. (2010). Mantle exhumation, crustal denudation, and gravity tectonics during Cretaceous rifting in the Pyrenean realm (SW Europe): Insights from the geological setting of the lherzolite bodies. *Tectonics*, 29(4), TC4012. <https://doi.org/10.1029/2009TC002588>
- Lagabrielle, Y., Clerc, C., Vauchez, A., Lahfid, A., Labaume, P., Azambre, B., et al. (2016). Very high

- geothermal gradient during mantle exhumation recorded in mylonitic marbles and carbonate breccias from a Mesozoic Pyrenean palaeomargin (Lherz area, North Pyrenean Zone, France). *From Rifting to Mountain Building: The Pyrenean Belt*, 348(3), 290–300. <https://doi.org/10.1016/j.crte.2015.11.004>
- Lago, M., Arranz, E., Pocoví, A., Galé, C., & Gil-Imaz, A. (2004). Permian magmatism and basin dynamics in the southern Pyrenees: a record of the transition from late Variscan transtension to early Alpine extension. *Geological Society, London, Special Publications*, 223(1), 439–464. <https://doi.org/10.1144/GSL.SP.2004.223.01.19>
- Lamare, P. (1936). *Recherches géologiques dans les Pyrénées basques d'Espagne* (Thèse). Université de Paris (1896-1968). Faculté des sciences, France.
- Larrasoaña, J. C., Parés, J. M., Millán, H., del Valle, J., & Pueyo, E. L. (2003a). Paleomagnetic, structural, and stratigraphic constraints on transverse fault kinematics during basin inversion: The Pamplona Fault (Pyrenees, north Spain). *Tectonics*, 22(6), n/a-n/a. <https://doi.org/10.1029/2002TC001446>
- Larrasoaña, J. C., Parés, J. M., del Valle, J., & Millán, H. (2003b). Triassic paleomagnetism from the Western Pyrenees revisited: implications for the Iberian–Eurasian Mesozoic plate boundary. *Paleomagnetism Applied to Tectonics. A Tribute to Rob Van Der Voo*, 362(1), 161–182. [https://doi.org/10.1016/S0040-1951\(02\)00636-4](https://doi.org/10.1016/S0040-1951(02)00636-4)
- Laumonier, BERNARD. (2008). Les Pyrénées pré-hercyniennes et hercyniennes. J. CANÉROT, J.-P. COLIN, J.-P. PLATEL & M. BILOTTE, *Pyrénées d'hier et d'aujourd'hui*, Pau, 20–21.
- Laumonier, Bernard, Barbey, P., Denèle, Y., Olivier, P., & Paquette, J.-L. (2014). Réconcilier les données stratigraphiques, radiométriques, plutoniques, vol-caniques et structurales au Pennsylvanien supérieur (Stéphanien–Autunien pp) dans l'Est des Pyrénées hercyniennes (France, Espagne). *Rev. Géol. Pyrén*, 1(2), 10.
- Lavier, L. L., & Manatschal, G. (2006). A mechanism to thin the continental lithosphere at magma-poor margins. *Nature*, 440, 324.
- Le Calvez, J. H., & Vendeville, B. C. (2002). Experimental designs to model along-strike fault interaction. *Journal of the Virtual Explorer*, 07, 1–17. <https://doi.org/10.3809/jvirtex.2002.00043>
- Le Pichon, X., & Sibuet, J.-C. (1971). Western extension of boundary between European and Iberian plates during the Pyrenean orogeny. *Earth and Planetary Science Letters*, 12, 83–88.
- Le Pochat, G. (1982). Reconnaissance des écaillés de cristallin et de Paléozoïque dans les massifs paléozoïques basques. *Progr. Géol. Prof. Fr., Bur. Rech. Géol. Min.*, 7, 285–287.
- Le Pochat, G., Bolthenhagen, C., Lenguin, M., Lorsignol, S., & Thibault, C. (1976). Feuille de Mauléon-Licharre. *Carte Géologique de La France A*, 1(50), 000.
- Le Pourhiet, L., May, D. A., Huille, L., Watremez, L., & Leroy, S. (2017). A genetic link between transform and hyper-extended margins. *Earth and Planetary Science Letters*, 465, 184–192. <https://doi.org/10.1016/j.epsl.2017.02.043>
- Lemirre, B., Duchêne, S., De Saint Blanquat, M., & Pujol, M. (2016). État thermique de la croûte varisque dans le massif nord-pyrénéen du Saint Barthélémy (p. 198). Presented at the 25^{ème} Réunion des sciences de la Terre (RST 2016).
- Lepvrier, C., & Martínez-García, E. (1990). Fault development and stress evolution of the post-Hercynian Asturian Basin (Asturias and Cantabria, northwestern Spain). *Tectonophysics*, 184(3–4), 345–356. [https://doi.org/10.1016/0040-1951\(90\)90447-G](https://doi.org/10.1016/0040-1951(90)90447-G)
- Leroy, S., Lucazeau, F., d'Acremont, E., Watremez, L., Autin, J., Rouzo, S., et al. (2010). Contrasted styles of rifting in the eastern Gulf of Aden: A combined wide-angle, multichannel seismic, and heat flow survey. *Geochemistry, Geophysics, Geosystems*, 11(7), n/a-n/a. <https://doi.org/10.1029/2009GC002963>
- Likerman, J., Burlando, J. F., Cristallini, E. O., & Ghiglione, M. C. (2013). Along-strike structural variations in the Southern Patagonian Andes: Insights from physical modeling. *Tectonophysics*, 590, 106–120. <https://doi.org/10.1016/j.tecto.2013.01.018>
- Lindholm, R. C. (1978). Triassic-Jurassic faulting in eastern North America— A model based on pre-Triassic structures. *Geology*, 6(6), 365. [https://doi.org/10.1130/0091-7613\(1978\)6<365:TFIENA>2.0.CO;2](https://doi.org/10.1130/0091-7613(1978)6<365:TFIENA>2.0.CO;2)
- Lister, G., Etheridge, M., & Symonds, P. (1986). Detachment faulting and the evolution of passive continental margins. *Geology*, 14(3), 246–250.
- Lizarralde, D., Axen, G. J., Brown, H. E., Fletcher, J. M., González-Fernández, A., Harding, A. J., et al. (2007). Variation in styles of rifting in the Gulf of California. *Nature*, 448, 466.
- Llanos, H. (1980). Estudio geológico del borde sur del macizo de Cinco Villas, Transversal Huici-Leiza (Navarra). *Univ. País Vasco, UPV, EHU*, 75–116.

- López-Gómez, J., Martín-González, F., Heredia, N., de la Horra, R., Barrenechea, J. F., Cadenas, P., et al. (2019). New lithostratigraphy for the Cantabrian Mountains: A common tectono-stratigraphic evolution for the onset of the Alpine cycle in the W Pyrenean realm, N Spain. *Earth-Science Reviews*, 188, 249–271. <https://doi.org/10.1016/j.earscirev.2018.11.008>
- Lowell, J. D. (1995). Mechanics of basin inversion from worldwide examples. *Geological Society, London, Special Publications*, 88(1), 39–57. <https://doi.org/10.1144/GSL.SP.1995.088.01.04>
- Lucas, C. (1987). Estratigrafía y datos Morfo-estructurales sobre el Permico y Triasico de fosas norte Pirenaicas. *Cuad. Geol. Iberica*, 11, 25–40.
- Lucazeau, F., & Le Douaran, S. (1985). The blanketing effect of sediments in basins formed by extension: a numerical model. Application to the Gulf of Lion and Viking graben. *Earth and Planetary Science Letters*, 74(1), 92–102. [https://doi.org/10.1016/0012-821X\(85\)90169-4](https://doi.org/10.1016/0012-821X(85)90169-4)
- Lucazeau, Francis, Leroy, S., Bonneville, A., Goutorbe, B., Rolandone, F., d'Acromont, E., et al. (2008). Persistent thermal activity at the Eastern Gulf of Aden after continental break-up. *Nature Geoscience*, 1, 854.
- Lundin, E. R., & Doré, A. G. (2011). Hyperextension, serpentinitization, and weakening: A new paradigm for rifted margin compressional deformation. *Geology*, 39(4), 347–350. <https://doi.org/10.1130/G31499.1>

M

- Macchiavelli, C., Vergés, J., Schettino, A., Fernández, M., Turco, E., Casciello, E., et al. (2017). A New Southern North Atlantic Isochron Map: Insights Into the Drift of the Iberian Plate Since the Late Cretaceous. *Journal of Geophysical Research: Solid Earth*, 122(12), 9603–9626. <https://doi.org/10.1002/2017JB014769>
- Manatschal, G. (2004). New models for evolution of magma-poor rifted margins based on a review of data and concepts from West Iberia and the Alps. *International Journal of Earth Sciences*, 93(3). <https://doi.org/10.1007/s00531-004-0394-7>
- Manatschal, G., & Müntener, O. (2009). A type sequence across an ancient magma-poor ocean–continent transition: the example of the western Alpine Tethys ophiolites. *Tectonophysics*, 473(1–2), 4–19. <https://doi.org/10.1016/j.tecto.2008.07.021>
- Manatschal, G., Lavier, L., & Chenin, P. (2015). The role of inheritance in structuring hyperextended rift systems: Some considerations based on observations and numerical modeling. *Gondwana Research*, 27(1), 140–164. <https://doi.org/10.1016/j.gr.2014.08.006>
- Martínez Catalán, J., Arenas, R., García, F. D., Cuadra, P. G., Gómez-Barreiro, J., Abati, J., et al. (2007). Space and time in the tectonic evolution of the northwestern Iberian Massif: Implications for the Variscan belt. In 4-D framework of continental crust (Vol. 200, pp. 403–423). Geological Society of America Memoir Boulder, Colorado.
- Martínez Catalán, J. R., Arenas, R., Díaz García, F., & Abati, J. (1997). Variscan accretionary complex of northwest Iberia: Terrane correlation and succession of tectonothermal events. *Geology*, 25(12), 1103. [https://doi.org/10.1130/0091-7613\(1997\)025<1103:VACONI>2.3.CO;2](https://doi.org/10.1130/0091-7613(1997)025<1103:VACONI>2.3.CO;2)
- Martínez-García, E. (2013). An Alleghenian orocline: the Asturian Arc, northwestern Spain. *International Geology Review*, 55(3), 367–381. <https://doi.org/10.1080/00206814.2012.713544>
- Martínez-Torres, L. (1992). El Manto de los Mármoles (Pirineo Occidental): geología estructural y evolución geodinámica. Servicio Editorial de la Universidad del País Vasco= Argitarapen Zerbitzua, Euskal Herriko Unibertsitatea.
- Martínez-Torres, L. M. (1993). Corte balanceado de la Sierra Cantabria (cabalgamiento de la Cuenca Vasco-Cantábrica sobre la Cuenca del Ebro).
- Masini, E., Manatschal, G., Mohn, G., Ghienne, J.-F., & Lafont, F. (2011). The tectono-sedimentary evolution of a supra-detachment rift basin at a deep-water magma-poor rifted margin: the example of the Samedan Basin preserved in the Err nappe in SE Switzerland. *Basin Research*, 23(6), 652–677. <https://doi.org/10.1111/j.1365-2117.2011.00509.x>
- Masini, E., Manatschal, G., & Mohn, G. (2013). The Alpine Tethys rifted margins: Reconciling old and new ideas to understand the stratigraphic architecture of magma-poor rifted margins. *Sedimentology*, 60(1), 174–196. <https://doi.org/10.1111/sed.12017>
- Masini, E., Manatschal, G., Tugend, J., Mohn, G., & Flament, J.-M. (2014). The tectono-sedimentary evolution of a hyper-extended rift basin: the example of the Arzacq–Mauléon rift system (Western Pyrenees, SW France). *International Journal of Earth Sciences*, 103(6), 1569–1596. <https://doi.org/10.1007/s00531-014-1023-8>
- Mathey, B. (1986). Les flyschs créacé supérieur des Pyrénées basques : âge, anatomie, origine du maté-

- riel, milieu de dépôt et relations avec l'ouverture du Golfe de Gascogne.
- Mathey, B., Floquet, M., & Miguel Martínez-Torres, L. (1999). The Leiza palaeo-fault: Role and importance in the Upper Cretaceous sedimentation and palaeogeography of the Basque Pyrenees (Spain). *Comptes Rendus de l'Académie Des Sciences - Series IIA - Earth and Planetary Science*, 328(6), 393–399. [https://doi.org/10.1016/S1251-8050\(99\)80105-0](https://doi.org/10.1016/S1251-8050(99)80105-0)
- Mattauer, M., & Séguret, M. (1971). Les relations entre la chaîne des Pyrénées et le golfe de Gascogne. J. Debyser, X. Le Pichon, and L. Montadert. *Technip*, Paris, 1–24.
- Mattauer, M., Dalmayrac, B., Laubacher, G., & Vidal, J. (1967). Contribution à l'étude des tectoniques superposées dans la chaîne hercynienne: le 'synclinal' paléozoïque de Villefranche-de-Conflent (Pyrénées orientales). *Comptes Rendus de l'Académie Des Sciences*, Paris, 265, 1361–1364.
- Mattauer, Maurice. (1968). Les traits structuraux essentiels de la chaîne pyrénéenne. *Revue de Geologie Dynamique et de Géographie Physique*, 10(1), 3–11.
- Mattauer, Maurice, & Henry, J. (1974). Pyrenees. *Geological Society*, London, Special Publications, 4(1), 3–21. <https://doi.org/10.1144/GSL.SP.2005.004.01.01>
- Matte, P. (2001). The Variscan collage and orogeny (480–290 Ma) and the tectonic definition of the Armorica microplate: a review. *Terra Nova*, 13(2), 122–128. <https://doi.org/10.1046/j.1365-3121.2001.00327.x>
- Mattioni, L., Le Pourhiet, L., & Moretti, I. (2006). Rifting through a heterogeneous crust: insights from analogue models and application to the Gulf of Corinth. *Geological Society*, London, Special Publications, 253(1), 213–231. <https://doi.org/10.1144/GSL.SP.2006.253.01.11>
- McClay, K., Muñoz, J.-A., & García-Senz, J. (2004). Extensional salt tectonics in a contractional orogen: A newly identified tectonic event in the Spanish Pyrenees. *Geology*, 32(9), 737. <https://doi.org/10.1130/G20565.1>
- McClay, K. R. (1990). Extensional fault systems in sedimentary basins: a review of analogue model studies. *Marine and Petroleum Geology*, 7(3), 206–233. [https://doi.org/10.1016/0264-8172\(90\)90001-W](https://doi.org/10.1016/0264-8172(90)90001-W)
- McClay, K. R., & White, M. J. (1995). Analogue modelling of orthogonal and oblique rifting. *Marine and Petroleum Geology*, 12(2), 137–151. [https://doi.org/10.1016/0264-8172\(95\)92835-K](https://doi.org/10.1016/0264-8172(95)92835-K)
- McDermott, K., Belligham, P., Pindell, J., Graham, R., & Horn, B. (2014). Some insights into rifted margin development and the structure of the continent-ocean transition using a global deep seismic reflection database. In *Go Deep: Back to the Source: 4th Atlantic Conjugate Margins Conference Abstracts Volume* (pp. 62–65).
- McKenzie, D. (1978). Some remarks on the development of sedimentary basins. *Earth and Planetary Science Letters*, 40(1), 25–32. [https://doi.org/10.1016/0012-821X\(78\)90071-7](https://doi.org/10.1016/0012-821X(78)90071-7)
- Mendia, M. S., & Ibarra, J. I. G. (1991). High-grade metamorphic rocks and peridotites along the Leiza Fault (Western Pyrenees, Spain). *Geologische Rundschau*, 80(1), 93–107. <https://doi.org/10.1007/BF01828769>
- Mercier de Lépinay, M., Loncke, L., Basile, C., Roest, W. R., Patriat, M., Maillard, A., & De Clarens, P. (2016). Transform continental margins – Part 2: A worldwide review. *Tectonophysics*, 693, 96–115. <https://doi.org/10.1016/j.tecto.2016.05.038>
- Meschede, M. (1987). The tectonic and sedimentary development of the Biscay synclinorium in Northern Spain. *Geologische Rundschau*, 76(2), 567–577. <https://doi.org/10.1007/BF01821092>
- Mohn, G., Manatschal, G., Masini, E., & Müntener, O. (2011). Rift-related inheritance in orogens: a case study from the Austroalpine nappes in Central Alps (SE-Switzerland and N-Italy). *International Journal of Earth Sciences*, 100(5), 937–961. <https://doi.org/10.1007/s00531-010-0630-2>
- Mohn, Geoffroy, Manatschal, G., Müntener, O., Beltrando, M., & Masini, E. (2010). Unravelling the interaction between tectonic and sedimentary processes during lithospheric thinning in the Alpine Tethys margins. *International Journal of Earth Sciences*, 99(1), 75–101. <https://doi.org/10.1007/s00531-010-0566-6>
- Mohn, Geoffroy, Manatschal, G., Beltrando, M., & Hauptert, I. (2014). The role of rift-inherited hyper-extension in Alpine-type orogens. *Terra Nova*, 26(5), 347–353. <https://doi.org/10.1111/ter.12104>
- Mohn, Geoffroy, Karner, G. D., Manatschal, G., & Johnson, C. A. (2015). Structural and stratigraphic evolution of the Iberia–Newfoundland hyper-extended rifted margin: a quantitative modelling approach. *Geological Society*, London, Special Publications, 413(1), 53. <https://doi.org/10.1144/SP413.9>
- Mohr, K., & Pilger, A. (1965). Das Nord-Süd-streichende Lineament von Elizondo in den westlichen Pyrenäen. *Geologische Rundschau*, 54(2), 1044–1060. <https://doi.org/10.1007/BF01820771>
- Montadert, L., Winnock, E., Deltiel, J. R., & Grau, G. (1974). Continental Margins of Galicia-Portugal

- and Bay of Biscay. In C. A. Burk & C. L. Drake (Eds.), *The Geology of Continental Margins* (pp. 323–342). Berlin, Heidelberg: Springer Berlin Heidelberg. https://doi.org/10.1007/978-3-662-01141-6_24
- Montigny, R., Azambre, B., Rossy, M., & Thuizat, R. (1986). K-Ar Study of cretaceous magmatism and metamorphism in the pyrenees: Age and length of rotation of the Iberian Peninsula. *The Geological Evolution of the Pyrenees*, 129(1), 257–273. [https://doi.org/10.1016/0040-1951\(86\)90255-6](https://doi.org/10.1016/0040-1951(86)90255-6)
- Morley, C., Nelson, R., Patton, T., & Munn, S. (1990). Transfer zones in the East African rift system and their relevance to hydrocarbon exploration in rifts (1). *AAPG Bulletin*, 74(8), 1234–1253.
- Mouthereau, F., Watts, A. B., & Burov, E. (2013). Structure of orogenic belts controlled by lithosphere age. *Nature Geoscience*, 6, 785.
- Mouthereau, F., Filleaudeau, P.-Y., Vacherat, A., Pik, R., Lacombe, O., Fellin, M. G., et al. (2014). Placing limits to shortening evolution in the Pyrenees: Role of margin architecture and implications for the Iberia/Europe convergence. *Tectonics*, 33(12), 2014TC003663. <https://doi.org/10.1002/2014TC003663>
- Muller, J., & Roger, P. (1977). L'Evolution structurale des Pyrénées (Domaine central et occidental) Le segment hercynien, la chaîne de fond alpine. *Géologie Alpine*, 53(2), 149–191.
- Muñoz, J. A. (1992). Evolution of a continental collision belt: ECORS-Pyrenees crustal balanced cross-section. *Thrust Tectonics*, 235–246.

N

- Nagel, T. J., & Buck, W. R. (2004). Symmetric alternative to asymmetric rifting models. *Geology*, 32(11), 937. <https://doi.org/10.1130/G20785.1>
- Nagel, T. J., & Buck, W. R. (2007). Control of rheological stratification on rifting geometry: a symmetric model resolving the upper plate paradox. *International Journal of Earth Sciences*, 96(6), 1047–1057. <https://doi.org/10.1007/s00531-007-0195-x>
- Naliboff, J. B., Buitter, S. J. H., Péron-Pinvidic, G., Osmundsen, P. T., & Tetreault, J. (2017). Complex fault interaction controls continental rifting. *Nature Communications*, 8(1), 1179. <https://doi.org/10.1038/s41467-017-00904-x>
- Neres, M., Font, E., Miranda, J. M., Camps, P., Terrinha, P., & Mirão, J. (2012). Reconciling Cretaceous paleomagnetic and marine magnetic data for Iberia: New Iberian paleomagnetic poles: IBERIA-PALEOMAGNETIC AND MAGNETIC DATA. *Journal of Geophysical Research: Solid Earth*, 117(B6), n/a-n/a. <https://doi.org/10.1029/2011JB009067>
- Neres, M., Miranda, J. M., & Font, E. (2013). Testing Iberian kinematics at Jurassic-Cretaceous times. *Tectonics*, 32(5), 1312–1319. <https://doi.org/10.1002/tect.20074>
- Nirrengarten, M., Manatschal, G., Yuan, X. P., Kuszniir, N. J., & Maillot, B. (2016). Application of the critical Coulomb wedge theory to hyper-extended, magma-poor rifted margins. *Earth and Planetary Science Letters*, 442(Supplement C), 121–132. <https://doi.org/10.1016/j.epsl.2016.03.004>
- Nirrengarten, M., Manatschal, G., Tugend, J., Kuszniir, N., & Sauter, D. (2018). Kinematic Evolution of the Southern North Atlantic: Implications for the Formation of Hyperextended Rift Systems: Kinematic of Hyperextended Rift Systems. *Tectonics*, 37(1), 89–118. <https://doi.org/10.1002/2017TC004495>
- Nirrengarten, Michael, Manatschal, G., Tugend, J., Kuszniir, N. J., & Sauter, D. (2017). Nature and origin of the J-magnetic anomaly offshore Iberia–Newfoundland: implications for plate reconstructions. *Terra Nova*, 29(1), 20–28.
- Nonn, C., Leroy, S., Khanbari, K., & Ahmed, A. (2017). Tectono-sedimentary evolution of the eastern Gulf of Aden conjugate passive margins: Narrowness and asymmetry in oblique rifting context. *Tectonophysics*, 721, 322–348. <https://doi.org/10.1016/j.tecto.2017.09.024>

O

- Oliva-Urcia, B., Román-Berdiel, T., Casas, A. M., Pueyo, E. L., & Osácar, C. (2010). Tertiary compressional overprint on Aptian–Albian extensional magnetic fabrics, North-Pyrenean Zone. *Journal of Structural Geology*, 32(3), 362–376. <https://doi.org/10.1016/j.jsg.2010.01.009>
- Olivet, J. (1996a). Kinematics of the Iberian plate. *Bulletin Des Centres de Recherches Exploration-Production Elf Aquitaine*, 20(1), 131–195.
- Olivet, J. (1996b). La cinématique de la plaque ibérique. *Bull. Cent. Rech. Explor. Prod. Elf Aquitaine*, 20(1), 131–195.
- Olivier, P. (2015). Comment on “Thermal control on the modes of crustal thinning leading to mantle

- exhumation: Insights from the Cretaceous Pyrenean hot paleomargins” by Clerc and Lagabrielle: Comment on Clerc & Lagabrielle [2014]. *Tectonics*, 34(10), 2271–2274. <https://doi.org/10.1002/2014TC003755>
- Omodeo-Salè, S., Guimerà, J., Mas, R., & Arribas, J. (2014). Tectono-stratigraphic evolution of an inverted extensional basin: the Cameros Basin (north of Spain). *International Journal of Earth Sciences*, 103(6), 1597–1620. <https://doi.org/10.1007/s00531-014-1026-5>
- Omodeo-Salé, S., Salas, R., Guimerà, J., Ondrak, R., Mas, R., Arribas, J., et al. (2017). Subsidence and thermal history of an inverted Late Jurassic-Early Cretaceous extensional basin (Cameros, North-central Spain) affected by very low- to low-grade metamorphism. *Basin Research*, 29, 156–174. <https://doi.org/10.1111/bre.12142>
- Osmundsen, P. T., & Ebbing, J. (2008). Styles of extension offshore mid-Norway and implications for mechanisms of crustal thinning at passive margins. *Tectonics*, 27(6), n/a–n/a. <https://doi.org/10.1029/2007TC002242>
- Osmundsen, Per Terje, & Redfield, T. F. (2011). Crustal taper and topography at passive continental margins: Crustal taper and topography. *Terra Nova*, 23(6), 349–361. <https://doi.org/10.1111/j.1365-3121.2011.01014.x>

P

- Pascal, A. (1985). Les systèmes biosédimentaires urgoniens (Aptien-Albien) sur la marge nord-ibérique.
- Pascal, C., van Wijk, J. W., Cloetingh, S. A. P. L., & Davies, G. R. (2002). Effect of lithosphere thickness heterogeneities in controlling rift localization: Numerical modeling of the Oslo Graben: NUMERICAL MODELING OF THE OSLO GRABEN. *Geophysical Research Letters*, 29(9), 69-1-69–4. <https://doi.org/10.1029/2001GL014354>
- Peacock, D. C. ., & Sanderson, D. . (1991). Displacements, segment linkage and relay ramps in normal fault zones. *Journal of Structural Geology*, 13(6), 721–733. [https://doi.org/10.1016/0191-8141\(91\)90033-F](https://doi.org/10.1016/0191-8141(91)90033-F)
- Pedreira, D., Pulgar, J. A., Gallart, J., & Díaz, J. (2003). Seismic evidence of Alpine crustal thickening and wedging from the western Pyrenees to the Cantabrian Mountains (north Iberia). *Journal of Geophysical Research: Solid Earth*, 108(B4), 2204. <https://doi.org/10.1029/2001JB001667>
- Pedreira, D., Pulgar, J. A., Gallart, J., & Torné, M. (2007). Three-dimensional gravity and magnetic modeling of crustal indentation and wedging in the western Pyrenees–Cantabrian Mountains. *Journal of Geophysical Research: Solid Earth*, 112(B12), B12405. <https://doi.org/10.1029/2007JB005021>
- Pedreira, David, Afonso, J. C., Pulgar, J. A., Gallastegui, J., Carballo, A., Fernández, M., et al. (2015). Geophysical-petrological modeling of the lithosphere beneath the Cantabrian Mountains and the North-Iberian margin: geodynamic implications. *Lithos*, 230, 46–68. <https://doi.org/10.1016/j.lithos.2015.04.018>
- Pedreira, A., García-Senz, J., Ayala, C., Ruiz-Constán, A., Rodríguez-Fernández, L. R., Robador, A., & González Menéndez, L. (2017). Reconstruction of the Exhumed Mantle Across the North Iberian Margin by Crustal-Scale 3-D Gravity Inversion and Geological Cross Section: Mantle Along the Basque-Cantabrian Basin. *Tectonics*, 36(12), 3155–3177. <https://doi.org/10.1002/2017TC004716>
- Pérez-Estaún, A., Bastida, F., Alonso, J. L., Marquínez, J., Aller, J., Alvarez-Marrón, J., et al. (1988). A thin-skinned tectonics model for an arcuate fold and thrust belt: The Cantabrian Zone (Variscan Ibero-Armorican Arc). *Tectonics*, 7(3), 517–537. <https://doi.org/10.1029/TC007i003p00517>
- Pérez-Gussinyé, M., & Reston, T. J. (2001). Rheological evolution during extension at nonvolcanic rifted margins: Onset of serpentinization and development of detachments leading to continental breakup. *Journal of Geophysical Research: Solid Earth*, 106(B3), 3961–3975. <https://doi.org/10.1029/2000JB900325>
- Péron-Pinvidic, G., Manatschal, G., Dean, S. M., & Minshull, T. A. (2008). Compressional structures on the West Iberia rifted margin: controls on their distribution. *Geological Society, London, Special Publications*, 306(1), 169–183. <https://doi.org/10.1144/SP306.8>
- Péron-Pinvidic, Gwenn, & Manatschal, G. (2010). From microcontinents to extensional allochthons: witnesses of how continents rift and break apart? *Petroleum Geoscience*, 16(3), 189. <https://doi.org/10.1144/1354-079309-903>
- Péron-Pinvidic, Gwenn, Manatschal, G., & Osmundsen, P. T. (2013). Structural comparison of archetypal Atlantic rifted margins: A review of observations and concepts. *Marine and Petroleum Geology*, 43(Supplement C), 21–47. <https://doi.org/10.1016/j.marpetgeo.2013.02.002>
- Péron-Pinvidic, Gwenn, Manatschal, G., Masini, E., Sutra, E., Flament, J. M., Hauptert, I., & Unternehr, P. (2017). Unravelling the along-strike variability of the Angola–Gabon rifted margin: a mapping

- approach. Geological Society, London, Special Publications, 438(1), 49–76.
- Petri, B., Lescoutre, R., Manatschal, G., Masini, E., & Müntener, O. (2018). A crustal view on the pyrenean rift system: the Arzacq-Mauléon basins (W Pyrenees) (Vol. 20, p. 10068). Presented at the EGU General Assembly Conference Abstracts.
- Petri, B., Duretz, T., Mohn, G., Schmalholz, S. M., Karner, G. D., & Müntener, O. (2019). Thinning mechanisms of heterogeneous continental lithosphere. *Earth and Planetary Science Letters*, 512, 147–162. <https://doi.org/10.1016/j.epsl.2019.02.007>
- Peybernes, B. (1978). Dans les Pyrenees la paleogeographie antecenomaniennne infirme la theorie d'un coulissement senestre de plusieurs centaines de kilometres le long de la "faille nord-pyreneenne" des auteurs. *Bulletin de La Société Géologique de France*, S7-XX(5), 701–709. <https://doi.org/10.2113/gssgfbull.S7-XX.5.701>
- Peybernes, B. (1979). L'Urgonien des Pyrénées; Essai de synthèse. *Geobios*, 12, 79–87. [https://doi.org/10.1016/S0016-6995\(79\)80052-2](https://doi.org/10.1016/S0016-6995(79)80052-2)
- Peybernes, B. (1982). Création puis évolution de la marge nord-ibérique des Pyrénées au Crétacé inférieur. *Cuadernos de Geología Ibérica*, Madrid, 8, 983–1000.
- Peybernes, B., & Souquet, P. (1984). Basement blocks and tecto-sedimentary evolution in the Pyrenees during Mesozoic times. *Geological Magazine*, 121(05), 397. <https://doi.org/10.1017/S0016756800029927>
- Pflug, R., & Schöll, W. (1976). Un bloque de material jurásico metamorizado en el Keuper del Diapiro de Estella (Navarra). *Munibe*, 4, 349–353.
- Pinto, V. H. G., Manatschal, G., Karpoff, A. M., & Viana, A. (2015). Tracing mantle-reacted fluids in magma-poor rifted margins: The example of Alpine Tethyan rifted margins. *Geochemistry, Geophysics, Geosystems*, 16(9), 3271–3308. <https://doi.org/10.1002/2015GC005830>
- Popov, A. A., & Sobolev, S. V. (2008). SLIM3D: A tool for three-dimensional thermomechanical modeling of lithospheric deformation with elasto-visco-plastic rheology. *Recent Advances in Computational Geodynamics: Theory, Numerics and Applications*, 171(1), 55–75. <https://doi.org/10.1016/j.pepi.2008.03.007>
- Portero, J., Ramírez del Pozo, J., & Aguilar, M. (1979). Mapa geológico 1: 50 000, Hoja 170 (Haro). IGME, Madrid.
- Poujol, M., Boulvais, P., & Kosler, J. (2010). Regional-scale Cretaceous albitization in the Pyrenees: evidence from *in situ* U–Th–Pb dating of monazite, titanite and zircon. *Journal of the Geological Society*, 167(4), 751. <https://doi.org/10.1144/0016-76492009-144>
- del Pozo, J. R. (1969). Síntesis estratigráfica y micropaleontológica de las facies Purbeckiense y Wealdense del Norte de España. Ed. CEPESA.
- Prave, A. R. (1986). An Interpretation of Late Cretaceous Sedimentation and Tectonics and the Nature of Pyrenean Deformation in the Northwestern Basque Pyrenees: A Thesis in Geology. Pennsylvania State University.
- Puelles, P., Ábalos, B., García de Madinabeitia, S., Sánchez-Lorda, M. E., Fernández-Armas, S., & Gil Ibarra, J. I. (2014). Provenance of quartz-rich metamorphic tectonite pebbles from the “Black Flysch” (W Pyrenees, N Spain): An EBSD and detrital zircon LA–ICP–MS study. *Tectonophysics*, 632, 123–137. <https://doi.org/10.1016/j.tecto.2014.06.004>
- Puigdefàbregas, C., & Souquet, P. (1986). Tecto-sedimentary cycles and depositional sequences of the Mesozoic and Tertiary from the Pyrenees. *The Geological Evolution of the Pyrenees*, 129(1), 173–203. [https://doi.org/10.1016/0040-1951\(86\)90251-9](https://doi.org/10.1016/0040-1951(86)90251-9)
- Puigdefàbregas, C., Rojas Tapia, B., Sánchez Carpintero, I., & del Valle, J. (1976). Mapa geológico de España E. 1:50.000, Serie MAGNA(Hoja de Aoiz, 142).
- Puigdefàbregas, C., Muñoz, J. A., & Vergés, J. (1992). Thrusting and foreland basin evolution in the Southern Pyrenees. In K. R. McClay (Ed.), *Thrust Tectonics* (pp. 247–254). Dordrecht: Springer Netherlands. https://doi.org/10.1007/978-94-011-3066-0_22
- Pujalte, V. (1977). El complejo Purbeck-Weald de Santander: estratigrafía y sedimentación. Unpublished Ph. D. Thesis. Univ. de Bilbao, 202.
- Pujalte, Victoriano. (1981). Sedimentary succession and palaeoenvironments within a fault-controlled basin: The ‘wealden’ of the Santander area, northern Spain. *Sedimentary Geology*, 28(4), 293–325. [https://doi.org/10.1016/0037-0738\(81\)90051-8](https://doi.org/10.1016/0037-0738(81)90051-8)
- Pulgar, J. A., Gallart, J., Fernández-Viejo, G., Pérez-Estaún, A., & Álvarez-Marrón, J. (1996). Seismic image of the Cantabrian Mountains in the western extension of the Pyrenees from integrated ESCIN reflection and refraction data. *Tectonophysics*, 264(1–4), 1–19. [https://doi.org/10.1016/S0040-1951\(96\)00114-X](https://doi.org/10.1016/S0040-1951(96)00114-X)

Q

- Quintana, L., Pulgar, J. A., & Alonso, J. L. (2015). Displacement transfer from borders to interior of a plate: A crustal transect of Iberia. *Tectonophysics*, 663, 378–398. <https://doi.org/10.1016/j.tecto.2015.08.046>
- Quintana, Luis, Alonso, J. L., Pulgar, J. A., & Rodríguez-Fernández, L. R. (2006). Transpressional inversion in an extensional transfer zone (the Saltacaballos fault, northern Spain). *Journal of Structural Geology*, 28(11), 2038–2048. <https://doi.org/10.1016/j.jsg.2006.06.013>

R

- Ramírez, J. I., Olivé, A., Aguilar, M. J., Ramírez, J., Meléndez, A., Pujalte, V., et al. (1986). Mapa geológico de España E. 1:50.000, Serie MAGNA(Hoja de Tolosa, 89).
- Ramírez Merino, J. J., Olivé Davo, A., Carballo Olivares, A., Villalobos Vilches, L., & León González, L. (1984). Mapa geológico de España E. 1:50.000, Serie MAGNA(Hoja de Estella, 140).
- Ranero, C. R., & Pérez-Gussinyé, M. (2010). Sequential faulting explains the asymmetry and extension discrepancy of conjugate margins. *Nature*, 468, 294.
- Rat, J., Mouthereau, F., Brichau, S., Crémades, A., Bernet, M., Balvay, M., et al. (2019). TECTONOTHERMAL EVOLUTION OF THE CAMEROS BASIN: IMPLICATIONS FOR TECTONICS OF NORTH-IBERIA. *Tectonics*. <https://doi.org/10.1029/2018TC005294>
- Rat, P. (1988). The Basque-Cantabrian basin between the Iberian and European plates: Some facts but still many problems. *Revista de La Sociedad Geológica de España*, 1(3–4), 327–348.
- Rat, P., Amiot, M., Feuillée, P., Floquet, M., Mathey, B., Pascal, A., et al. (1983). Vue sur le Cretace basco-cantabrique et nord-ibérique. Une Marge et Son Arrière-Pays, Ses Environments Sédimentaires. *Mémoires Géologiques de l'Université de Dijon*, 9, 191.
- Rat, Pierre. (1959). Les pays crétacés: basco-cantabriques (Espagne) (Vol. 18). Presses universitaires de France.
- Ravier, J. (1959). Le métamorphisme des terrains secondaires des Pyrénées (Vol. 86). *Mém. Soc. Géol. Fr.*
- Razin, P. (1989). Evolution tecto-sédimentaire alpine des Pyrénées Basques à l'Ouest de la transformante de Pamplona(province du Labourd).
- Reston, T., & Manatschal, G. (2011). Rifted Margins: Building Blocks of Later Collision. In D. Brown & P. D. Ryan, *Arc-Continent Collision* (pp. 3–21). Berlin, Heidelberg: Springer Berlin Heidelberg. https://doi.org/10.1007/978-3-540-88558-0_1
- Reston, T. J., & McDermott, K. G. (2011). Successive detachment faults and mantle unroofing at magma-poor rifted margins. *Geology*, 39(11), 1071–1074. <https://doi.org/10.1130/G32428.1>
- Reynolds, D., & Rosendahl, B. (1984). Tectonic expressions of continental rifting. *EOS, Trans. Am. Geophys. Union*, 65, 1055.
- Richard, P. (1986). Structure et évolution alpine des massifs paléozoïques du Labourd (Pays Basque français). *Éditions du Bureau de recherches géologiques et minières*.
- Ring, U. (1994). The influence of preexisting structure on the evolution of the Cenozoic Malawi rift (East African rift system). *Tectonics*, 13(2), 313–326. <https://doi.org/10.1029/93TC03188>
- Robert, P. (1971). Etude pétrographique des matières organiques insolubles par la mesure de leur pouvoir réflecteur: contribution à l'exploration pétrolière et à la connaissance des bassins sédimentaires. *Rev. Inst. Franç. Pétrole*, 26, 105–135.
- Roca, E., Muñoz, J. A., Ferrer, O., & Ellouz, N. (2011). The role of the Bay of Biscay Mesozoic extensional structure in the configuration of the Pyrenean orogen: constraints from the MARCONI deep seismic reflection survey. *Tectonics*, 30(2). Retrieved from <http://onlinelibrary.wiley.com/doi/10.1029/2010TC002735/full>
- Roest, W. R., & Srivastava, S. P. (1991). Kinematics of the plate boundaries between Eurasia, Iberia, and Africa in the North Atlantic from the Late Cretaceous to the present. *Geology*, 19(6), 613. [https://doi.org/10.1130/0091-7613\(1991\)019<0613:KOTPBB>2.3.CO;2](https://doi.org/10.1130/0091-7613(1991)019<0613:KOTPBB>2.3.CO;2)
- Rosenbaum, G., Lister, G. S., & Duboz, C. (2002). Relative motions of Africa, Iberia and Europe during Alpine orogeny. *Tectonophysics*, 359(1), 117–129. [https://doi.org/10.1016/S0040-1951\(02\)00442-0](https://doi.org/10.1016/S0040-1951(02)00442-0)
- Rossi, P., Cocherie, A., Fanning, C. M., & Ternet, Y. (2003). Datation U-Pb sur zircons des dolérites tholéitiques pyrénéennes (ophites) à la limite Trias–Jurassique et relations avec les tufs volcaniques dits « infra-liasiques » nord-pyrénéens. *Comptes Rendus Geoscience*, 335(15), 1071–1080.

<https://doi.org/10.1016/j.crte.2003.09.011>

- Rossy, M. (1988). Contribution à l'étude du magmatisme mésozoïque du domaine pyrénéen: I, le Trias dans l'ensemble du domaine, II le Crétacé dans les provinces basques d'Espagne.
- Roure, F., Choukroune, P., Berastegui, X., Munoz, J. A., Villien, A., Matheron, P., et al. (1989). Ecore deep seismic data and balanced cross sections: Geometric constraints on the evolution of the Pyrenees. *Tectonics*, 8(1), 41–50. <https://doi.org/10.1029/TC008i001p00041>
- Roure, F., Howell, D., Guellec, S., & Casero, P. (1990). Shallow structures induced by deep-seated thrusting. *Petroleum and Tectonics in Mobile Belts*, 15–30.
- Ruiz, M., Gallart, J., Díaz, J., Olivera, C., Pedreira, D., López, C., et al. (2006). Seismic activity at the western Pyrenean edge. *Tectonophysics*, 412(3–4), 217–235. <https://doi.org/10.1016/j.tecto.2005.10.034>
- Rybacki, E., & Dresen, G. (2000). Dislocation and diffusion creep of synthetic anorthite aggregates. *Journal of Geophysical Research: Solid Earth*, 105(B11), 26017–26036. <https://doi.org/10.1029/2000JB900223>

S

- de Saint Blanquat, M., Bajolet, F., Grand'Homme, A., Proietti, A., Zanti, M., Boutin, A., et al. (2016). Cretaceous mantle exhumation in the central Pyrenees: New constraints from the peridotites in eastern Ariège (North Pyrenean zone, France). From Rifting to Mountain Building: The Pyrenean Belt, 348(3), 268–278. <https://doi.org/10.1016/j.crte.2015.12.003>
- Salomon, J.-N., Rat, P., Ros, A. P., Amiot, M., Floquet, M., & Mathey, B. (1982). Évolution de la marge cantabrique et de son arrière-pays ibérique au Crétacé. *Cuadernos de Geología Ibérica= Journal of Iberian Geology: An International Publication of Earth Sciences*, (8), 37–64.
- Sanderson, D. J., & Marchini, W. R. . (1984). Transpression. *Journal of Structural Geology*, 6(5), 449–458. [https://doi.org/10.1016/0191-8141\(84\)90058-0](https://doi.org/10.1016/0191-8141(84)90058-0)
- Saura, E., & Teixell, A. (2006). Inversion of small basins: effects on structural variations at the leading edge of the Axial Zone antiformal stack (Southern Pyrenees, Spain). *Journal of Structural Geology*, 28(11), 1909–1920. <https://doi.org/10.1016/j.jsg.2006.06.005>
- Savva, D., Pubellier, M., Franke, D., Chamot-Rooke, N., Meresse, F., Steuer, S., & Auxietre, J. L. (2014). Different expressions of rifting on the South China Sea margins. *Evolution, Structure, and Sedimentary Record of the South China Sea and Adjacent Basins*, 58(Part B), 579–598. <https://doi.org/10.1016/j.marpetgeo.2014.05.023>
- Scharer, de Parseval, Polve, & de Saint Blanquat. (1999). Formation of the Trimouns talc-chlorite deposit (Pyrenees) from persistent hydrothermal activity between 112 and 97 Ma. *Terra Nova*, 11(1), 30–37. <https://doi.org/10.1046/j.1365-3121.1999.00224.x>
- Schoeffler, J. (1982). Les transversales basco-landaises. *Bulletin Des Centre de Recherches ELF-Aquitaine*, 6, 257–263.
- Schott, J. J., & Peres, A. (1988). Paleomagnetism of Permo-Triassic red beds in the western Pyrenees: evidence for strong clockwise rotations of the Paleozoic units. *Tectonophysics*, 156(1–2), 75–88. [https://doi.org/10.1016/0040-1951\(88\)90284-3](https://doi.org/10.1016/0040-1951(88)90284-3)
- Sclater, J. G., Jaupart, C., & Galson, D. (1980). The heat flow through oceanic and continental crust and the heat loss of the Earth. *Reviews of Geophysics*, 18(1), 269–311. <https://doi.org/10.1029/RG018i001p00269>
- Scotese, C. R., & Schettino, A. (2017). Late Permian-Early Jurassic Paleogeography of Western Tethys and the World. In *Permo-Triassic Salt Provinces of Europe, North Africa and the Atlantic Margins* (pp. 57–95). Elsevier. <https://doi.org/10.1016/B978-0-12-809417-4.00004-5>
- Seguret, M. (1972). Étude tectonique des nappes et séries décollées de la partie centrale du versant sud des Pyrénées. *Pub. Estela, Ser Geol. Struct.*, 2, 1–155.
- Seguret, M., & Daignières, M. (1985). Coupes balancées d'échelle crustale des Pyrénées. *Comptes Rendus de l'Académie Des Sciences. Série 2, Mécanique, Physique, Chimie, Sciences de l'univers, Sciences de La Terre*, 301(5), 341–346.
- Seguret, M., & Daignières, M. (1986). Crustal scale balanced cross-sections of the Pyrenees; discussion. *Tectonophysics*, 129(1–4), 303–318. [https://doi.org/10.1016/0040-1951\(86\)90258-1](https://doi.org/10.1016/0040-1951(86)90258-1)
- Şengör, A. M. C. (2016). The structural evolution of the Albula Pass region, Graubünden, eastern Switzerland: the origin of the various vergences in the structure of the Alps. *Canadian Journal of Earth Sciences*, 53(11), 1279–1311. <https://doi.org/10.1139/cjes-2016-0020>
- Şengör, A. M. C., Lom, N., & Sağdıç, N. G. (2018). Tectonic inheritance, structure reactivation and lithospheric strength: the relevance of geological history. *Geological Society, London, Special*

- Publications, SP470.8. <https://doi.org/10.1144/SP470.8>
- Serrano, O., Delmas, J., Hanot, F., Vially, R., Herbin, J. P., Houel, P., & Tourlière, B. (2006). Le Bassin d'Aquitaine : valorisation des données sismiques, cartographie structurale et potentiel pétrolier. BRGM. <https://doi.org/10.13140/2.1.1304.2241>
- Sibuet, J.-C., Srivastava, S. P., & Spakman, W. (2004). Pyrenean orogeny and plate kinematics. *Journal of Geophysical Research: Solid Earth*, 109(B8), B08104. <https://doi.org/10.1029/2003JB002514>
- Sinclair, H., Gibson, M., Naylor, M., & Morris, R. (2005). Asymmetric growth of the Pyrenees revealed through measurement and modeling of orogenic fluxes. *American Journal of Science*, 305(5), 369–406. <https://doi.org/10.2475/ajs.305.5.369>
- Skogseid, J. (2010). The Orphan Basin—A key to understanding the kinematic linkage between North and NE Atlantic Mesozoic rifting (pp. 13–23). Presented at the II Central & North Atlantic Conjugate Margins Conference.
- Sleep, N. H., & Wolery, T. J. (1978). Egress of hot water from midocean ridge hydrothermal systems: Some thermal constraints. *Journal of Geophysical Research: Solid Earth*, 83(B12), 5913–5922.
- Smith, L., & Chapman, D. S. (1983). On the thermal effects of groundwater flow: 1. Regional scale systems. *Journal of Geophysical Research: Solid Earth*, 88(B1), 593–608.
- Soler, R. (1971). El Jurásico Marino de la Sierra de Aralar (Cuenca Cantábrica occidental): los problemas poskinméricos. *Cuadernos de Geología Ibérica= Journal of Iberian Geology: An International Publication of Earth Sciences*, (2), 509–532.
- Soto, R., Casas-Sainz, A. M., VILLALAIN, J. J., Gil-Imaz, A., Fernández-González, G., Del Río, P., et al. (2008). Characterizing the Mesozoic extension direction in the northern Iberian plate margin by anisotropy of magnetic susceptibility (AMS). *Journal of the Geological Society*, 165(6), 1007–1018. <https://doi.org/10.1144/0016-76492007-163>
- Souche, A., Medvedev, S., Andersen, T. B., & Dabrowski, M. (2013). Shear heating in extensional detachments: Implications for the thermal history of the Devonian basins of W Norway. *Tectonophysics*, 608, 1073–1085. <https://doi.org/10.1016/j.tecto.2013.07.005>
- Souche, A., Dabrowski, M., & Andersen, T. B. (2014). Modeling thermal convection in supradetachment basins: example from western Norway. *Geofluids*, 14(1), 58–74. <https://doi.org/10.1111/gfl.12042>
- Souche, Alban, Schmid, D. W., & Rüpke, L. (2017). Interrelation between surface and basement heat flow in sedimentary basins. *AAPG Bulletin*, 101(10), 1697–1713. <https://doi.org/10.1306/12051615176>
- Soula, J. C., Debat, P., Deramond, J., & Pouget, P. (1986). A dynamic model of the structural evolution of the Hercynian Pyrenees. *The Geological Evolution of the Pyrenees*, 129(1), 29–51. [https://doi.org/10.1016/0040-1951\(86\)90244-1](https://doi.org/10.1016/0040-1951(86)90244-1)
- Soula, J.-C., Lucas, C., & Bessiere, G. (1979). Genesis and evolution of Permian and Triassic basins in the Pyrenees by regional simple shear acting on older Variscan structures: field evidence and experimental models. *Tectonophysics*, 58(3–4), T1–T9. [https://doi.org/10.1016/0040-1951\(79\)90307-7](https://doi.org/10.1016/0040-1951(79)90307-7)
- Souquet, P., Debroas, E.-J., Boirie, J.-M., Pons, P., Fixari, G., Roux, J.-C., et al. (1985). Le groupe du Flysch noir (albo-cénomanién) dans les Pyrénées. *Bull. Cent. Rech. Explo.-Prod. Elf-Aquitaine Pau*, 9, 183–252.
- Souquet, Pierre, Peybernes, B., Bilotte, M., & Debroas, E.-J. (1977). La chaîne alpine des Pyrénées. *Géologie Alpine*, 53(fasc. 2), 193–216.
- Stampfli, G. ., & Borel, G. . (2002). A plate tectonic model for the Paleozoic and Mesozoic constrained by dynamic plate boundaries and restored synthetic oceanic isochrons. *Earth and Planetary Science Letters*, 196(1), 17–33. [https://doi.org/10.1016/S0012-821X\(01\)00588-X](https://doi.org/10.1016/S0012-821X(01)00588-X)
- Stern, R. J. (2004). Subduction initiation: spontaneous and induced. *Earth and Planetary Science Letters*, 226(3–4), 275–292. <https://doi.org/10.1016/j.epsl.2004.08.007>
- Stevaux, J., & Winnock, E. (1974). Les bassins du Trias et du Lias inférieur d'Aquitaine et leurs épisodes évaporitiques. *Bulletin de La Société Géologique de France*, S7-XVI(6), 679–695. <https://doi.org/10.2113/gssgfbull.S7-XVI.6.679>
- Suess, E., Bertrand, M., & Termier, P. (1900). *Antlitz der Erde* (Vol. 2). A. Colin et cie.
- Sutra, E., Manatschal, G., Mohn, G., & Unternehr, P. (2013). Quantification and restoration of extensional deformation along the Western Iberia and Newfoundland rifted margins. *Geochemistry, Geophysics, Geosystems*, 14(8), 2575–2597. <https://doi.org/10.1002/ggge.20135>
- Svartman Dias, A. E., Lavier, L. L., & Hayman, N. W. (2015). Conjugate rifted margins width and asymmetry: The interplay between lithospheric strength and thermomechanical processes. *Journal of Geophysical Research: Solid Earth*, 120(12), 8672–8700. <https://doi.org/10.1002/2015JB012074>

T

- Tapponnier, P., Armijo, R., Manighetti, I., & Courtillot, V. (1990). Bookshelf faulting and horizontal block rotations between overlapping rifts in southern Afar. *Geophysical Research Letters*, 17(1), 1–4. <https://doi.org/10.1029/GL017i001p00001>
- Tavani, S., Bertok, C., Granado, P., Piana, F., Salas, R., Vigna, B., & Muñoz, J. A. (2018). The Iberia-Eurasia plate boundary east of the Pyrenees. *Earth-Science Reviews*, 187, 314–337. <https://doi.org/10.1016/j.earscirev.2018.10.008>
- Tavani, Stefano, & Muñoz, J. A. (2012). Mesozoic rifting in the Basque-Cantabrian Basin (Spain): Inherited faults, transversal structures and stress perturbation: Mesozoic rifting in the Basque-Cantabrian Basin. *Terra Nova*, 24(1), 70–76. <https://doi.org/10.1111/j.1365-3121.2011.01040.x>
- Tavani, Stefano, Carola, E., Granado, P., Quintà, A., & Muñoz, J. A. (2013). Transpressive inversion of a Mesozoic extensional forced fold system with an intermediate décollement level in the Basque-Cantabrian Basin (Spain): INVERSION OF EXTENSIONAL FORCED FOLDS. *Tectonics*, 32(2), 146–158. <https://doi.org/10.1002/tect.20019>
- Taylor, G. H., Teichmüller, M., Davis, A., Diessel, C., Littke, R., & Robert, P. (1998). Organic petrology. *Bulletin de La Societe Geologique de France*, VI(2), 241. <https://doi.org/10.2113/gssgfbull.VI.2.241>
- Teixell, A. (1990). Alpine thrusts at the western termination of the Pyrenean axial zone. *Bulletin de La Societe Geologique de France*, VI(2), 241. <https://doi.org/10.2113/gssgfbull.VI.2.241>
- Teixell, A. (1993). Coupe géologique du massif d'Igountze: implications sur l'évolution structurale de la bordure sud de la zone nord-pyrénéenne occidentale. *Comptes Rendus de l'Académie Des Sciences. Série 2, Mécanique, Physique, Chimie, Sciences de l'univers, Sciences de La Terre*, 316(12), 1789–1796.
- Teixell, A. (1996). The Ansó transect of the southern Pyrenees: basement and cover thrust geometries. *Journal of the Geological Society*, 153(2), 301–310. <https://doi.org/10.1144/gsjgs.153.2.0301>
- Teixell, A. (1998). Crustal structure and orogenic material budget in the west central Pyrenees. *Tectonics*, 17(3), 395–406. <https://doi.org/10.1029/98TC00561>
- Teixell, A., Labaume, P., Ayarza, P., Espurt, N., de Saint Blanquat, M., & Lagabrielle, Y. (2018). Crustal structure and evolution of the Pyrenean-Cantabrian belt: A review and new interpretations from recent concepts and data. *Tectonophysics*, 724–725, 146–170. <https://doi.org/10.1016/j.tecto.2018.01.009>
- Teixell, Antonio, Labaume, P., & Lagabrielle, Y. (2016). The crustal evolution of the west-central Pyrenees revisited: Inferences from a new kinematic scenario. *Comptes Rendus Geoscience*, 348(3–4), 257–267. <https://doi.org/10.1016/j.crte.2015.10.010>
- Tentler, T. (2007). Focused and diffuse extension in controls of ocean ridge segmentation in analogue models: OCEAN RIDGE SEGMENTATION. *Tectonics*, 26(5), n/a-n/a. <https://doi.org/10.1029/2006TC002038>
- Tentler, T., & Acocella, V. (2010). How does the initial configuration of oceanic ridge segments affect their interaction? Insights from analogue models. *Journal of Geophysical Research*, 115(B1). <https://doi.org/10.1029/2008JB006269>
- Tesauro, M., Kaban, M. K., & Cloetingh, S. A. P. L. (2009). A new thermal and rheological model of the European lithosphere. *Tectonophysics*, 476(3), 478–495. <https://doi.org/10.1016/j.tecto.2009.07.022>
- Tetreault, J. L., & Buitter, S. J. H. (2017). The influence of extension rate and crustal rheology on the evolution of passive margins from rifting to break-up. *Tectonophysics*. <https://doi.org/10.1016/j.tecto.2017.08.029>
- Teyssonnières, M. (1983). Approche analytique du Flysch crétaé supérieur des Pyrénées-Atlantiques, 222.
- Theissen, S., & Rüpke, L. H. (2009). Feedbacks of sedimentation on crustal heat flow: New insights from the Vøring Basin, Norwegian Sea. *Basin Research*. <https://doi.org/10.1111/j.1365-2117.2009.00437.x>
- Thinon, I., Matias, L., Réhault, J. P., Hirn, A., Fidalgo-González, L., & Avedik, F. (2003). Deep structure of the Armorican Basin (Bay of Biscay): a review of Norgasis seismic reflection and refraction data. *Journal of the Geological Society*, 160(1), 99–116. <https://doi.org/10.1144/0016-764901-103>
- Thinon, Isabelle, Fidalgo-González, L., Réhault, J.-P., & Olivet, J.-L. (2001). Déformations pyrénéennes dans le golfe de Gascogne. *Comptes Rendus de l'Académie Des Sciences - Series IIA - Earth and Planetary Science*, 332(9), 561–568. [https://doi.org/10.1016/S1251-8050\(01\)01576-2](https://doi.org/10.1016/S1251-8050(01)01576-2)
- Thomas, W. A. (2006). Tectonic inheritance at a continental margin. *GSA Today*, 16(2), 4–11.
- Torne, M., Fernández, M., Vergés, J., Ayala, C., Salas, M. C., Jimenez-Munt, I., et al. (2015). Crust and mantle lithospheric structure of the Iberian Peninsula deduced from potential field modeling and

- thermal analysis. Special Issue on Iberia Geodynamics: An Integrative Approach from the Topo-Iberia Framework, 663(Supplement C), 419–433. <https://doi.org/10.1016/j.tecto.2015.06.003>
- Tugend, J., Manatschal, G., Kuszniir, N. J., Masini, E., Mohn, G., & Thimon, I. (2014). Formation and deformation of hyperextended rift systems: Insights from rift domain mapping in the Bay of Biscay-Pyrenees. *Tectonics*, 33(7), 2014TC003529. <https://doi.org/10.1002/2014TC003529>
- Tugend, J., Manatschal, G., Kuszniir, N. J., & Masini, E. (2015). Characterizing and identifying structural domains at rifted continental margins: application to the Bay of Biscay margins and its Western Pyrenean fossil remnants. *Geological Society, London, Special Publications*, 413(1), 171. <https://doi.org/10.1144/SP413.3>
- Tugend, J., Manatschal, G., & Kuszniir, N. J. (2015). Spatial and temporal evolution of hyperextended rift systems: Implication for the nature, kinematics, and timing of the Iberian-European plate boundary. *Geology*, 43(1), 15–18. <https://doi.org/10.1130/G36072.1>
- Turner, J. P. (1996). Switches in subduction direction and the lateral termination of mountain belts: Pyrenees-Cantabrian transition, Spain. *Journal of the Geological Society*, 153(4), 563–571. <https://doi.org/10.1144/gsjgs.153.4.0563>

U

- Ungerer, P., Burrus, J., Doligez, B. (Institut F. du petrole, Rueil-Malmaison (France)), Chenet, P. Y. (BEICIP, Rueil-Malmaison (France)), & Bessis, F. (CILIA, Rueil-Malmaison (France)). (1990). Basin evaluation by integrated two-dimensional modeling of heat transfer, fluid flow, hydrocarbon generation, and migration. *AAPG Bulletin (American Association of Petroleum Geologists); (USA)*. Retrieved from <http://www.osti.gov/scitech/servlets/purl/6990099>
- Ustaszewski, K., Schumacher, M., Schmid, S., & Nieuwland, D. (2005). Fault reactivation in brittle?viscous wrench systems?dynamically scaled analogue models and application to the Rhine?Bresse transfer zone. *Quaternary Science Reviews*, 24(3–4), 363–380. <https://doi.org/10.1016/j.quascirev.2004.03.015>

V

- Vacherat, A., Mouthereau, F., Pik, R., Bernet, M., Gautheron, C., Masini, E., et al. (2014). Thermal imprint of rift-related processes in orogens as recorded in the Pyrenees. *Earth and Planetary Science Letters*, 408(Supplement C), 296–306. <https://doi.org/10.1016/j.epsl.2014.10.014>
- Vacherat, A., Mouthereau, F., Pik, R., Bellahsen, N., Gautheron, C., Bernet, M., et al. (2016). Rift-to-collision transition recorded by tectonothermal evolution of the northern Pyrenees. *Tectonics*, 35(4), 907–933. <https://doi.org/10.1002/2015TC004016>
- Vacherat, A., Mouthereau, F., Pik, R., Huyghe, D., Paquette, J.-L., Christophoul, F., et al. (2017). Rift-to-collision sediment routing in the Pyrenees: A synthesis from sedimentological, geochronological and kinematic constraints. *Earth-Science Reviews*, 172, 43–74. <https://doi.org/10.1016/j.earsci-rev.2017.07.004>
- Van der Voo, R. (1969). Paleomagnetic evidence for the rotation of the Iberian Peninsula. *Tectonophysics*, 7(1), 5–56. [https://doi.org/10.1016/0040-1951\(69\)90063-8](https://doi.org/10.1016/0040-1951(69)90063-8)
- Vargas, H., Gaspar-Escribano, J. M., López-Gómez, J., Van Wees, J.-D., Cloetingh, S., de La Horra, R., & Arche, A. (2009). A comparison of the Iberian and Ebro Basins during the Permian and Triassic, eastern Spain: A quantitative subsidence modelling approach. *Tectonophysics*, 474(1–2), 160–183. <https://doi.org/10.1016/j.tecto.2008.06.005>
- Vaucher, A., Clerc, C., Bestani, L., Lagabrielle, Y., Chauvet, A., Lahfid, A., & Mainprice, D. (2013). Preorogenic exhumation of the North Pyrenean Agly massif (Eastern Pyrenees-France): EXHUMATION OF THE NORTH PYRENEAN MASSIFS. *Tectonics*, 32(2), 95–106. <https://doi.org/10.1002/tect.20015>
- Velasque, P. C., Ducasse, L., Muller, J., & Scholten, R. (1989). The influence of inherited extensional structures on the tectonic evolution of an intracratonic chain: the example of the Western Pyrenees. *Tectonophysics*, 162(3), 243–264. [https://doi.org/10.1016/0040-1951\(89\)90247-3](https://doi.org/10.1016/0040-1951(89)90247-3)
- Vergés, J. (2003). Evolución de los sistemas de rampas oblicuas de los Pirineos meridionales: fallas del Segre y Pamplona. *Bol. Geol. Min*, 114(1), 87–101.
- Vergés, Jaume, & García-Senz, J. (2001). Mesozoic evolution and Cainozoic inversion of the Pyrenean rift. *Mémoires Du Muséum National d'histoire Naturelle*, 186, 187–212.
- Verhoef, J., & Srivastava, S. (1989). Correlation of Sedimentary Basins Across the North Atlantic as Obtained from Gravity and Magnetic Data, and Its Relation to the Early Evolution of the North

Atlantic: Chapter 9: North Atlantic Perspectives.

- Vielzeuf, D. (1984). Relations de phases dans le faciès granulite et implications géodynamiques: l'exemple des granulites des Pyrénées.
- Vielzeuf, D., & Kornprobst, J. (1984). Crustal splitting and the emplacement of Pyrenean lherzolites and granulites. *Earth and Planetary Science Letters*, 67(1), 87–96. [https://doi.org/10.1016/0012-821X\(84\)90041-4](https://doi.org/10.1016/0012-821X(84)90041-4)
- Virgili, C., Hernando, S., Ramos, A., & Sopeña, A. (1976). Le Permien en Espagne. In *The Continental Permian in Central, West, and South Europe* (pp. 91–109). Springer.
- Vissers, R. L. M. (1992). Variscan extension in the Pyrenees. *Tectonics*, 11(6), 1369–1384. <https://doi.org/10.1029/92TC00823>
- Vissers, Reinoud L.M., van Hinsbergen, D. J. J., van der Meer, D. G., & Spakman, W. (2016). Cretaceous slab break-off in the Pyrenees: Iberian plate kinematics in paleomagnetic and mantle reference frames. *Gondwana Research*, 34(Supplement C), 49–59. <https://doi.org/10.1016/j.gr.2016.03.006>
- Voort, H. B. (1964). Zum Flyschproblem in den Westpyrenäen. *Geologische Rundschau*, 53(1), 220–233. <https://doi.org/10.1007/BF02040748>

W

- Walgenwitz, F. (1976). Etude pétrologique des roches intrusives triasiques, des écailles du socle profond et des gites de chlorite de la région d'Elizondo, Navarre espagnole.
- Wang, Y., Chevrot, S., Monteiller, V., Komatitsch, D., Mouthereau, F., Manatschal, G., et al. (2016). The deep roots of the western Pyrenees revealed by full waveform inversion of teleseismic P waves. *Geology*, 44(6), 475–478. <https://doi.org/10.1130/G37812.1>
- Wegener, A. (1912). Die entstehung der kontinente. *Geologische Rundschau*, 3(4), 276–292.
- Weil, Arlo B, Van der Voo, R., van der Pluijm, B. ., & Parés, J. . (2000). The formation of an orocline by multiphase deformation: a paleomagnetic investigation of the Cantabria–Asturias Arc (northern Spain). *Journal of Structural Geology*, 22(6), 735–756. [https://doi.org/10.1016/S0191-8141\(99\)00188-1](https://doi.org/10.1016/S0191-8141(99)00188-1)
- Weil, Arlo Brandon. (2006). Kinematics of orocline tightening in the core of an arc: Paleomagnetic analysis of the Ponga Unit, Cantabrian Arc, northern Spain: KINEMATICS OF OROCLINE TIGHTENING. *Tectonics*, 25(3), n/a-n/a. <https://doi.org/10.1029/2005TC001861>
- Wernicke, B. (1985). Uniform-sense normal simple shear of the continental lithosphere. *Canadian Journal of Earth Sciences*, 22(1), 108–125. <https://doi.org/10.1139/e85-009>
- Whitchurch, A. L., Carter, A., Sinclair, H. D., Duller, R. A., Whittaker, A. C., & Allen, P. A. (2011). Sediment routing system evolution within a diachronously uplifting orogen: Insights from detrital zircon thermochronological analyses from the South-Central Pyrenees. *American Journal of Science*, 311(5), 442–482. <https://doi.org/10.2475/05.2011.03>
- Whitmarsh, R. B., Manatschal, G., & Minshull, T. A. (2001). Evolution of magma-poor continental margins from rifting to seafloor spreading. *Nature*, 413, 150.
- Willett, S., Beaumont, C., & Fullsack, P. (1993). Mechanical model for the tectonics of doubly vergent compressional orogens. *Geology*, 21(4), 371. [https://doi.org/10.1130/0091-7613\(1993\)021<0371:MMFTTO>2.3.CO;2](https://doi.org/10.1130/0091-7613(1993)021<0371:MMFTTO>2.3.CO;2)
- Wilson, D. S. (1990). Kinematics of overlapping rift propagation with cyclic rift failure. *Earth and Planetary Science Letters*, 96(3–4), 384–392. [https://doi.org/10.1016/0012-821X\(90\)90014-O](https://doi.org/10.1016/0012-821X(90)90014-O)
- Wilson, J. T. (1965). A new class of faults and their bearing on continental drift. *Nature*, 207(4995), 343.
- Wilson, J. T. (1966). Did the Atlantic Close and then Re-Open? *Nature*, 211, 676.
- Withjack, M. O., & Jamison, W. R. (1986). Deformation produced by oblique rifting. *Tectonophysics*, 126(2–4), 99–124. [https://doi.org/10.1016/0040-1951\(86\)90222-2](https://doi.org/10.1016/0040-1951(86)90222-2)

Z

- Ziegler, P. (1978). North-western Europe: tectonics and basin development. *Geologie En Mijnbouw*, 57(4), 589–626.
- Ziegler, P. A., & Cloetingh, S. (2004). Dynamic processes controlling evolution of rifted basins. *Earth-Science Reviews*, 64(1–2), 1–50. [https://doi.org/10.1016/S0012-8252\(03\)00041-2](https://doi.org/10.1016/S0012-8252(03)00041-2)
- Zolnai, G. (1971). Le front nord des Pyrénées occidentales. *Histoire Structural Du Golfe de Gascogne*. Technip, 1–10.
- Zwaan, F., Schreurs, G., Naliboff, J., & Buitter, S. J. H. (2016). Insights into the effects of oblique extension on continental rift interaction from 3D analogue and numerical models. *Tectonophysics*, 693, 239–260. <https://doi.org/10.1016/j.tecto.2016.02.036>

ANNEXES

1. MATÉRIEL SUPPLÉMENTAIRE CHAPITRE II

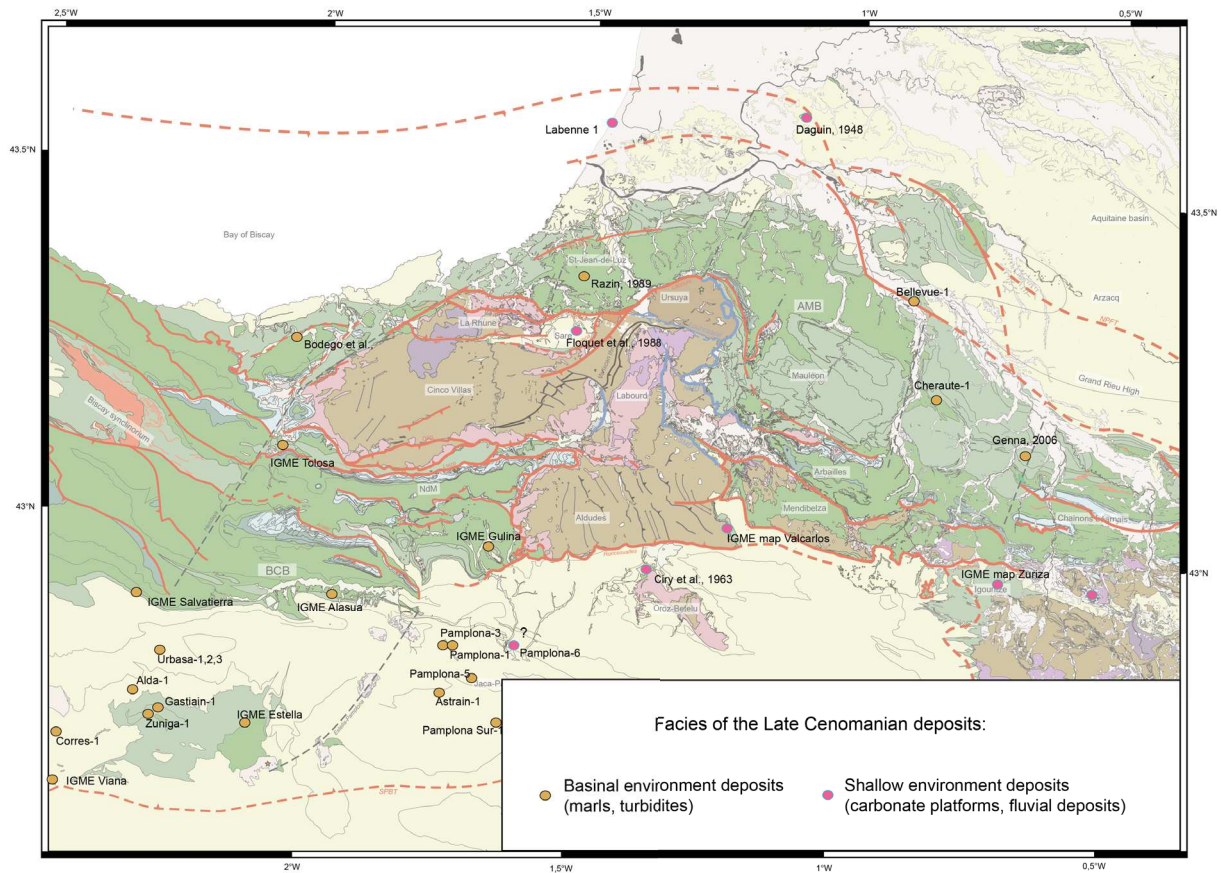


Figure S1: Carte des faciès du Cénomanién Supérieur autour des massifs basques à partir des données de puits, de littérature et des cartes géologiques.

2. MATÉRIEL SUPPLÉMENTAIRE CHAPITRE IV

Supporting Information for

Thermal evolution of asymmetric hyperextended magma-poor rift systems: results from numerical modelling and Pyrenean field observations

Rodolphe Lescoutre¹, Julie Tugend^{1,2,3}, Sascha Brune^{4,5}, Emmanuel Masini³,
Gianreto Manatschal¹

¹*IPGS, EOST-CNRS, Université de Strasbourg, Strasbourg, France*

²*Sorbonne Université, CNRS-INSU, Institut des Sciences de la Terre Paris, ISTeP UMR 7193, F-75005 Paris, France.*

³*Total R&D, CSTJF, Pau, France*

⁴*GFZ Potsdam, German Research Centre for Geosciences, Potsdam, Germany*

⁵*Institute of Earth and Environmental Sciences, University of Potsdam, Germany*

Contents of this file

Table S1: Thermo-mechanical parameters used for the numerical model.

Figure S2: Numerical model with sediments.

Movie S3: Numerical model of asymmetric rifting and top basement heat flow evolution (snapshots extracted from the movie).

Table S4: RSCM datasets of the Mauléon basin compiled for this study.

Figure S5: Vitrinite reflectance data from the Arzacq-Mauléon basin (courtesy of Total)

Summary

This supporting information file contains the parameters used for the numerical model (Table S1). The same numerical model is run with progressive sediment infill and depicted in Figure S2. Movie S3 shows the complete evolution of the numerical model of asymmetric rifting and the evolution of topography and top basement heat flow from where are extracted the 3 snapshots of Figure 3. We include new vitrinite reflectance data from the Arzacq-Mauléon basin in Figure S5 and compile the full data sets of RSCM data (Table S4) available in the literature for the Mauléon-Arzacq basin.

| Parameter | Upper Crust | Lower Crust | Strong Mantle | Weak Mantle |
|---|-------------|-------------|---------------|-------------|
| Density, ρ (kg m ⁻³) | 2700 | 2850 | 3280 | 3300 |
| Thermal expansivity, α_T (10 ⁻⁵ K ⁻¹) | 2.7 | 2.7 | 3.0 | 3.0 |
| Bulk modulus, K (GPa) | 55 | 63 | 122 | 122 |
| Shear modulus, G (GPa) | 36 | 40 | 74 | 74 |
| Heat capacity, C_p (J kg ⁻¹ K ⁻¹) | 1200 | 1200 | 1200 | 1200 |
| Heat conductivity, λ (W K ⁻¹ m ⁻¹) | 2.5 | 2.5 | 3.3 | 3.3 |
| Radiogenic heat production, A (μ W m ⁻³) | 1.5 | 0.2 | 0.0 | 0.0 |
| Initial friction coefficient, μ (-) | 0.5 | 0.5 | 0.5 | 0.5 |
| Cohesion, c (MPa) | 5.0 | 5.0 | 5.0 | 5.0 |
| Pre-exponential constant for diffusion creep, $\log(B_{\text{Diff}})$ (Pa ⁻¹ s ⁻¹) | - | - | -8.65 | -8.66 |
| Activation energy for diffusion creep, E_{Diff} (kJ / mol) | - | - | 375 | 335 |
| Activation volume for diffusion creep, V_{Diff} (cm ⁻³ / mol) | - | - | 6 | 4 |
| Pre-exponential constant for dislocation creep, $\log(B_{\text{Disloc}})$ (Pa ⁻ⁿ s ⁻¹) | -28.00 | -15.40 | -15.56 | -15.05 |
| Power law exponent for dislocation creep, n | 4.0 | 3.0 | 3.5 | 3.5 |
| Activation energy for dislocation creep, E_{Disloc} (kJ / mol) | 223 | 356 | 530 | 480 |
| Activation volume for dislocation creep, V_{Disloc} (cm ⁻³ /mol) | 0 | 0 | 13 | 10 |

Table S1: Thermo-mechanical parameters. During frictional and viscous strain softening, μ and B_{Disloc} respectively vary linearly for brittle and viscous strain between 0 and 1. For strains larger than 1, they remain constant. We thereby use a minimum friction coefficient of 0.05 and a maximum pre-exponential factor that is 30 times larger than the listed value, representing a modest viscosity decrease between 0.3 and 0.4 if compared to unstrained material (Brune et al., 2014). We mimic the heterogeneous distribution of faults by randomizing the initial strain distribution between values of 0 and 0.2, which results in an initial spread of friction coefficients between 0.4 and 0.5.

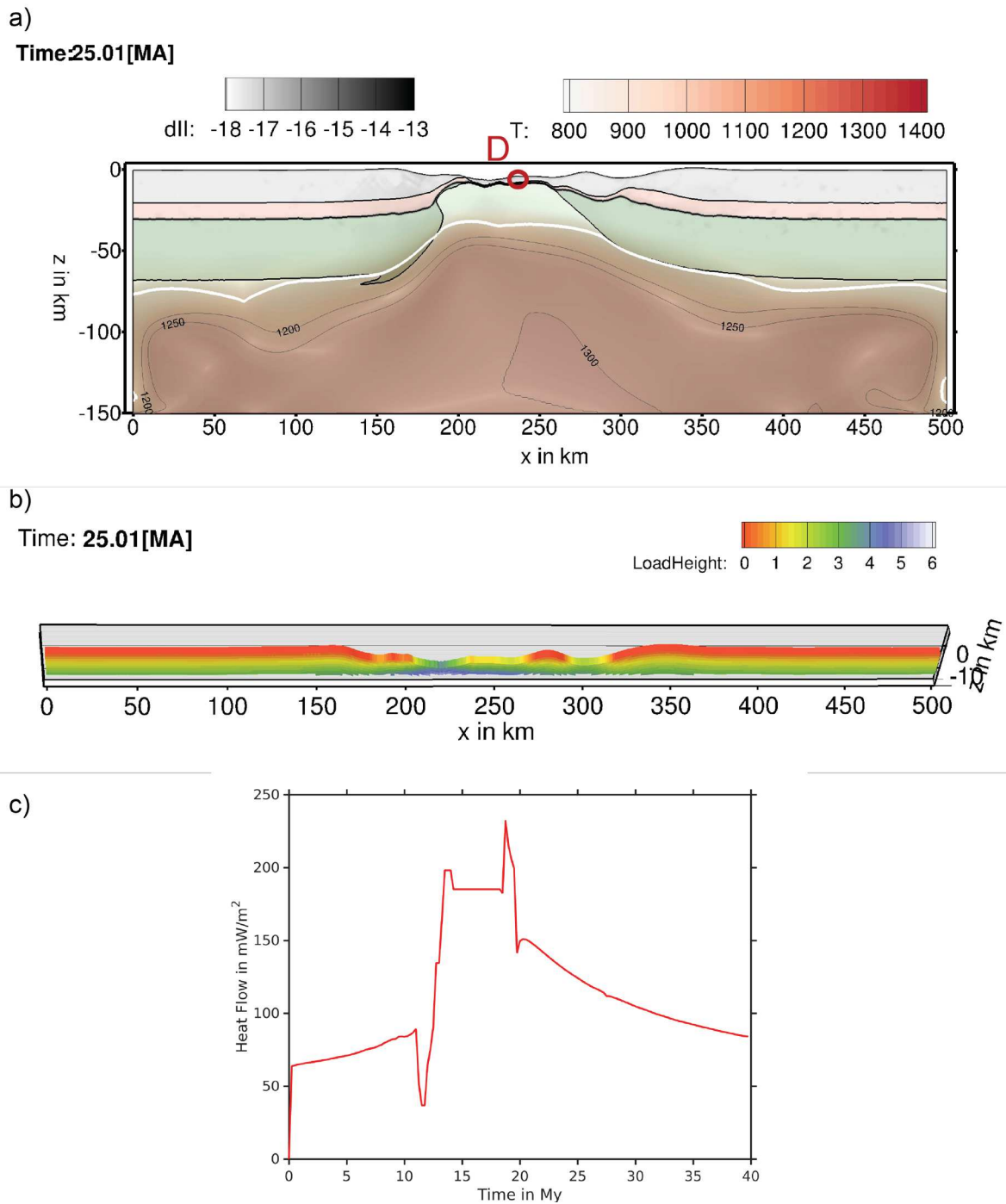


Figure S2: Role of sediments on the mode of deformation. a) The model is identical to the setup shown in Figure 3 and Movie S3 but here we add sediments at each step in a way that the basin is always filled to 3 km below the surface. The thermal gradient in the sediments is set to $80^{\circ}\text{C}/\text{km}$. The model shows similar brittle asymmetric deformation. b) Sediment thickness (LoadHeight in km) is represented along the aborted rift system at 25My. Note that the deepest part (upper-lower plate transition) records about 4.5 km of sediments during rifting. c) Heat flow evolution of marker D (see location at the end of rifting on a)). We conclude that the shape of the heat flow evolution is similar to the model without sediments, however, maximum heat flow remains high for much longer.

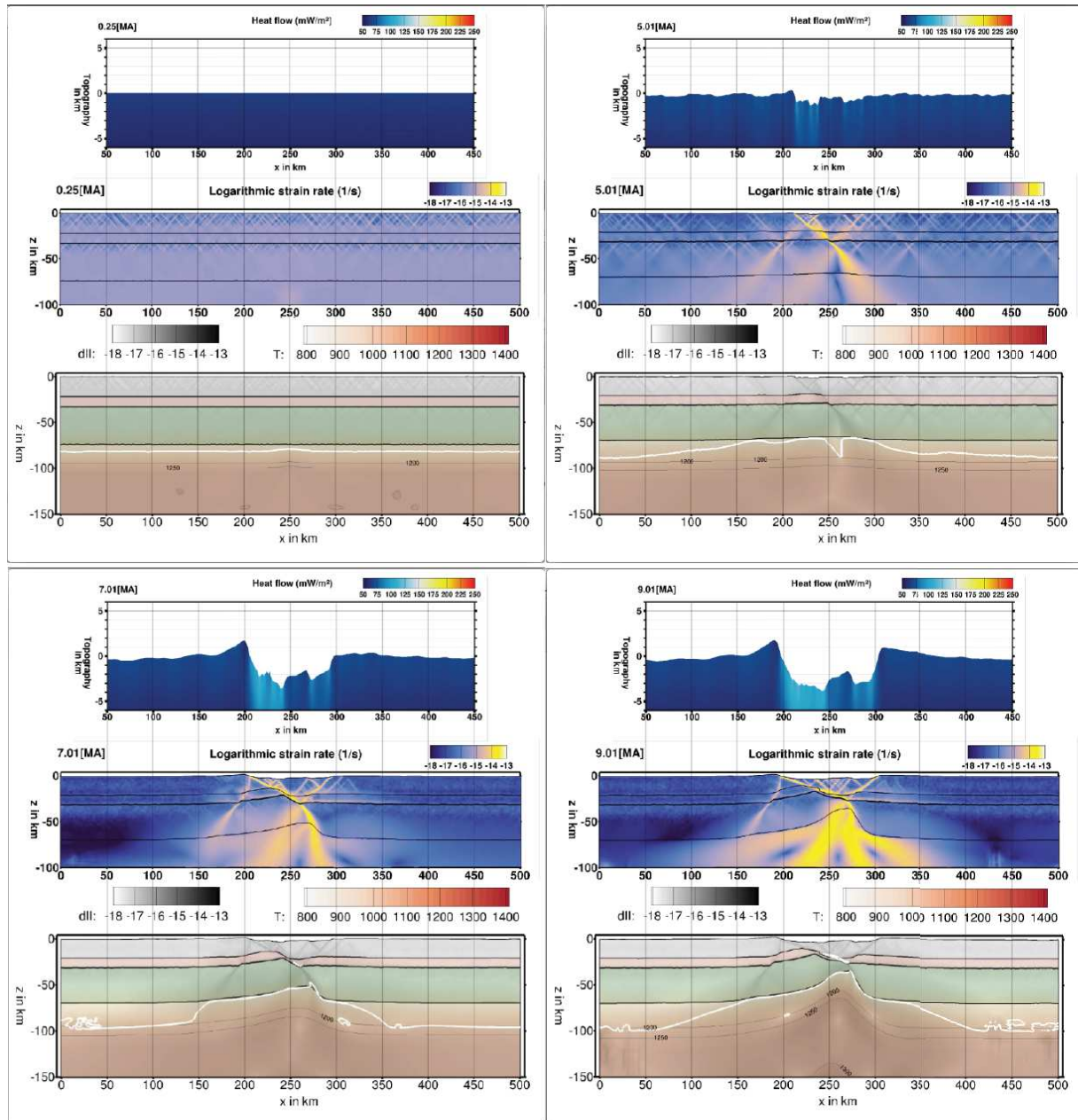


Figure S3: See caption below.

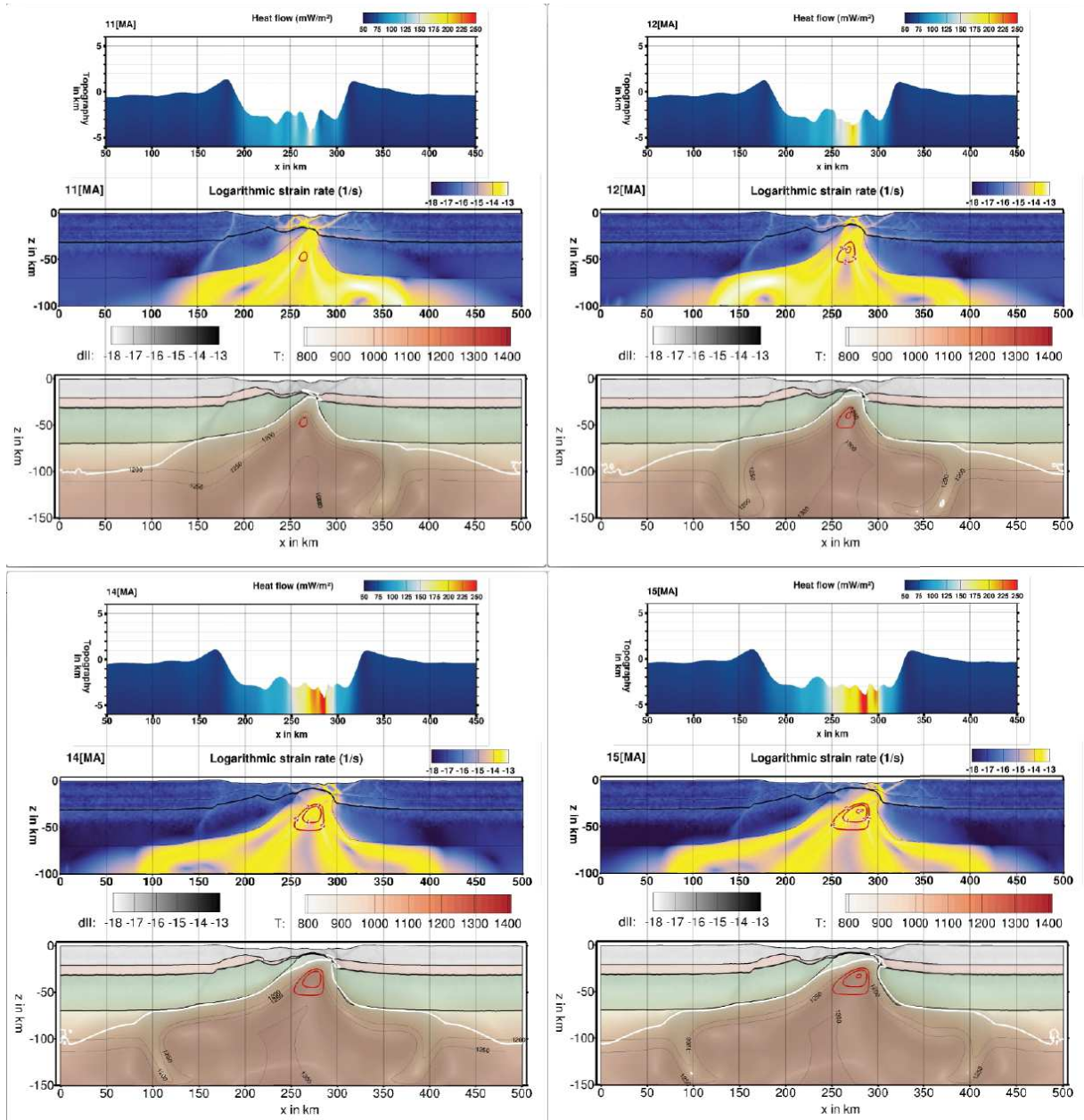


Figure S3: See caption below.

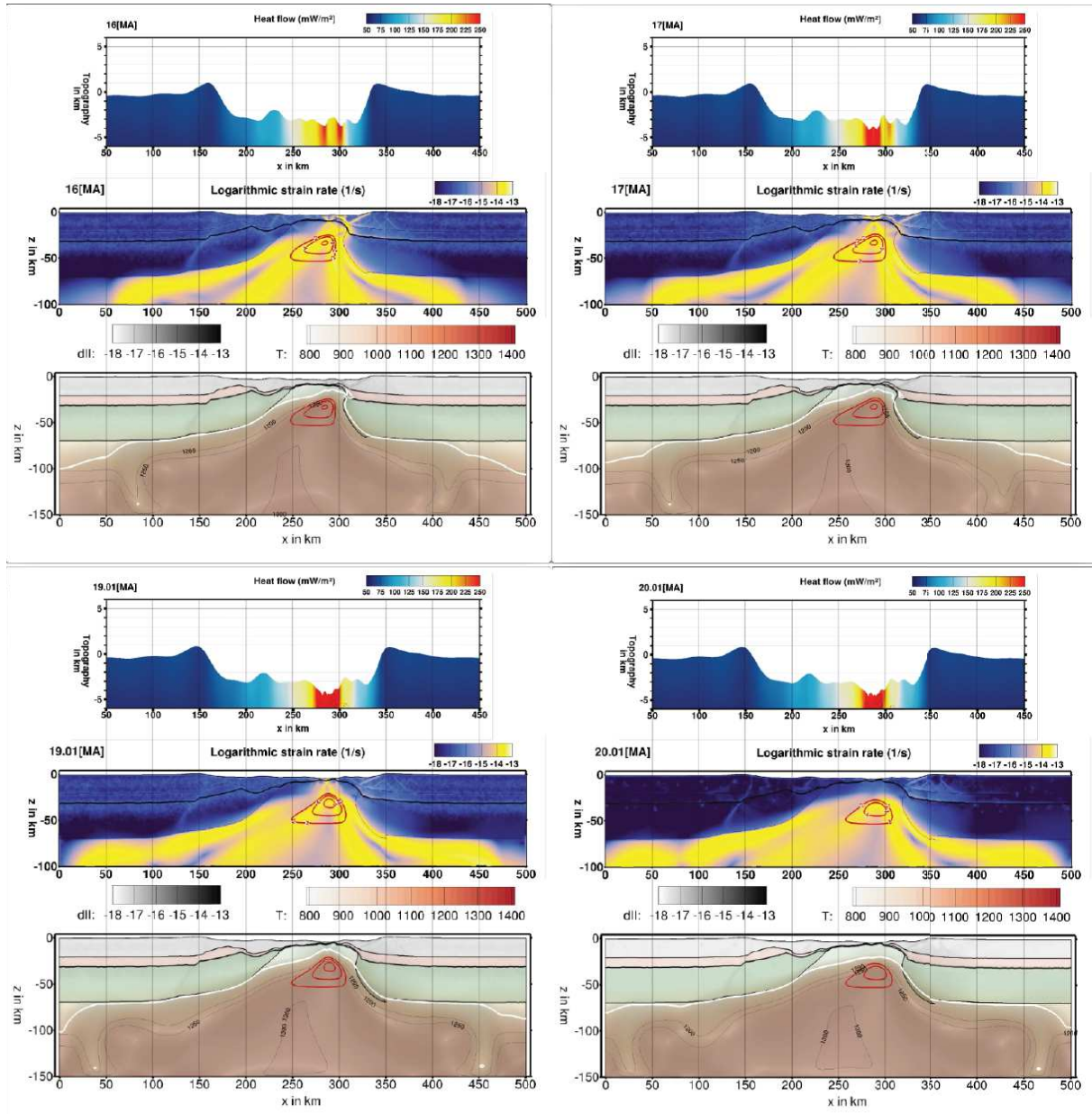


Figure S3: See caption below.

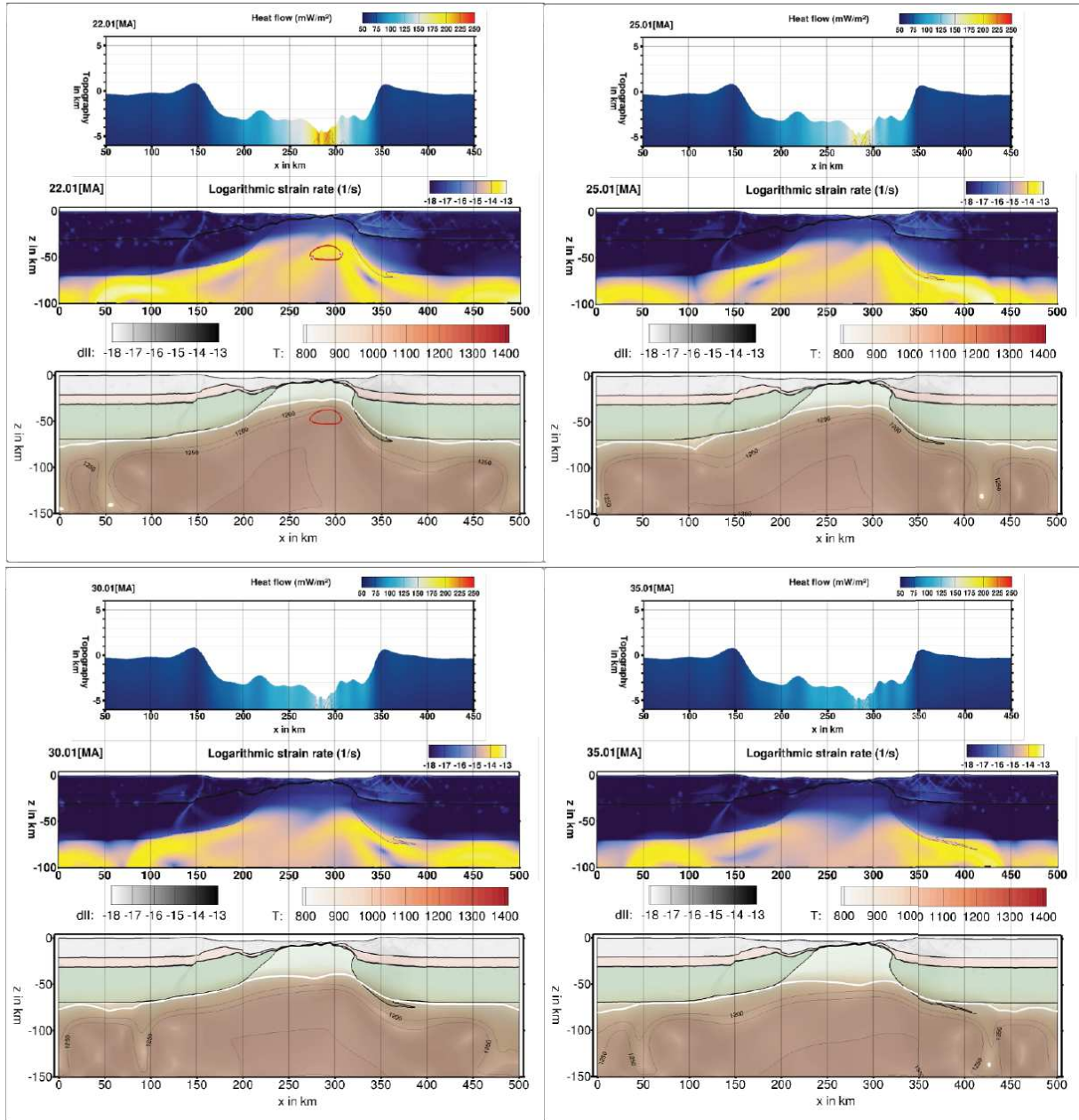


Figure S3: Selected snapshots of the numerical model of asymmetric rifting and top basement heat flow evolution.

| Longitude | Latitude | Sample | Location | Lithology | Temperature (°C) | Reference |
|-----------|------------|--------|-----------------|-----------------------------------|------------------|-----------------------|
| 403280.81 | 6223889.38 | SAR5 | Sarailié | Urgonian | 297 | Clerc et al., 2015 |
| 403513.57 | 6223926.57 | SAR7 | Sarailié | Urgonian | 328 | Clerc et al., 2015 |
| 401783.58 | 6231308.06 | URD11 | Urdach | Cenomanian | 215 | Clerc et al., 2015 |
| 401783,58 | 6231308,06 | URD14 | Urdach | Cenomanian | 233 | Clerc et al., 2015 |
| 356379,02 | 6259200,47 | 12PB02 | Abarratia | Turonian? | 157 | Clerc et al., 2015 |
| 372996,99 | 6230030,98 | 12PB03 | Col d'Ibarburia | Aptian-Albian "Marnes à Spicules" | 249 | Clerc et al., 2015 |
| 372472,96 | 6227574,43 | 12PB05 | Arhansus | Albian-Cenomanian | 224 | Clerc et al., 2015 |
| 372282,97 | 6227494,43 | 12PB06 | Arhansus | Albian-Cenomanian | 235 | Clerc et al., 2015 |
| 391102,76 | 6223631,29 | 12PB07 | Barlanès | Albian-Cenomanian | 156 | Clerc et al., 2015 |
| 390732,65 | 6224895,19 | 12PB08 | Barlanès | Liassic | 288 | Clerc et al., 2015 |
| 390341,98 | 6227752,51 | 12PB09 | Barlanès | Albian-Cenomanian | 366 | Clerc et al., 2015 |
| 386132,21 | 6230520,05 | 12PB10 | Roquiague | Albian-Cenomanian | 255 | Clerc et al., 2015 |
| 389934,96 | 6232608 | 12PB11 | Roquiague | early-Cenomanian | 331 | Clerc et al., 2015 |
| 393016,45 | 6237184,27 | 12PB12 | Roquiague | early-Cenomanian | 330 | Clerc et al., 2015 |
| 389997,09 | 6234654,94 | 12PB13 | Roquiague | late-Cenomanian | 247 | Clerc et al., 2015 |
| 375326,66 | 6242430,16 | 12PB15 | Roquiague | Cenomanian-Turonian | 224 | Clerc et al., 2015 |
| 378207,29 | 6238398,25 | 12PB16 | Roquiague | Aptian-Albian | 295 | Clerc et al., 2015 |
| 401185,32 | 6223544,26 | 12PB17 | Sarailié | Albian-Cenomanian | 278 | Clerc et al., 2015 |
| 404127,81 | 6222487,18 | 12PB18 | Sarailié | Albian-Cenomanian | 263 | Clerc et al., 2015 |
| 406468,2 | 6225279,1 | 12PB19 | Sarailié | Jurassic | 298 | Clerc et al., 2015 |
| 365155 | 6258276 | LU-1 | NE Ursuya | Albian-Cenomanian | 200 | Vacherat et al., 2014 |

Table S4: RSCM datasets compiled for this study. Longitudes (x) and latitudes (y) are in Lambert 93 coordinate system (in meters).

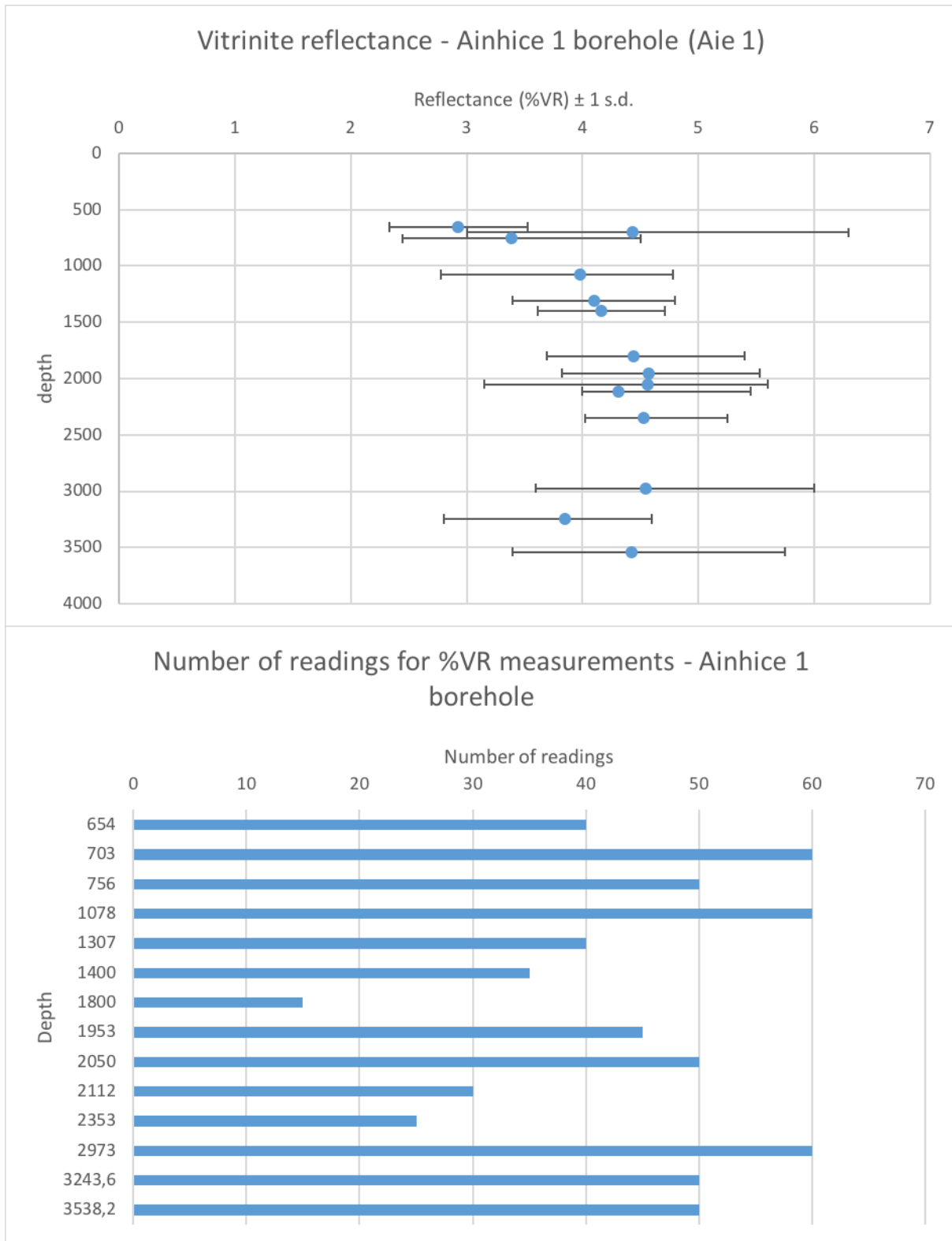
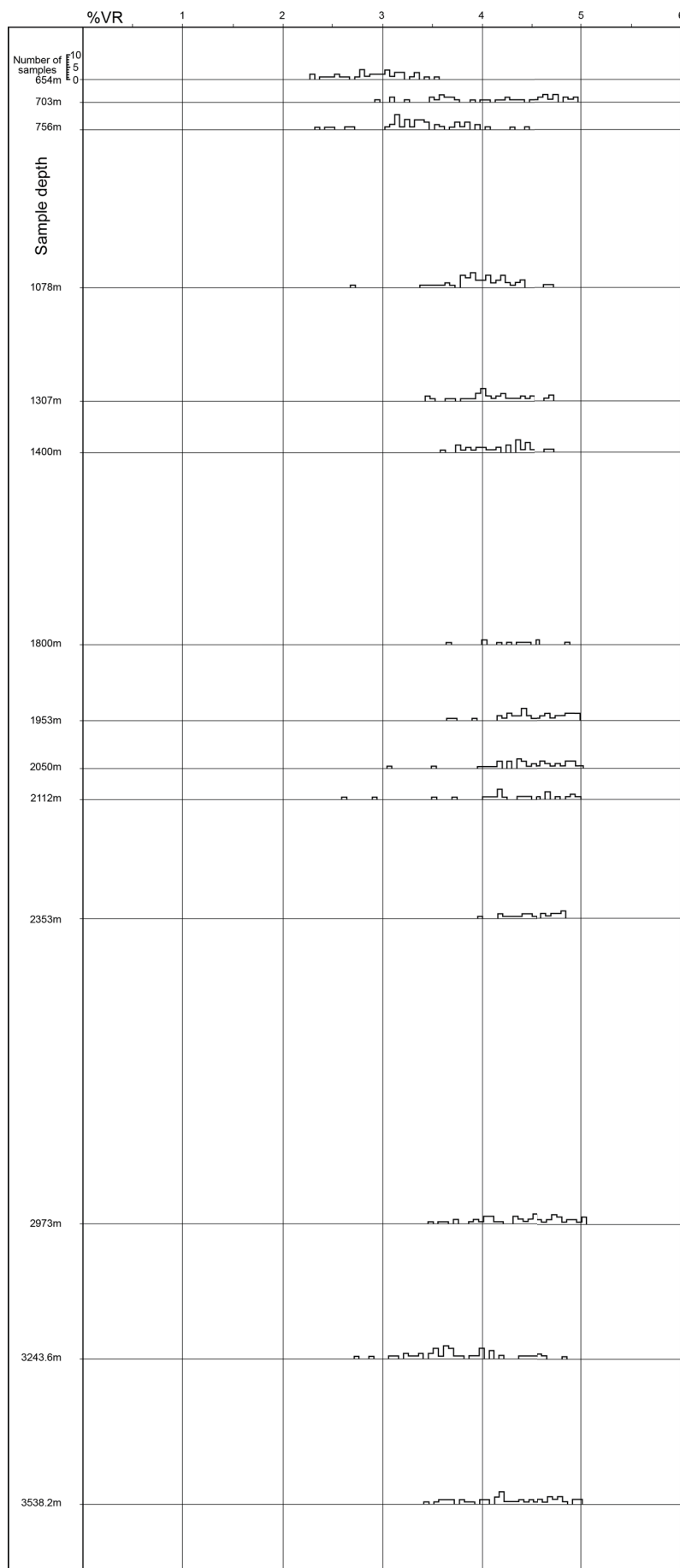


Figure S5: See caption below.

Ainhice 1 borehole



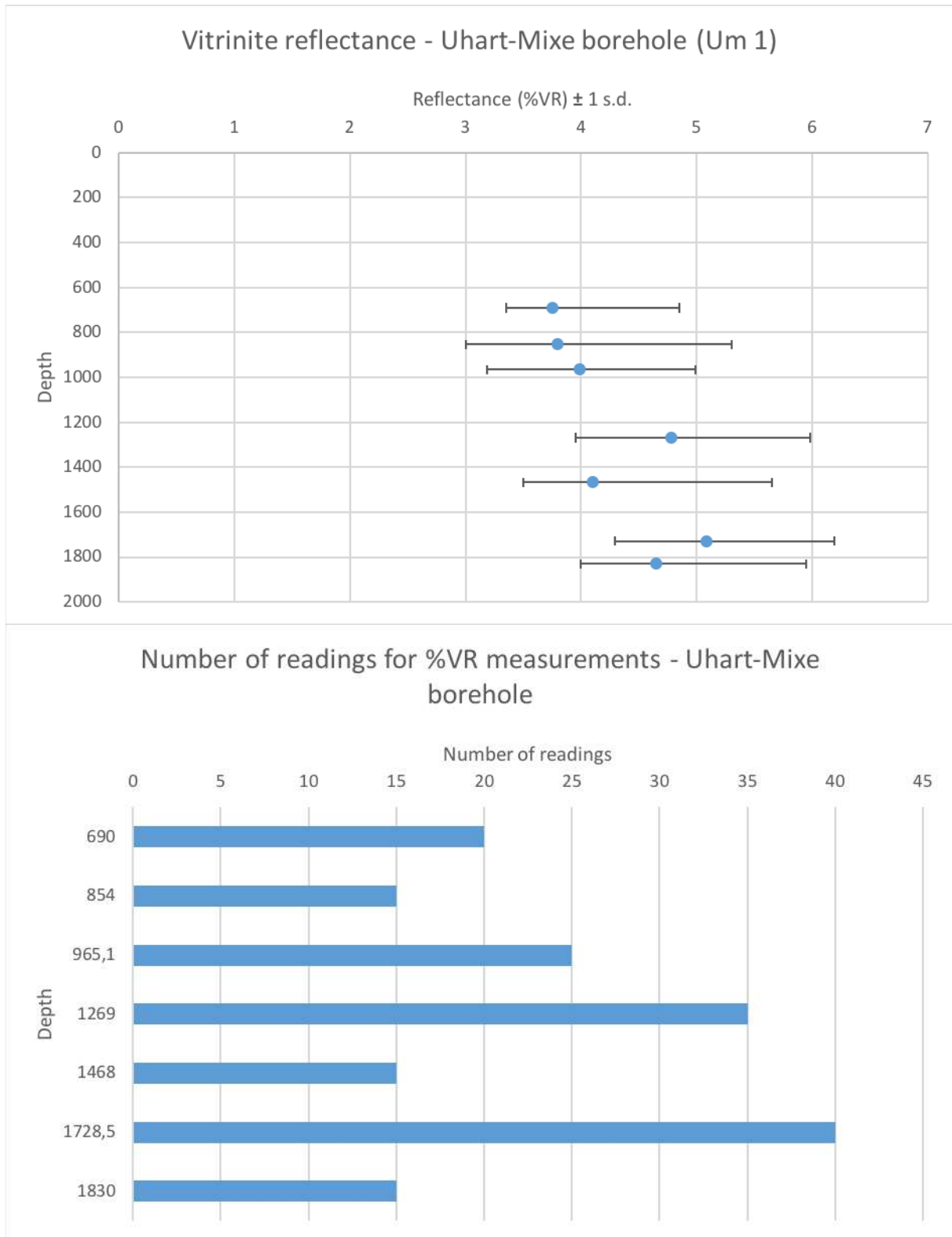
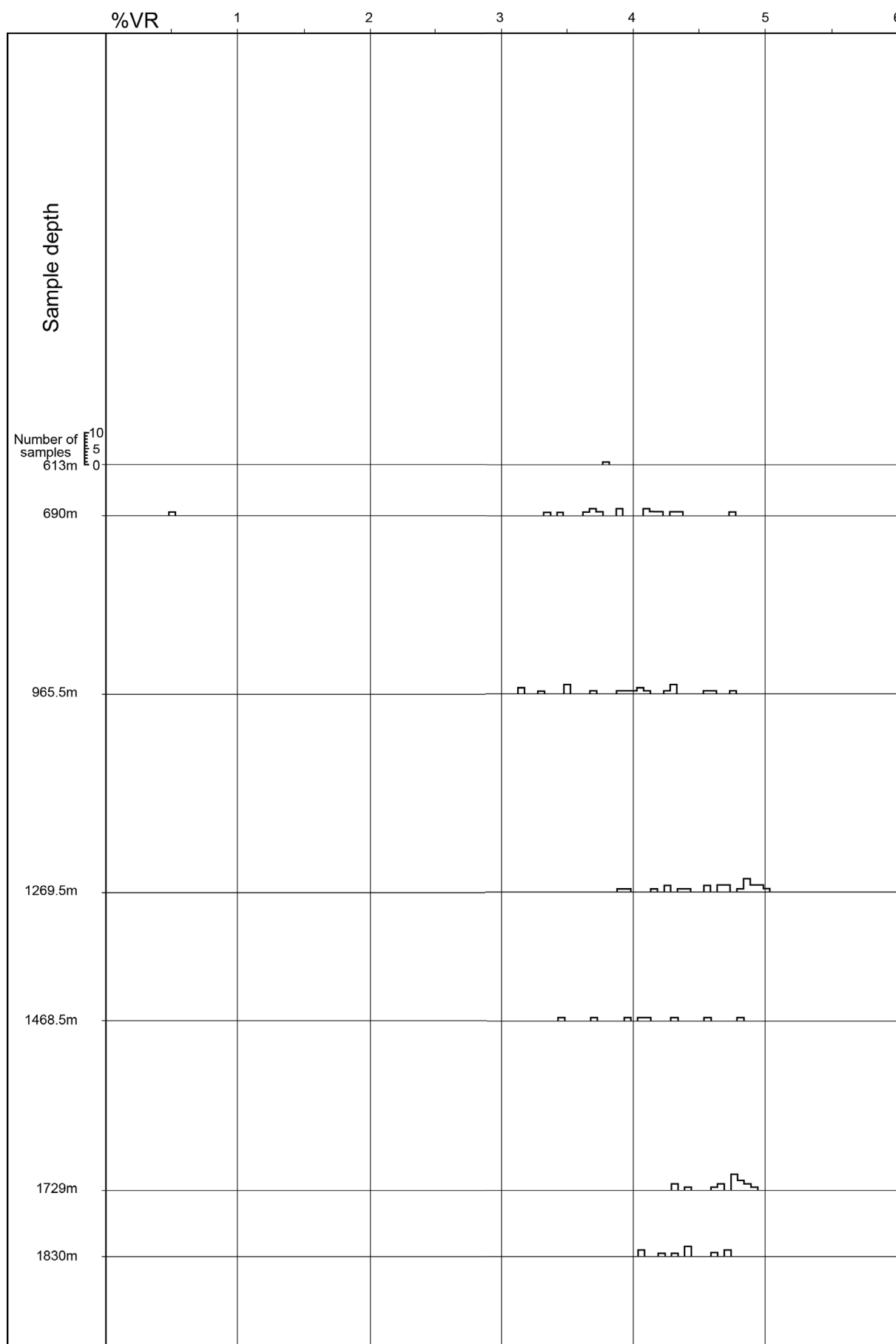


Figure S5: See caption below.

Uhart-Mixe 1 borehole



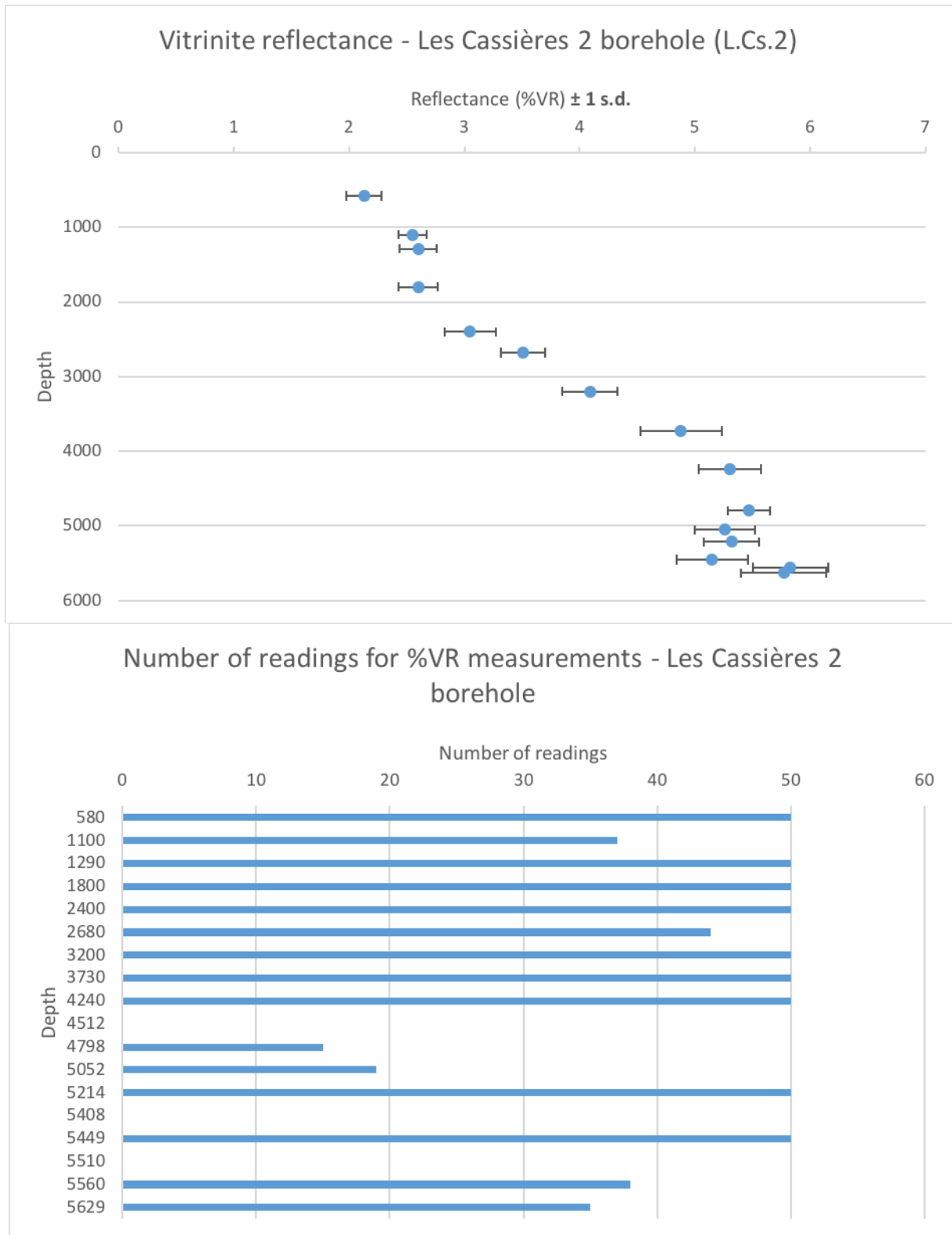
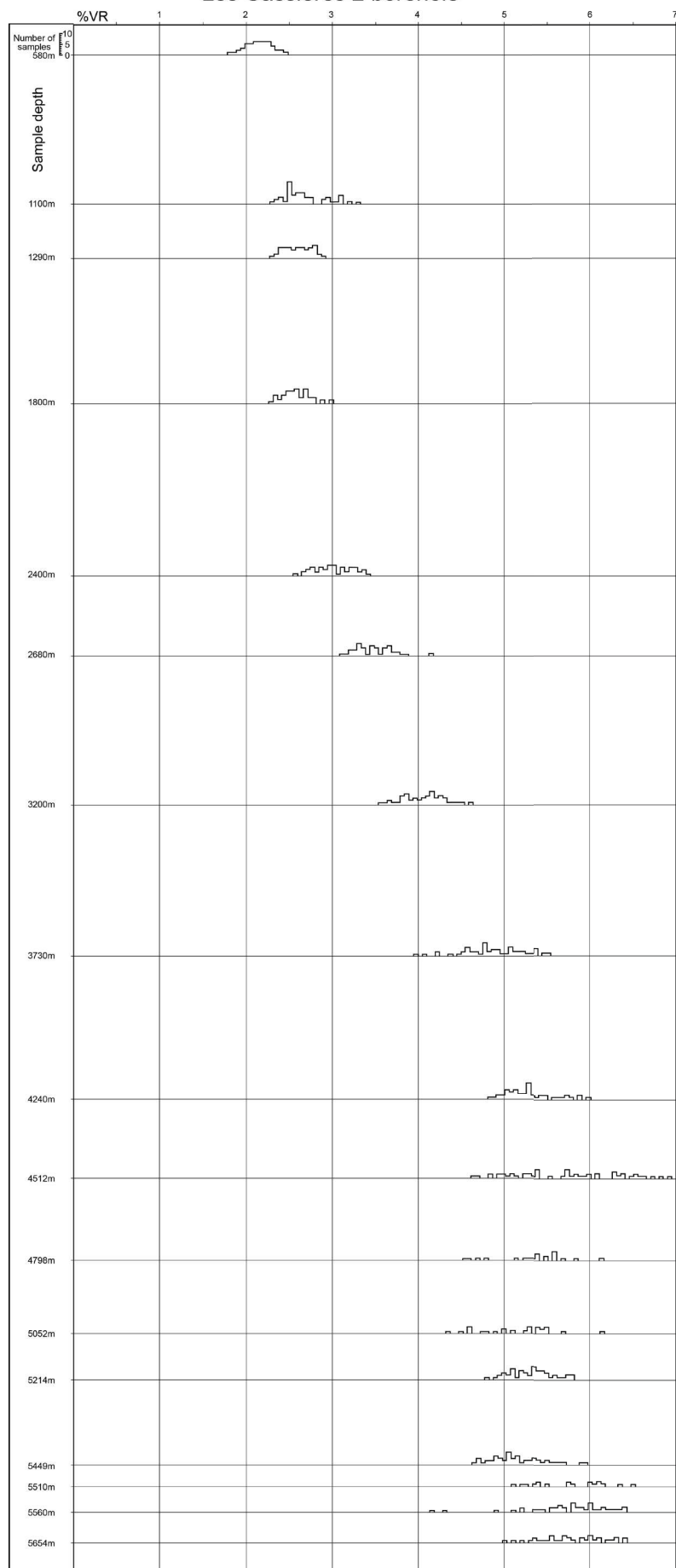
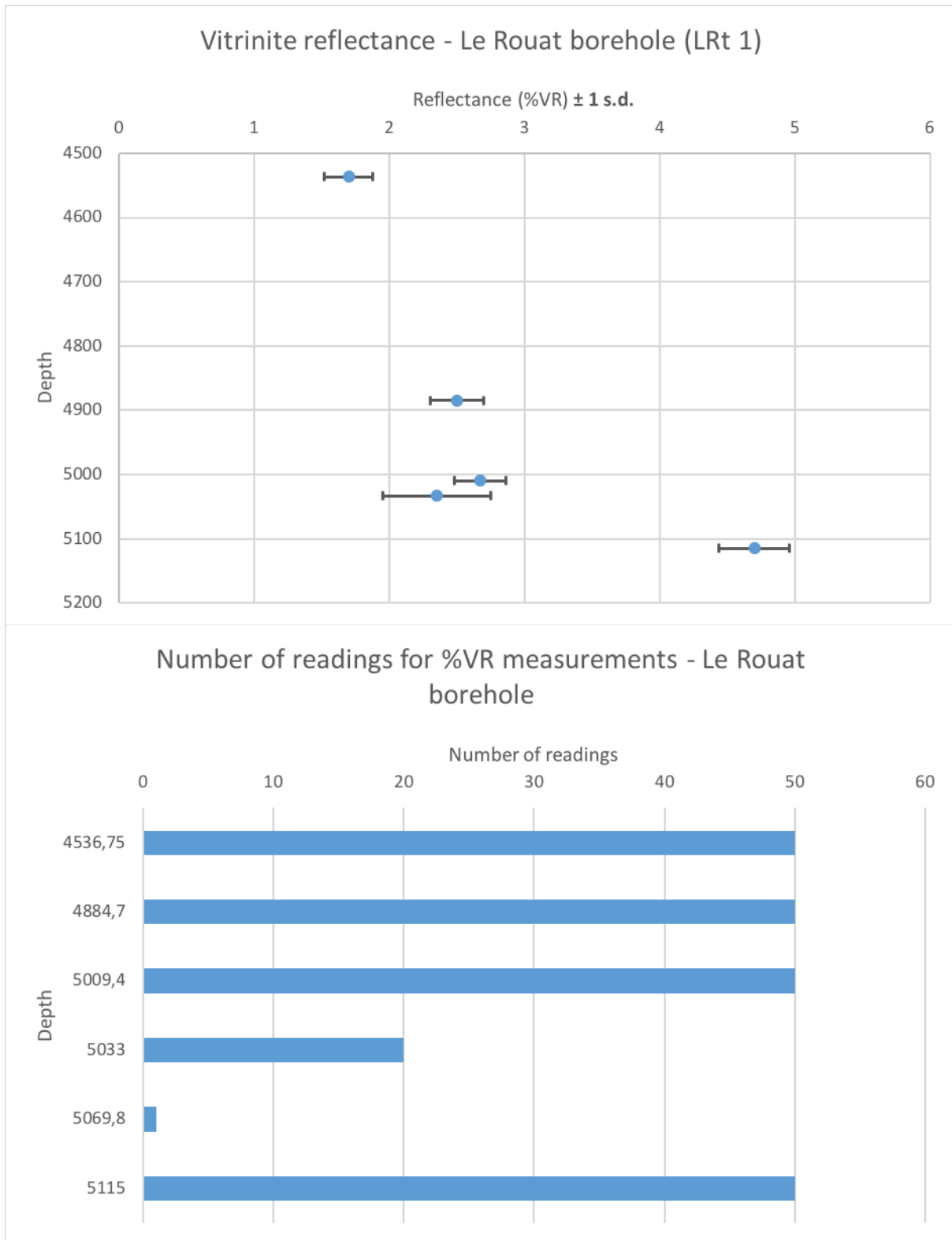


Figure S5: See caption below.

Les Cassières 2 borehole





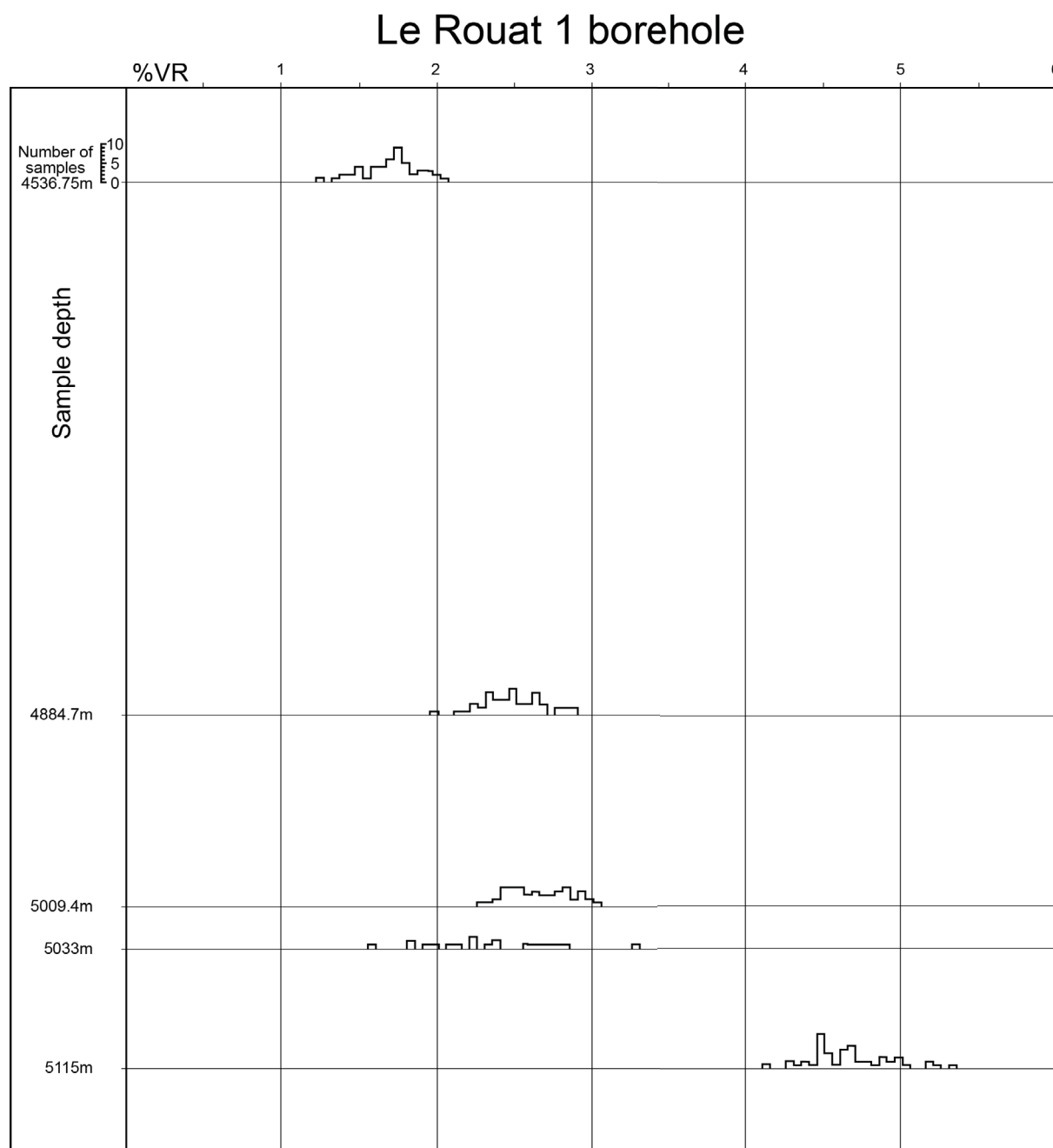


Figure S5: Vitrinite reflectance data from the Arzacq-Mauléon basin (courtesy of Total). The measurements for each depth and the number of samples are shown. We also present the histograms provided by the Total company.

3. INTERPRÉTATIONS SISMIQUES DANS LE BASSIN BASQUE-CANTABRE

Une interprétation de certaines données sismiques disponibles dans le bassin Basque-Cantabre est proposée ici (Fig. 1). L'intérêt de ce travail est avant tout de produire une interprétation 3D cohérente de la zone à partir des données disponibles. Ainsi, au vu de la qualité des données, les horizons n'ont pas été suivis de façon rigoureuse mais peuvent être corrélés aux cartes géologiques de surface et aux données de puits.

Les interprétations sismiques ont été effectuées avec le logiciel Move (Midland Valley) à partir des lignes sismiques et des données de puits mis à disposition par l'IGME (©Instituto Geológico y Minero de España – IGME ; <http://info.igme.es/SIGEOF>).

L'échelle verticale des coupes sismiques étant en seconde (temps de parcours aller-retour), la conversion appliquée est de 4,5 secondes (TWT) correspondent à 10'000 mètres. Les horizons de couleurs correspondent au « top » de la séquence sédimentaire considérée (voir Fig. 2 pour la légende des horizons). Les intersections avec les autres lignes sismiques sont indiquées par les croix sur les sections.

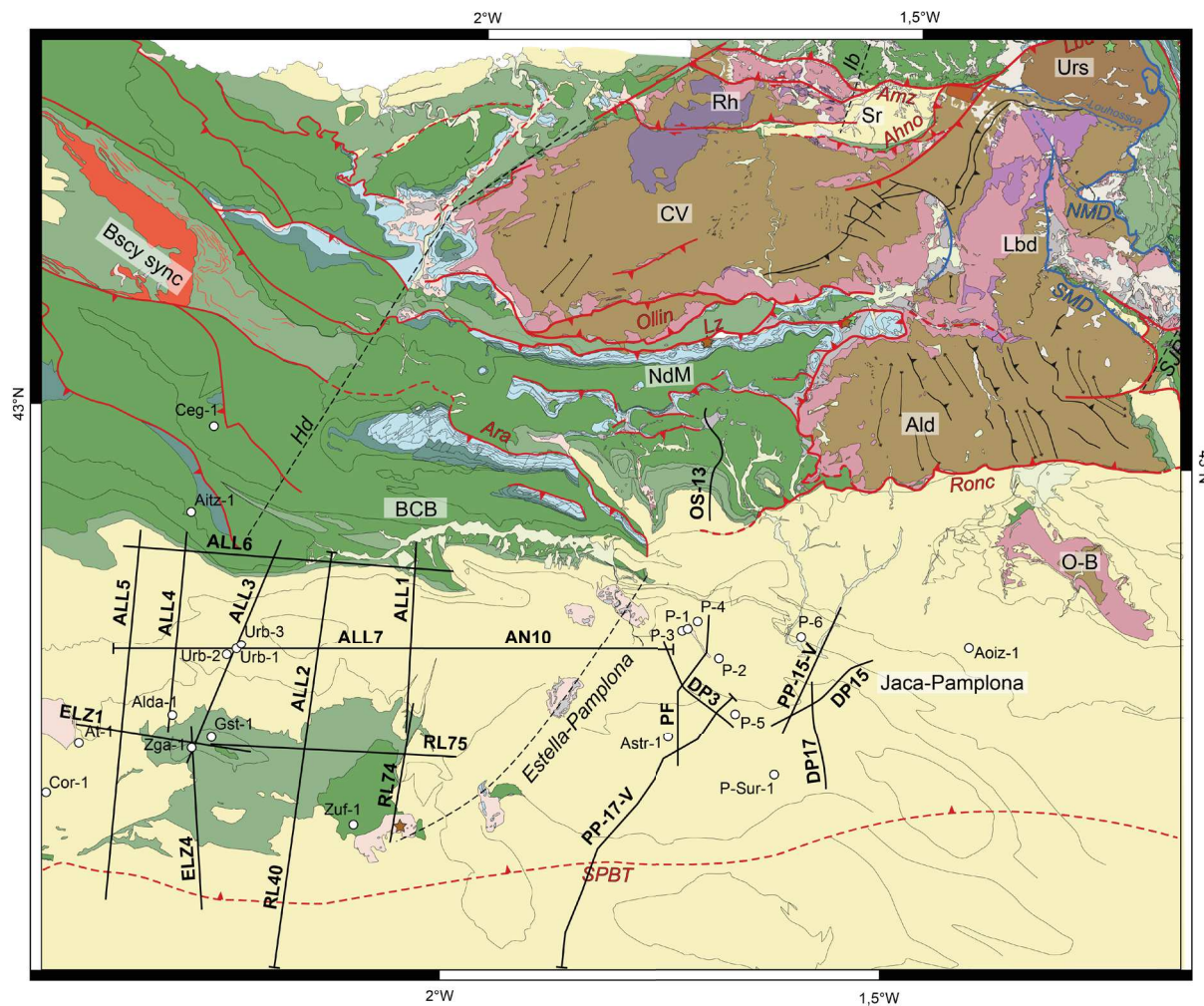


Figure 1: Carte de localisation des lignes sismiques interprétées

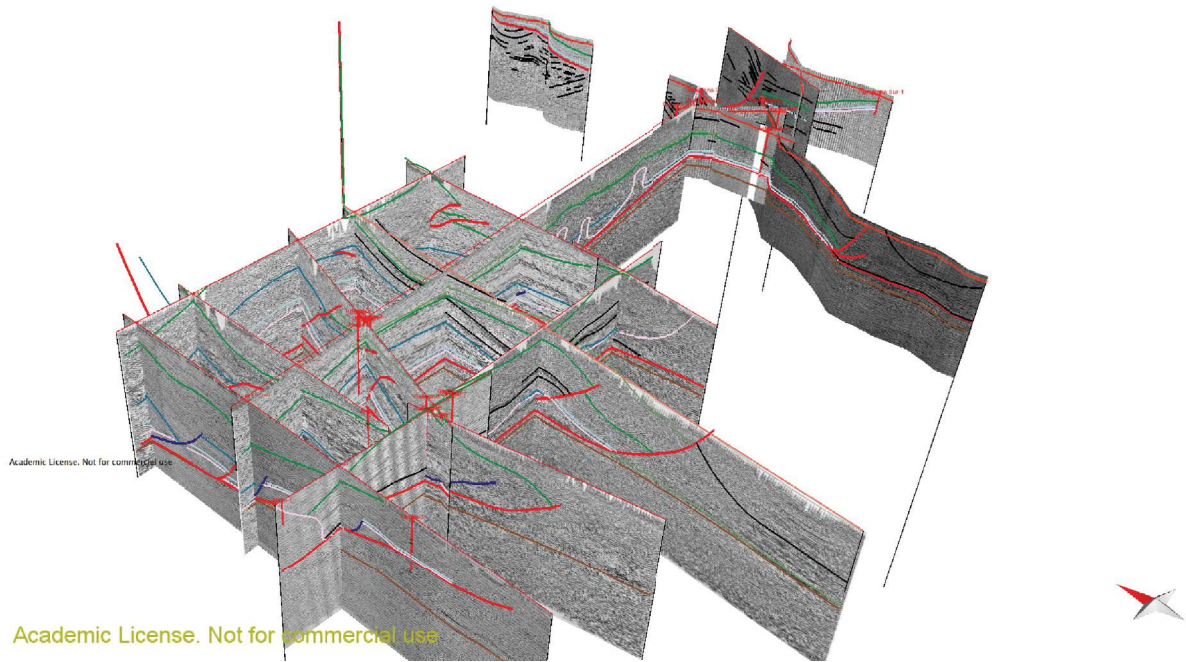
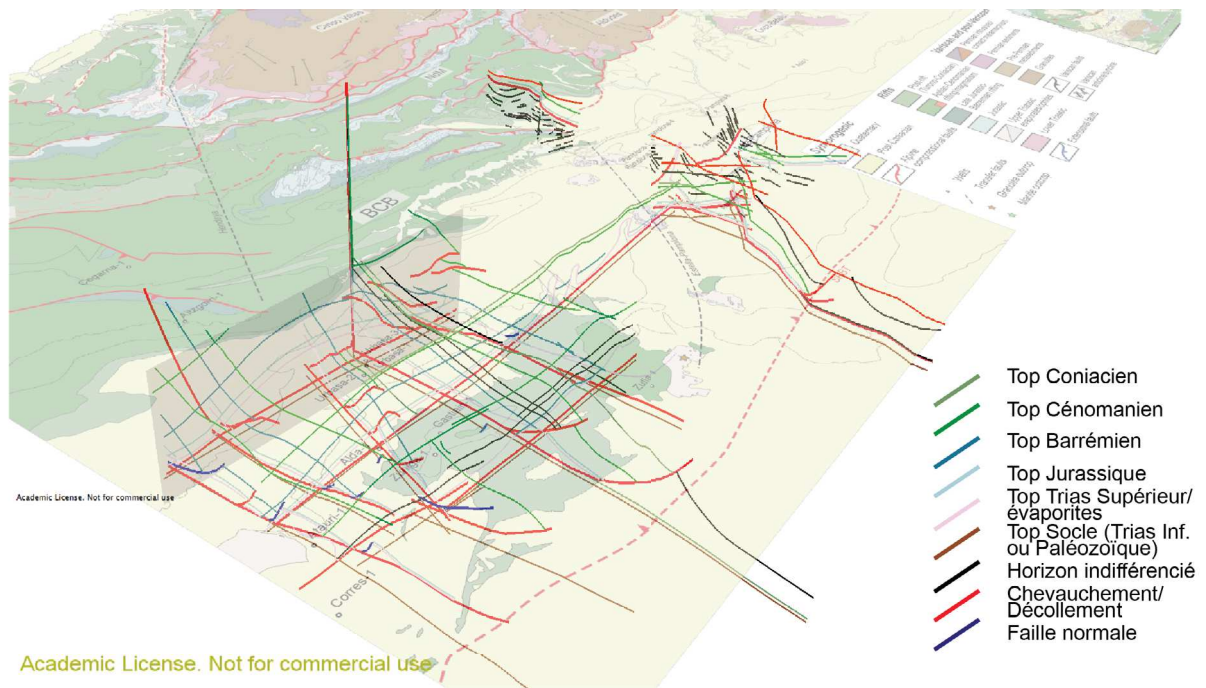


Figure 2: Vue 3D des lignes interprétées

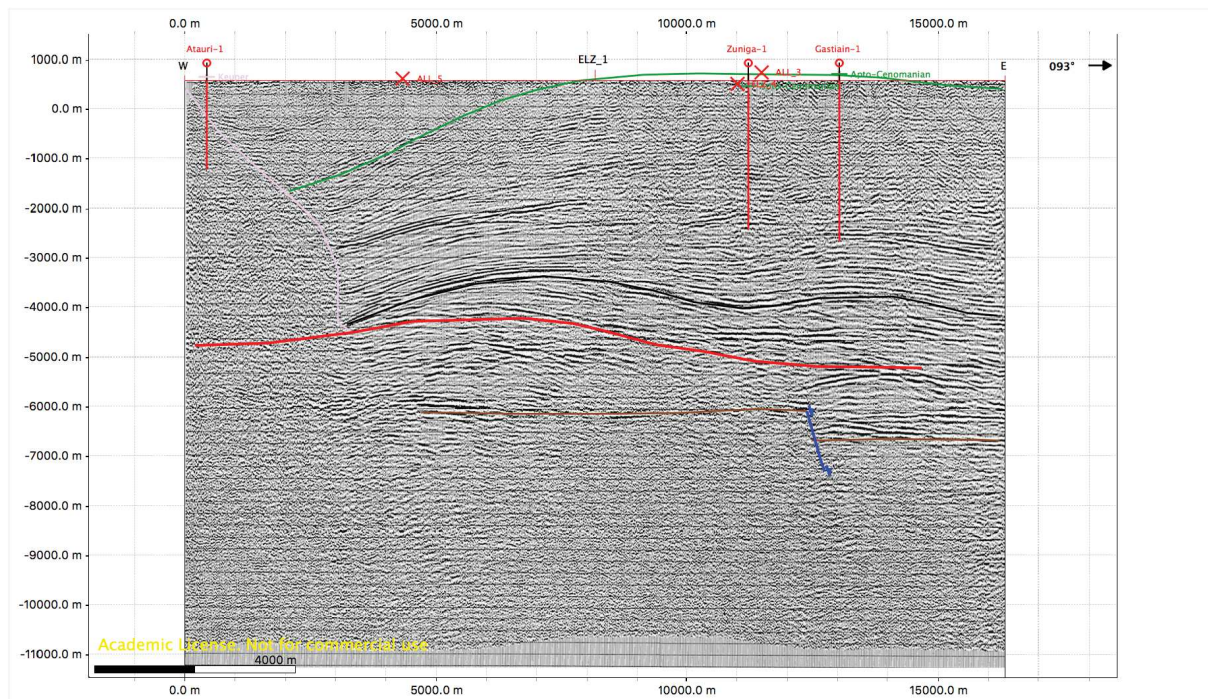


Figure 3: Ligne sismique ELZ1

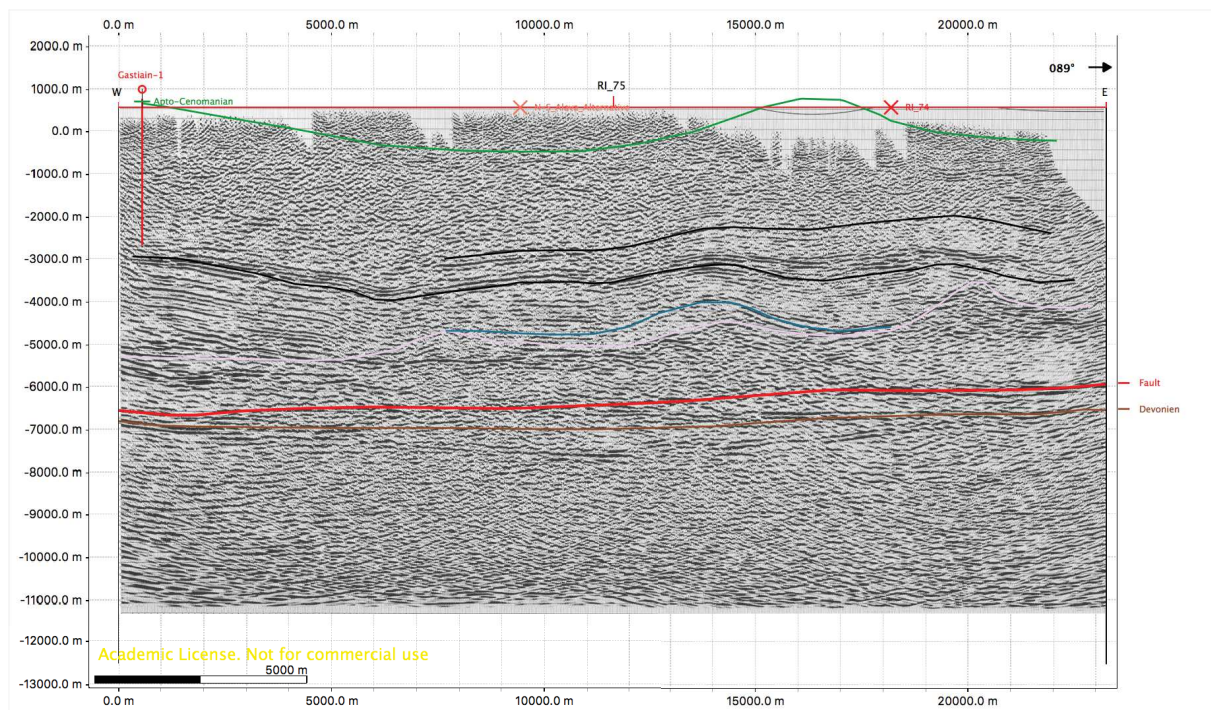


Figure 4: Ligne sismique RL75

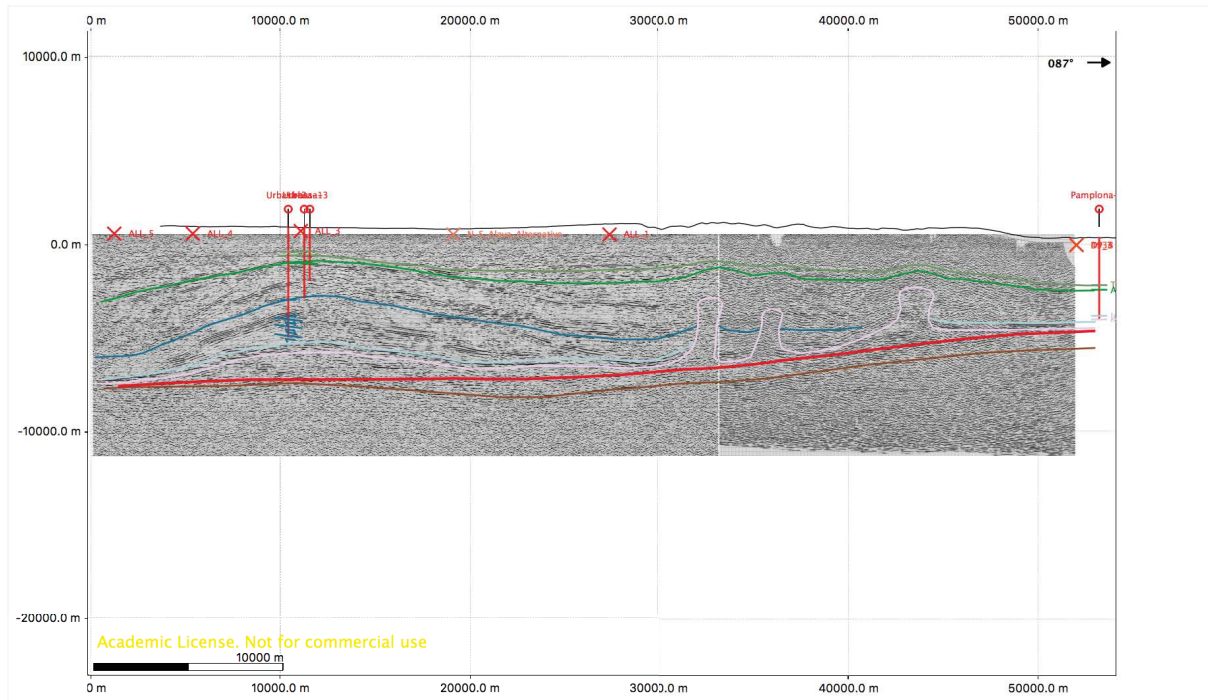


Figure 5: Lignes sismiques ALL7+AN10

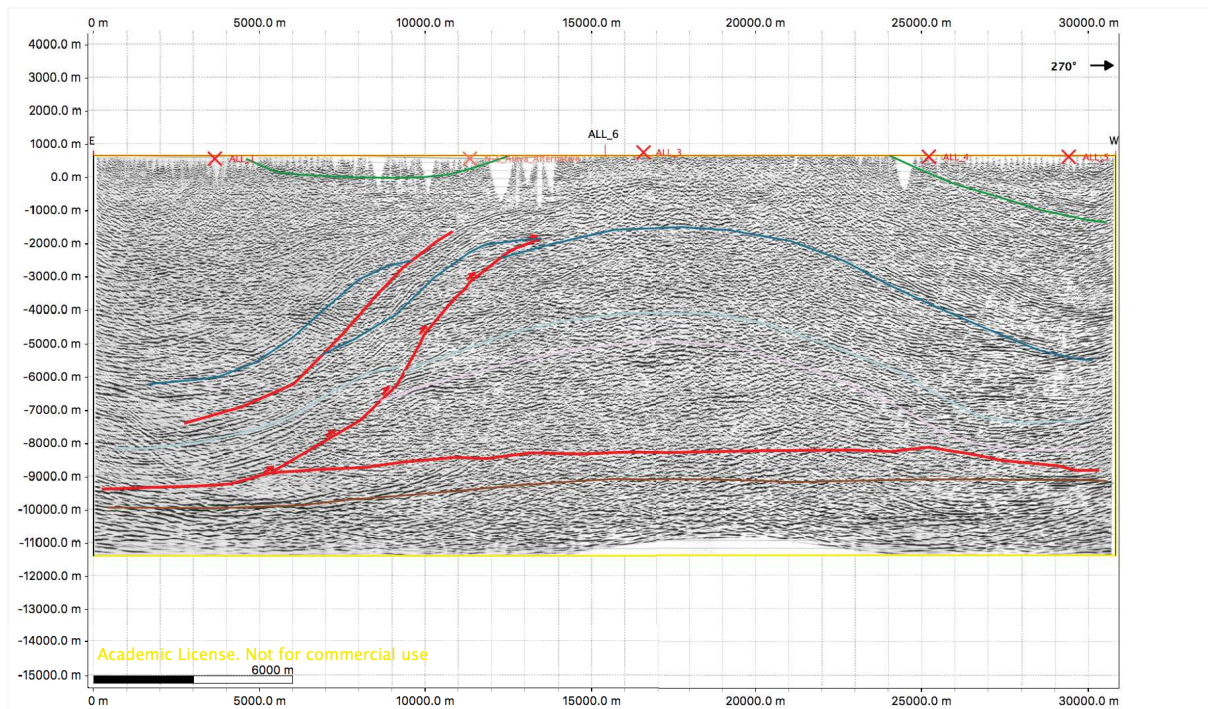


Figure 6: Ligne sismique ALL6

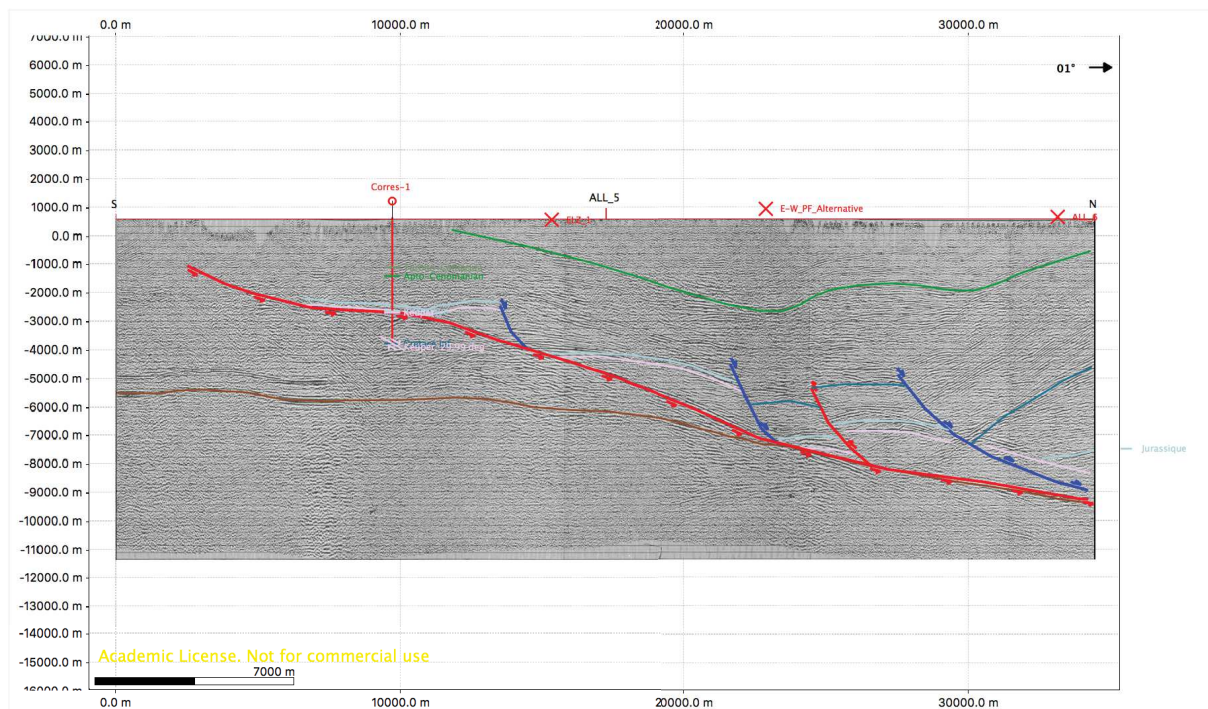


Figure 7: Ligne sismique ALL5

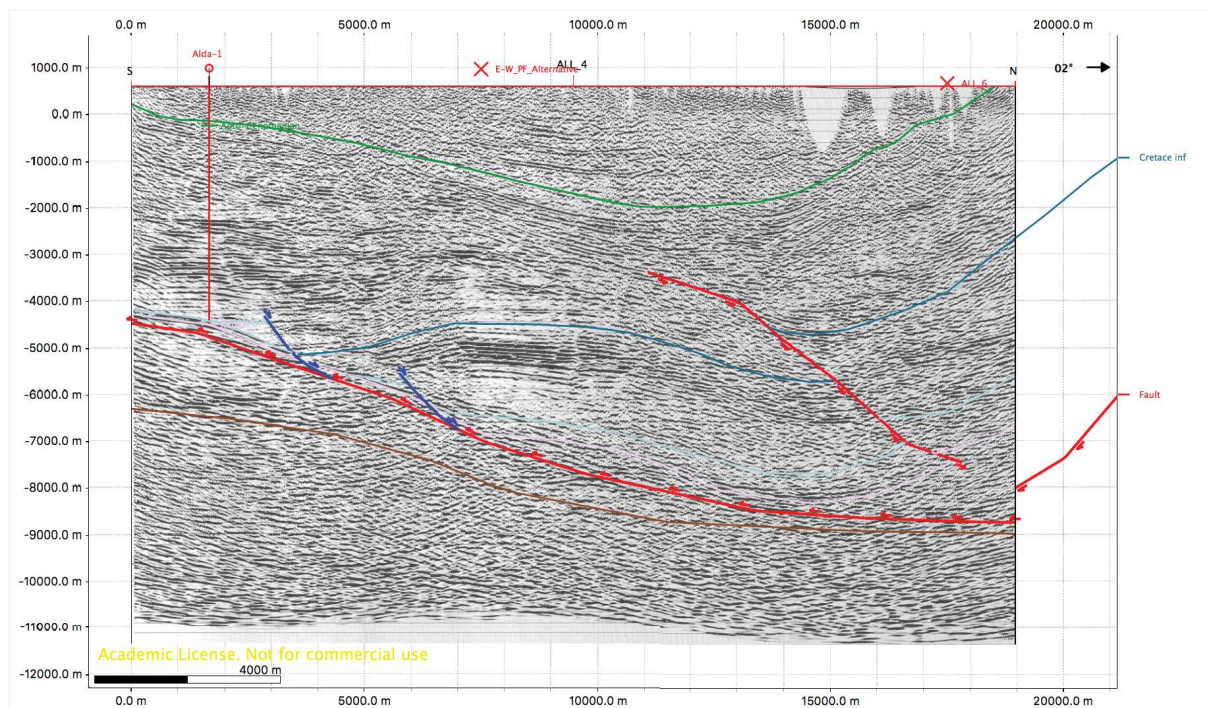


Figure 8: Ligne sismique ALL4

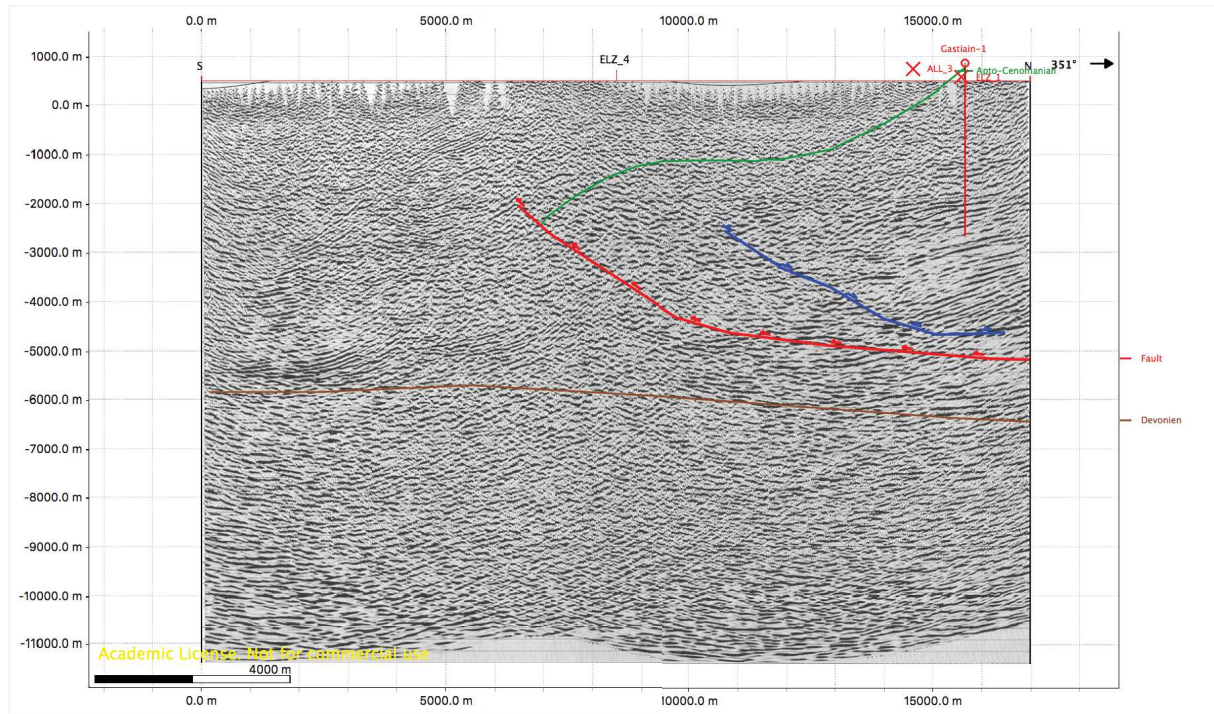


Figure 9: Ligne sismique ELZ4

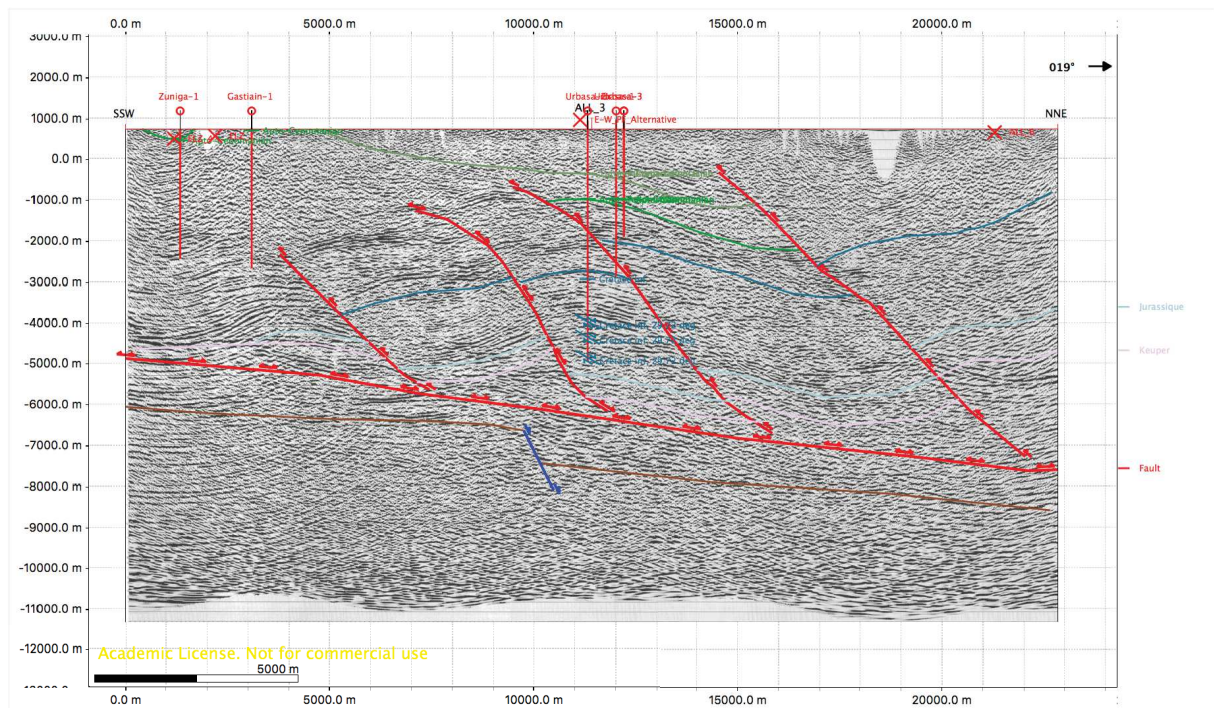


Figure 10: Ligne sismique ALL3

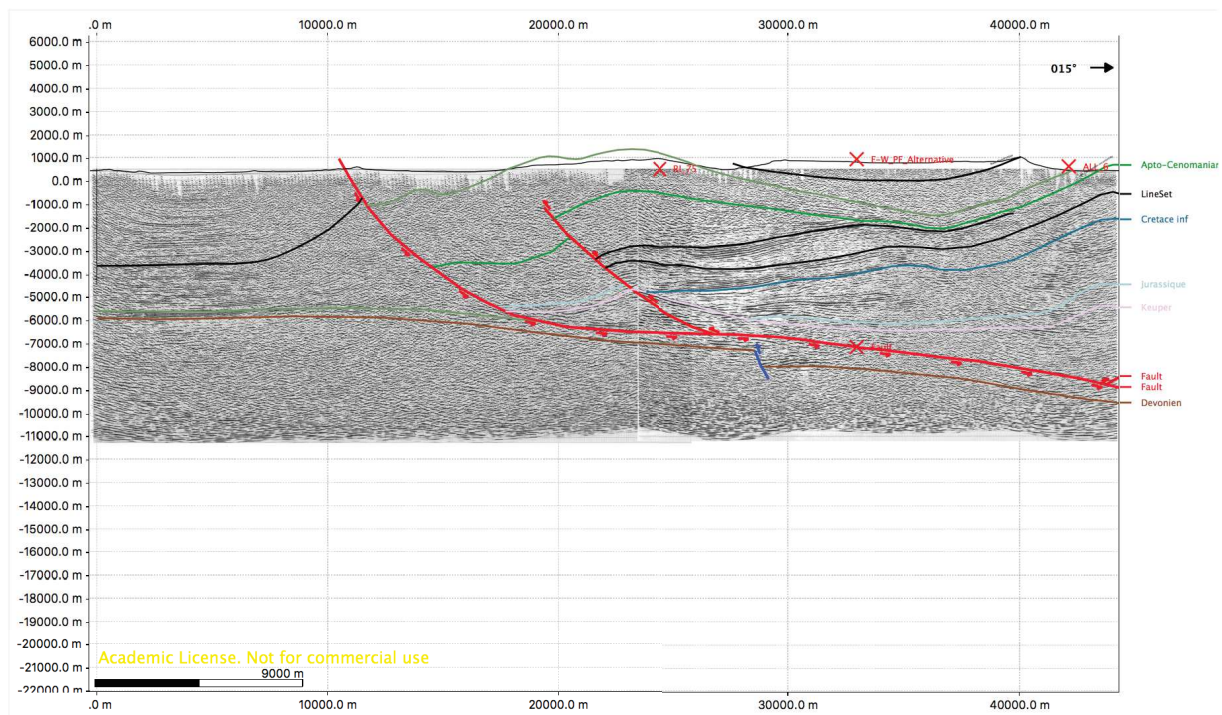


Figure 11: Lignes sismiques RL40+ALL2

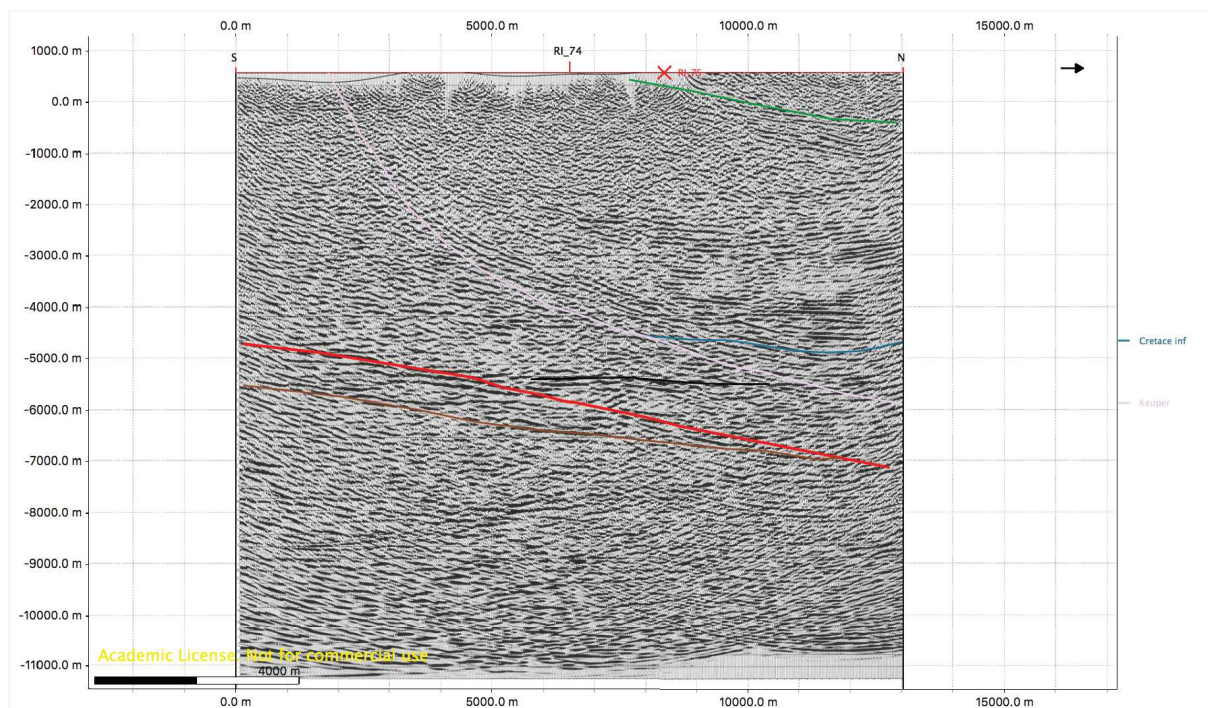


Figure 12: Ligne sismique RL74

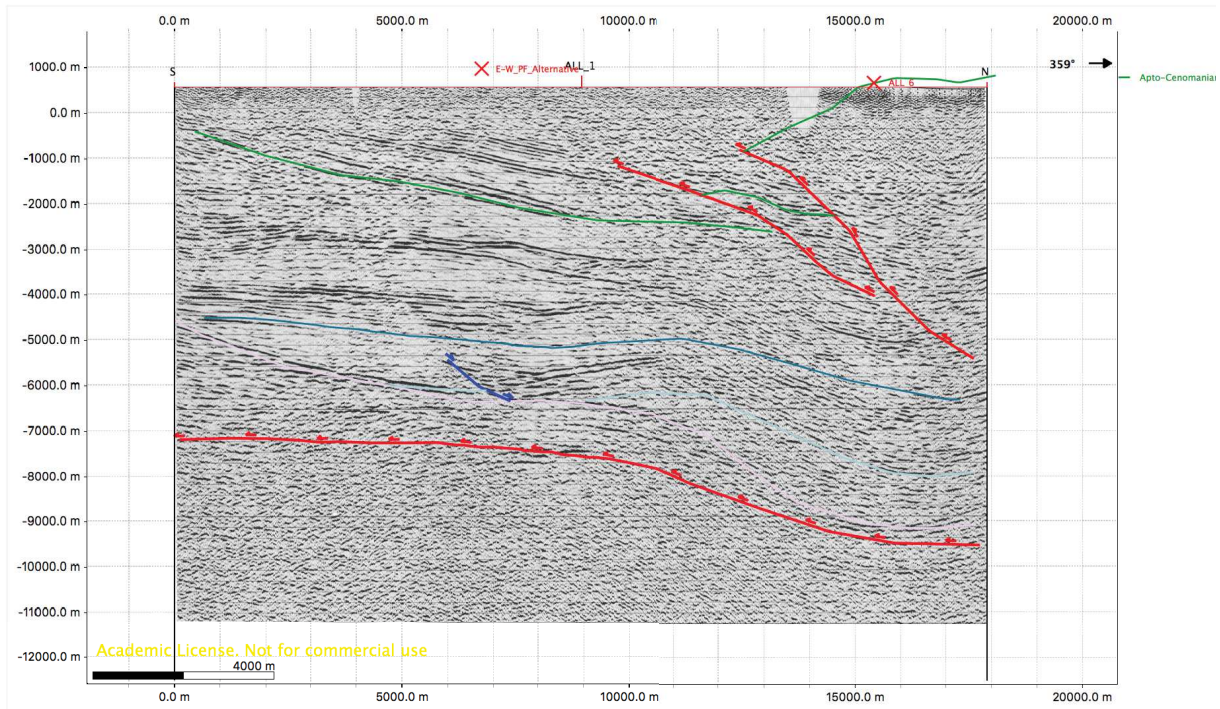


Figure 13: Ligne sismique ALL1

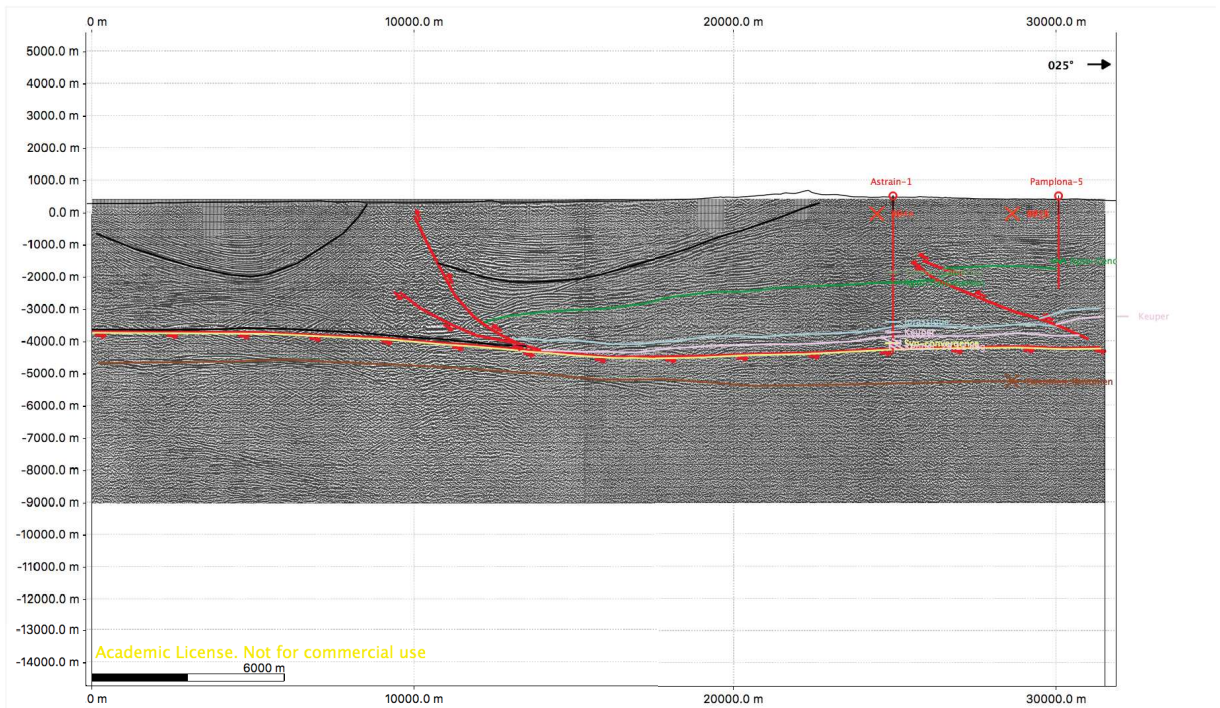


Figure 14: Ligne sismique PP-17-V

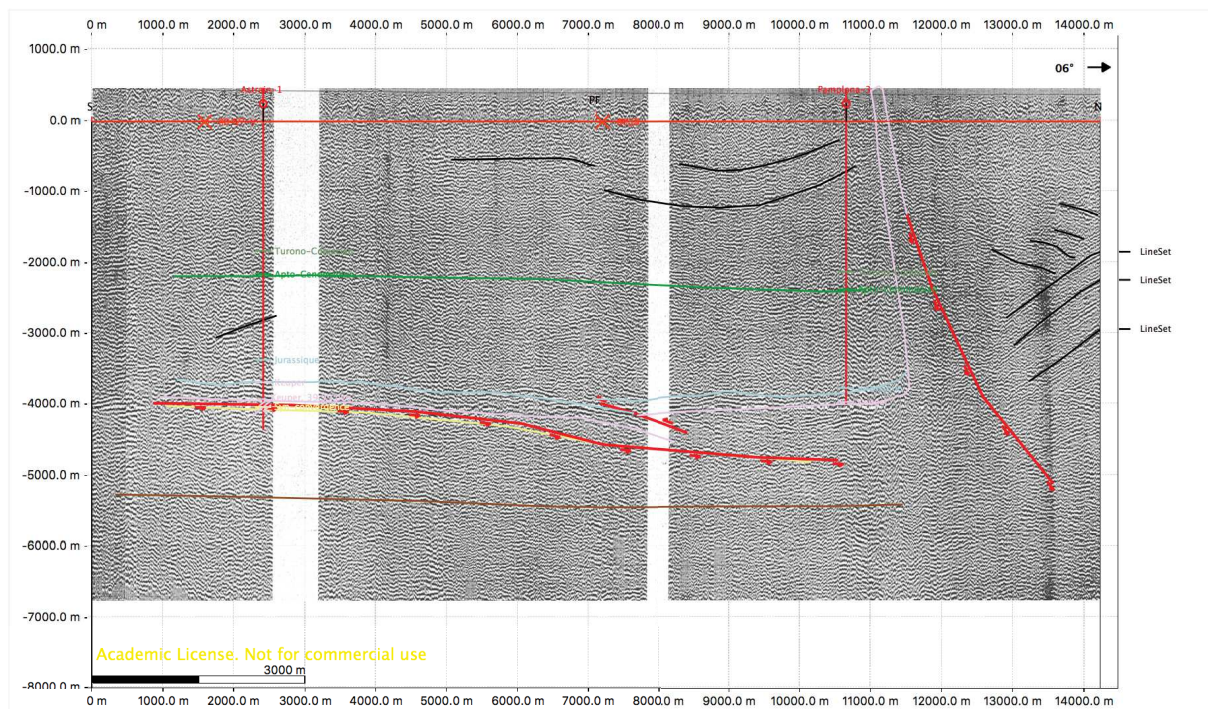


Figure 15: Ligne sismique PF

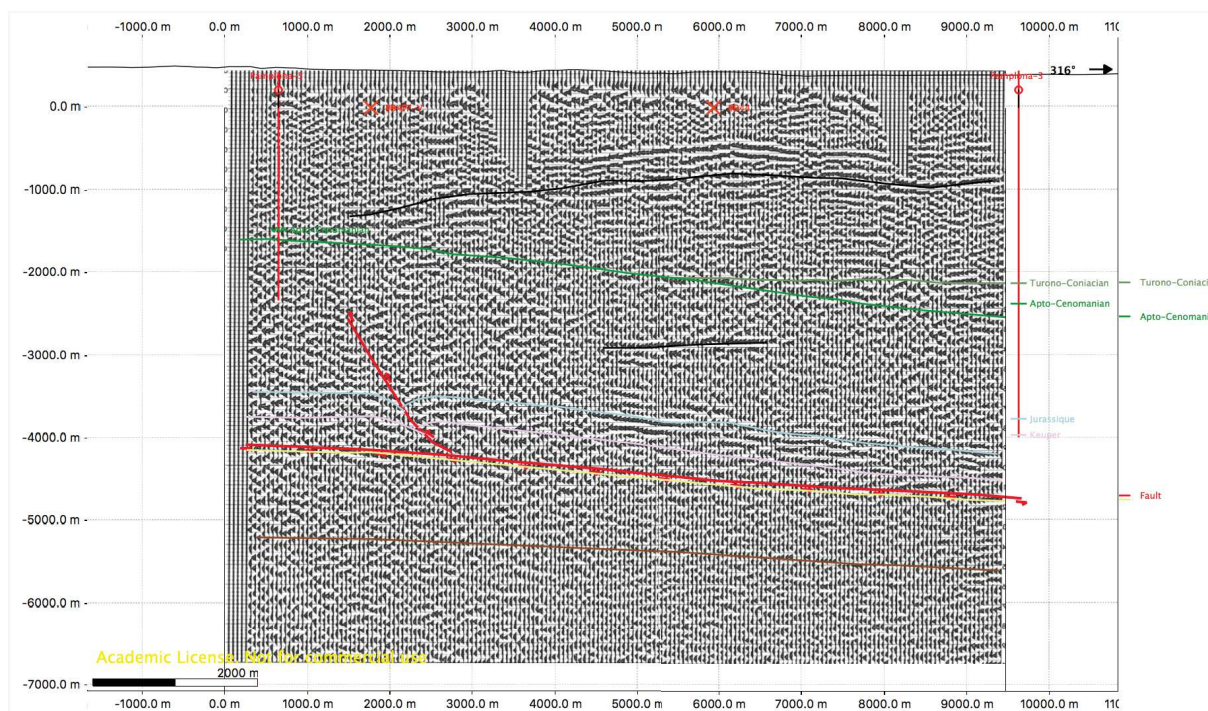


Figure 16: Ligne sismique DP3

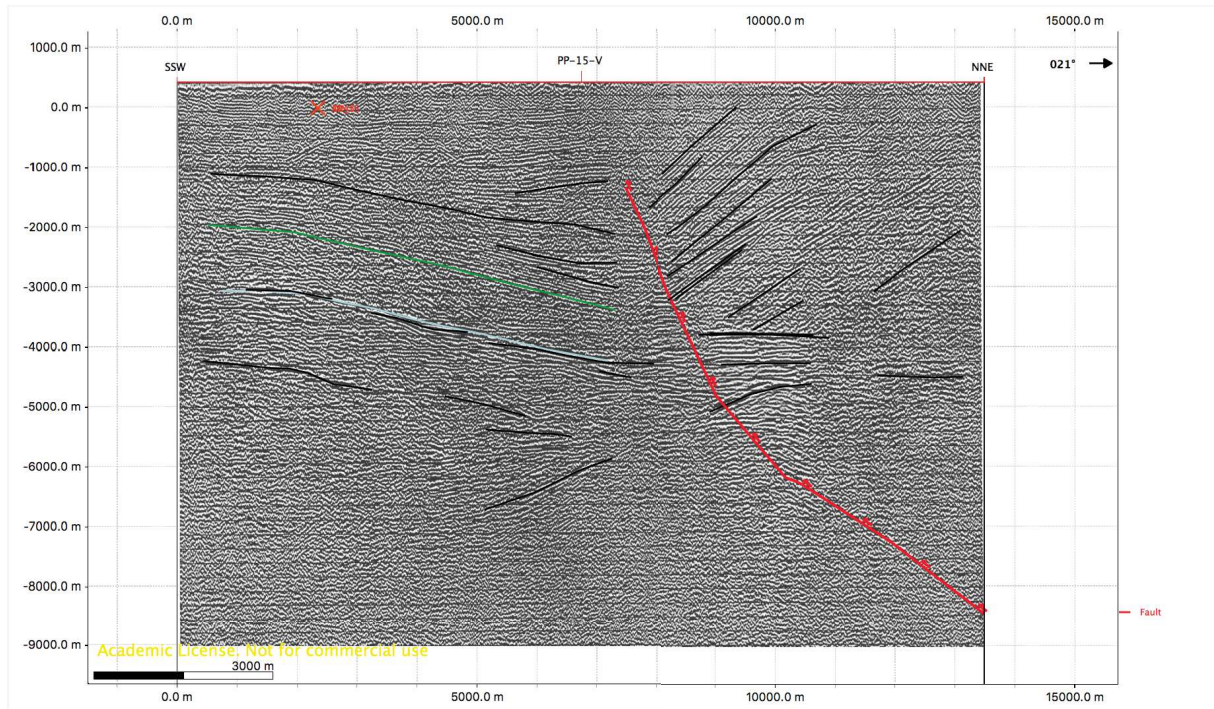


Figure 17: Ligne sismique PP-15-V

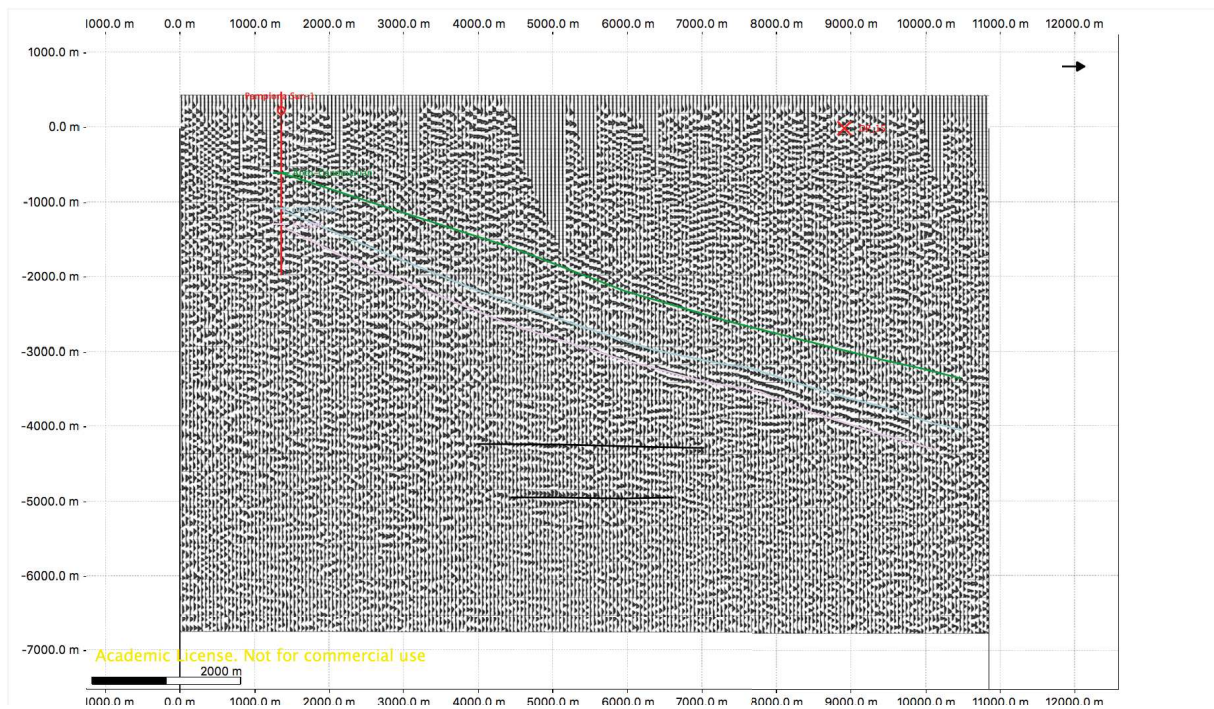


Figure 18: Ligne sismique DP17

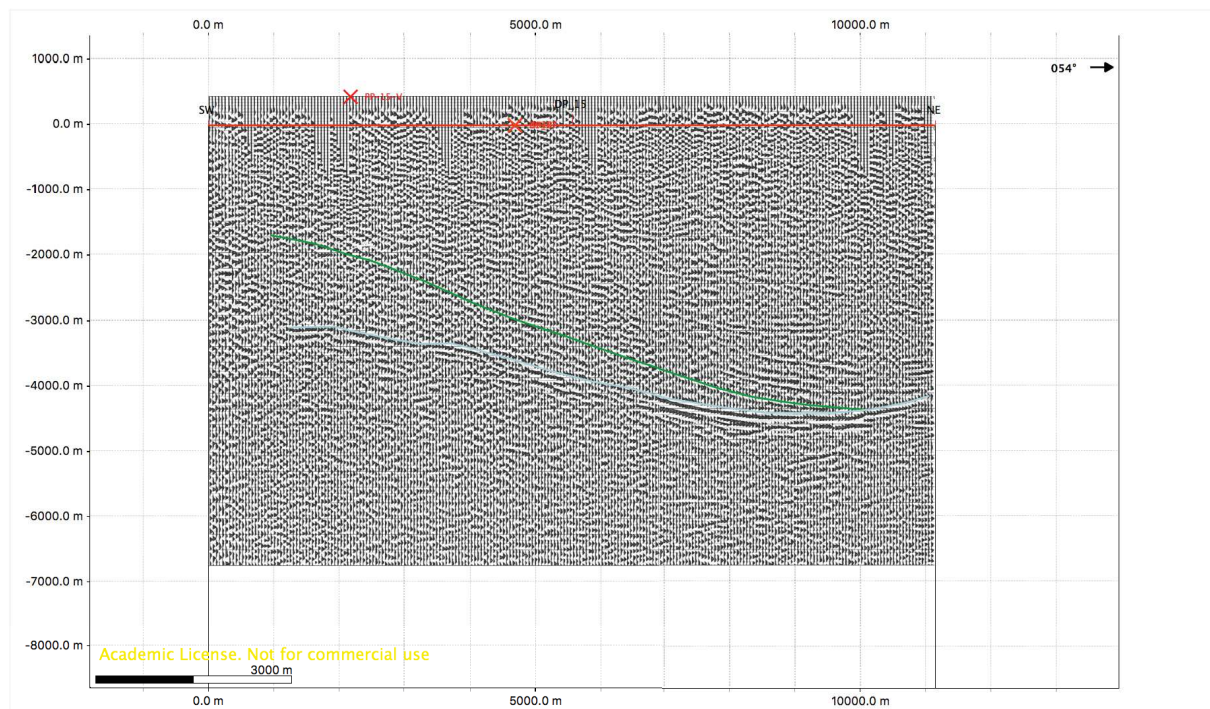


Figure 19: Ligne sismique DP15

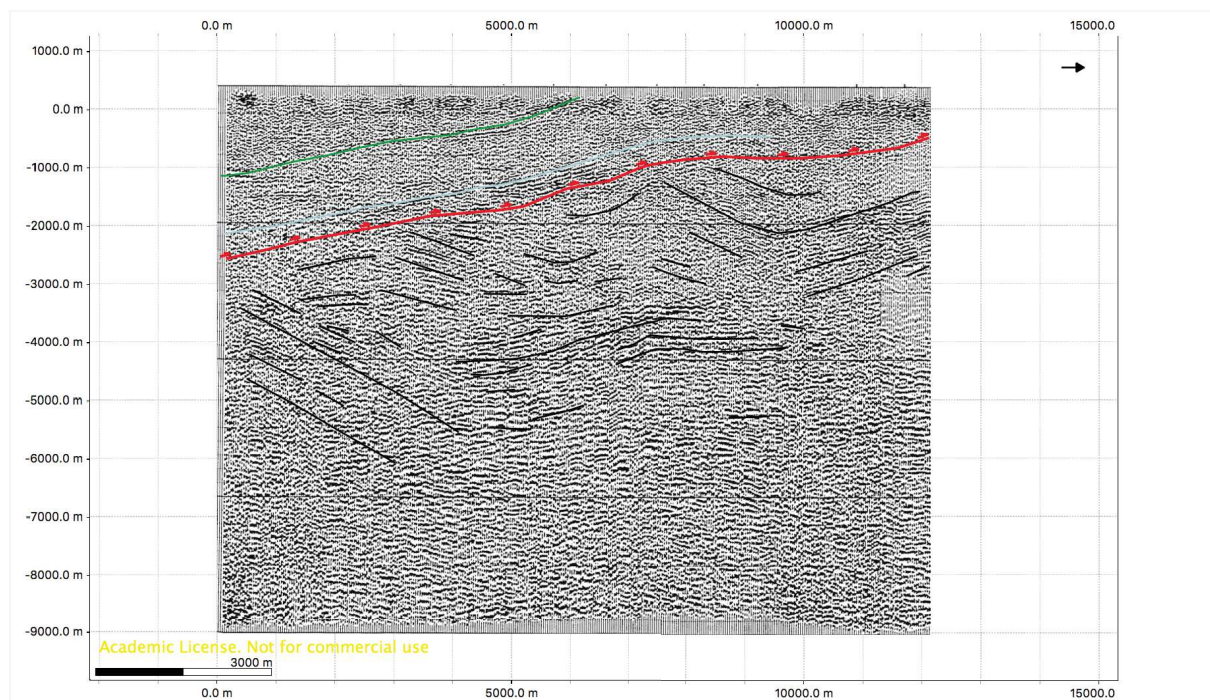


Figure 20: Ligne sismique OS-13

4. OBSERVATIONS ET COUPES DE TERRAIN: EXHUMATION DES GRANULITES DE L'URSUYA ET ORGANISATION STRUCTURALE LE LONG DE LA TRACE DE LA « FAILLE DE PAMPELUNE ».

4.1 Exhumation des granulites de l'Ursuya

Un panorama a été réalisé à partir des données et observations de terrain afin de déterminer les relations entre le massif du Labourd et l'unité des granulites de l'Ursuya (Fig. 1), ainsi que l'âge relatif de l'exhumation et/ou dénudation des granulites. Des observations de terrain à proximité du village du Louhossoa viennent compléter le panorama.

On observe que les séries détritiques du Trias Inférieur (Buntsandstein) du massif du Labourd présentent une stratification sub-horizontale, discordants sur le bassin permien de Bidarray (Fig. II-4). Ces séries sont basculées vers le nord à nord-est en s'approchant du linéament de Louhossoa où le Trias Inférieur est totalement absent. Le Trias est également absent dans l'unité granulitique d'Ursuya. Ce linéament de Louhossoa apparait dans la topographie de la région comme une crête d'orientation E-O composée principalement des méta-sédiments

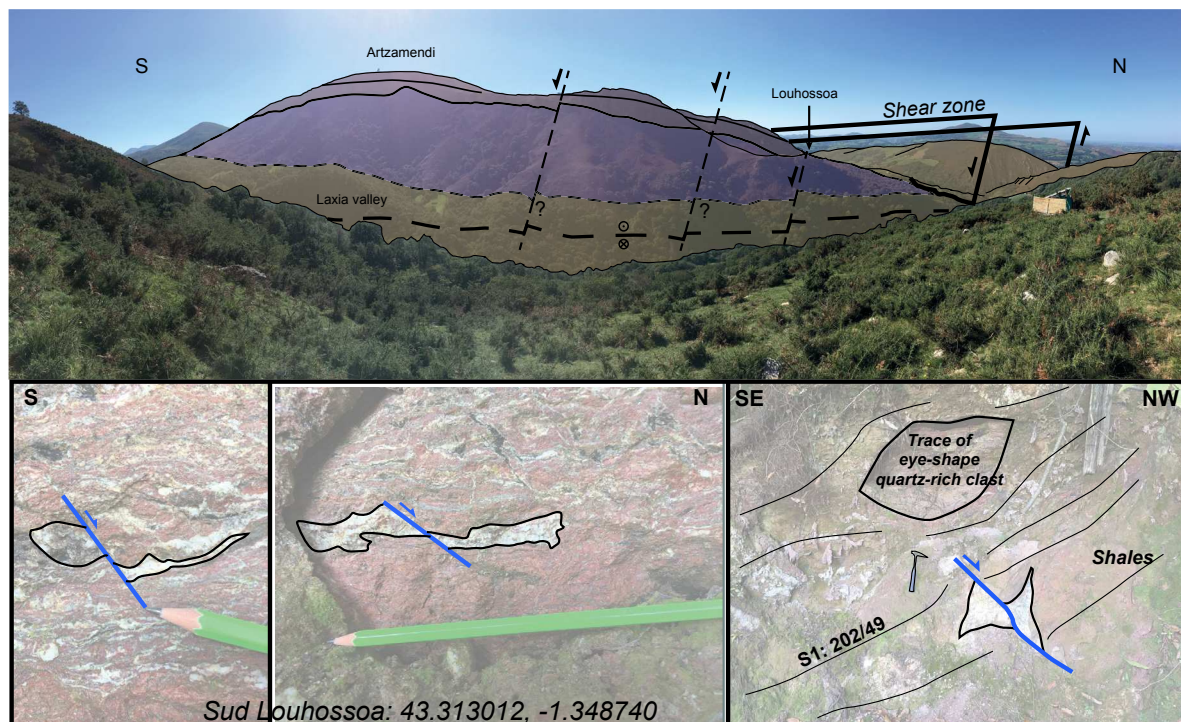


Figure 1: Panorama à partir du point 43°18'09.4"N 1°25'17.5"W, au sud-ouest du Pas de Roland, en regardant vers l'est vers le massif d'Artzamendi (photographie en miroir). Photographies des structures observées au sud de Louhossoa. Voir explications dans le texte.

riches en quartz ordoviciens dont la foliation est fortement inclinée vers le sud (Sn: 171/60 à 202/49). De plus, les observations de terrain (point GPS : 43.313012°N, -1.348740°E) ont révélé l'existence d'une zone de cisaillement affectant des roches très altérées, attribuée au Paléozoïque, au sud du village de Louhossoa. Cette zone de cisaillement, dont l'épaisseur atteint un minimum de 20 mètres, se compose de schistes altérées rougeâtres dont le plan de schistosité est inclinée vers le sud (Sn : 202/49), ainsi que de lentilles de quartz de tailles décimétriques. Ces lentilles de quartz (et feldspaths?) se déforment de façon ductile dans la direction de la schistosité de la matrice argileuse puis sont recoupées par une déformation cassante qui se caractérise par des failles normales orientées approximativement vers le nord.

Ces observations suggèrent qu'une déformation ductile puis cassante, probablement associée à un même épisode extensif, a affecté les roches paléozoïques à la limite entre le massif du Labourd et les granulites de l'Ursuya. Cet épisode pourrait être partiellement responsable de l'exhumation des granulites et du basculement vers le nord (nord-est en relation avec des failles secondaires orientées N-S à faible rejet) des séries triasiques dans le toit de la zone de cisaillement. Ainsi, l'âge de la structure de Louhossoa devrait être postérieur aux dépôts du Trias Inférieur. Cependant, des études complémentaires seraient nécessaires afin de mieux contraindre l'âge relatif des déformations.

4.2 Organisation structurale le long de la trace de la « faille de Pampelune ».

Des coupes géologiques ont été réalisées (Fig. 2) entre le massif de Cinco Villas et le massif du Labourd (Figs. 3 et 4), et entre la Nappe des Marbres et les massifs de Cinco Villas et des Aldudes (Figs. 5 et 6), afin d'étudier les relations structurales le long du tracé de la « faille de Pampelune ».

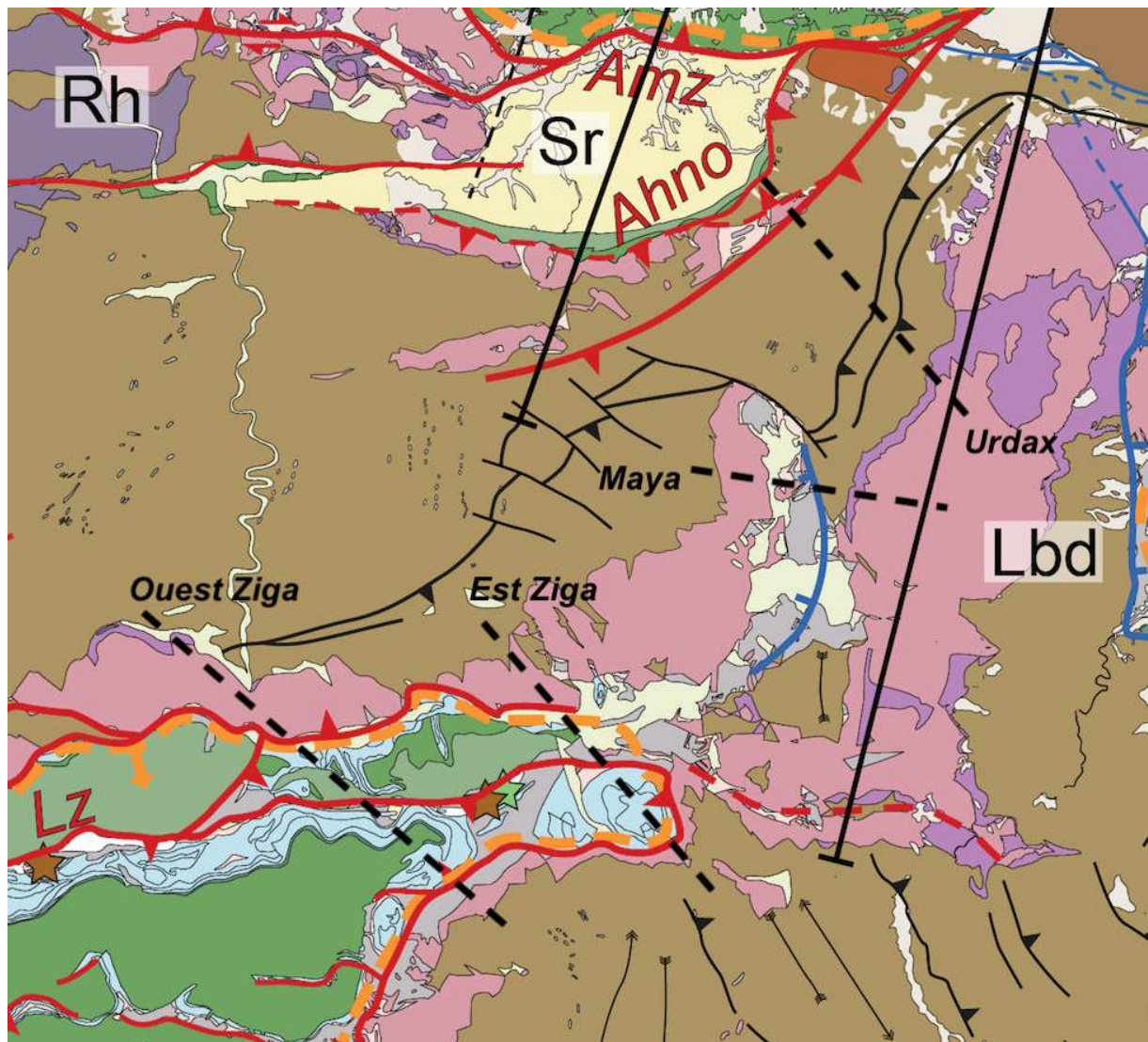


Figure 2: Carte de localisation des coupes

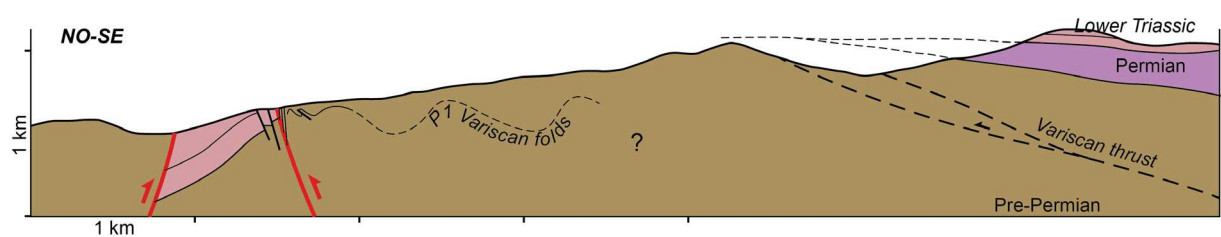


Figure 3: Coupe « Urdax » NO-SE entre le massif du Labourd et le massif de Cinco Villas

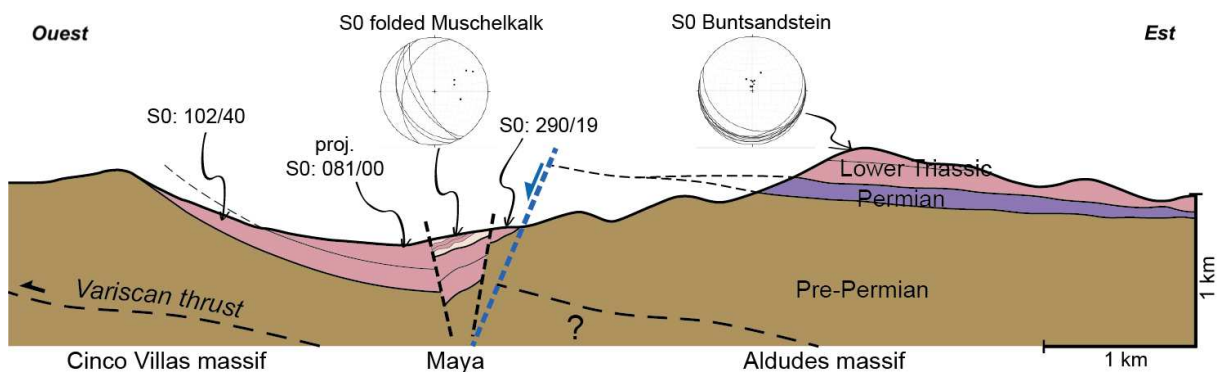


Figure 4: Coupe « Maya » E-O entre le massif du Labourd et la massif de Cinco Villas

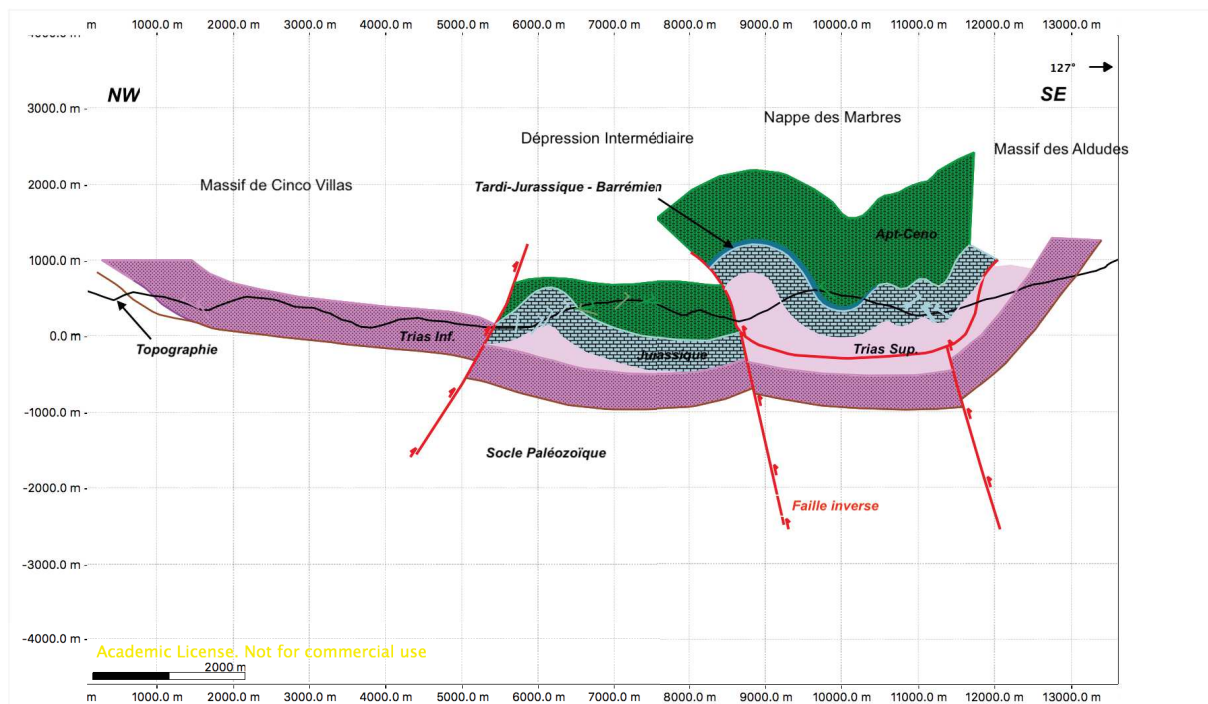


Figure 5: Coupe « ouest Ziga » entre le massif de Cinco Villas et des Aldudes

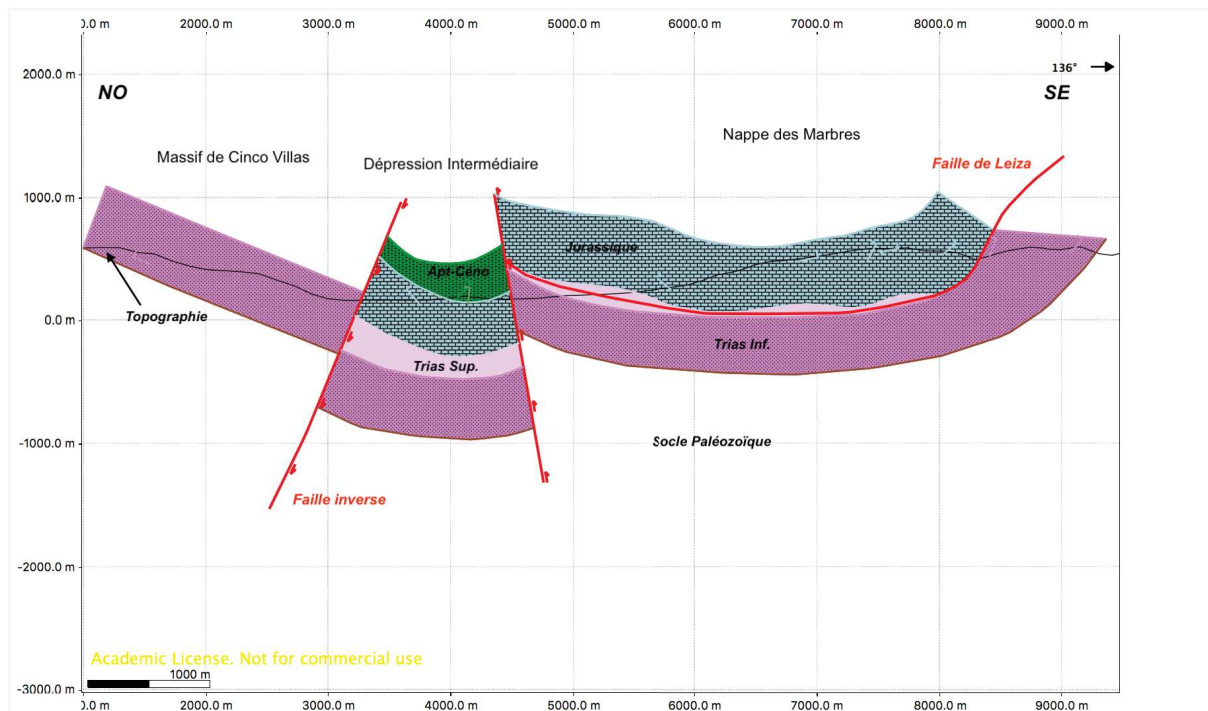


Figure 6: Coupe « Est Ziga » entre le massif de Cinco Villas et des Aldudes

5. RAPPORT D'OBSERVATION DES CAROTTES ET CUTTINGS DU PUIT D'AINHICE (BASSIN DE MAULÉON) (COLLAB. EMMANUEL MASINI, JULIE TUGEND ET MAXIME DUCOUX)

5.1 Rapport d'observation des carottes du puit d'Ainhice-1 à Boussens

Participants : Emmanuel Masini, Julie Tugend, Maxime Ducoux, Rodolphe Lescoutre

L'objectif était de caractériser le contact entre le socle Paléozoïque et les évaporites du Trias Supérieur tel que décrit sur le rapport des activités de forage (Fig. 1).

Les observations correspondent au premier ordre avec le rapport des activités de sondages décrivant une alternance d'ophites tardi-triasiques avec des ardoises indurées. Les carottes montrent des changements abruptes de pendages ainsi que des déformations compressives de types boudinage, plis et failles inverses suggérant au minimum deux phases de déformations. Uniquement dans les carottes 1 et 3 apparaissent des déformations extensives (failles/zones de cisaillement, structures S-C) remplies par de la calcite parfois de couleur verdâtre (Fig. 2). La déformation extensive semble s'intensifier du bas vers le haut de la série (de 3248m à 2969m). Il est difficile de déterminer un âge relative entre les déformations extensives et compressives.

| N° | Profondeur | | Longueur | Récupération | Lithologie |
|----|------------|---------|----------|--------------|-------------------------------|
| | de | à | | | |
| 1 | 2969 | 2974,20 | 5,20 | 5,20 | Argile - Calcaire |
| 2 | 3199 | 3201,00 | 2,00 | 1,80 | Ophite-Gresquartzite-Calcaire |
| 3 | 3241,60 | 3248,30 | 6,70 | 6,70 | Argile - Calcaire |
| 4 | 3536,30 | 3540,85 | 4,55 | 4,00 | Quartzite-Argile-Calcaire |

Figure 1: Extrait du rapport d'activité de forage du puit d'Ainhice indiquant les carottes observées pour ce rapport.

Nos commentaires sont que les roches observées, très indurées et plissées, ne correspondent pas aux évaporites triasiques tel qu'énoncées dans le rapport de sondage. Nous supposons que la présence d'ophites ainsi que l'absence des grès triasiques inférieurs plus profond dans le puit ont porté à confusion et que la série carottée ici (3536 à 2969m) a été attribuée à tort au Trias Supérieur. Ces roches présentent en revanche des similarités avec les roches du socle paléozoïque (Ordovicien, Silurien ou Dévonien) tel que décrit par Heddebaut (1973).

Nous proposons que ces carottes soient constituées de roches du socle paléozoïque affectées par des intrusions de magma ophitique lors du Trias Supérieur. Ces résultats placent la limite socle-couverture à un niveau plus haut dans le puit où, notons, aucune évidence de grès triasique (Buntsandstein) n'a été relevée. Ces observations, couplées au fait que la déformation extensive s'intensifie vers le haut de la séquence observée, suggèrent que la limite socle-couverture pourrait correspondre à une surface tectonique de type extensive.



Figure 2: Échantillons de carottes montrant les veines de calcites remplissant les failles et les fractures.

5.2 Rapport d'observation des cuttings

L'objectif était d'identifier et de décrire la limite entre les argiles noires et les anhydrites indiquée sur les rapport d'activité de sondage à ~2900m de profondeur. Cette limite pourrait correspondre au contact tectonique suggéré dans le paragraphe précédent.

Les observations de cuttings montrent une transition abrupte entre les ardoises indurées (échantillons centimétriques) et les anhydrites blanches (sable fin) entre 2904m et 2898m (l'intervalle n'étant pas disponible). Aucune structure de déformation n'a été observée sur les quelques échantillons d'ardoises. Les anhydrites sont parfois associées avec des argiles vertes et rouges que l'on peut distinctement attribuer aux séries évaporitiques du Trias Supérieur.

Ces observations suggèrent que le contact entre les ardoises (probablement paléozoïques) et les évaporites (Trias Supérieur) représente une discordance, qu'elle soit sédimentaire ou tectonique.

6. CARACTÉRISATION STRUCTURALE ET PÉTROLOGIQUE DES PYRÉNÉES DE L'OUEST PAR LA MÉTHODE MAGNÉTIQUE À DIFFÉRENTES ÉCHELLES (COLLAB. PAULINE LE MAIRE).

Ce travail résulte d'une collaboration avec Pauline Le Maire (IPGS/Cardem). P. Le Maire a effectué les mesures en drone et traité les données magnétiques tandis que les choix d'études et interprétations ont été principalement guidés par les résultats et observations de mon travail de thèse.

6.1 Objectif et lieu d'étude

L'objectif de la mission était de caractériser et localiser certaines structures et objets géologiques du massif du Labourd, dans les Pyrénées occidentales (Pays Basque français). L'étude s'est focalisée sur 3 zones où des objets géologiques majeurs sont représentés sur les cartes géologiques (carte géologique BRGM Iholdi 1/50000) mais ne sont pas précisément identifiables sur le terrain. En effet, la végétation et le niveau d'altération des roches rend l'observation des zones de contacts tectonique ou pétrologique difficile.

Ainsi, l'étude de carte de l'intensité de l'anomalie magnétique dans ces zones permettrait de mieux localiser et caractériser ces zones clefs pour la compression du système ouest Pyrénéen.

6.2 Contexte général

Le système pyrénéo-cantabrique, qui s'étend au nord de l'Espagne selon une orientation est-ouest, résulte de la fermeture des bassins de rift créacés lors de l'orogénèse pyrénéenne/alpine du Crétacé Supérieur au Miocène. L'architecture de la chaîne présente une disposition générale en éventail dissymétrique associée à une subduction à pendage nord de la plaque Ibérique. Elle se situe à la limite des plaques Ibérie et Eurasie où différents évènements tectoniques ont façonné l'architecture lithosphérique et crustale (ex : orogénèse varisque, rifts triasique et créacé). De nombreux témoins de ces épisodes sont préservés dans la chaîne ainsi que dans les domaines externes.

La carte des anomalies magnétiques à l'échelle du système pyrénéo-cantabrique est représentée sur la figure 1b. Cette carte est obtenue en faisant une dérivée verticale à l'ordre 1 de la grille EMAG2 (Maus et al., 2009). Elle montre des objets ponctuels (3D) ou des structures linéaires (2D). Les principaux objets ponctuels sont localisés près de Bilbao et d'Aurignac

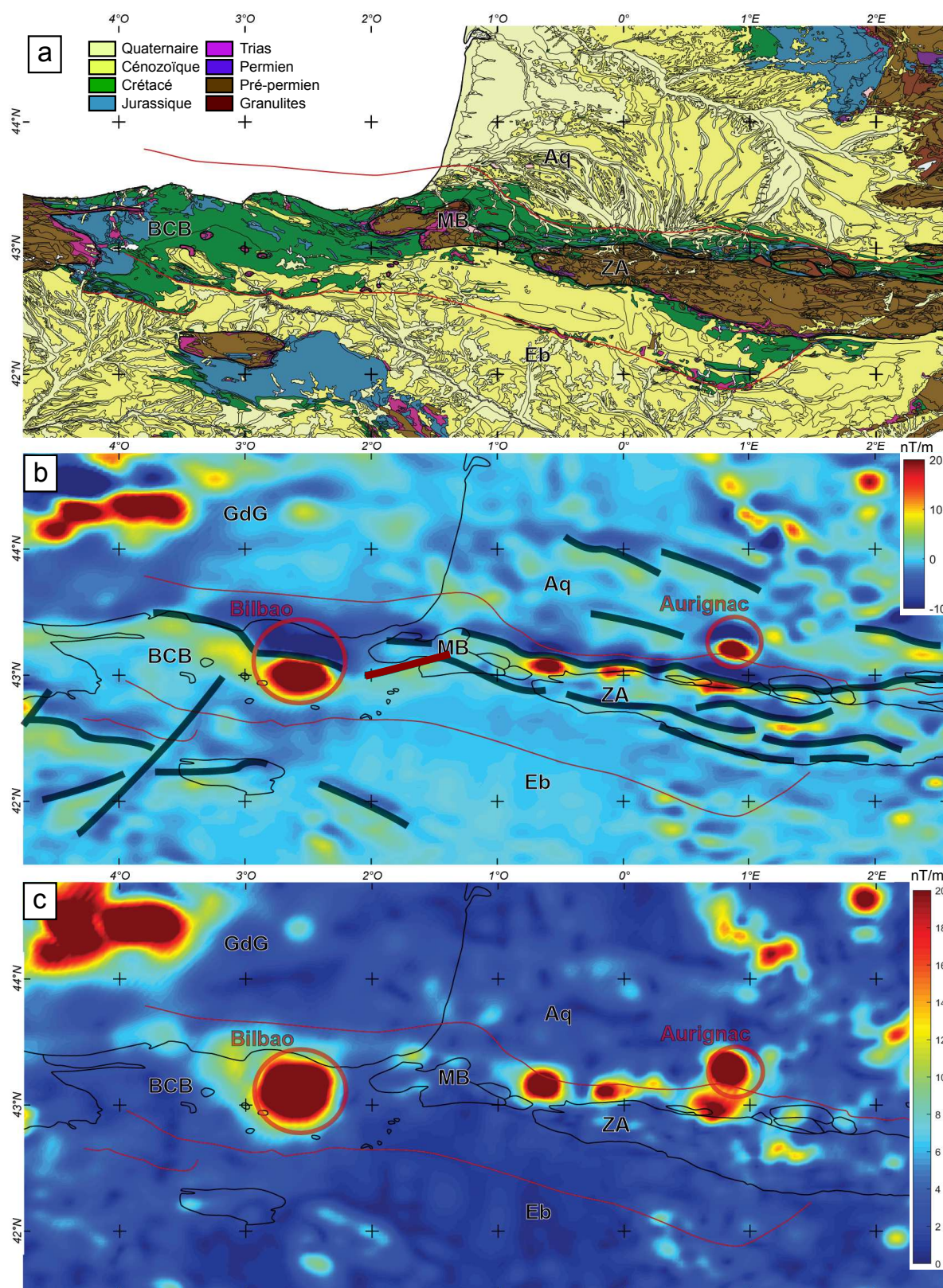


Figure 1: Carte géologique (a), carte des anomalies magnétiques (b), et carte du signal analytique (c) du système pyrénéo-cantabrique. GdG : Golfe de Gascogne ; BCB : Bassin Basque-Cantabre ; Aq : Bassin Aquitaine ; Eb : Bassin de l'Èbre ; MB : Massifs Basques ; ZA : Zone Axiale.

(cercles rouges, Figure 1b). Afin d'estimer une profondeur, des inversions sur le signal analytique (Nabighian, 1972 ; Roest et al., 1992 ; Salem et al., 2002) ont été faites sur ces deux anomalies (Fig. 1c; hypothèse sur la géométrie : sphère). Pour l'anomalie de Bilbao, une profondeur d'environ 35km a été trouvée, alors que pour l'anomalie d'Aurignac la profondeur estimée est d'environ 15km. Dans les Pyrénées, les linéations magnétiques sont préférentiellement alignées selon un axe E-O à ONO-ESE parallèle à l'orientation de la chaîne, excepté aux environs des massifs basques où seule une orientation OSO-ENE semble se détacher (trait rouge, Fig. 1b). De façon générale, le domaine est-pyrénéen présente de nombreuses anomalies orientées ONO-ESE (quatre linéations principales) au sein de la zone axiale tandis qu'elles semblent moins nombreuses (deux linéations principales) dans la partie ouest. De faibles anomalies sont observées dans les bassins de l'Èbre et Aquitain. Notons cependant l'existence d'une anomalie NE-SO au sud du bassin Basque-Cantabre qui correspond à une orientation généralement attribuée aux épisodes tardi-varisque à triasique.

Il existe également une campagne aéromagnétique de plus grande résolution effectuée par CGG en 1968 pour la compagnie ESSO au niveau du chevauchement du Labourd. Les données ont été acquises à 1.5 km de hauteur, avec un espacement des profils de 8 km. La carte présentée dans la figure 2 a été obtenue en numérisant une carte du BRGM de 1980 qui compile certains levés détaillés.

Sur cette figure 2, on constate la présence d'anomalies ponctuelles et l'absence de linéations E-O comme observées sur la figure 1.

- L'anomalie au sud, de haute fréquence et de plus forte intensité, indique que la source est proche de la surface. La carte géologique nous indique la présence d'ophite dans la zone que l'on pourrait donc rapprocher à cette anomalie ponctuelle.

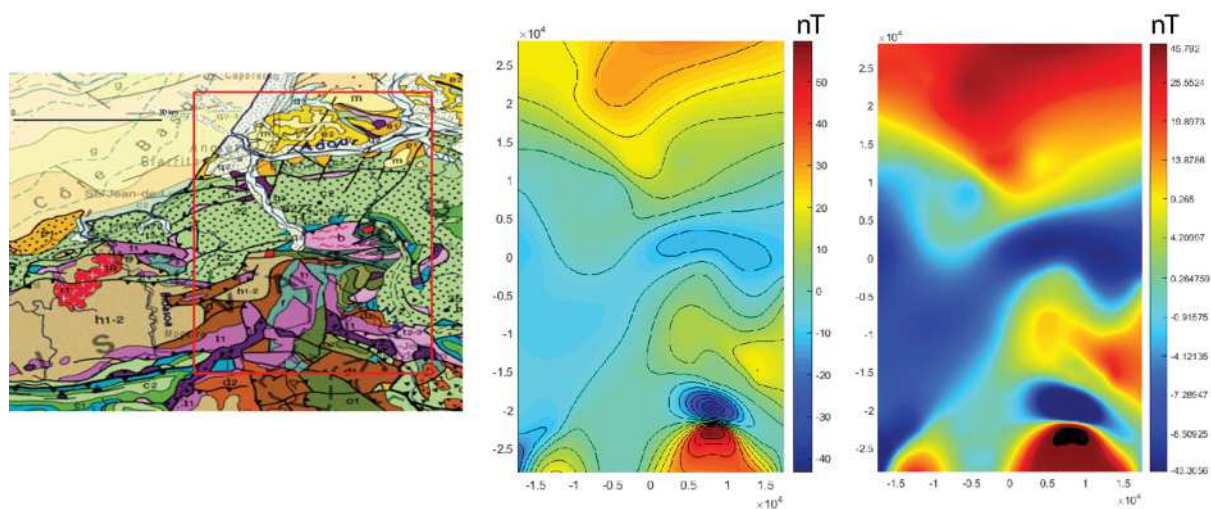


Figure 2: Carte géologique au 1/106 (BRGM) et cartes des anomalies magnétiques montrant les anomalies ponctuelles associées au massif du Labourd.

- Au centre, on aperçoit une anomalie de plus grande longueur d'onde et de plus faible intensité, dont la géométrie semble s'accorder avec la limite nord du massif du Labourd.

Cependant, on remarque qu'aucune anomalie ne semble associée au linéament de Louhossoa. C'est pourquoi nous avons effectué de nouvelles acquisitions de plus haute résolution dans la zone afin de caractériser les objets géologiques.

6.3 Description des zones cartographiées

Les 3 zones définies (Fig. 3) pour la cartographie des anomalies magnétiques par drone sont :

1) Hasparren (entre Hasparren en Cambo-les-bains)

La zone sélectionnée recouvre le chevauchement du Labourd qui superpose les roches à faciès métamorphique « granulite » de l'unité d'Ursuya sur les sédiments non métamorphiques du bassin de Mauléon. L'unité d'Ursuya est composée de métasédiments et migmatites (faciès granulites et protolithe inconnu) ainsi que de gabbros. La formation des gabbros et le métamorphisme granulitique est probablement tardi-varisque (300Ma). Les sédiments du bassin de Mauléon ont des lithologies variables (sel, calcaires, marnes, et turbidites calcaires) d'âge tardi-triasique à crétacé supérieur. Le chevauchement du Labourd, bien qu'observé indirectement par l'étude des déformations dans les bassins de Mauléon et St-Jean-de-Luz et la cartographie, n'a pas été clairement identifié à l'affleurement. Ainsi, l'angle de la faille et le déplacement accommodé par le chevauchement ne sont pas bien contraints.

2) Louhossoa, au pied du mont Baïgoura

La zone d'étude se situe au pied nord du massif du Baïgoura, sur la structure de Louhossoa qui juxtapose les granulites de l'unité d'Ursuya (cf. zone d'Hasparren) aux roches paléozoïques et triasiques du Baïgoura. Les roches du Baïgoura se composent de métasédiments de l'Ordovicien à Dévonien déformés lors de l'orogénèse varisque et de grès du Trias Inférieur. Une augmentation du métamorphisme est observée du haut du massif du Baïgoura vers la structure de Louhossoa en contrebas. Cette structure de Louhossoa a été décrite comme une faille ou zone de cisaillement extensive à pendage sud accommodant une partie de l'exhumation des granulites de l'Ursuya. Cependant, l'âge et l'angle de cette structure restent peu connus. Les précédentes estimations de son angle, basées sur les interprétations géologiques, varient de 30° à 70° et ne permettent pas de contraindre le processus à l'origine de l'exhumation de ces granulites (Louhossoa seule ou faille d'exhumation à pendage nord).

3) Sohano

Cette zone correspond au seul affleurement connu de manteau (péridotite) du Labourd. Il se situe au nord de l'unité granulitique de l'Ursuya, dans la vallée située au sud du village de Sohano. La péridotite est fortement serpentinisée et affleure sous la forme d'un ellipsoïde d'orientation ONO-ESE (carte géologique) entourée des granulites et des gabbros. Les questions autour de cette roche ultramafique anime la communauté pyrénéenne puisque son origine et ses implications pour l'architecture crustale synrift crétacée sont largement discutées : péridotite mantellique (= croûte très amincie) ou cumulât (magma associé à la mise en place des gabbros). Bien que l'origine mantellique a récemment été confirmée par B. Petri (comm. pers.), sa position dans la croûte reste incertaine : 1) Fenêtre sur le manteau sous-continentale, auquel cas le contact granulite-manteau représenterait ici le Moho crétacée ; 2) Lentille de manteau insérée dans la croûte inférieure à moyenne lors d'un précédent événement tectonique.

Ainsi, une cartographie de l'étendue et profondeur du manteau de Sohano permettrait à priori d'argumenter en faveur de l'un ou de l'autre scénario.

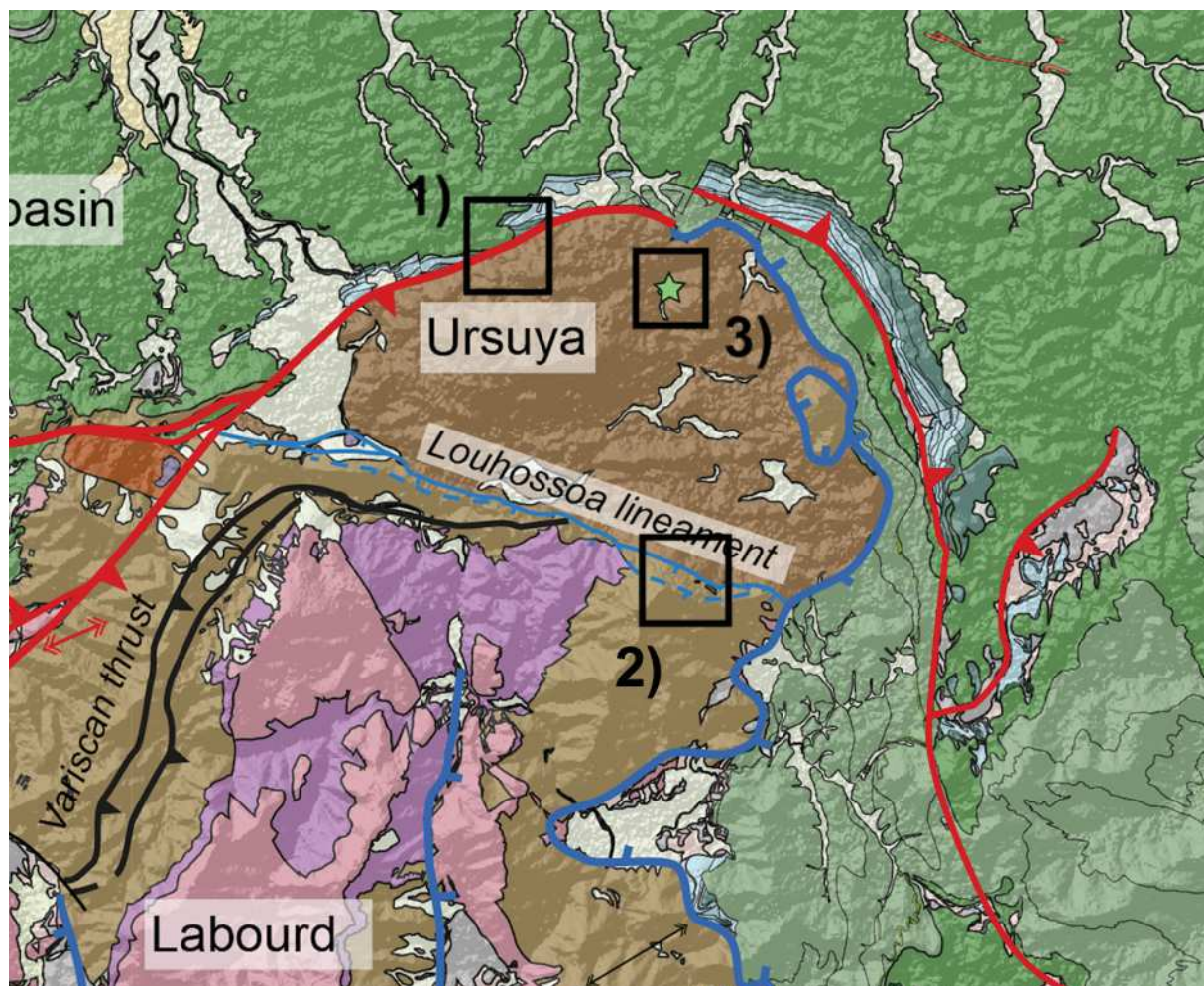


Figure 3: Carte géologique du massif du Labourd, avec les 3 zones étudiées.

6.4 Méthode

La cartographie magnétique par drone permet d'obtenir un jeu de données de haute résolution sur les anomalies magnétiques localisées à faible profondeur correspondant à l'échelle des structures observées sur le terrain. De plus, elle permet de couvrir de vastes zones éventuellement inaccessibles à pied.

L'acquisition en drone a été réalisée avec une électronique de type 15F1 (15F1000). Pour l'ensemble des fichiers les mesures ont été faites à une cadence de 25 Hz avec un filtre sur 36 échantillons. Aucune perturbation anthropique particulière n'a été notée.

Un capteur magnétique de type fluxgate (Bartington Mag03) a été placé à 41 cm (à partir du milieu du drone) à l'avant du drone. Le porteur de l'équipement est le drone M210 RTK du fabricant DJI (Fig. 4). Lors des acquisitions, une antenne de base a été placée sur le terrain, afin de fournir des corrections aux deux antennes placées sur le drone.



Figure 4: Le drone avec le système magnétique.

A chaque point de décollage, la base RTK est déployée et des étalonnages au sol et/ou en vol sont réalisés, en début et/ou en fin de profil.

Les conditions météorologiques doivent être bonnes (pas de vent, pluie). Les vols ont été faits de façon manuelle et automatique, selon le contexte et l'altitude (Fig. 5).

| Lieu | Altitude | Espacement des profils | Temps de vol | Distance |
|------------------|----------|------------------------|--------------|----------|
| Hasparren | 50 m | 50 m | 22 min | 10 km |
| <u>Louhossoa</u> | 10 m | 10 m | 35 min | 4 km |
| <u>Sohano</u> | 80 m | 80m | 9 min | 3 km |
| <u>Sohano</u> | 60 m | 60m | 22 min | 9 km |

Figure 5: Tableau des paramètres de vols.

6.5 Résultats de la campagne aéromagnétique

1) Hasparren

Les résultats (Fig. 6) montrent un gradient positif vers le nord, mais l'anomalie n'est pas complète et il est donc difficile de l'interpréter. Sur la zone, la carte géologique indique la présence de chevauchement du Labourd où le contact granulites - sédiments ne semble être associé à aucune anomalie magnétique de haute fréquence.

Ces résultats peuvent être mis en perspective par rapport à une première mission de mesure au sol (capteur à un mètre du sol) effectuée dans la zone nord-est du massif du Labourd (carrière de Garralda). A cet endroit, le même contact lithologique existe (granulite – sédiments mésozoïques) et son anomalie mesurée était d'une dizaine de nano-Tesla.

Ainsi, si l'on souhaite cartographier magnétiquement ce contact, il est nécessaire que le capteur soit placé à quelques mètres du sol.

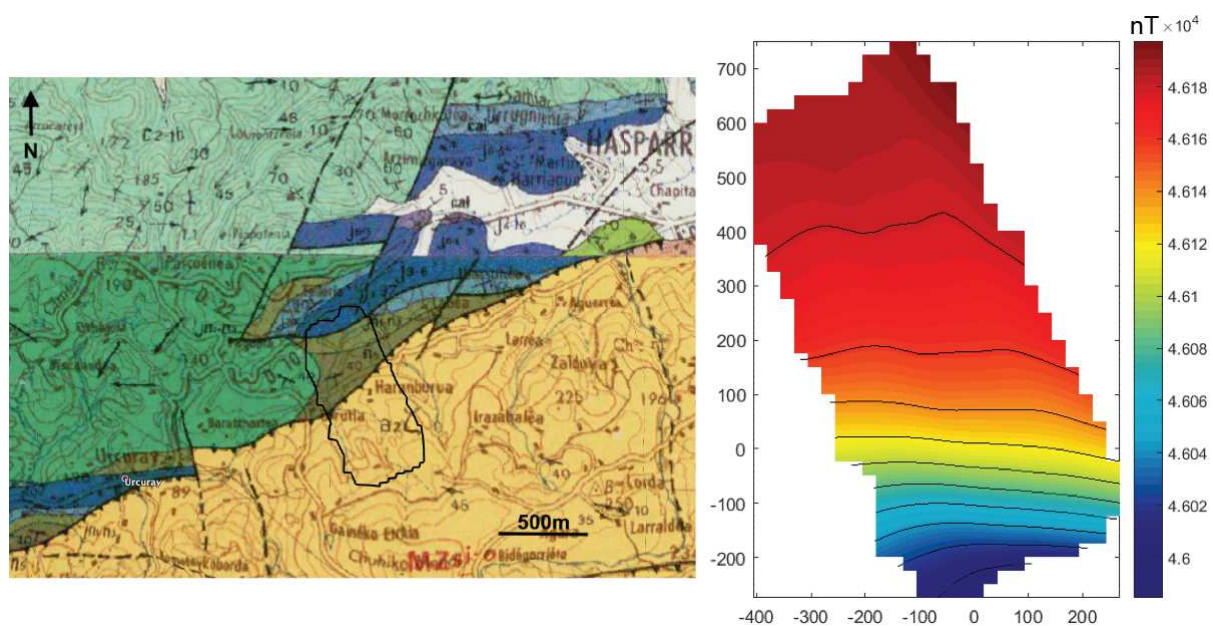


Figure 6: Carte géologique (Iholdy 1/50000, BRGM) et carte de l'intensité de l'anomalie magnétique pour la zone d'Hasparren.

2) Louhossoa

Les cartes magnétiques ne montrent pas d'anomalie corrélées à la géologie que ce soit en drone ou au sol. Ainsi, un chemin de randonnée est observable sur la bordure ouest du profil mais aucun objet géologique n'est mesuré. Ce constat peut être expliqué par deux hypothèses :

- Un contraste faible des propriétés magnétiques entre l'infra-structure (granulites) et la supra-structure (métasédiments paléozoïques).
- La zone de cisaillement de Louhossoa pouvant être diffuse, le couloir cartographié devrait potentiellement être étendu.

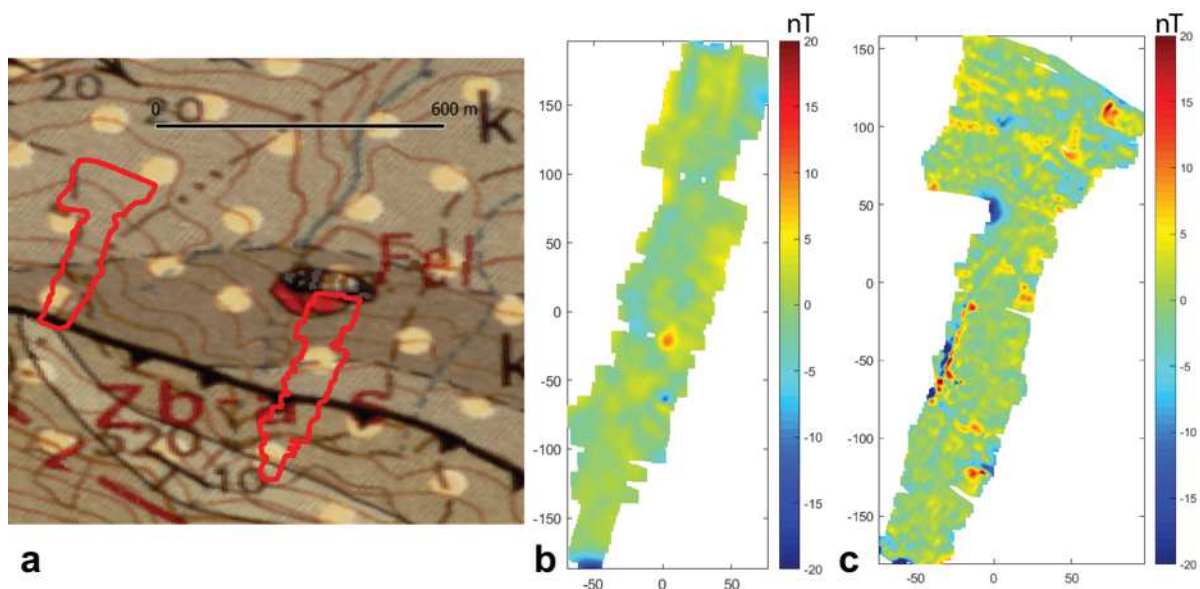


Figure 7: Carte géologique (a) (Iholdy 1/50000, BRGM) et carte des anomalies magnétiques par drone (b) et au sol (c) pour la zone de Louhossoa.

3) Sohano

Les résultats montrent une anomalie de forme ellipsoïde orientée E-O à ENE-OSO que l'on peut associer aux roches de manteau serpentinisé décrites sur la carte géologique comme orientée ONO-ESE. Au nord-ouest de la zone cartographiée à 60m, on observe la partie positive d'une anomalie de grande longueur d'onde qui ne semble pas corrélée aux orientations de la géologie de surface. Un gradient linéaire orienté ENE-OSO est également observable au sud de la carte. Il semble parallèle au tracé d'une faille inverse de la carte géologique.

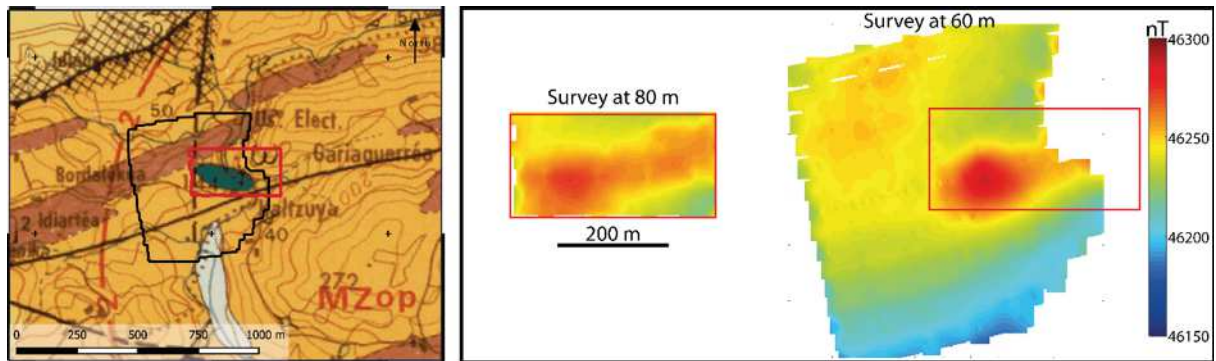


Figure 8: Carte géologique (Iholdy 1/50000, BRGM) et cartes de l'intensité de l'anomalie magnétique pour la zone de Sohano.

6.6 Conclusion générale et perspectives

L'analyse à l'échelle du système pyrénéo-cantabrique des cartes magnétiques (EMAG2) a mis en évidence de nombreuses structures globalement orientées E-O ainsi qu'une différence d'architecture entre l'est et l'ouest.

Avec les données de moyenne résolution dans le Pays Basque, on remarque que les anomalies ne sont plus aussi linéaires. Dans le cas du chevauchement du Labourd, une anomalie semble dessiner son contact nord. Cependant, le linéament de Louhossoa ne semble pas être associé à une anomalie magnétique.

Avec des données de haute résolution, nous avons mis en évidence que les anomalies magnétiques pouvaient être corrélées plus facilement avec les objets géologiques cartographiés.

Cette étude préliminaire met en évidence que le magnétisme permet de mieux caractériser les structures à toutes les échelles du système.

Les données satellitaires montrent une asymétrie E-O à travers le système pyrénéen. Il serait intéressant de combiner ces données aux données géophysiques existantes ainsi qu'aux observations géologiques afin d'établir un modèle crustal cohérent du système pyrénéo-cantabrique.

Les données plus hautes résolutions (aéromagnétisme et drone) permettent de faire le lien avec la géologie de surface. Une campagne de plus haute résolution permettrait de mieux contraindre les relations géologiques de sub-surface qui sont à l'heure actuelle mal définies (végétation dense, urbanisation, données géophysiques pas assez résolutes).

6.7 Références

- Maus, S., Barckhausen, U., Berkenbosch, H., Bournas, N., Brozena, J., Childers, V., Dostaler, F., Fairhead, J.D., Finn, C., von Frese, R.R.B., Gaina, C., Golynsky, S., Kucks, R., Lühr, H., Milligan, P., Mogren, S., Müller, R.D., Olesen, O., Pilkington, M., Saltus, R., Schreckenberger, B., Thébault, E., Caratori Tontini, F., 2009. EMAG2: A 2-arc min resolution Earth Magnetic Anomaly Grid compiled from satellite, airborne, and marine magnetic measurements: EARTH MAGNETIC ANOMALY GRID. *Geochemistry, Geophysics, Geosystems* 10, n/a-n/a. <https://doi.org/10.1029/2009GC002471>
- Nabighian, M.N., 1972. The analytic signal of two-dimensional magnetic bodies with polygonal cross-section; its properties and use for automated anomaly interpretation. *Geophysics* 37, 507–517. <https://doi.org/10.1190/1.1440276>
- Roest, W.R., Verhoef, J., Pilkington, M., 1992. Magnetic interpretation using the 3-D analytic signal. *Geophysics* 57, 116–125. <https://doi.org/10.1190/1.1443174>
- Salem, A., Ravat, D., Gamey, T.J., Ushijima, K., 2002. Analytic signal approach and its applicability in environmental magnetic investigations. *Journal of Applied Geophysics* 49, 231–244.

LIST OF FIGURES

RÉSUMÉ ÉTENDU

| | |
|--|----|
| Fig. Résumé-1: Coupe et carte de la jonction pyrénéo-cantabrique. | 15 |
| Fig. Résumé-2: Blocs 3D de l'évolution des segments de rift lors de la convergence. | 17 |
| Fig. Résumé-3: Captures du modèle numérique de rift hyper-étiré asymétrique. | 19 |
| Fig. Résumé-4: Évolution thermique premier-ordre d'un rift hyper-étiré asymétrique. | 20 |

CHAPTER I: INTRODUCTION

| | |
|--|----|
| Fig. I-1: Conceptual view of a reactivated passive margin in the 80's. | 36 |
| Fig. I-2: Role of inheritance for rifted margins and collisional orogens. | 37 |
| Fig. I-3: Comparison of symmetric and asymmetric rifting. | 41 |
| Fig. I-4: Representation of accommodation zones, transfer zone and transform fault. | 42 |
| Fig. I-5: Geological and structural maps of the Hadibo rift transfer zone. | 43 |
| Fig. I-6: New lithospheric extensional models and the McKenzie model. | 45 |
| Fig. I-7: Mantle bodies and HT/LP metamorphic rocks. | 47 |
| Fig. I-8: Geological map of the Pyrenean and Cantabrian segments. | 48 |
| Fig. I-9: Main stages in the evolution of the Pyrenean Wilson cycle. | 49 |
| Fig. I-10: Major structures and orogenic domains of the Variscan belt. | 50 |
| Fig. I-11: Map of the Late Variscan transcurrent faults in Western Europe. | 52 |
| Fig. I-12: Paleogeographic map of Western Europe at Late Permian. | 53 |
| Fig. I-13: Paleogeographic map of Western Europe at Late Triassic. | 55 |
| Fig. I-14: Geodynamic evolution of the Iberia-Eurasia plate boundary. | 57 |
| Fig. I-15: Distribution of Neocomian sedimentary facies. | 58 |
| Fig. I-16: Map of rift domains prior to the onset of compression. | 61 |
| Fig. I-17: Cross-section evolution of the Eastern Pyrenees. | 63 |
| Fig. I-18: Cross-sections across the Pyrenean-Cantabrian system. | 64 |

CHAPTER II

| | |
|--|----|
| Fig. II-1: Present-day map and kinematic models of Eurasia - Iberia plate boundary. | 75 |
| Fig. II-2: Geological map of the Western Pyrenean – Eastern Cantabrian system. | 81 |
| Fig. II-3: N-S cross-sections across the eastern and western Labourd massif. | 87 |
| Fig. II-4: Geological map of the Labourd – Ursuya area with structural data. | 89 |

| | |
|--|-----|
| Fig. II-5: N-S cross-section across the St-Jean-de-Luz basin. | 91 |
| Fig. II-6: N-S cross-section and seismic interpretation across the BCB. | 92 |
| Fig. II-7: Geological map and structural data of the northern BCB. | 93 |
| Fig. II-8: Field photographs and structural data from the eastern BCB. | 97 |
| Fig. II-9: E-W seismic interpretation across the Estella-Pamplona diapirs. | 98 |
| Fig. II-10: N-S seismic interpretation across the Jaca – Pamplona basin. | 99 |
| Fig. II-11: Present-day crustal cross-section across the BCB to St-Jean-de-Luz basin. | 103 |
| Fig. II-12: Thin- and thick-skinned deformation at the Pyrenean-Cantabrian junction. | 105 |
| Fig. II-13: Schematic cross-section across the eastern Nappe des Marbres. | 106 |

CHAPTER III

| | |
|--|-----|
| Fig. III-1: Geological map of the Pyrenean-Cantabrian system. | 116 |
| Fig. III-2: Structural and rheological characteristics of rift domains. | 119 |
| Fig. III-3: Restored rift domain maps and cross-sections. | 120 |
| Fig. III-4: Schematic evolution of the Pyrenean-Cantabrian system. | 131 |
| Fig. III-5: Schematic 3D evolution of the Pyrenean-Cantabrian junction. | 134 |

CHAPTER IV

| | |
|--|-----|
| Fig. IV-1: Examples of asymmetric rifted margins from the Northern Atlantic. | 145 |
| Fig. IV-2: Wheeler diagram and architecture of upper and lower plates. | 146 |
| Fig. IV-3: Snapshots from the numerical model of asymmetric rifting. | 149 |
| Fig. IV-4: Heat flow evolution for the 3 markers A, B and C during rifting. | 151 |
| Fig. IV-5: Geological map of the Mauléon-Arzacq basin. | 153 |
| Fig. IV-6: Key field observations, rift domains and plate polarity. | 155 |
| Fig. IV-7: Synthetic well logs and restored cross-section of the AMB. | 158 |
| Fig. IV-8: Conceptual figure of T_{\max} and heat flow evolution during hyperextension. | 161 |
| Fig. IV-9: Role of sedimentation rates on the thermal architecture. | 162 |

CHAPTER V: GENERAL DISCUSSION

| | |
|--|-----|
| Fig. V-1: Crustal section and structural map of the Pyrenean-Cantabrian junction. | 171 |
| Fig. V-2: Schematic 3D evolution of the Pyrenean-Cantabrian junction. | 173 |
| Fig. V-3: First order thermal evolution during hyperextension. | 175 |

ANNEXES

| | |
|--|-----|
| Fig. S1: Carte des faciès du Cénomanién Supérieur. | 223 |
| Fig. S2: Role of sediments on the numerical model evolution. | 226 |
| Fig. S3: Selected snapshots of the numerical model of asymmetric rifting. | 230 |
| Fig. S5: Vitrinite reflectance data from the Arzacq-Mauléon basin. | 239 |
| Fig. 1: Carte de localisation des lignes sismiques interprétées dans le BCB. | 241 |
| Fig. 2: Vue 3D des lignes interprétées (Move software). | 242 |
| Fig. 3: Ligne sismique ELZ1. | 243 |
| Fig. 4: Ligne sismique RL75. | 243 |
| Fig. 5: Lignes sismiques ALL7+AN10. | 244 |
| Fig. 6: Ligne sismique ALL6. | 244 |
| Fig. 7: Ligne sismique ALL5. | 245 |
| Fig. 8: Ligne sismique ALL4. | 245 |
| Fig. 9: Ligne sismique ELZ4. | 246 |
| Fig. 10: Ligne sismique ALL3. | 246 |
| Fig. 11: Lignes sismiques RL40+ALL2. | 247 |
| Fig. 12: Ligne sismique RL74. | 247 |
| Fig. 13: Ligne sismique ALL1. | 248 |
| Fig. 14: Ligne sismique PP-17-V. | 248 |
| Fig. 15: Ligne sismique PF. | 249 |
| Fig. 16: Ligne sismique DP3. | 249 |
| Fig. 17: Ligne sismique PP-15-V. | 250 |
| Fig. 18: Ligne sismique DP17. | 250 |
| Fig. 19: Ligne sismique DP15. | 251 |
| Fig. 20: Ligne sismique OS-13. | 251 |
| Fig. 1: Panorama vers le massif d'Artzamendi et structures de Louhossoa. | 252 |
| Fig. 2: Carte de localisation des coupes. | 254 |
| Fig. 3: Coupe « Urdax ». | 254 |
| Fig. 4: Coupe « Maya ». | 254 |
| Fig. 5: Coupe « Ouest Ziga ». | 255 |
| Fig. 6: Coupe « Est Ziga ». | 255 |
| Fig. 1: Extrait du rapport d'activité de forage du puit d'Ainhice. | 256 |
| Fig. 2: Photographies d'échantillons de carottes du puit d'Ainhice. | 257 |
| Fig. 1: Carte géologique, carte des anomalies magnétiques, et carte du signal analytique. | 259 |
| Fig. 2: Carte géologique et cartes des anomalies magnétiques du massif du Labourd. | 260 |

| | |
|--|-----|
| Fig. 3: Carte géologique du massif du Labourd, avec les 3 zones étudiées. | 262 |
| Fig. 4: Le drone avec le système magnétique. | 263 |
| Fig. 5: Tableau des paramètres de vols. | 264 |
| Fig. 6: Carte géologique et carte des anomalies magnétiques pour Hasparren. | 264 |
| Fig. 7: Carte géologique et carte des anomalies magnétiques pour Louhossoa. | 265 |
| Fig. 8: Carte géologique et carte des anomalies magnétiques pour Sohano. | 266 |

Formation et réactivation du système de rift pyrénéo-cantabrique : héritage, segmentation et évolution thermique

Résumé

Cette étude vise à décrire le rôle de l'héritage et de la segmentation associé au rifting pour la réactivation ainsi qu'à étudier l'importance de l'asymétrie tectonique sur l'évolution thermique syn-rift, en utilisant le système de rift pyrénéo-cantabrique comme laboratoire naturel.

L'architecture de la jonction entre les segments pyrénéen et cantabrique a été décrite grâce à l'établissement de coupes géologiques, d'interprétations sismiques et de données de puits. Elle montre un découplage important entre la déformation « thin-skinned » et « thick-skinned ». Les résultats infirment l'hypothèse d'une faille transformante de Pampelune au Crétacé moyen et mettent en évidence une zone d'accommodation, où les segments de rifts se propagent au nord et au sud des massifs basques, associée à une direction d'extension globalement nord-sud.

L'établissement d'une carte des domaines de rift et de coupes restaurées montrent que deux phases peuvent être observées lors de la convergence dans les segments de rift en fonction du point de couplage : une phase de subduction et une phase de collision. Cependant, à la jonction entre les segments, un proto-prisme orogénique bordé par des structures néoformées s'est développé dès la phase de subduction. Ces résultats soulignent l'importance de l'héritage 3D pour l'initiation de la réactivation et l'architecture locale de la chaîne orogénique.

L'évolution thermique associée aux rifts hyper-étirés asymétriques a été étudiée en utilisant un modèle numérique et l'analogie du bassin de Mauléon. Les résultats montrent que l'asymétrie structurale est associée à une évolution thermique asymétrique et diachrone. Ils soulignent l'importance de comprendre l'évolution lithosphérique afin de contraindre l'architecture thermique.

Mots clefs : héritage, segmentation, réactivation, Pyrénées, évolution thermique, hyper-extension

Abstract

This study aims to describe the role of rift-inheritance and segmentation for reactivation and to investigate the influence of asymmetric rifting on the syn-rift thermal evolution, using the Pyrenean-Cantabrian system as a natural laboratory.

The architecture of the Pyrenean-Cantabrian junction has been described thanks to geological cross-sections, seismic interpretations and borehole data. It shows a strong decoupling between the thin- and thick-skinned deformations. Results argue against the existence of a Pamplona transform fault at mid-Cretaceous time and describe an accommodation zone where rift segments overlapped north and south of the Basque massifs, in relation with a roughly north-south direction of extension.

Rift domain mapping and restored cross-sections show that two phases can be recognized with respect to the coupling point during the reactivation of rift segments: a subduction and a collisional phase. However, at rift segment boundaries, a proto-crustal wedge bounded by newly formed structures already developed during the subduction phase. These results highlight the importance of 3D inheritance for the initiation of reactivation and the local architecture.

The thermal evolution associated with asymmetric hyperextended rifting has been investigated using numerical modelling and the Mauléon rift basin analogue. Results show that structural asymmetry is associated with asymmetric and diachronous thermal evolution, and highlight the importance of understanding lithospheric evolution to better constrain the thermal architecture.

Keywords: rift-inheritance, segmentation, reactivation, Pyrenees, thermal evolution, hyperextension